NGU RAPPORT 2019.027

Miljøgeokjemiske data og dateringsresultater fra indre Kongsfjorden og indre Rijpfjorden, samt områdene SK01 og SK02 vest for Svalbard - MAREANO

GEOLOGI FOR SAMFUNNET

SIDEN 1858

NORGES GEOLOGISKE UNDERSØKELSE

- NGU -

NORGES GEOLOGISKE UNDERSØKELSE
· NGU ·

RAPPORT

Norges geologiske undersøkelse
Postboks 6315 Sluppen
7491 TRONDHEIM
Tlf. 73 90 40 00

Rapport nr.: 2019.027
ISSN: 0800-3416 (trykt)
ISSN: 2387-3515 (online)
Gradering: Åpen

Tittel:
Miljøgeokjemiske data og dateringsresultater fra indre Kongsfjorden og indre Rijpfjorden samt områdene SK01 og SK02 vest for Svalbard - MAREANO.

Forfatter:
Henning K.B. Jensen og Valerie Bellec

Oppdragsgiver:
MAREANO

Fylke:

Kommune:

Kartblad (M=1:250.000)

Kartbladnr. og -navn (M=1:50.000)

Forekomstens navn og koordinater:

Sidetall: 50 sider,143 sider vedl **Pris:** 530 kr.
Kartbilag: 0

Feltarbeid utført:
Okt. 2017 og aug. 2018.

Rapportdato:
15.12.2019

Prosjektnr.: 311730

Ansvarlig:
Reidulv Bøe

Sammendrag:
På MAREANO-toktene med FF G.O. Sars i 2017 og 2018 ble det tatt sedimentkjerner for miljøundersøkelser på 8 prøvetakingsstasjoner, fordelt med 1 stasjon i SK01, 1 stasjon i SK02, 3 stasjoner i indre Kongsfjorden og 3 stasjoner i indre Rijpfjorden (Svalbard). Arsen (As) har konsentrasjoner tilsvarende moderat forurensning (Klasse III i Miljødirektoratets klassifisering for kyst og fjordsedimenter) på alle 8 stasjoner (Klasse III: 18 – 71 mg/kg sediment). Bly (Pb), kadmium (Cd), kobber (Cu), nikkel (Ni) og sink (Zn) har enkelte prøver med konsentrasjoner i Klasse II, mens de øvrige stasjonene har konsentrasjoner i Klasse I. For metallene krom (Cr) og kvikksølv (Hg) er konsentrasjonene i Klasse I i overflatesedimentene. Barium er tilstede i relativt konstante konsentrasjoner, med høyest konsentrasjon i SK02. ^{137}Cs er tilstede i lave konsentrasjoner i de 3 analyserte sedimentkjernene fra SK02, indre Kongsfjorden og indre Rijpfjorden.

Tre sedimentkjerner fra SK02, indre Kongsfjorden og indre Rijpfjorden ble valgt ut for kjemisk analyse ned gjennom kjernene, ble datert med bruk av ^{210}Pb, og analysert for innhold av ^{137}Cs. ^{210}Pb-dateringsanalysene er av god kvalitet. ^{14}C-analyser ble utført på foraminiferer i et intervall i sedimentkjernen fra indre Kongsfjorden. Det er forskjell i avsetningsrater når ^{210}Pb og ^{14}C dateringsresultatene sammenliknes. ^{14}C-resultatet viser en sedimentasjonsrate på 0,35 mm/år. Lineære sedimentasjonsrater basert på ^{210}Pb-dataene gir sedimentasjonsrater varierende fra 1,5 til 2,0 millimeter pr. år for de 3 sedimentkjernene med høyest sedimentasjonsrate i indre Rijpfjorden, og lavest i indre Kongsfjorden.

Arsen er tilstede i høye konsentrasjoner i de øverste 3-5 cm i de analyserte sedimentkjernene, med inntil 5 ganger økning i forhold til bakgrunnsnivået dypere i kjernene. Det er ikke klart hvorfor denne økning skjer øverst i sedimentkjernene. Mulig årsak kan være binding av As i toppsjiktet gjennom redoksprosesser i sedimentene etter at sedimentene er avsatt. Hg og Pb øker også i de øverste 10 cm, fra bakgrunnsnivå dypere i kjernene. De høyere verdiene av Hg og Pb mot toppen av disse sedimentkjernene tilskrives langtransportert forurensning primært knyttet til havstrømmer eller atmosfærisk transport. Økningen knyttes primært til forbrenning av kull (Hg) og blyholdig bensin (Pb). For alle øvrige metaller og barium er det relativt stabile konsentrasjoner gjennom de 3 analyserte sedimentkjernene. Disse metallene vurderes å være på naturlig bakgrunnsnivå.

Mikroplast av 10 prøver inklusive overflateprøver fra indre Kongsfjorden og indre Rijpfjorden, samt en test av kontaminering er presentert i en egen rapport fra NGI som vedlegg til denne rapporten. Resultatene viser at det finnes mikroplast i de analyserte overflateprøvene. Resultatene i NGI rapporten viser også at kontaminering er en utfordring i alle ledd fra prøvetaking, uttak av prøver fra sedimentkjerner til analyse, og det er en rekke anbefalinger som må tas med i videre arbeid med mikroplast, inkl. valg av materialer og lokalisering for uttak av prøver til mikroplast-analyse.

Emneord: Maringeologi	Sediment	Forurensning
Tungmetall	Prøvetaking	MAREANO
Geokjemi	Datering	Mikroplast

INNHOLD

VEDLEGG (Vedlegg 1 tilgjengelig digitalt ved nedlasting fra www.mareano.no/resultater/geokjemirapporter.)

Vedlegg 1. Prøveliste og analyseresultater. Kornstørrelsesfordeling (Coulter), Leco (total S, total C og organisk C), HNO_3-ekstrahert og analysert med AAS (Hg) og ICP-AES (Ba, Cd, Cr, Cu, Ni, Pb og Zn). Naturlige standarder Hynne og Nordkyn er inkludert i prøvelistene.

Vedlegg 2. Cd, Cr, Cu, Zn og ^{137}Cs kart i prøvene 0-1 cm dyp og sedimentasjonsrater basert på ^{210}Pb-data.

Vedlegg 3. XRI-bilder av sedimentkjerner.

Vedlegg 4. ^{210}Pb- og ^{137}Cs-analyserapporter fra tre sedimentkjerner. Leverandør av rapporter: Gamma Dating Center, Københavns Universitet, Danmark.

Vedlegg 5. ^{14}C-analyserapport fra R1869MC016 sedimentkjerne. Leverandør av rapport: $^{14}Chrono$, Queens University, Belfast, Nord-Irland.

Vedlegg 6. NGI-rapport: Mikroplastdata fra indre Kongsfjorden, indre Rijpfjorden, Bjørnøytransektet, samt testanalyser for kontaminering.

1. INNLEDNING

MAREANO er et nasjonalt program for kartlegging av havbunnen. De første sedimentprøvene ble samlet inn i 2006. Resultater av målinger av uorganiske miljøgifter fra prøver innsamlet i 2006 - 2017 er rapportert tidligere (rapporter og kart er tilgjengelige på www.mareano.no).

Sedimentkjerner fra 8 stasjoner er analysert for innhold av tungmetaller, arsen, barium, kornstørrelse, total organisk karbon, totalkarbon og total svovel (Fig. 1). Utvalgte sedimentkjerner er i tillegg datert (^{210}Pb, ^{137}Cs samt ^{14}C). Sedimentkjerner er undersøkt med røntgen (XRI) for å studere strukturer i sedimentene, skjell og større partikler. Kart med mikroplastanalyser av 20 sedimentprøver fra forskjellige deler av de kartlagte områdene inklusiv prøver fra de to Svalbardfjordene er inkludert i rapporten.

2. TOKT OG PRØVETAKING

På toktene 2017115 og 2018109 ble det tatt prøver på 8 stasjoner i Norskehavet (SK01 og SK02), indre Kongsfjorden og indre Rijpfjorden (Figur 1). Tabell 1 gir en oversikt over havdyp, geografiske posisjoner og lengde på sedimentkjernene samt antall prøver tatt ut til analyse fra hver stasjon. Prøvetakingsutstyret består av en multicorer som har seks PVC-rør med 106 millimeter indre diameter og 60 cm lengde (Figur 2 og 3). Syv stasjoner ble tatt med multicorer og en stasjon med boxcorer (Figur 4). Boxcoreren ble brukt på en enkelt stasjon hvor det ikke var mulig å bruke multicoreren (SK01).

Tabell 1a. Prøvetakingsstasjoner.

Stasjon	Område	Geografiske koordinater (WGS 84)		Havdyp [m]	Prøvetaking utstyr
		Nord	Øst		
Tokt 2017-115					
R1823MC012A	SK02	77.68550	11.24950	303	Multicorer
R1843BC043	SK01	76.52150	14.58117	277	Boxcorer
Tokt 2018-109					
R1846MC014A	indre Kongsfjorden	78.98480	11.70747	311	Multicorer
R1865MC015A	indre Kongsfjorden	79.10484	11.64824	275	Multicorer
R1869MC016A	indre Kongsfjorden	79.01981	11.41530	346	Multicorer
R1872MC019A	indre Rijpfjorden	80.03960	22.25330	145	Multicorer
R1878MC021A	indre Rijpfjorden	80.09196	22.15351	213	Multicorer
R1887MC023A	indre Rijpfjorden	80.17150	22.13449	208	Multicorer

Tabell 1b. Prøvetakingsstasjoner med analyserte sedimentprøver.

Stasjon	Prøvetaking utstyr	Kjernelengde [cm]	Antall prøver til kjemisk analyse
Tokt 2017-115			
R1823MC012A	Multicorer	37	7
R1843BC043	Boxcorer	32	1
Tokt 2018-109			
R1846MC014A	Multicorer	33	1
R1865MC015A	Multicorer	37	1
R1869MC016A	Multicorer	35	7
R1872MC019A	Multicorer	26	1
R1878MC021A	Multicorer	31	1
R1887MC023A	Multicorer	36	7

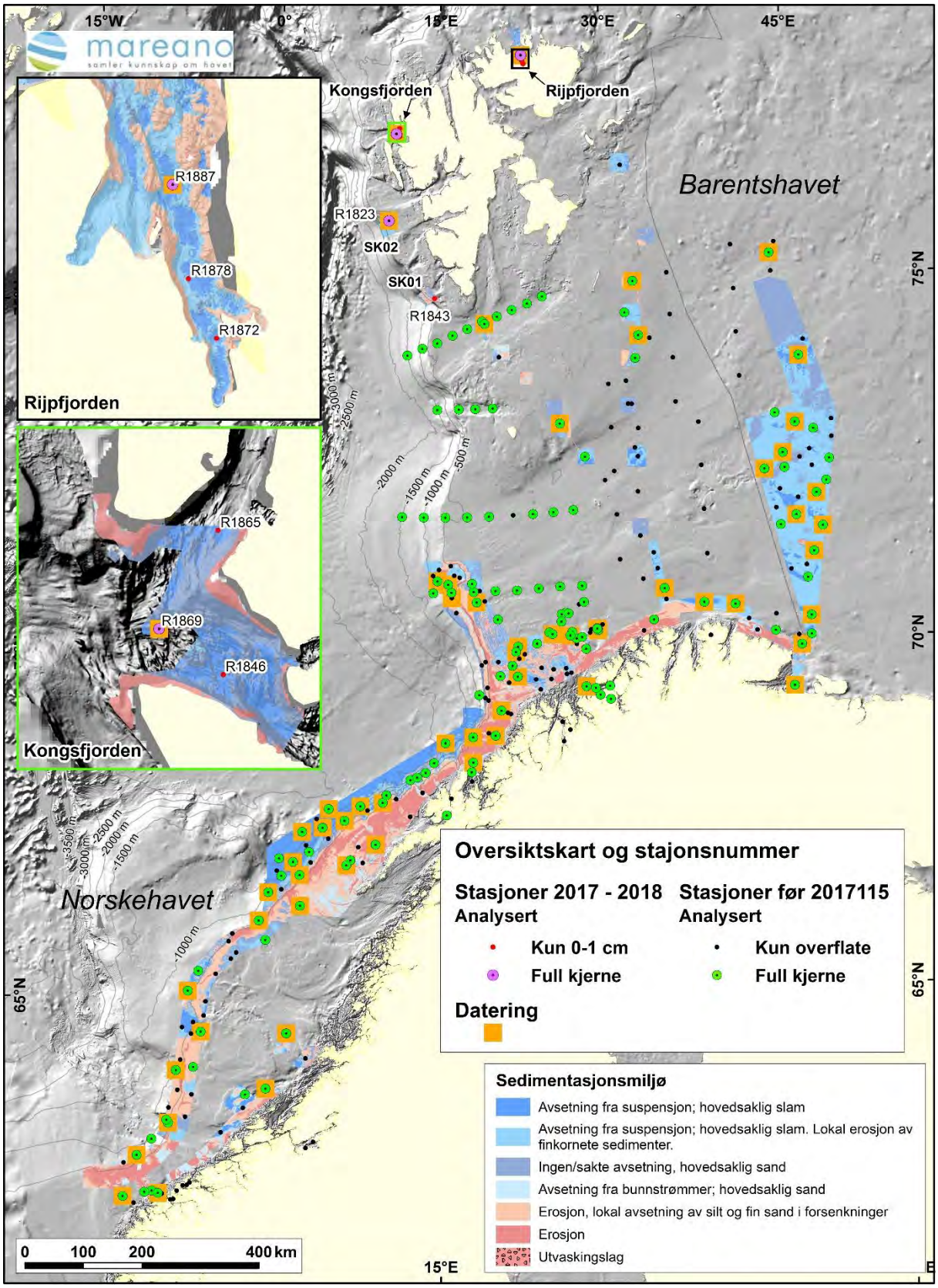

Figur 1. Kart over alle MAREANOs prøvetakingsstasjoner i perioden 2006-2018, inkludert stasjoner prøvetatt i 2003 og 2004. R1843 i SK01 og R1823 i SK02 er lokalisert vest for Svalbard. Stasjonene i indre Kongsfjorden og indre Rijpfjorden er vist i kartutsnittene for de to Svalbardfjordene.

Figur 2. R1887MC023 (indre Rijpfjorden) sedimentkjerner stående i multicoreren. Rørene er 60 cm lange og sedimentkjernene har vannsøyle på toppen.

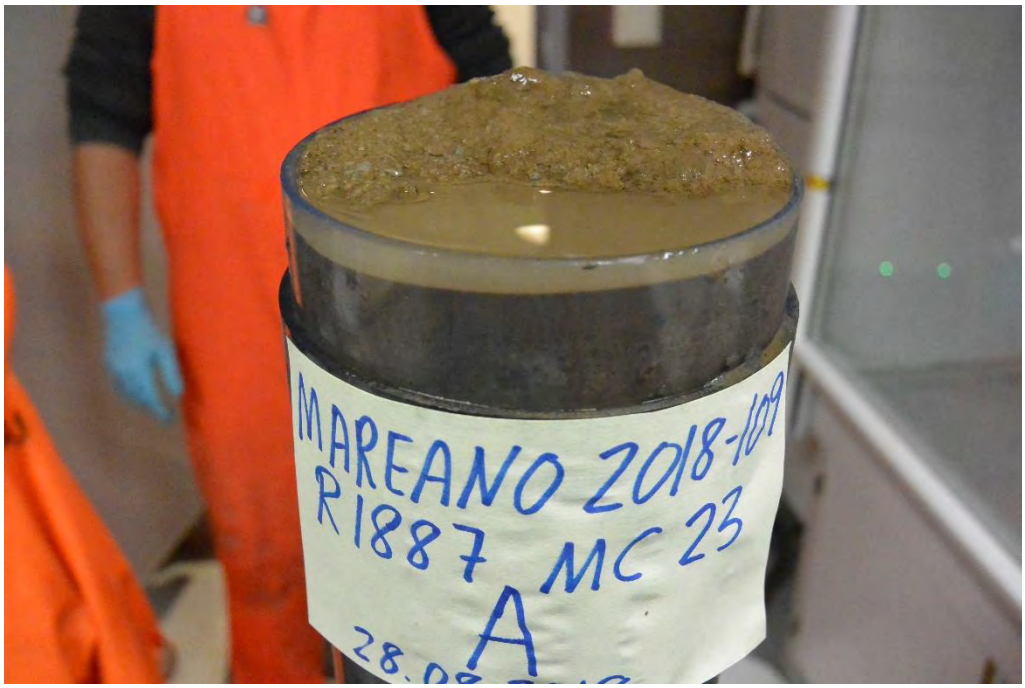

Figur 3. Toppen av sedimentkjerne A med litt ujevn overflate fra stasjon R1887MC023 fra indre Rijpfjorden, før sedimentkjernen deles opp i 1-cm skiver til uorganisk kjemiske analyser. De øverste centimeterne i sedimentkjernen har høyt vanninnhold.

3. DATA OG METODIKK

Det ble gjennomført skiving av kjerner ombord for hver centimeter. Prøvetakingsrøret har en indre diameter på 106 mm. Sedimentkjernen ble presset ut av røret v.h.a. et stempel. Figur 5 viser toppen av en sedimentkjerne som blir presset ut, klar for å ta en sedimentprøve (0-1 cm). Prøvene ble pakket i polyetylenposer med ziplås før innfrysing til ÷18 ºC.

Ved NGU Lab ble frysetørking og uttak til følgende analyser gjennomført:

- Bestemmelse av organisk karbon (TS, TC og TOC) ved hjelp av Leco.
- Innvekt 1,1 g til 7M HNO_3-ekstraksjon etter NS 4770 for påfølgende analyse med ICP-AES og CV-AAS. As, Ba, Cd, Cr, Cu, Ni, Pb og Zn analysene ble gjort ved et eksternt laboratorium. Hg-analysene er gjort ved NGU-lab.

Resultatene er rapportert som mg/kg tørrvekt sediment.

Det er brukt varierende prøvemengde for våtsikting med sikteåpning 16, 8, 4, 2 og 1 mm, samt 500, 250, 125 og 63 µm (avhengig av antatt kornstørrelsesfordeling). Fraksjonen mindre enn 2 mm er så analysert for kornstørrelse med Coulter laserdiffraksjon, slik at kornfordelingskurve kan beregnes for kornstørrelse ned til 0,4 µm. Vedlegg 1 gjengir analyserapporten fra NGU Lab og Eurofins i sin helhet. Prøver til dateringsanalyse ble tatt ut fra samme sedimentkjerne som prøvene til uorganisk kjemiske analysene nevnt ovenfor.

4. KVALITETSKONTROLL

Kornstørrelses- og organisk kullstoff-analysene ved NGU-Lab er gjennomført i henhold til akkrediterte metoder. Syreekstraksjon og tungmetallanalysene samt Ba ble utført ved Eurofins i Moss i henhold til akkrediterte metoder. Dateringsanalysene (^{210}Pb og ^{137}Cs) er ikke akkrediterte, men er etablerte metoder ved Gamma Dating Center presentert i vitenskapelige artikler (Andersen, 2017). ^{14}C-analysen ble utført ved ^{14}Chrono Lab, Belfast. Tabell 2 oppsummerer analytiske metoder, analyseusikkerhet og -presisjon for parametrene vist i rapporten og som kart. De samme parametrene, i tillegg til flere elementer fra ICP-AES analysen som ikke rapporteres, kan ses i Vedlegg 1.

For kvalitetskontroll av de uorganiske kjemiske analysene er det satt inn sedimentprøver fra Trondheimsfjorden (Hynne) og en standardprøve fra Nordkyn i Finnmark i prøvesettet. Det er gjennomført i alt 4 parallelle analyser av hver av de to innsatte sedimentprøvene. Analyseresultatene er presentert sammen med de øvrige resultatene i Vedlegg 1.

5. RESULTATER

Geokjemiske data fra samtlige analyser finnes i Vedlegg 1 og 2. I de fleste sammenhenger benyttes konsentrasjonsenheten mg/kg bortsett fra TOC, TC, TS (vektprosent), ^{210}Pb, ^{137}Cs og ^{14}C. For å kunne operere med statistikk og kart for alle observasjoner er alle analyseresultater rapportert "< deteksjonsgrense" satt til verdien 0,5 × deteksjonsgrensen for det gjeldende stoff.

5.1 Sedimentklassifikasjon og beregning av vektprosent karbonat

NGU har etablert en sedimentklassifikasjon (Bøe m. fl., 2010), som revideres ved behov. Deler av sedimentklassifikasjonen relevant i MAREANO-sammenheng er presentert i Tabell 3.

Tabell 2. Oversikt over analytiske metoder, kvalitetssikring og akkreditering.

Parameter	Instrument	Akkreditering	Analytisk usikkerhet	Nedre detekt.
Opparbeiding av prøver til analyser: Frysetørker FreeZone 6L med FreeZone Bulk Tray Dryer (BTD) fra Labconco (- 55 grd), med Vacuubrand RC-6 pumpe. Er akkreditert.				
Sedimentkarakteristikk – analysemetoder				
Total karbon (TC)	Leco SC-632	Ja	±15 %	0,06
Total organisk karbon (TOC)	"	Ja	±25 %	0,1
Total svovel (TS)	"	Ja	±30 %	0,02
Kornstørrelsesanalyse	Coulter LS 13320	Ja	±10 %	Ikke angitt
Opparbeiding av prøver til kjemiske elementanalyser: Syreekstraksjon av 1,1 gr tørket sediment 30 minutt i autoklav med 20 ml 7M HNO_3,				
As	ICP-AES: Perkin Elmer Optima 4300 Dual View	Ja	±20 %	0,5 mg/kg
Ba	"	ja	±25 %	0,5 mg/kg
Cd	"	ja	±25 %	0,01 mg/kg
Cr	"	ja	±25 %	0,5 mg/kg
Cu	"	ja	±25 %	0,5 mg/kg
Ni	"	ja	±25 %	0,5 mg/kg
Pb	"	ja	±25 %	0,5 mg/kg
Zn	"	ja	±25 %	2,0 mg/kg
Hg	FIMS 100 Flow Injection Mercury System fra Perkin Elmer	ja	±20 %	0.002 mg/kg
^{210}Pb	Canberra ultralow-background Ge-detector	Nei	Ikke relevant	Ikke relevant
^{137}Cs	"	Nei	Ikke relevant	Ikke relevant
^{14}C		Nei	Ikke relevant	Ikke relevant

Tabell 3. Sedimentklassifikasjon og kornstørrelser. Klassifikasjonen er i henhold til NGUs sedimentklassifikasjon.

Kornstørrelse	Definisjon/beskrivelse
Leir	Leir:silt > 2:1 og leir+silt > 90 %, sand < 10 %, grus < 2%
Organisk slam	Leir:silt fra 1:2 til 2:1 og leir+silt > 90 %, sand < 10 %, grus < 2 %. Høyt innhold av organisk material
Slam	Leir:silt fra 1:2 til 2:1 og leir +silt > 90 %, sand < 10%, grus < 2%.
Sandholdig leir	Leir+silt > 2:1 og leir+silt > 50 %, sand < 50 %, grus < 2 %.
Sandholdig slam	Leir:silt = fra 1:2 til 2:1 og leir+silt > 50%, sand < 50%, grus < 2%.
Silt	Leir:silt < 1:2 og leir+silt > 90 %, sand < 10%, grus < 2 %.
Sandholdig silt	Silt:leir >2:1 og leir+silt > 50 %, sand < 50 %, grus < 2 %.
Leirholdig sand	Sand > 50 %, leir:silt > 2:1 og leir+silt < 50 %, grus < 2 %.
Slamholdig sand	Sand > 50 %, leir:silt = fra 1:2 til 2:1og leir+silt < 50 %, grus < 2 %.
Siltholdig sand	Sand > 50 %, silt:leir > 2:1 og leir+silt < 50 %, grus < 2 %.
Fin sand	Sand > 90 %, inkluderer fin og veldig fin sand (Wentworth, 1922).
Sand	Sand > 90 %, leir+silt < 10 %, grus < 2 %.
Grov sand	Sand > 90 %, inkluderer medium, grov og veldig grov sand (Wentworth, 1922).
Grusholdig slam	Sand:silt+leir < 1:9, grus 2 – 30 %.
Grusholdig sandholdig slam	Sand:silt+leir fra 1:9 til 1:1, grus 2 – 30 %.
Grusholdig slamholdig sand	Sand:silt+leir fra 1:1 til 9:1, grus 2 – 30 %.
Grusholdig sand	Sand:silt+leir > 9:1, grus 2 – 30 %.
Slamholdig grus	Grus 30 – 80 %, sand:silt+leir < 1:1.
Slamholdig sandholdig grus	Grus 30 – 80 %, sand:silt+leir fra 1:1 til 9:1.
Sandholdig grus	Grus 30 – 80 %, sand:silt+leir>9:1.
Grus	Grus > 80 %.
Grus, stein og blokk	Dominans av grus, stein og blokk.
Stein og blokk	Dominans av stein og blokk.
Sand og blokk	Dominans av sand og blokk.
Diamikton	Sediment med blandede kornstørrelser og dårlig sortering.

Innholdet av karbonat i sedimentene beregnes fra analyser med LECO, og gjøres ut fra antakelsen om at karbon (C) som ikke er av organisk opprinnelse er bundet i karbonat ($CaCO_3$). Karbonatverdiene i vektprosent beregnes fra følgende formel:

$$(TC - TOC) \times (CaCO_3/C) = (TC - TOC) \times 8{,}33$$

TC er innholdet av totalt karbon, mens TOC er innhold av total organisk karbon.

Karbonat i sedimentene antas å ha opprinnelse i biologisk materiale – i hovedsak skjell fra mikroorganismer og større bunnlevende dyr, for eksempel foraminiferer, kråkeboller og koraller.

5.2 Overflateprøver (0-1 cm)

De geokjemiske resultatene for overflateprøvene (0-1 cm) rapporteres for å gi oversikt over dagens miljøtilstand. Parametrene som presenteres her er sedimentenes finstoffandel, innhold av TOC, innhold av karbonat og innholdet av tungmetallene kadmium (Cd), kobber (Cu), krom (Cr), kvikksølv (Hg), nikkel (Ni), bly (Pb) og sink (Zn), samt elementene arsen (As) og barium (Ba). Kart for de nevnte parametrene finnes i Vedlegg 2. Videre rapporteres radioaktiv ^{137}Cs, som blir analysert i forbindelse med dateringsanalysene utført på sedimentkjerner fra tre utvalgte stasjoner.

5.2.1 Kornstørrelsesfordeling, organisk karbon, karbonat og svovel

I utgangspunktet er prøvetaking for miljøanalyser gjennomført i områder med finkornige sedimenter. De fleste prøvetakingsstasjonene er valgt ut før tokt på bakgrunn av blant annet multistråledata (dybde og bunnreflektivitet). Metodikken for geologisk havbunnskartlegging er gitt i Bøe m. fl. (2010) og Bellec m. fl. (2017). Prøvetaking planlegges der en forventer at det avsettes slamholdige sedimenter, typisk i dype områder eller områder med svake havstrømmer. Andel finstoff (<63µm) i overflateprøvene er vist i Figur 6. Tabell 3 viser sedimentklassifikasjonen som er brukt for beskrivelse av overflateprøvene.

Tabell 4 viser kornstørrelsesfordelingen i leir-, silt-, sand- og grusfraksjoner for overflateprøvene for de 8 stasjonene. Seks av de 8 prøvene består av silt, en prøve består av sandholdig silt og en enkelt prøve grusholdig silt. Siltfraksjonen utgjør 60 – 87 %, mens sandfraksjonen varierer fra 2 til 32 %. Andelen leir utgjør 9 til 15 %. En enkelt prøve, R1865MC015 fra indre Kongsfjorden, har 5 % grus. Forekomsten av grus i denne overflateprøven kan muligvis forklares med grovere sediment tilført fra sedimentholdig is fra breer i Kongsfjorden. Finstoff, bestående av leir + silt, utgjør 68 til 98 % av prøvene. Andel finstoff er vist i Figur 5. Det er viktig å merke seg at kornfordelingsanalyse med Coulter gir lavere leirinnhold og høyere siltinnhold enn andre tradisjonelle metoder for kornfordelingsanalyse (Rise og Brendryen, 2013). Andelen leir kan i enkelte tilfeller ganges med fire og siltandelen deles med fire, slik at for eksempel sandholdig silt kan klassifiseres som sandholdig slam (Tabell 4).

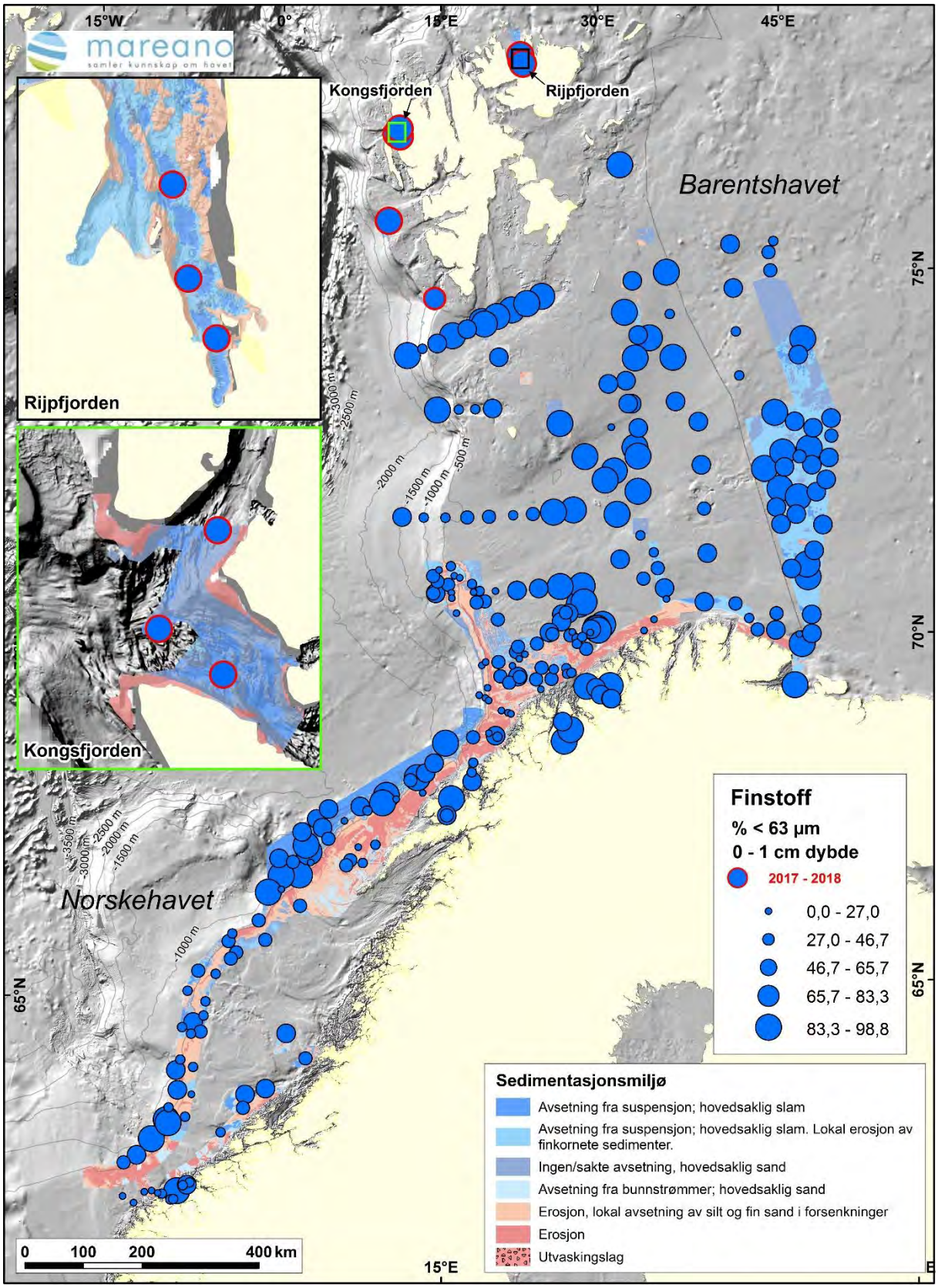

Figur 5. Andel finstoff (<63µm) i overflateprøvene. Prøvene fra toktene 2017115 (SK01og SK02), og 2018109 (indre Kongsfjorden og indre Rijpfjorden) er markert med rød ring.

Tabell 4. Kornstørrelsesfordeling[1] og sedimentklassifikasjon for overflateprøvene (0-1 cm dybde) basert på Coulter data.

Stasjon	Område	Leir < 2 µm [%]	Silt 2- 63 µm [%]	Finstoff <63µm [%]	Sand 63-2000 µm [%]	Grus >2000 µm [%]	NGU sediment Klassifikasjon
R1823MC012A	SK02	12.4	82.4	94,8	5,2	0	Silt
R1843BC043	SK01	8.9	59.6	68,4	31,6	0	Sandholdig silt
R1846MC014A	Kongsfjorden indre	11.4	85.2	96,6	3,4	0	Silt
R1865MC015A	Kongsfjorden indre	10.4	79.4	89,8	4,8	5,4	Grusholdig slam
R1869MC016A	Kongsfjorden indre	11.1	86.7	97,8	2,2	0	Silt
R1872MC019A	Rijpfjorden indre	9.3	84.6	93,9	6,1	0	Silt
R1878MC021A	Rijpfjorden indre	14.1	83.5	97,6	2,4	0	Silt
R1887MC023A	Rijpfjorden indre	15.4	80.6	96,0	4,0	0	Silt

TOC i overflateprøvene er presentert i Figur 6. Prøvene har TOC som varierer fra 1,08 (R1865, Kongsfjorden) til 1,88 vektprosent (R1823, SK02) (Figur 6). De analyserte prøvene har TOC-verdier som tidligere analyserte prøver i Barentshavet og denne delen av Norskehavet (Figur 6).

Innhold av karbonat varierer fra 3,7 til 14,7 vektprosent (Figur 7). Høyest karbonatinnhold er i de tre prøvene fra indre Kongsfjorden (12,4 – 14,7 vektprosent), mens det er lav andel karbonat i SK01, SK02 og indre Rijpfjorden (3,7 – 5,4 vektprosent). Den generelt lave andelen karbonat kan forklares med at kalkskallene løses opp når organismene dør. Alternativt kan det skyldes at det finnes færre kalkdannende organismer i disse havområdene sammenlignet med havområdene lengre mot sør i Barentshavet og Norskehavet (Figur 7) (Steinsund og Hald, 1993). Slik sett er andelen karbonat høy i prøvene fra Kongsfjorden sammenlignet med prøver sør for Kongsfjorden, inkl. SK01 og SK02 og tidligere analyserte prøver i Barentshavet (Figur 7). Visuell inspeksjon av frysetørkete prøver viser at det er forekomst av mikrofossiler i prøver fra indre Kongsfjorden.

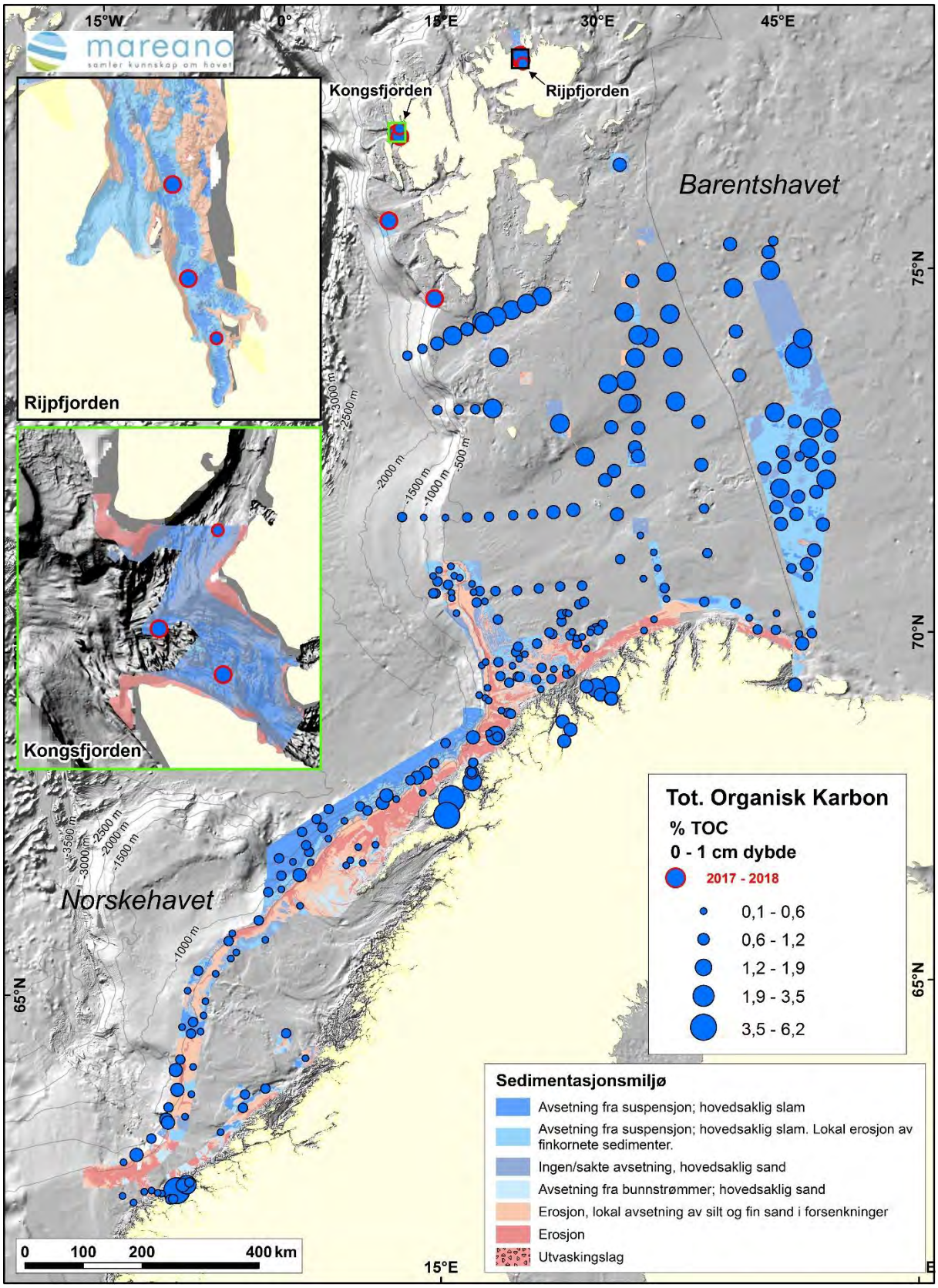

Figur 6. TOC i overflateprøver. Prøvene fra 2017115 og 2018109 fra SK01, SK02, indre Kongsfjorden og indre Rijpfjorden er markert med rød ring.

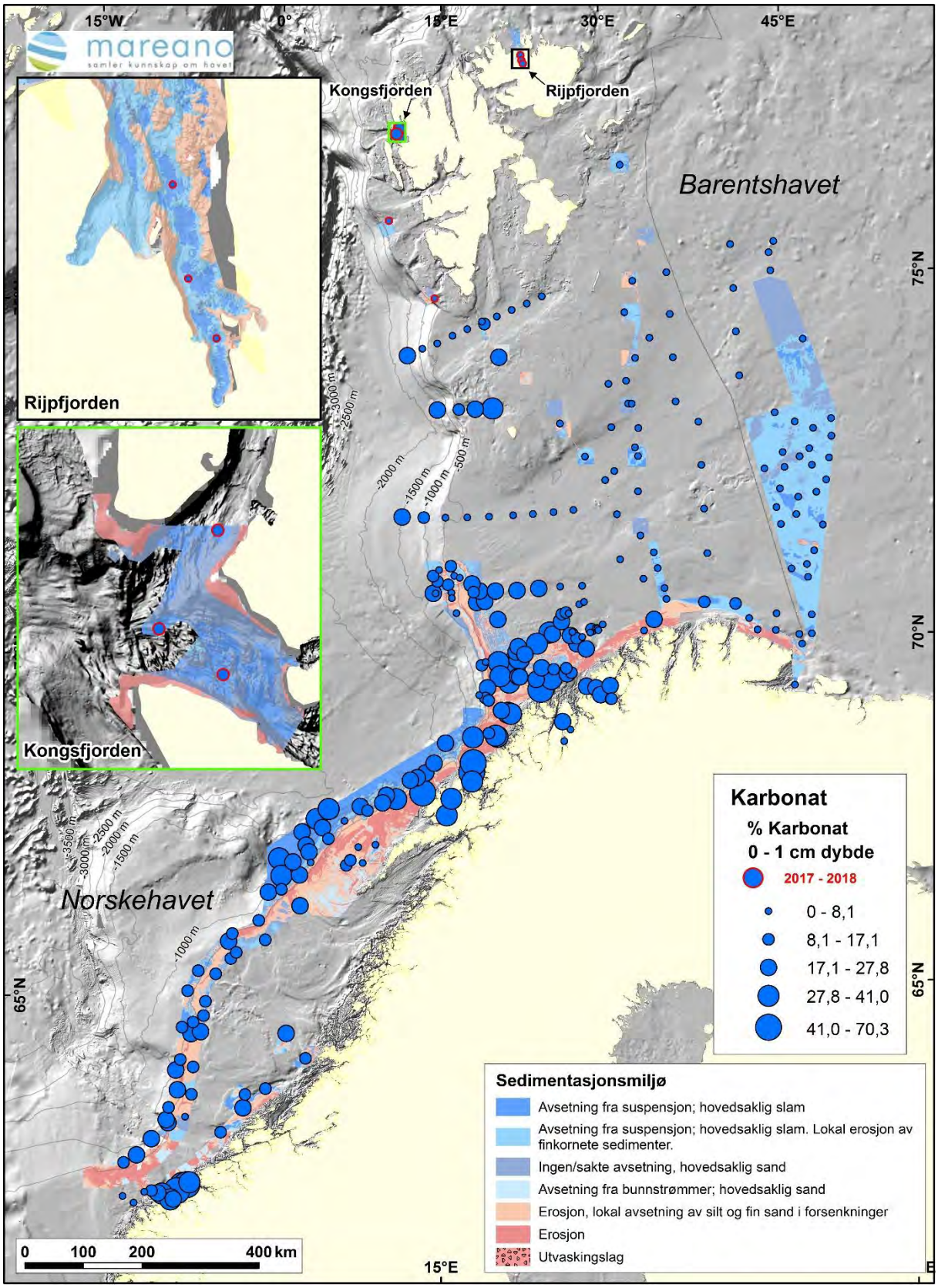

Figur 7. Karbonat i overflateprøver (vektprosent). Prøvene fra 2017115 og 2018109 fra SK01, SK02, indre Kongsfjorden og indre Rijpfjorden er markert med rød ring.

5.2.2 Innhold av tungmetaller, arsen og barium

Det er analysert for tungmetallene bly (Pb), kadmium (Cd), kobber (Cu), krom (Cr), kvikksølv (Hg), nikkel (Ni), sink (Zn), samt arsen (As) i overflateprøvene fra de 8 prøvetakingsstasjonene. Tungmetall- og arsenkonsentrasjonene i sedimentprøvene er sammenlignet med Miljødirektoratets klassifikasjonssystem for forurensningsnivåer i sedimenter i kyst- og fjordområder (Molvær m. fl., 1997; SFT, 2007) og nå sist justert i 2016 (Miljødirektoratet Veileder M-608). Her er det skjedd noen justeringer for inndeling i tilstandsklasser for en rekke metaller og arsen. Justeringene i grenseverdiene medfører også at metallkonsentrasjonskartene blir justert i forhold til de nye grenseverdiene. Klassifikasjonssystemet er delt inn i følgende tilstandsklasser:

tilstandsklasse I: bakgrunn; tilstandsklasse II: god; tilstandsklasse III: moderat; tilstandsklasse IV: dårlig; tilstandsklasse V: svært dårlig

Barium (Ba) er også inkludert selv om Ba ikke er et toksisk element. Olsgård og Gray (1995) og Rye (1996) har rapportert om utslipp av barytt fra norsk offshorevirksomhet i Nordsjøen. Ba i sedimenter i Skagerrak er rapportert, og de forhøyede verdiene øverst i havbunnen er tolket som tilførsel av barium fra boreslam brukt i Nordsjøen og transportert med havstrømmer til Skagerrak (Sæther m. fl., 1996; Thorsnes og Klungsøyr, 1997; Lepland m. fl., 2000). Dehairs m. fl. (1980) og Nuernberg m. fl. (1997) beskriver andre prosesser for forekomst av Ba i sedimenter: det dannes små baryttkrystaller i mikronisjer i organisk materiale som brytes ned i vannsøylen, spesielt i områder med høy biologisk produktivitet. Kart som viser konsentrasjoner av tungmetallene, arsen og barium i overflatesedimentene finnes også i Vedlegg 3. Radioaktivt ^{137}Cs blir rapportert for overflatesedimentene. ^{137}Cs blir analysert sammen med den radioaktive ^{210}Pb-isotopen, som brukes for datering av sedimentkjerner (avsnitt 5.3.4).

Arsen (As)

Prøvene varierer fra 19 til 58 mg/kg sediment, slik at alle 8 prøver har konsentrasjoner høyere enn 18 mg/kg sediment og er dermed i tilstandsklasse III (18-71 mg/kg). Figur 8 viser As-konsentrasjon i toppsedimentene. Prøvene i SK01, SK02, indre Kongsfjorden og indre Rijpfjorden er på samme nivå som de øvrige analyserte prøvene i Barentshavet og det nordlige Norskehavet (Figur 8).

Bly (Pb)

Prøvene varierer fra 16 til 31 mg/kg, med høyeste konsentrasjon på stasjon R1823 i SK01(Figur 9). Seks sedimentprøver har Pb-konsentrasjoner i tilstandsklasse I (tilstandsklasse I: <25 mg/kg) (Figur 9), mens to prøver er i tilstandsklasse II (25 – 150 mg/kg), som vist i Figur 9.

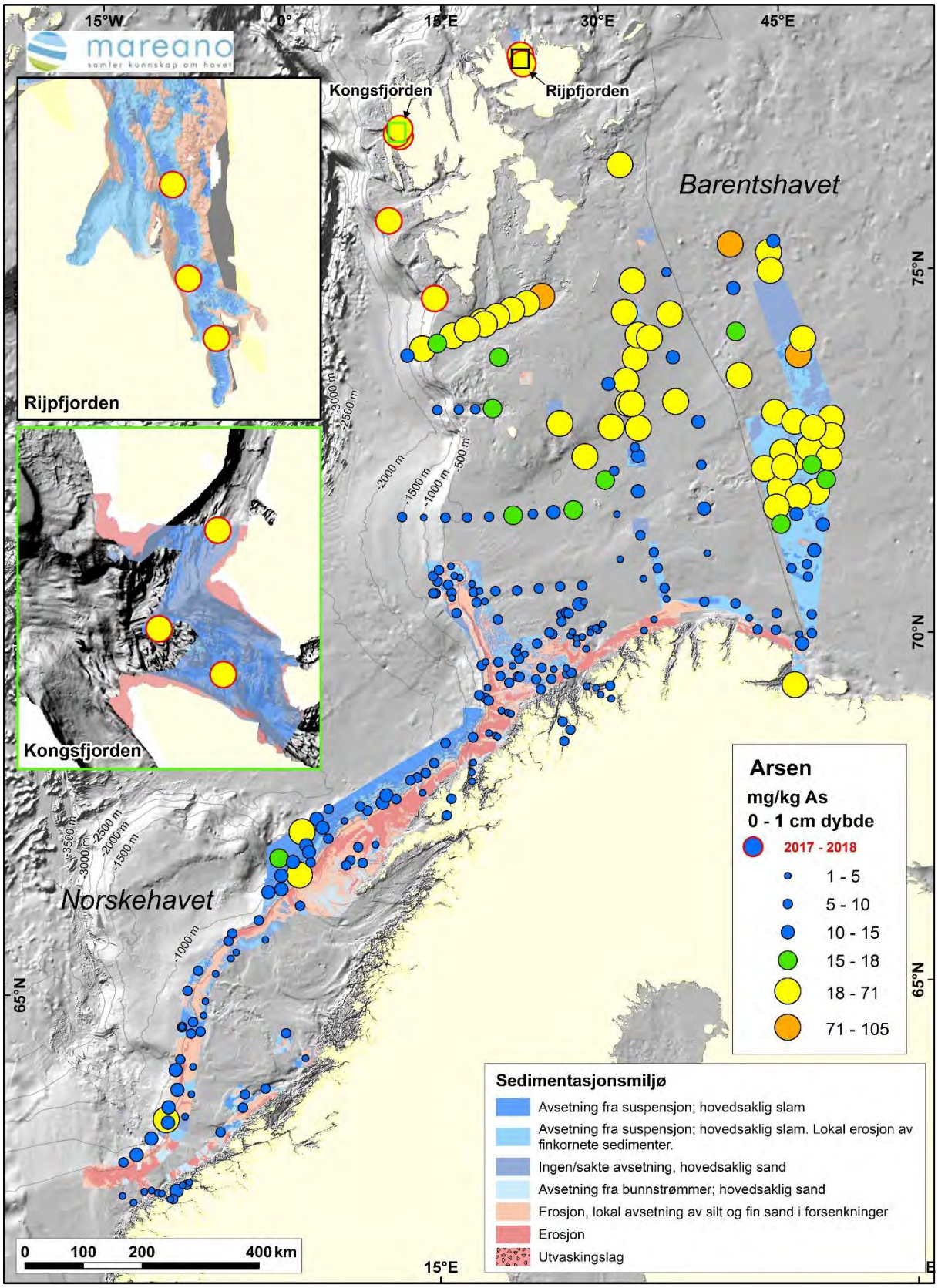

Figur 8. As-konsentrasjon i overflateprøver (0-1 cm). Grønne punkt angir tilstandsklasse II (15-18 mg/kg). Gule punkt angir tilstandsklasse III (18 – 71 mg/kg). Oransje punkt angir tilstandsklasse IV (71 – 580 mg/kg). Prøvene fra 2017 og 2018 fra SK01, SK02, indre Kongsfjorden og indre Rijpfjorden er markert med rød ring.

Kadmium (Cd)

Prøvene har lave kadmiumkonsentrasjoner fra 0,05 til 0,29 mg/kg sediment. Seks av de 8 prøvene er i tilstandsklasse I - bakgrunn for kyst- og fjordsedimenter (<0,25 mg/kg), og to prøver (R1878 og R1887) fra indre Rijpfjorden er i tilstandsklasse II (0,25 – 2,5 mg/kg sediment).

Kobber (Cu)

Prøvene har Cu-konsentrasjoner varierende fra 12 til 20 mg/kg med høyest konsentrasjon i R1872 og R1878 i Rijpfjorden, som er i tilstandsklasse II (20 – 84 mg/kg sediment), mens de øvrige 6 prøvene er i tilstandsklasse I – bakgrunn for kyst og fjordsedimenter (< 20 mg/kg sediment).

Krom (Cr)

Prøvene har Cr-konsentrasjoner varierende fra 23 til 42 mg/kg med høyest konsentrasjon i R1823 (SK02). Samtlige overflateprøver har konsentrasjoner i tilstandsklasse I (<60 mg/kg).

Kvikksølv (Hg)

Hg i overflateprøvene er vist i Figur 10. Prøvene har Hg-konsentrasjoner varierende fra 0,030 til 0,044 mg/kg. Samtlige 8 prøver er i tilstandsklasse I (<0,050 mg/kg sediment) for fjord og kystsedimenter.

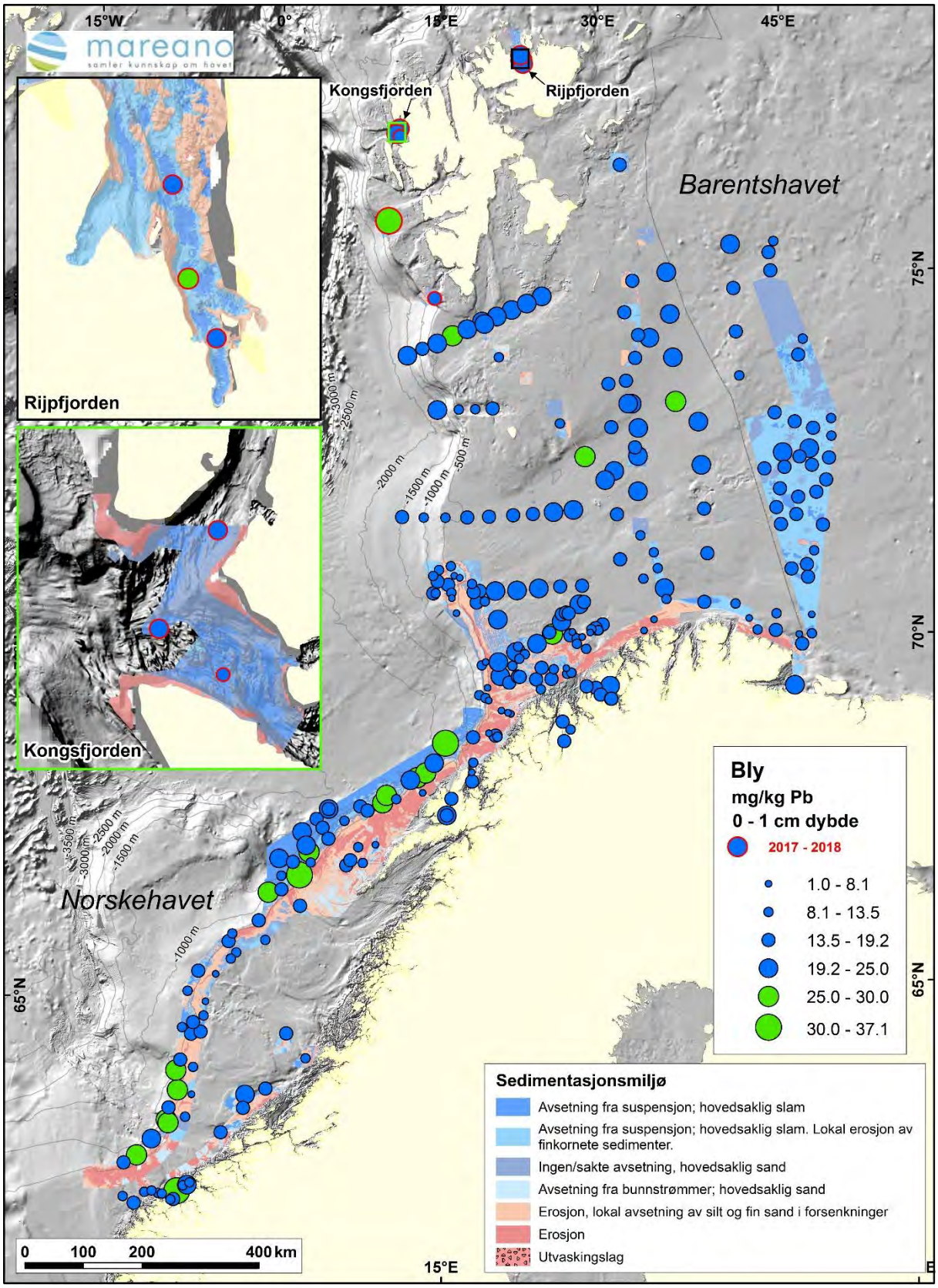

Figur 9. Pb-konsentrasjon i overflateprøver (0-1 cm). Blå punkt angir tilstandsklasse I for kyst- og fjordsedimenter (<25 mg/kg). Grønne punkt angir tilstandsklasse II (25-150 mg/kg). Prøvene fra toktene 2017115 og 2018109 er markert med rød ring.

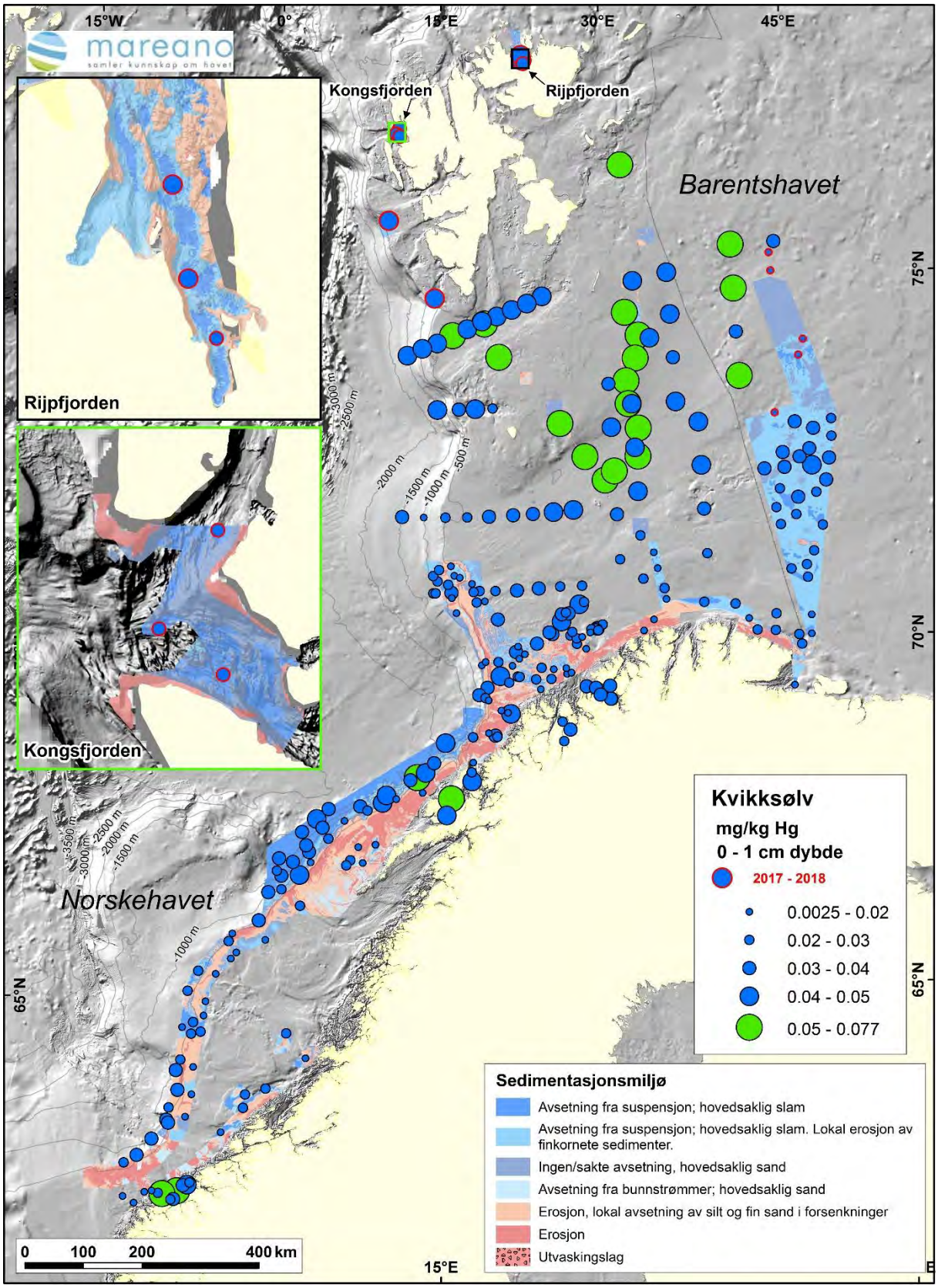

Figur 10. Hg i overflateprøvene. Blå punkt angir tilstandsklasse I for kyst- og fjordsedimenter (<0,05 mg/kg). Grønne punkt angir tilstandsklasse II (0,05- 0,52 mg/kg). Prøvene fra toktene 2017115 og 2018109 er markert med rød ring.

Nikkel (Ni)

Figur 11 viser Ni-konsentrasjon i overflateprøvene. Prøvene har Ni-konsentrasjoner varierende fra 23 til 35 mg/kg med den høyeste konsentrasjonen i R1823, som er den eneste stasjon i tilstandsklasse II (30 – 42 mg/kg sediment). De øvrige 7 prøvene er i tilstandsklasse I (< 30 mg/kg sediment).

Sink (Zn)

Sink varierer fra 57 til 95 mg/kg med den høyeste konsentrasjon i R1878 i indre Rijpfjorden. Tre av de 8 overflateprøvene er i tilstandsklasse II: to prøver i indre Rijpfjorden og en prøve fra indre Kongsfjorden (god, 90 – 139 mg/kg sediment), mens de øvrige 5 prøvene er i tilstandsklasse I (<90 mg/kg).

Barium (Ba)

Ba analyseres for å vurdere om eventuelle utslipp fra olje- og gassboring kan spores i sedimentene, men det er viktig å være klar over at også naturlige kilder kan gi forhøyde verdier. Ba i overflatesedimentene er presentert i Figur 12. Prøvene har konsentrasjoner varierende fra 98 til 190 mg/kg, med den høyeste konsentrasjonen i R1823 (SK02).

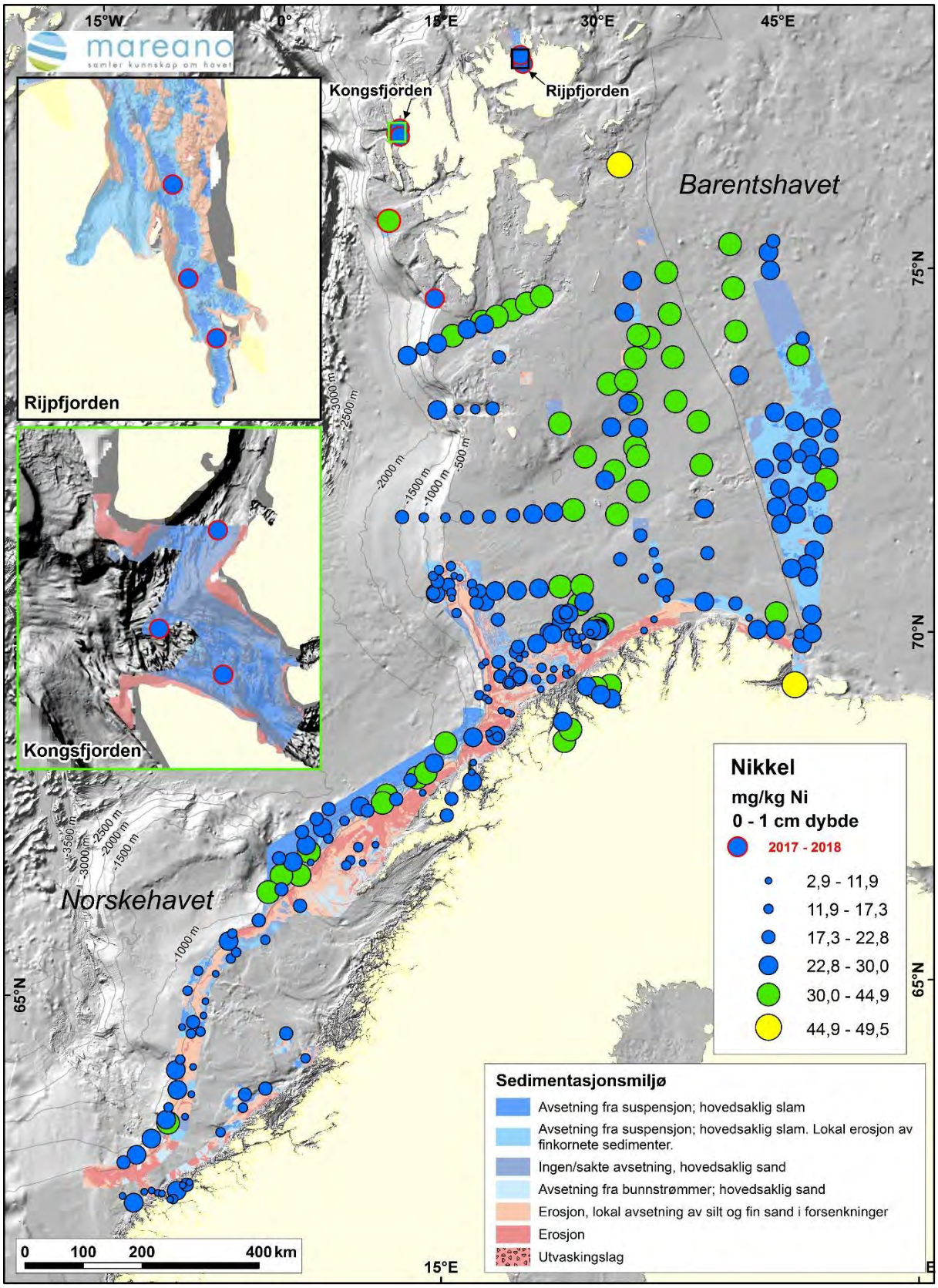

Figur 11. Nikkel i overflateprøver. Blå punkt angir tilstandsklasse I for kyst- og fjordsedimenter. Grønne punkter angir tilstandsklasse II (30-42 mg/kg). Gule punkt angir tilstandsklasse III (42 – 271 mg/kg TS). Prøvene fra toktene 2017115 og 2018109 er markert med rød ring.

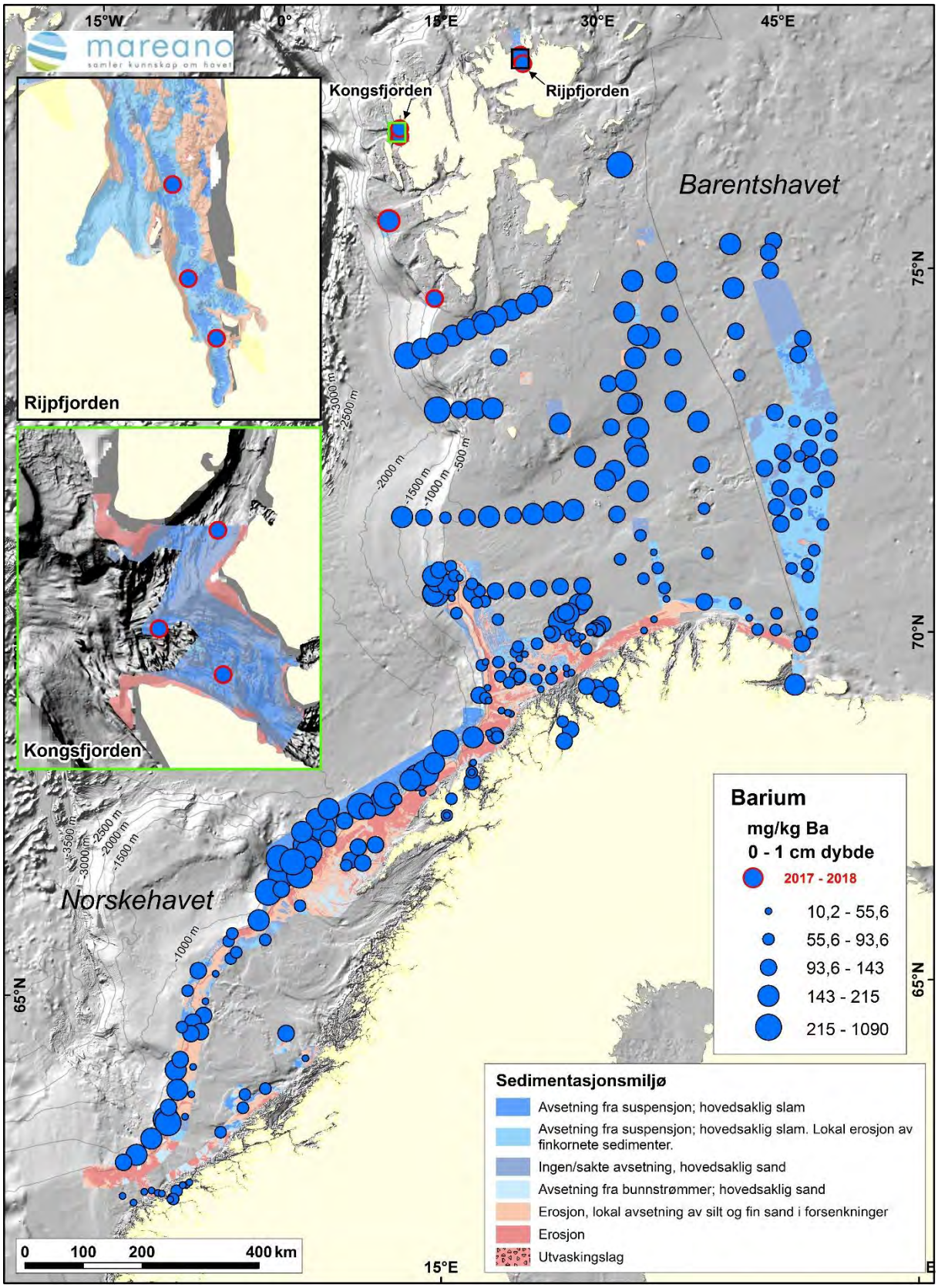

Figur 12. Barium i overflatesedimenter. Prøvene fra toktene 2017115 og 2018109 er markert med rød ring.

Cesium-137 (^{137}Cs)

^{137}Cs er et menneskeskapt radioaktivt element. De viktigste kildene er utslippet fra Tsjernobyl (1986) og de atmosfæriske atomprøvesprengningene på Novaja Zembla på 1950- og 1960-tallet. Resultatene fra ^{137}Cs er presentert på kart i Vedlegg 2. ^{137}Cs-konsentrasjonen i overflatesedimentene på de tre analyserte stasjonene R1823, R1869 og R1887 er henholdsvis 3,0, 2,0 og 4,0 Bq/kg sediment i overflateprøvene. Se kapittel 5.3.4 for mer detaljer vedr. ^{137}Cs resultatene.

Resultatene fra metallanalysene av overflatesedimentene er oppsummert i Tabell 5, hvor tilstandsklassene for metallene er vist, samt antall prøver innenfor hver av tilstandsklassene i henhold til Miljødirektoratets klassifikasjonssystem for sedimenter (Miljødirektoratet, M-608, 2016). http://www.miljodirektoratet.no/no/Publikasjoner/2016/September-2016/Grenseverdier-for-klassifisering-av-vann-sediment-og-biota/

Tabell 5. Metaller og arsen (8 stasjoner fra tokt 2017115 og 2018109) i henhold til Miljødirektoratets tilstandsklasser for marine overflatesedimenter. Uthevet skrift viser antall prøver i overflateprøver i hver av klassene I-V.

Parametere	Forurensningsnivåer				
	I Bakgrunn	II God	III Moderat	IV Dårlig	V Svært dårlig
Arsen (mg/kg) As	<15 **0**	15-18 **0**	18-71 **8**	71 – 580 **0**	>580 **0**
Bly (mg/kg) Pb	<25 **7**	25 -150 **1**	150-1480 **0**	1480-2000 **0**	>2000 **0**
Kadmium (mg/kg) Cd	<0,25 **6**	0,25 – 2,5 **2**	2,5 –16 **0**	16 – 157 **0**	>157 **0**
Kobber (mg/kg) Cu	<20 **8**	20-84 **0**	84 **0**	84-114 **0**	>114 **0**
Krom (mg/kg) Cr	<60 **8**	60 – 660 **0**	660 – 6000 **0**	6000 – 15500 **0**	>15500 **0**
Kvikksølv (mg/kg) Hg	<0,050 **8**	0,05 – 0,52 **0**	0,52 – 0,75 **0**	0,75 – 1,45 **0**	>1,45 **0**
Nikkel (mg/kg) Ni	<30 **7**	30 – 42 1	42 – 271 0	271 – 533 0	>533 **0**
Sink (mg/kg) Zn	<90 **5**	90 – 139 **3**	139 – 750 **0**	750 – 6690 **0**	>6690 **0**

5.2.3 Mikroplast

Mikroplast (<1 millimeter) er analysert på i alt 20 sedimentprøver (Knutsen m. fl., 2019; Vedlegg 6). Rapporten viser noen forskjeller i analysemetodikk og prøveuttak i forhold til tidligere metodikk beskrevet i Jensen og Cramer (2017). Metodene brukt i de to prosjektene er oppsummert i Tabell 6. Resultatene fra mikroplastanalysene er presentert i Figur 13, og viser at prøvene langs norskekysten har høyest antall plastpartikler/kg sediment tørrvekt. De tre prøvene lengst mot sør i Norskehavet har inntil 300 plastpartikler/kg sediment, mens det er noen færre i prøvene lengre mot nord i Varangerfjorden. Resultatene fra Kongsfjorden og Rijpfjorden viser at det er registrert litt høyere antall partikler i indre Rijpfjorden enn i indre Kongsfjorden. Antall mikroplastpartikler i Bjørnøytransektet nordvest for Bjørnøya (Figur 13) viser større variasjon. Dette kan skyldes variasjoner i avsetningsmiljøet i Bjørnøytransektet. Resultatene fra kjemianalysene i Bjørnøytransektet, inkludert kornstørrelsesanalyser, vil foreligge i 2020.

Tabell 6. Oversikt over metoder brukt til opparbeiding av sedimentprøver til mikroplastanalyser.

Parameter	University of Ghent	NGI
Prøvetaker og sedimentlagtykkelse	8 multicorer og 2 boxcorer, 3 cm prøver	10 multicorer, 2 cm prøver
Mikroplastseperasjon, saltløsning	30 % H_2O_2, 24 timer Natriumiodid (1,6 gr/cm^3)	30 % H_2O_2 og 10 M NaOH $ZnCl_2$ solution (1,52 g/cm^3)
Filter	5 µm	45 µm

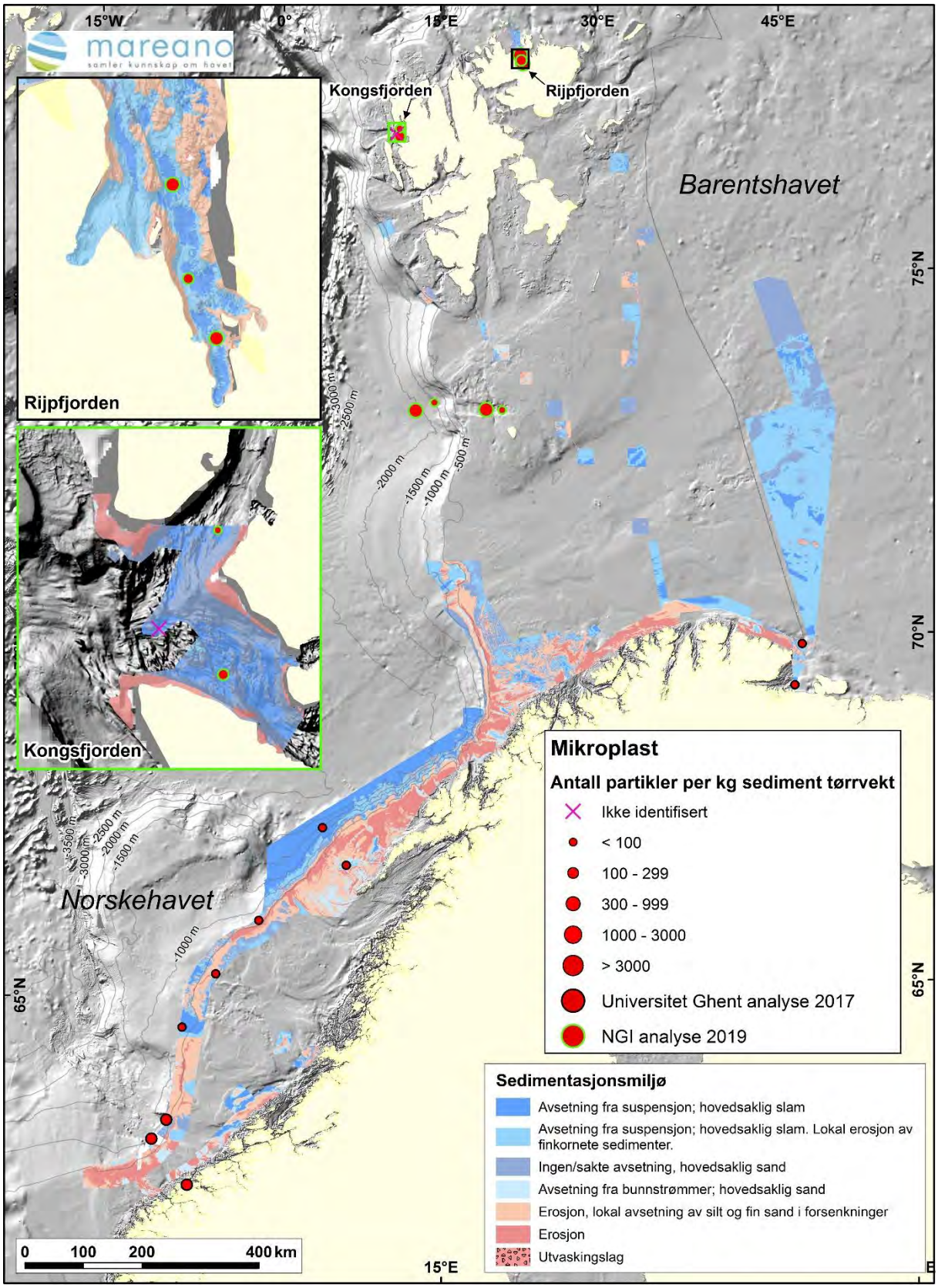

Figur 13. Mikroplast i sedimentprøver.

5.3 Analyser av sedimentkjerner

5.3.1 Visuell bedømmelse og XRI-analyser

Sedimentkjernene blir beskrevet om bord før de blir delt opp i 1 cm tykke skiver. På de fleste stasjonene er det også tatt hele sedimentkjerner som tas med til laboratoriet, hvor de blir analysert med røntgen (XRI). Dette gjøres for å få en kvalitativ vurdering for valg av stasjoner for dateringsanalyse, og geokjemisk analyse av hele sedimentkjerner. XRI-bildene kan gi informasjon om det er lagdelte sedimenter, eller om det f.eks. er homogene og bioturberte sedimenter. XRI-bildene er presentert i Vedlegg 4. Eksempler fra de forskjellige områdene er presentert, med vekt på sedimentkjerner fra de tre stasjonene der det er gjennomført dateringsanalyser (kapittel 5.4). Dette gjelder stasjonene R1823 (SK02), R1869 fra indre Kongsfjorden og R1887fra indre Rijpfjorden. XRI-utstyret er et Geotek-instrument med tilhørende programvare, som med røntgenstråler gjør det mulig å se gjennom sedimentkjernene og på den måten få et inntrykk av om det finnes sedimentære strukturer, bioturbasjon, skallfragmenter eller større sedimentære partikler som grus. Figurene 14 – 16 viser sedimentkjernene fra R1823, R1869 og R1887. R1823 (SK02) i Figur 14 viser en 33 cm lang sedimentkjerne med tydelige tegn på bioturbasjon, spesielt i den øverste delen. Sedimentkjernen fra indre Kongsfjorden (R1869MC016) i Figur 15 viser også tydelig av bioturbasjon i deler av sedimentkjernen. Gruspartikler forekommer spredd i sedimentkjernene, sannsynligvis avsatt som droppstein fra flytende isfjell.

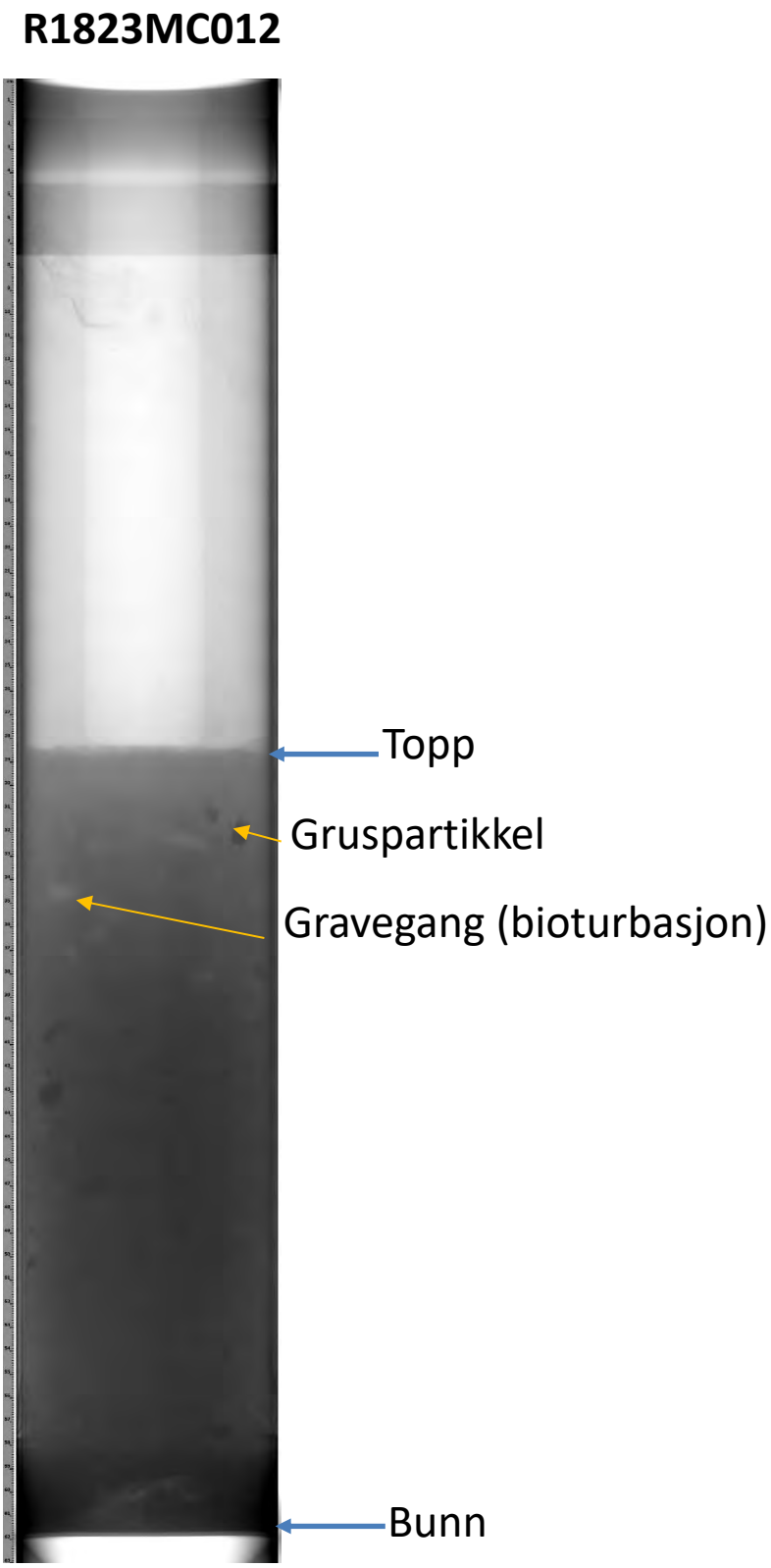

Figur 14. XRI-bilder av sedimentkjerne R1823MC012 fra SK02. Sedimentkjernen er 33 cm lang (målestokk med 1 cm enhet til venstre).

R1869MC016

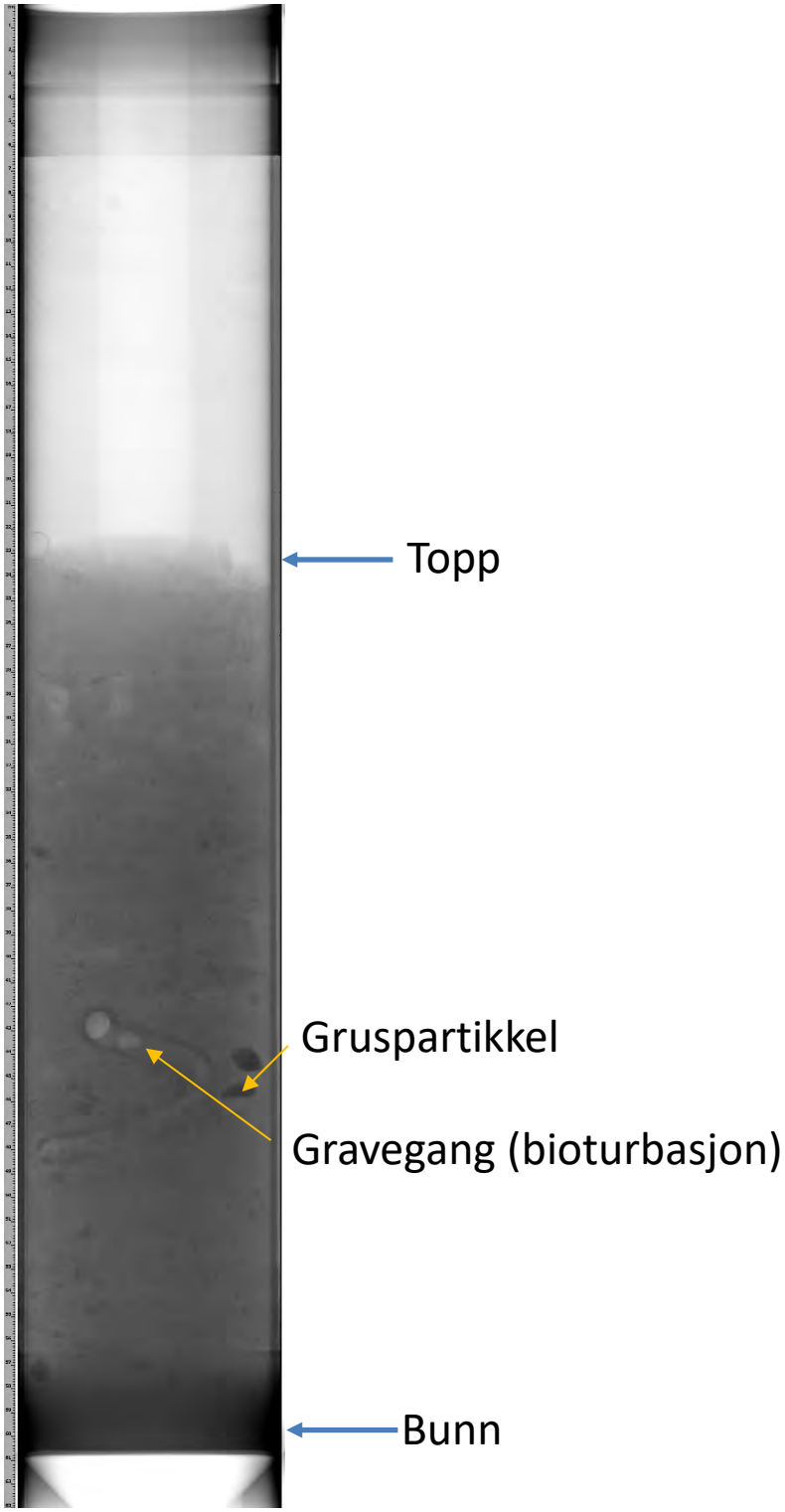

Figur 15. XRI-bilde av sedimentkjerne R1869MC016 fra indre Kongsfjorden. Bioturbasjon er tydelig i nedre delen av sedimentkjernen. Sedimentkjernen er 38 cm lang (målestokk med 1 cm enhet til venstre).

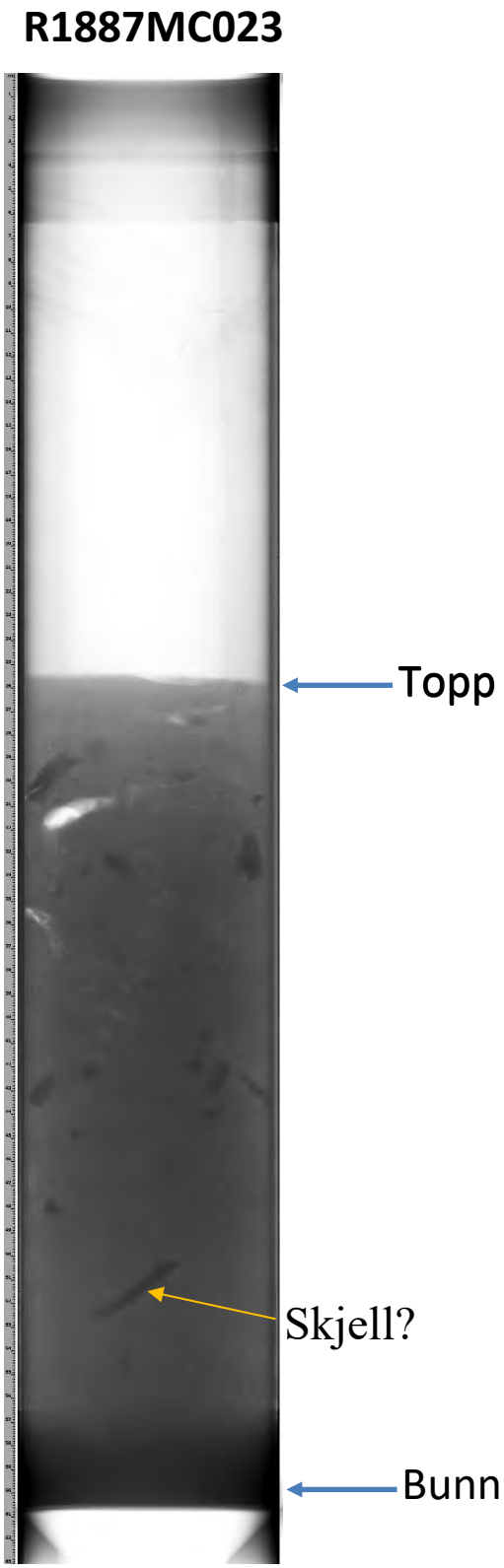

Figur 16. XRI-bilde av sedimentkjerne R1887MC023, indre Rijpfjorden. Sedimentkjernen er 35 cm lang (målestokk med 1 cm enhet til venstre).

5.3.2 Kornstørrelsesfordeling i sedimentkjerner

De tre sedimentkjernene R1823, R1869 og R1887 viser lite forskjell i kornfordeling (leir, silt, sand) (Figur 17). Andelen av finstoff (fraksjonene <2 µm + 2-63 µm) er større enn 90 % i stort sett alle prøver i de tre analyserte sedimentkjernene. Den konstante andel finstoff i de tre sedimentkjernene tyder på konstante sedimentasjonsforhold på de tre lokalitetene i henholdsvis SK02, indre Kongsfjorden og indre Rijpfjorden. Silt (2 – 63 µm) utgjør den største andel av sedimentene med generelt mer enn 80 % i alle tre sedimentkjernene, og leir med en andel på 10 – 16 %. Leir utgjør en litt større andel i R1887 (indre Rijpfjorden) sammenlignet med sedimentkjernene fra SK02 (R1823) og indre Kongsfjorden (R1869) (Figur 17). Andelen sand i R1823 minker gradvis fra 16 % nederst til ca. 5 % øverst. Samtidig øker andel leir og silt tilsvarende.

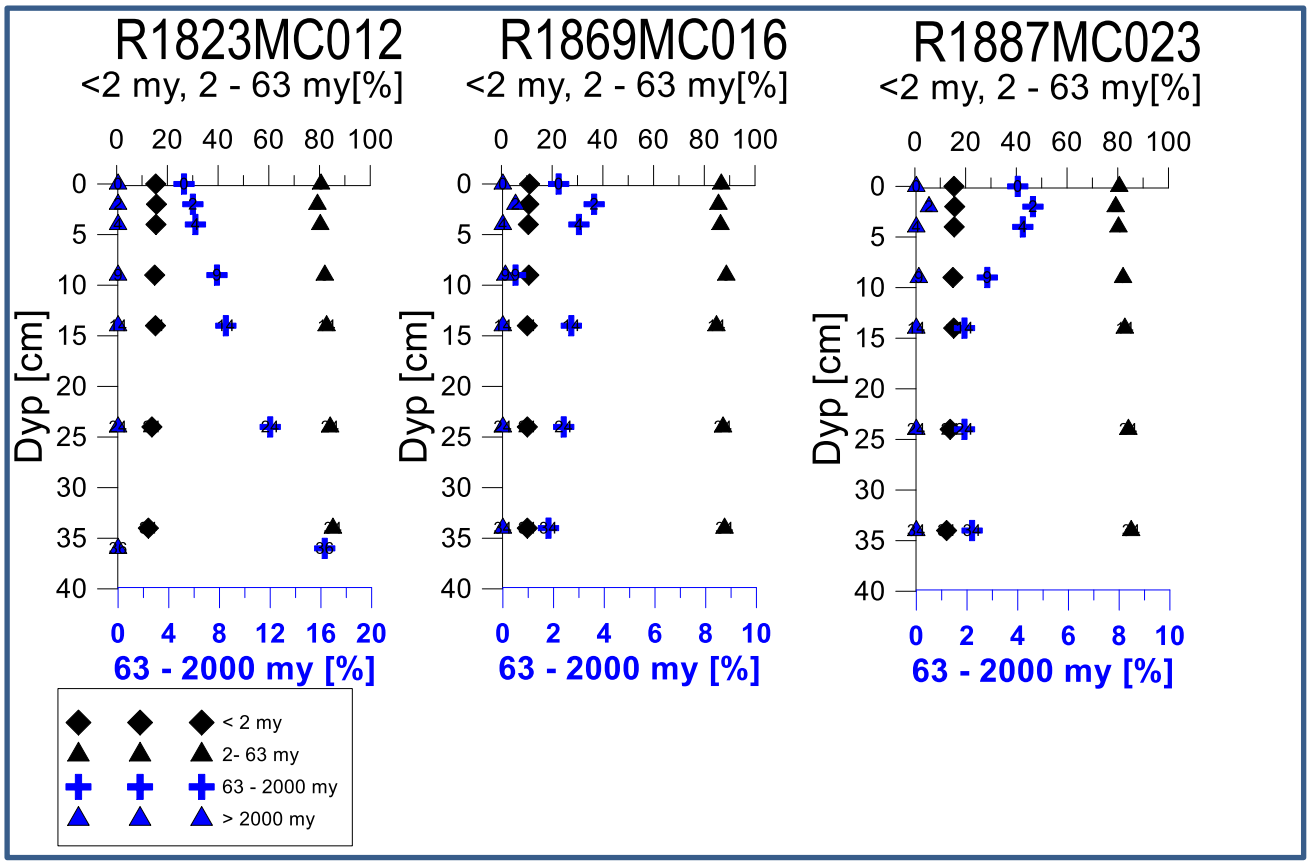

Figur 17. Kornfordelingskurver for R1823 (SK02), R1869 (indre Kongsfjorden) og R1887 (indre Rijpfjorden) (fraksjonene <2 µm, 2-63 µm, 63-2000 µm og >2000 µm). Dybdeskalaen er i cm. Merk at det er valgt skalaer på 20 % for R1823, og 10 % for R1869 og R1887 for andel sand (blå skala langs X-aksen nederst).

5.3.3 Total organisk karbon, karbonat og svovel

Innholdet av total organisk karbon (TOC), total svovel (TS) og karbonat ($CaCO_3$) varierer i de 3 sedimentkjernene R1823, R1869 og R1887. R1823 (SK02) har høyest TOC varierende fra 1.45 nederst (36 – 37 cm) økende til 2.0 vektprosent i toppen av sedimentkjernen. R1869 fra indre Kongsfjorden har TOC varierende fra 1.42 til 1.79 vektprosent, og dermed relativ konstant innhald fra topp til bunn (34 – 35 cm). R1887 fra indre Rijpfjorden har TOC fra 1.00 i toppen til 1.77 vektprosent i den nederste prøven. Denne prøven, i intervallet 34 – 35 cm, har betydelig høyere TOC sammenlignet med prøvene nevnt over (Figur 18). Sedimentkjernen fra indre Rijpfjorden har mindre andel TOC i toppen enn sedimentkjernene fra SK02 og indre Kongsfjorden (Figur 18). Muligvis spiller den høyere sedimentasjonsraten i R1887 en rolle med en uttynningseffekt på sedimentasjonen av organisk material (se kapittel 5.3.4 for dateringsresultatene).

Karbonatinnhold i sedimentkjernene viser markante forskjeller. R1869 fra indre Kongsfjorden har 2-3 ganger meir karbonat (12.0-14.4 vektprosent) enn R1823 (SK02) (3.2-5.5 vektprosent) og R1887 (indre Rijpfjorden) (4.2-5.0 vektprosent). Mikroskopi av prøvene viser at mange foraminiferer i R1869 sannsynligvis er årsaken til det høye karbonatinnholdet. Lavere innhald av karbonat i de øvrige sedimentkjernene kan skyldes enten manglende tilstedeværelse av organismer med kalkskall, eller oppløsning av skjellene som følge av stor akkumulasjon av organisk karbon, noe som forekommer i store deler av Barentshavet (Steinsund m. fl., 1996). Høyere innhold av karbonat i indre Kongsfjorden i sedimentkjerne R1869 og SK02 indikerer at varmere atlantiske vannmasser kan spille en større rolle her enn i indre Rijpfjorden og i SK02. Det kan muligvis forklares med at det utenfor Kongsfjorden er lokal upwelling av næringsrikt atlantisk vann (Winkelmann og Knies, 2005), som fører til høyere marin organisk produksjon i dette området og da også påvirker Kongsfjorden innenfor terskelen (indre Kongsfjorden) i forhold til marin produksjon.

Total svovel (TS) i de tre sedimentkjernene er vist i Figur 18. R1823 (SK02) har TS økende fra 0.18 vektprosent dypest (34-35 cm) til 0.23 vektprosent øverst (0-1 cm). Denne økningen kan ha sammenheng med en tilsvarende økning i TOC fra bunn til topp i sedimentkjernen. I R1869 fra indre Kongsfjorden minker TS-innholdet fra nederst (34-35 cm og 24-25 cm) fra ca. 0,5 vektprosent til drøye 0,2 vektprosent i prøvene fra 14-15 cm til 0-1 cm. R1887 fra indre Rijpfjorden har høy TS innhold nederst (34-35 cm) på 0.68 vektprosent, og minker til ca. 0,2 vektprosent mellom 24-25 cm og 0-1 cm.

Den høye TS andel nederst i R1869 og R1887 indikerer at det kan ha vært anoksiske forhold i de dypere delene av de to sedimentkjernene fra Kongsfjorden og Rijpfjorden. Beskrivelsen av sedimentene i dekksloggene fra R1869 og R1887 viser mørke sedimenter med svarte flekker i intervallet 10 – 35 cm. De svarte flekkene kan være jernsulfider.

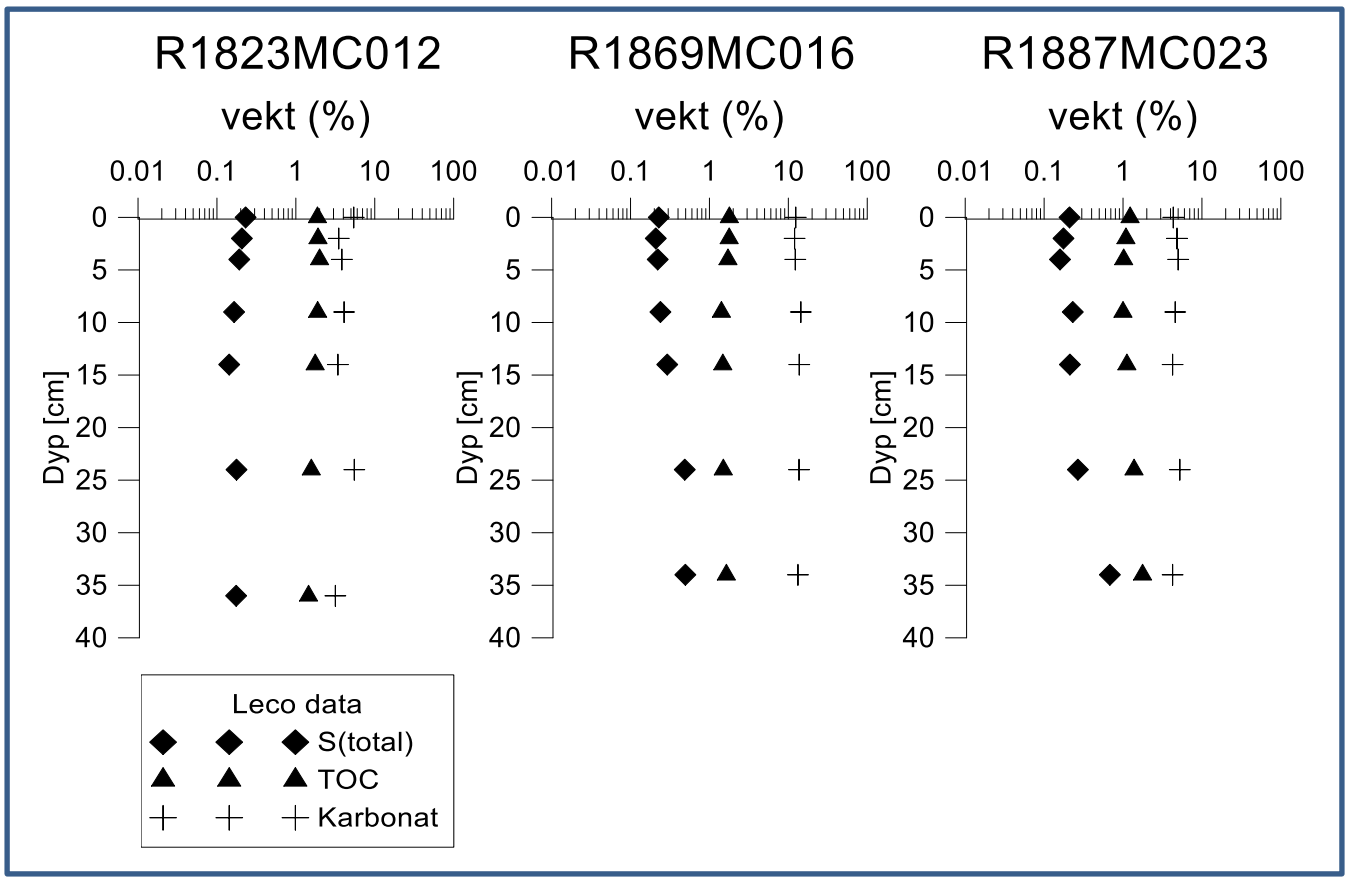

Figur 18. Variasjon i TOC, karbonat ($CaCO_3$) og svovel (TS) i sedimentkjerner fra stasjonene R1823, R1869 og R1887. Dybdeskalaen til venstre er i centimeter. Vektprosentskala for de 3 sedimentkjernene er logaritmisk.

5.3.4 Blyisotop 210 (^{210}Pb) -datering, ^{137}Cs-målinger og akkumulasjonsrater

Bestemmelse av akkumulasjonsrater i sedimentkjernene er viktig for å vurdere om det skjer en tilførsel av sedimenter, og hvorvidt denne tilførselen er stabil eller preget av perioder med manglende avsetning eller erosjon. Daterte sedimentkjerner gir også informasjon om mengden tilførsel av forurensende stoffer i moderne tid. Alderen på de øverste sedimentlagene og akkumulasjonsrater kan bestemmes ved måling av ^{210}Pb-aktiviteten i sedimentene. Isotopen ^{210}Pb har en halveringstid på 22,3 år. Bakgrunnsverdien for ^{210}Pb bestemmes ut fra mengden av bakgrunnsstråling ^{210}Pb ("supported" ^{210}Pb), som er uavhengig av sedimentasjon. Bestemmelsen av ^{210}Pb-bakgrunnsstråling skjer fra de dypere sjiktene i sedimentet, hvor konsentrasjonen er konstant fordi all ^{210}Pb ("unsupported" ^{210}Pb) fra atmosfærisk nedfall er nedbrutt. I tillegg til ^{210}Pb-datering, ble cesiumisotoper (^{137}Cs) målt i alle kjernene for å identifisere begynnelsen av atomprøvesprengninger i 1950- og 1960 årene. I moderne tid er disse sprengningene den største kilden til radioaktiv forurensning av miljøet og det største utslaget er i 1963. Økte konsentrasjoner av ^{137}Cs i marine sedimenter kan ikke bare indikere begynnelsen av atomprøvesprengninger, men også radioaktive ulykker i Tsjernobyl (Ukraina) i 1986, og Fukushima (Japan) i 2011.

Datering og bestemmelse av akkumulasjonsrater ble gjennomført på 3 sedimentkjerner R1823 (SK02), R1869 (indre Kongsfjorden) og R1887 (indre Rijpfjorden). Analysene ble gjennomført på Gamma Dating Center (GDC), Universitet i København. ^{210}Pb- og ^{137}Cs-analyserapporten inkludert analytiske metoder, og usikkerheter er presentert i Vedlegg 4 inkludert data og GDC sin tolkning av data for hver av de 3 analyserte sedimentkjernene.

Sedimentakkumulasjonsrater i denne rapporten baseres hovedsakelig på ^{210}Pb- og ^{137}Cs-analyseresultater. En enkel prøve er datert med AMS^{14}C radiokarbondatering på foraminiferskjell (R1869, 24-25 cm, indre Kongsfjorden) (Tabell 7). ^{14}C-alderen for denne prøven er 1287 AD ±18 år.

Kjerne R1823MC012A, SK02

R1823 har høy ^{210}Pb-aktivitet (Figur 19) med en svak tendens til eksponentielt lavere verdier med dybden, noe som indikerer sedimentmiksing og bioturbasjon. Eksponentielt lavere verdier observeres først under 5 cm kjernedyp. Alder versus dyp i Figur 20 er tolket ned til 21,5 cm tilsvarende 1885 (Figur 20). Basert på alder og dyp i sedimentene er den gjennomsnittlige sedimentasjonsraten på ca. 1,7 millimeter pr. år. ^{137}Cs-toppen ved 6–7 cm (Figur 19) tilsvarer 1987. Bioturbasjon bidrar til blanding av sedimentene. Det er derfor sannsynlig at denne ^{137}Cs-toppen har bidrag fra Tsjernobylutslippet i 1986. Den totale vurderingen av ^{137}Cs/^{210}Pb-baserte sedimentasjonsmodeller på dypere lag i denne kjernen må derfor ses som foreløpig, med mulige justeringer i dypere sjikt i sedimentene.

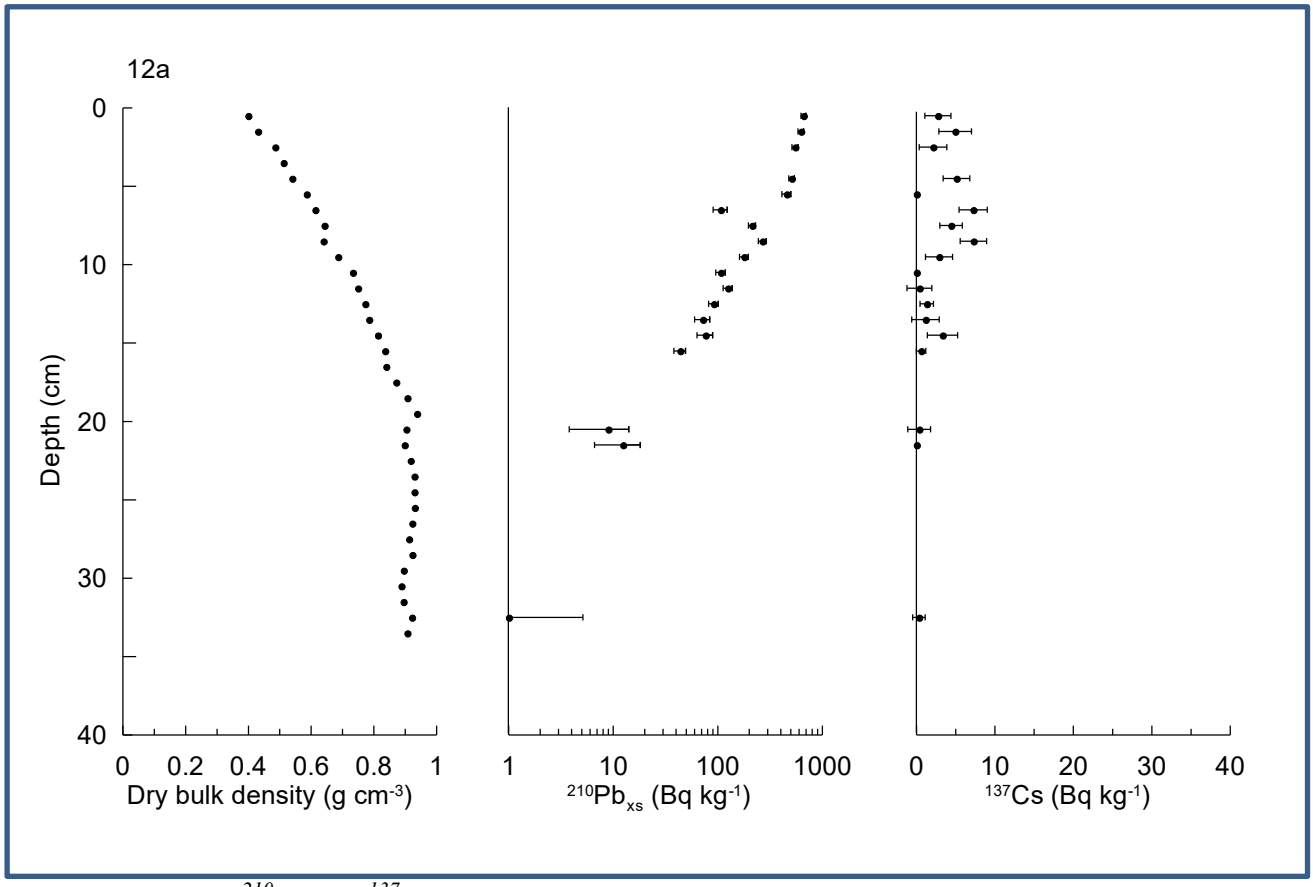

Figur 19. Tetthet, ^{210}Pb- og ^{137}Cs-aktivitetsmålinger i R1823MC012A, SK02.

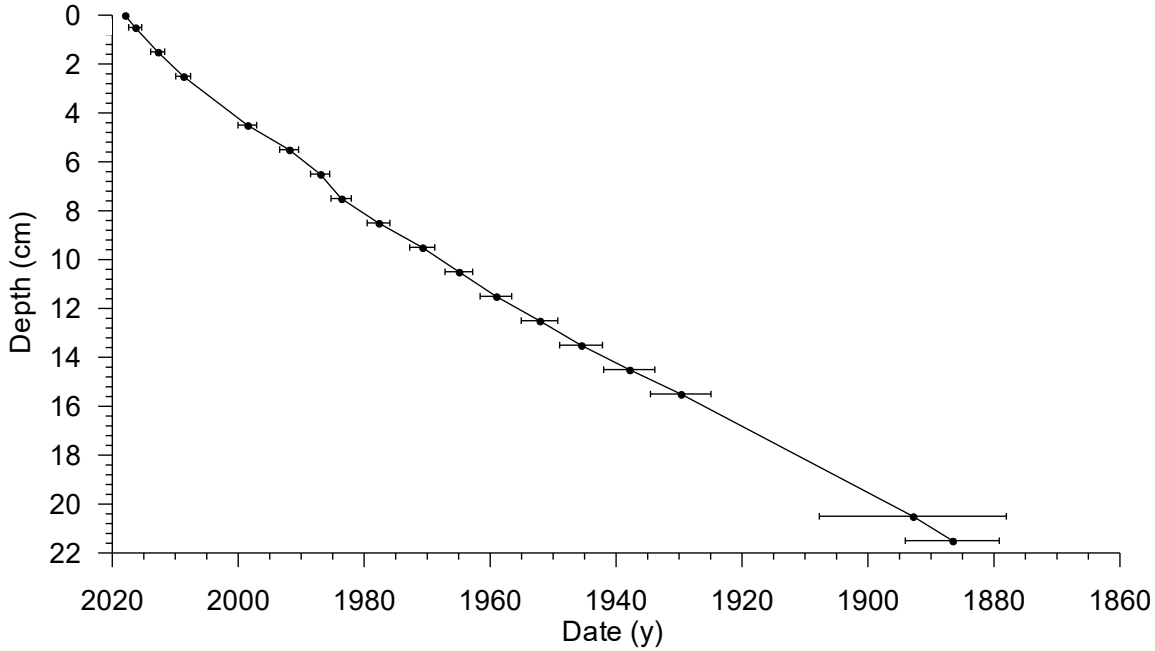

Figur 20. Alder versus dyp i sedimentene i R1823MC012A, SK02.

Kjerne R1869MC016A, indre Kongsfjorden

R1869 fra indre Kongsfjorden har middels høy ^{210}Pb-aktivitet (Figur 21) med en svak tendens til eksponentielt lavere verdier i de øverste 19 cm. Eksponentielt lavere verdier observeres først under 5 cm kjernedyp (Figur 21). Alder versus dyp i Figur 22 er tolket ned til 18-19 cm tilsvarende 1887 (Vedlegg 4). Basert på alder og dyp i sedimentene er den gjennomsnittlige sedimentasjonsraten ca. 1,5 millimeter pr. år. ^{210}Pb-kronologien er underbygget av ^{137}Cs-innholdet, som indikererer at sedimentene mellom 0 og 11 cm er avsatt siden ca. 1963. AMS ^{14}C-dateringen på foraminiferer i den nedre delen av kjernen (24-25 cm) viser en alder på 692 år BP (1950). Denne alderen strider imot konklusjonen basert på ^{210}Pb- og ^{137}Cs-kronologien, og skyldes muligvis resedimentasjon. Alternativt viser de to andre dateringsmetodene for høye sedimentasjonsrater. ^{14}C-dateringsanalyseresultatet er oppsummert i Tabell 7. Sedimentasjonsraten basert på ^{14}C er 0,35 mm/år, som er ca. en fjerdedel sammenlignet med sedimentasjonsraten basert på ^{210}Pb-analysene.

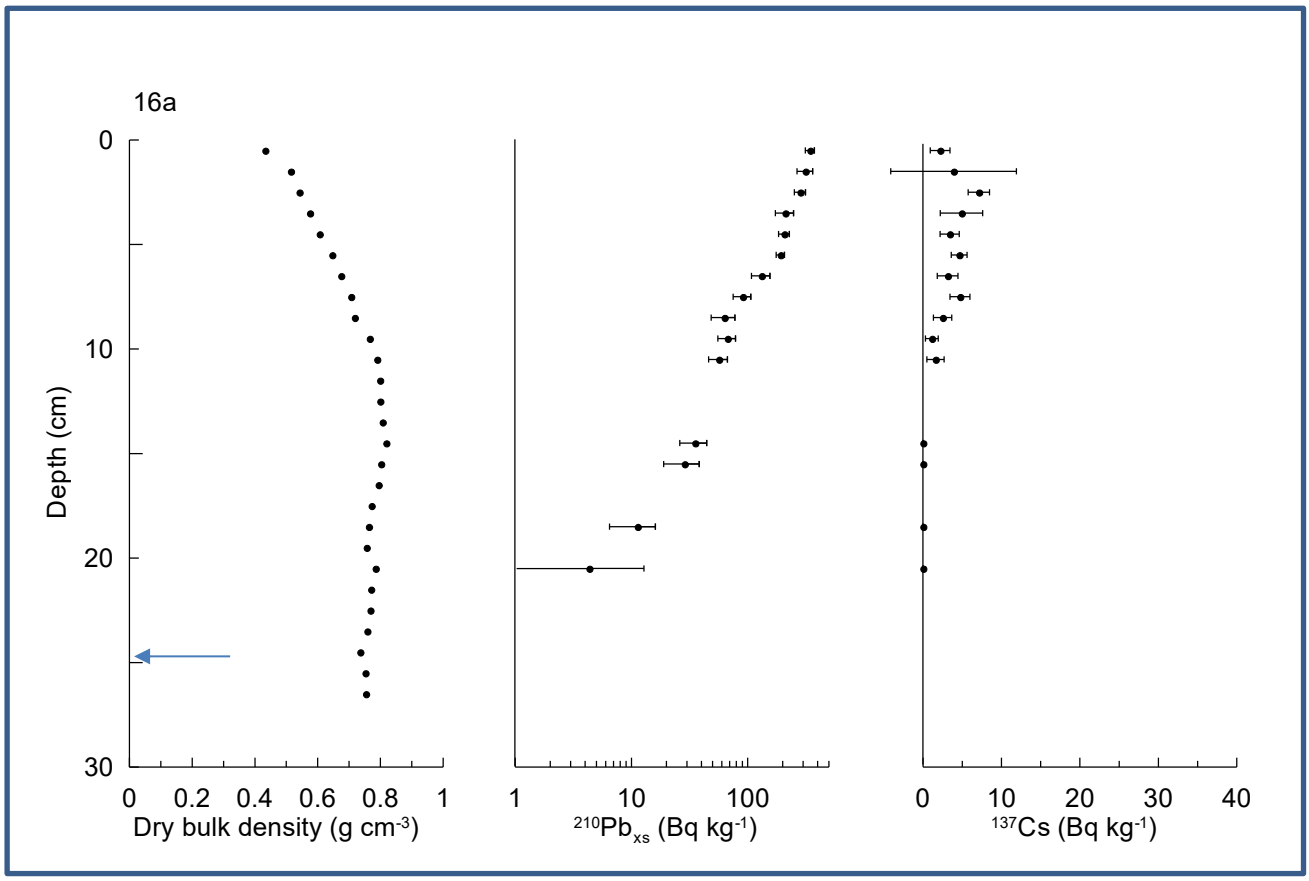

Figur 21. Tetthet, ^{210}Pb- og ^{137}Cs-aktivitetsmålinger i R1869MC016. Blå pil i plottet til venstre indikerer prøvenivået for AMS^{14}C radiokarbondatering, gjennomført på foraminiferer (Tabell 7).

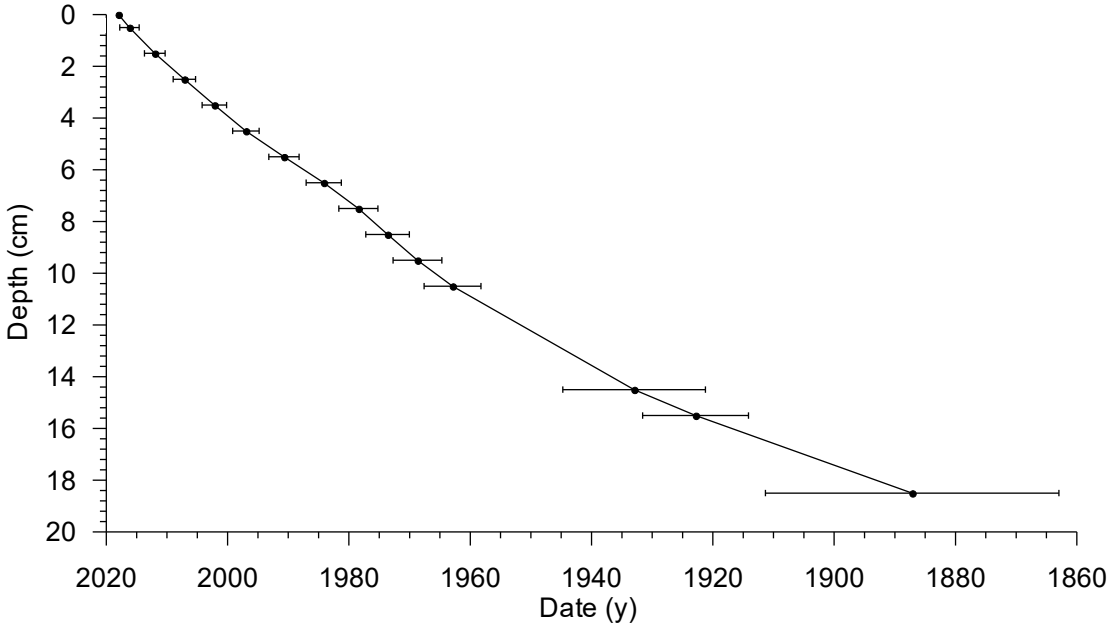

Figur 22. Alder versus dyp i sedimentene i R1869MC016, indre Kongsfjorden.

Tabell 7. AMS ^{14}C-datering i kjerne R1869MC016, indre Kongsfjorden.

Lab kode	Kjerne	Dyp (cm)	^{14}C alder	Avvik År	Materiale	2s max alder (AD)	2s min alder (AD)	Median (år AD)
UBA-41563	R1869 MC016A	24-25 cm	692	±18	Foramini-ferer.	1300	1273	1287

Kjerne R1887MC022, indre Rijpfjorden

R1887MC022 har ^{210}Pb- og ^{137}Cs-aktivitet på omtrent samme nivå som R1869MC016. ^{210}Pb- og ^{137}Cs-aktivitetskurvene er vist i Figur 23. ^{210}Pb-aktivitet er målbar ned til 23 cm under overflaten. ^{137}Cs-nivået er generelt litt høyere enn i R1823 og R1869 men fremdeles til stede med lav aktivitet i de fleste prøver. (Figur 23). Prøven 12-13 cm med desidert høyest ^{137}Cs-aktivitet representerer 1963. Nedgang i ^{210}Pb-aktivitet er eksponentiell og alder versus dyp er pålitelig ned til 23 cm. Beregnet gjennomsnittlig sedimentasjonsrate over de øverste 23 cm er 2,0 mm/år. Alder versus dyp er vist i Figur 24, som viser at det er mulig å datere sedimentene tilbake til ca. 1907.

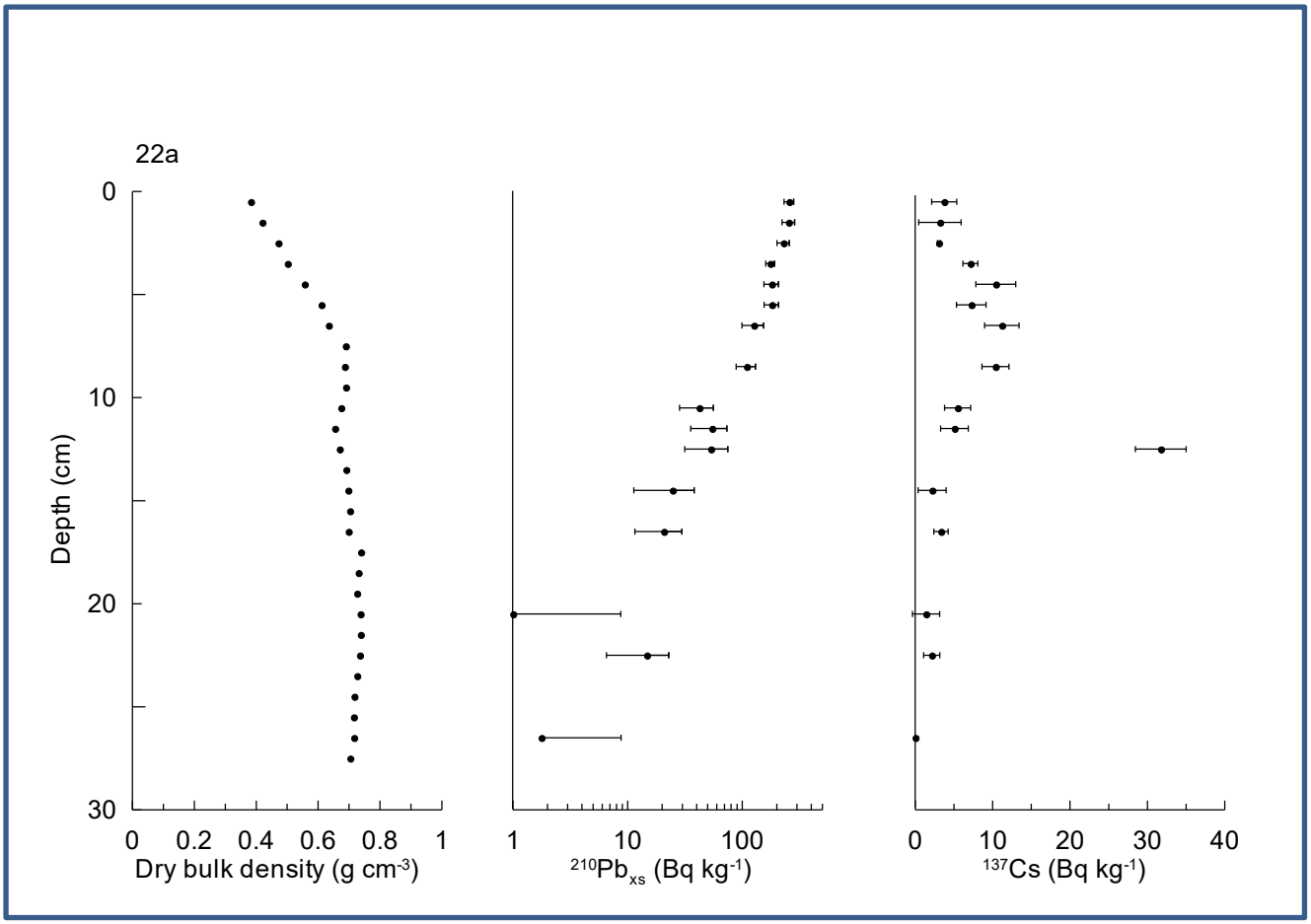

Figur 23. Tetthet, ^{210}Pb- og ^{137}Cs-aktivitetsmålinger i R1887MC022, indre Rijpfjorden.

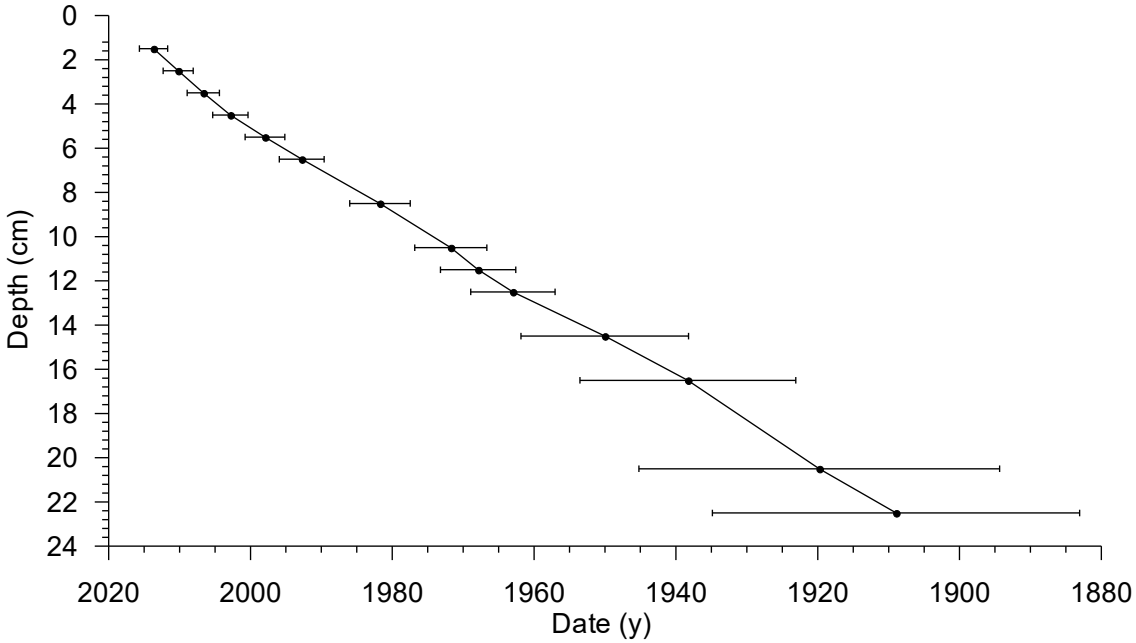

Figur 24. Alder versus dyp i sedimentene i R1887MC023.

Sedimentasjonsrater og vurdering av dateringenes kvalitet basert på ^{210}Pb- og ^{137}Cs-dateringsanalysene er oppsummert i Tabell 8.

Tabell 8. Daterte sedimentkjerner fra MAREANO-tokt 2017115 og 2018109. LSR: Lineær sedimentasjonsrate for intervaller karakterisert som pålitelig basert på ^{210}Pb-aktivitetskurver. Dateringskvalitet karakteriseres av aldersmodeller som viser en tydelig eksponsensiell nedgang av ^{210}Pb-aktivitet og langsom utflating av ^{137}Cs-konsentrasjon.

Stasjon	Område	LSR (mm/år)	Dateringens kvalitet
R1823MC012	SK02	1,7	God
R1869MC016	indre Kongsfjorden	1,5	God
R1887M0C23	indre Rijpfjorden	2,0	God

5.4 Tungmetaller, arsen og barium i tre ^{210}Pb-daterte sedimentkjerner

For å vurdere dagens forurensningstilstand sammenlignet med tidligere tider er de tre ^{210}Pb-daterte sedimentkjernene analysert for innhold av tungmetaller, arsen og barium. Analyseresultatene finnes i Vedlegg 1.

R1823MC012, SK02

R1823MC010 er lokalisert i SK02 (Figur 1). Minimum, gjennomsnitt, median og maksimum konsentrasjoner for en rekke tungmetaller, arsen og barium er vist i Tabell 9. Cr, Cu, Ni, Zn og Ba har stabilt lave konsentrasjoner (Figur 25) og anses for å være på naturlig bakgrunnsnivå i sedimentkjernen. Årstallene til høyre i Figur 25 er basert på resultatene av dateringsanalysene og da primært Pb-dataene (avsnitt 5.3). Hg øker fra et nivå på 0,035 mg/kg sediment nederst (36 – 37 cm) til maksimalt 0,052 mg/kg sediment ved 4 – 5 cm og avtar så til 0,044 mg/kg sediment øverst (0 – 1 cm). Pb øker fra et bakgrunnsnivå på 15 og 18 mg/kg sediment ved de to nederste prøvene, til et maksimalt nivå på 34 mg/kg sediment ved 9 – 10 cm og holder seg på et litt lavere nivå i de øverste 3 prøvene. Dette er i tråd med at det er antropogen tilførsel av Pb i den øvre delen av kjernen og deretter en gradvis reduksjon sannsynligvis relatert til forbudet mot blyholdig bensin gjeldende fra 1970-tallet i en rekke industriland. As øker fra et bakgrunnsnivå på 10 mg/kg sediment eller lavere i intervallet 9 – 35 cm til et markant høyere nivå i de øverste 3 prøvene, med maksimum på 58 mg/kg sediment ved 2 – 3 cm og 40 mg/kg sediment øverst, tilsvarende tilstandsklasse III, moderat forurensningsnivå (se avsnitt 5.5 for nærmere diskusjon). Cd har lave konsentrasjoner på maksimalt 0,19 mg/kg sediment dypt i sedimentkjernen, og et gjennomsnitt på 0,12 mg/sediment. Analyseresultatene viser at Hg og Pb øker svakt fra rundt år 1900, fra lave bakgrunnsnivåer på henholdsvis 0,035 mg/kg og 15 mg/kg (Figur 25).

Tabell 9. Sedimentkjerne R1823MC012 (0-37 cm): minimums-, gjennomsnitts-, median- og maksimumsverdier for tungmetaller, arsen og barium (mg/kg).

Antall prøver		As mg/kg	Ba mg/kg	Cd mg/kg	Cr mg/kg	Cu mg/kg	Hg mg/kg	Ni mg/kg	Pb mg/kg	Zn mg/kg
N = 7	Min.	8,7	140,0	0,05	28,0	13,0	0,033	27,0	15,0	58,0
	Gns.	25,4	148,5	0,12	31,7	15,0	0,043	29,7	26,4	66,7
	Med.	10,0	140,0	0,14	30,0	15,0	0,044	28,0	30,0	66,5
	Max.	58,0	190,0	0,19	35,0	17.0	0,052	35,0	34,0	80,0

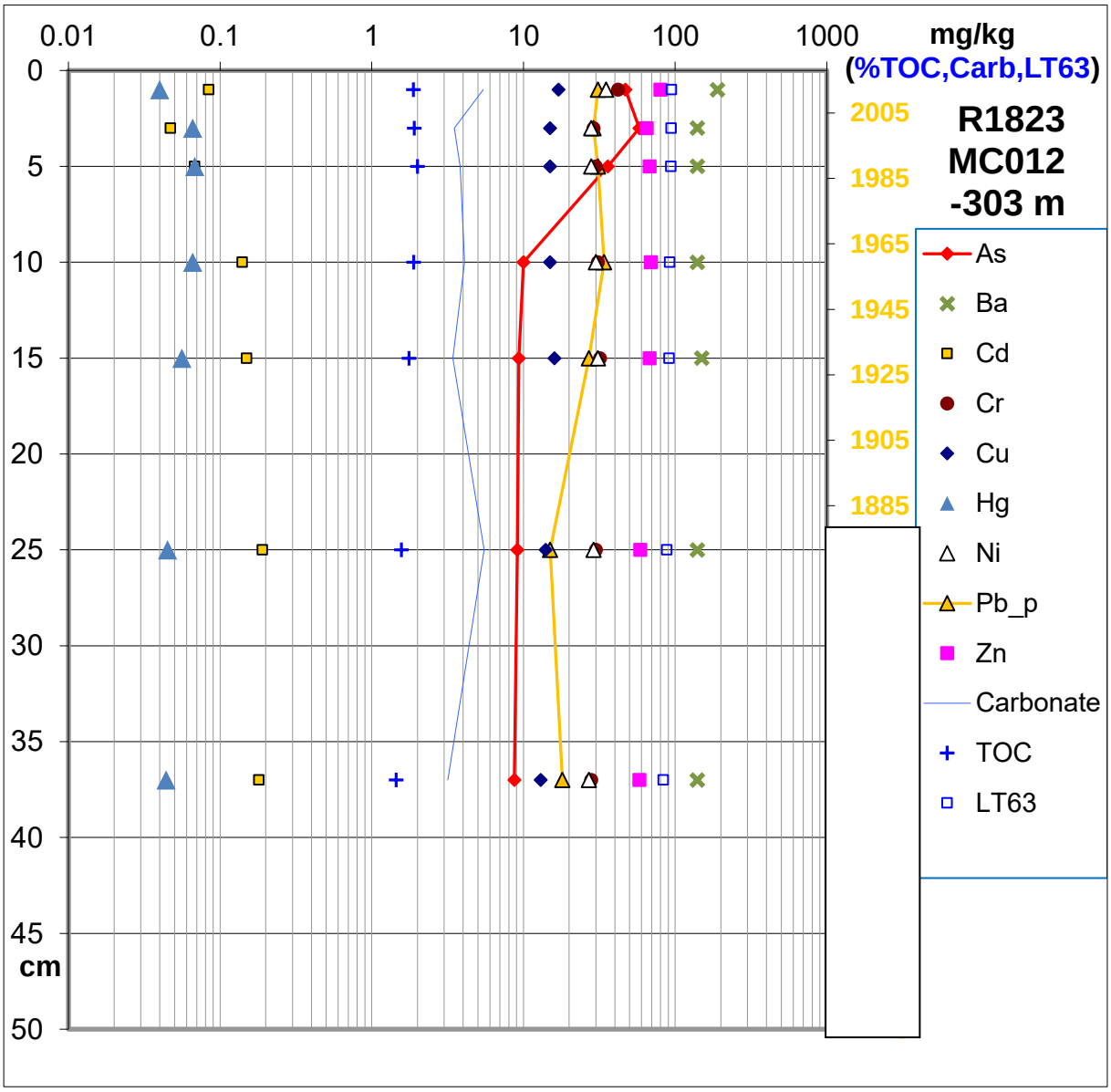

Figur 25. Tungmetall, arsen, barium, TOC, karbonat og finstoff i sedimentkjerne R1823MC012 (0-35 cm). X-skalaen (konsentrasjoner) er logaritmisk. Årstallene til høyre er basert på ^{210}Pb-dateringsanalysene presentert i avsnitt 5.3.4.

R1869MC016, indre Kongsfjorden

R1869MC016 er lokalisert i indre Kongsfjorden (Figur 1). Sedimentkjernen er analysert i intervallet 0-35 cm med 7 prøver fra dette intervallet. Minimum, gjennomsnitt, median og maksimum konsentrasjoner for en rekke tungmetaller, arsen og barium er vist i Tabell 10. Ba, Cr, Cu, Ni og Zn har relativt stabile konsentrasjoner gjennom hele kjernen med svakt økte konsentrasjoner mot toppen (Figur 26). Hg øker gradvis fra konsentrasjon på 0,027 mg/kg sediment ved 34 – 35 cm til maksimalt 0,046 mg/kg sediment ved 2 – 3 cm og reduseres så til 0,038 mg/kg sediment ved 0 – 1 cm. Pb øker gradvis fra et bakgrunnsnivå på 18 mg/kg i den nedre delen av kjernen til maksimalt 26 mg/kg sediment ved 1 – 2 cm (Figur 26). Det er ikke mulig å si mer presist i hvilket intervall i kjernen økningen finner sted. Cd har generelt lav konsentrasjon gjennom hele kjernen. Cd-konsentrasjonen minker fra 0,22 mg/kg sediment ved 24-25 cm til 0,11 mg/kg sediment øverst (0-1 cm). As har relativt stabil konsentrasjon med 10 – 15 mg/kg sediment i intervallet 2-3 cm til 34-35 cm og høyeste verdi ved 0-1 cm med 40 mg/kg sediment. Dette tilvarer klasse III forurensningsnivå i marine sedimenter. Figur 26 viser at Hg og Pb øker litt fra bakgrunnsnivåer i tidsrommet ca. 1885 – 1925 og så minker igjen etter 2005. As øker markant fra 2-3 cm til 0-1 cm, og endringen ser ut til å skje over kort tid (2005 – 2018). De høye As-verdiene tas opp i kapittel 5.5.

Tabell 10. Sedimentkjerne R1869MC016 (0-35 cm): minimums-, gjennomsnitts-, median- og maksimumsverdier for tungmetaller, arsen og barium (mg/kg).

Antall prøver		As mg/kg	Ba mg/kg	Cd mg/kg	Cr mg/kg	Cu mg/kg	Hg mg/kg	Ni mg/kg	Pb mg/kg	Zn mg/kg
N = 7	Min.	10,0	95,0	0,11	32,0	17,0	0,027	27,0	18,0	69,0
	Gns.	16,0	102,7	0,16	35,0	17,6	0,037	27,9	22,7	74,0
	Med.	12,0	100,0	0,15	34,0	17,0	0,038	28,0	24,0	72,0
	Max.	40,0	120,0	0,22	41,0	19,0	0,046	29,0	26,0	82,0

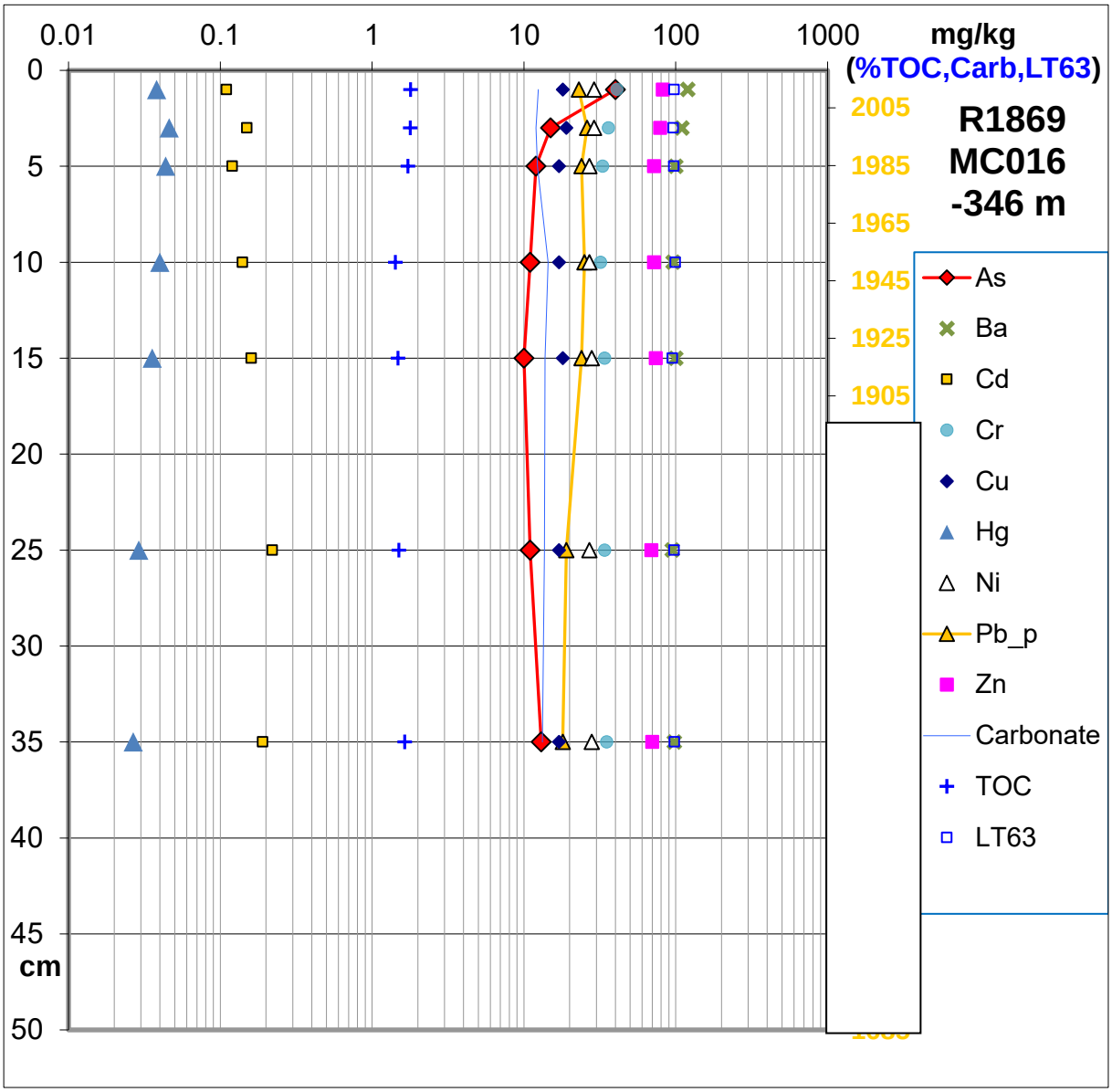

Figur 26. Tungmetall, arsen, barium, TOC, karbonat og finstoff i sedimentkjerne R1869MC016 i indre Kongsfjorden (0 - 35 cm). X-skalaen (konsentrasjon) er logaritmisk.

R1887MC023, indre Rijpfjorden

Stasjon R1887 i indre Rijpfjorden er dominert av slam (Figur 2). Den daterte sedimentkjernen R1887MC023 er analysert i intervallet 0 - 35 cm med 7 prøver. Minimum, gjennomsnitt, median og maksimum konsentrasjoner for en rekke tungmetaller, arsen og barium er vist i Tabell 11. Metallene Cr, Cu, Hg, Ni, Pb og Zn, samt Ba har relativt stabile konsentrasjoner gjennom sedimentkjernen (Figur 27), noe som også er reflektert i minimum-, gjennomsnitt-, median- og maksimumverdiene (Tabell 11). Den ^{210}Pb-baserte tidsskalaen til høyre i Figur 27 viser at Hg øker fra en bakgrunnskonsentrasjon på 0,027 mg/kg sediment nederst (34-35 cm) til 0,039 mg/kg sediment ved 14-15 cm, og en maksimal konsentrasjon i intervallet 5 – 10 cm, tilsvarende ca. 1970 til 1995, dvs. en økning på ca. 40 %. Hg minker litt øverst i kjernen fra en konsentrasjon på 0,043 mg/kg sediment vd 4-5 cm til 0,041 mg/kg sediment øverst. Om dette er en reell reduksjon er imidlertid usikkert med tanke på 20 % måleunøyaktighet (Tabell 2). Pb har relativt stabil konsentrasjon fra 24-25 cm til toppen med verdier varierende fra 22 til 25 mg/kg sediment. Cd har konsentrasjoner fra 0,12 mg til 0,35 mg/kg sediment, generelt avtakende fra bunn til topp i kjernen, og laveste verdi i prøven ved 2-3 cm. As har et bakgrunnsnivå på 12 til 18 mg/kg sediment i prøvene fra 34-35 cm til 14-15 cm. As-konsentrasjonn øker markant fra 9-10 cm til toppen av kjernen, med høyeste konsentrasjon ved 2-3 cm (61 mg/kg sediment). Konsentrasjonen reduseres til 32 mg/kg sediment øverst (0-1 cm). As-konsentrasjoner beskrives mer detaljert i kapittel 5.5.

Tabell 11. Sedimentkjerne R1887MC023 (0-35 cm): minimums-, gjennomsnitts-, median- og maksimumsverdier for tungmetaller, arsen og barium.

Antall prøver		As mg/kg	Ba mg/kg	Cd mg/kg	Cr mg/kg	Cu mg/kg	Hg mg/kg	Ni mg/kg	Pb mg/kg	Zn mg/kg
N = 7	Min.	12,0	82,0	0,12	19,0	17,0	0,027	21,0	21,0	74,0
	Gns.	31,4	98,3	0,27	24,6	18,3	0,037	24,6	23,1	83,7
	Med.	23,0	97,0	0,27	23,0	18,0	0,039	24,0	22,0	83,0
	Max.	61,0	110,0	0,35	34,0	20,0	0,045	29,0	26,0	92,0

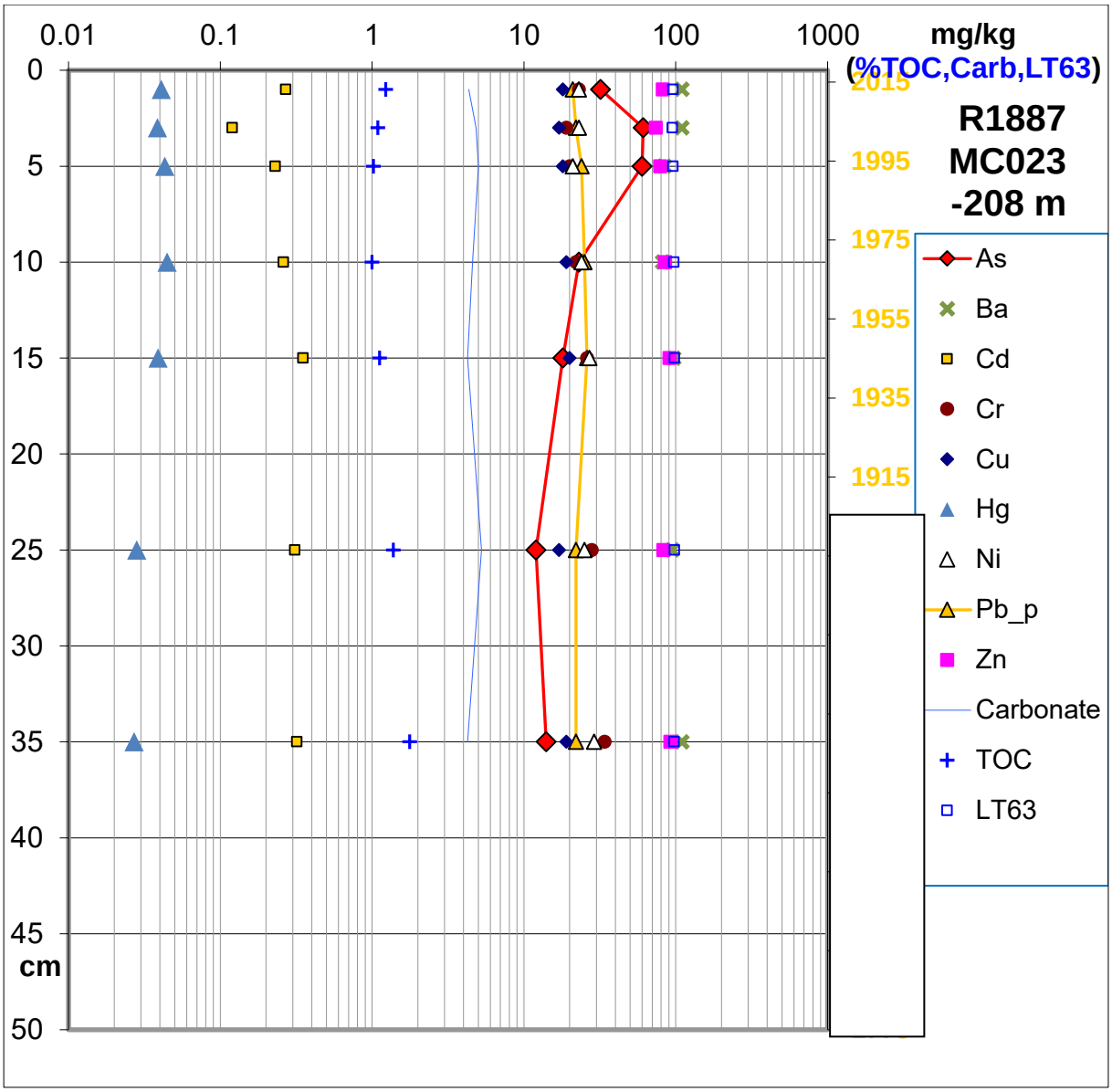

Figur 27. Tungmetall, arsen, barium, TOC, karbonat og finstoff i sedimentkjerne R1887MC023 (0 - 35 cm), indre Rijpfjorden. X-skalaen (konsentrasjon) er logaritmisk.

5.5 Arsenkonsentrasjoner i overflatesedimentene og variasjon over tid

Figur 9 viser en geografisk forskjell når hele det kartlagte MAREANO-området vurderes, med høyere arsenkonsentrasjoner i overflatesedimentene i sentrale og nordlige deler av Barentshavet og rundt Svalbard enn i sørlige Barenthavet, områdene rundt Lofoten og Vesterålen og i Norskehavet. Punktkilder er ikke en sannsynlig årsak til de høye konsentrasjonene. Flomsedimentdata fra Svalbard (Ottesen m. fl., 2010) indikerer at kilder på Svalbard kan være årsak til de høye konsentrasjonene i de marine sedimentene i Kongsfjorden, da det er relativt høye As-konsentrasjoner (inntil 57,4 mg/kg sediment) for en del prøver. Det er ikke mulig å si noe om Rijpfjorden og for SK01 da det ikke er analysert flomsedimenter på landområder her. Flomsedimenter på Svalbard nær SK02 har relativt lave As-verdier, med konsentrasjoner <14 mg/kg sediment. AMAP (1998) viser at As-nivåene i finkornige sedimenter i Barentshavet, Karahavet og i sedimenter nær den russiske kysten (Pechorahavet) er på samme nivå eller høyere enn de nivåene som er funnet i MAREANO-prøvene fra Barentshavet. Hvorvidt de høye As-nivåene skyldes forurensing er ikke fastslått (AMAP, 1998).

De 3 analyserte sedimentkjerner viser omtrent like variasjoner i As-konsentrasjon. Det er høye As-konsentrasjoner i de øverste 1-5 cm, tilsvarende tilstandsklasse III, moderat forurensning. Under dette toppsjiktet er As-konsentrasjonene markant lavere, tilsvarende tilstandsklasse I, bakgrunnsnivå (<15 mg/kg sediment). Sammenlikning mellom de tre nye sedimentkjernene og tidligere analyserte sedimentkjerner fra Norskehavet og andre områder, viser at bakgrunnsnivået er betydelig lavere i de sistnevnte områdene (Jensen m. fl. 2014; Jensen m. fl. 2016). De nye resultatene er sammenliknbare med sedimentkjerner i den nordlige og sentrale delen av Barentshavet (Jensen m. fl., 2018). Økning i As-konsentrasjon er opp til 3 – 5 ganger bakgrunnsnivået i de øverste cm i sedimentkjernene. De høye As-konsentrasjonene i topplagene sammenlignet med dypere lag kan muligens knyttes til prosesser i sedimentene, såkalte redoksprosesser, der reduserende forhold erstattes med oksiderende forhold i et grensesjikt noen centimeter under sedimentoverflaten. Det fører til mobilisering av arsen i dypere lag og utfelling i lag nær overflaten (Farmer and Lovell, 1986). Alternativt kan økningen forklares med økt tilførsel i nyere tid. Da må arsen sannsynligvis knyttes til utslipp fra menneskelige kilder. Følgende oppsummering kan gjøres:

1. Bakgrunnsnivået av As varierer i områdene kartlagt av MAREANO.
2. As-konsentrasjonen i de øverste 3-5 cm av sedimentkjerner øker 3-5 ganger i forhold til bakgrunnsnivået i områdene kartlagt av MAREANO. Økningen er inntil 5 ganger for de tre analyserte sedimentkjernene fra SK02, indre Kongsfjorden og indre Rijpfjorden.
3. Årsaken til den markante økningen øverst i sedimentkjernene, spesielt i Barentshavet, er ikke kjent. En mulig mekanisme kan være naturlige redoksprosesser øverst i havbunnen som binder As i topplagene, men menneskelig tilførsel kan ikke utelukkes.

6. OPPSUMMERING

Tungmetallkonsentrasjonene i overflatesedimentene i SK01, SK02, indre Kongsfjorden og indre Rijpfjorden er analysert. As er tilstede i relativt høye konsentrasjoner på alle 8 stasjoner tilsvarende tilstandsklasse III (moderat forurensning) i Miljødirektoratets klassifisering for kyst og fjordsedimenter. Cd, Cu, Ni, Pb og Zn er tilstede i tilstandsklasse II på enkelte stasjoner, og tilstandsklasse I (bakgrunn) på øvrige stasjoner. Cr, Hg og Zn har konsentrasjoner i tilstandsklasse I (bakgrunn) på samtlige 8 stasjoner.

De 3 analyserte sedimentkjernene fra SK02, indre Kongsfjorden og indre Rijpfjorden har noen felles trekk: Det er stabile konsentrasjoner av Cr, Cu, Ni, Zn og Ba i alle kjernene. Disse elementene vurderes å stamme utelukkende fra naturlige geologiske kilder. Hg og Pb følger like trender i de fleste analyserte sedimentkjernene. De dypeste prøvene har Hg- og Pb-konsentrasjoner på naturlig bakgrunnsnivå. Bakgrunnsnivået varierer, avhengig av innhold av finstoff og TOC, men er typisk 0,03 mg/kg sediment for Hg og ca. 10 mg/kg sediment for Pb. Hg øker fra ca. 0,03 mg/kg sediment (bakgrunnsnivå) til maksimale konsentrasjoner i størrelsesorden 0,04 – 0,05 mg/kg sediment litt under overflaten i sedimentkjernene. For Pb er økningen i de øverste delene av sedimentkjernene 50 – 100 % i forhold til bakgrunnsnivåene i de tre sedimentkjernene. Høyeste Pb-konsentrasjoner er for de fleste sedimentkjerner noen få cm under toppen. Pb-konsentrasjonen avtar litt øverst i sedimentkjernene.

^{210}Pb-dateringsanalysene viser at økningen i Hg og Pb skjer rundt 1900 i R1823 fra SK02, mens det er vanskeligere å si når økningen i R1869 (indre Kongsfjorden) og R1887 (indre Rijpfjorden) skjer. Økningen i Hg og Pb tilskrives menneskelig tilførsel fra primært fossil energibruk (Hg: kullforbrenning; Pb: blyholdig bensin). Tilførsel og avsetning i sedimentene har vært med havstrømmer og lufttransport. Nedgangen i Pb øverst i sedimentkjernene kan sannsynligvis knyttes til forbudet mot bruk av blyholdig bensin i flere industrialiserte land fra 1970-tallet. For Hg er det tendens til litt avtakende konsentrasjon i samtlige sedimentkjerner i de øverste få cm.

As øker inntil 5 ganger fra et bakgrunnsnivå på 10 mg/kg sediment til inntil 61 mg/kg sediment i de øverste 3-5 cm i sedimentkjernene. Årsaken til den markante økningen øverst i sedimentkjernene er ikke kjent. En mulig mekanisme kan være naturlige redoksprosesser øverst i havbunnen som binder As i topplagene, men menneskelig tilførsel kan ikke utelukkes. Cd minker til lave konsentrasjoner øverst i sedimentkjernene med konsentrasjoner på 0.10-0.15 mg/kg sediment.

Mikroplast er funnet overflateprøver i Kongsfjorden og Rijpfjorden, samt i et transekt nordvest for Bjørnøya.

7. REFERANSER

AMAP 1998. AMAP Assessment Report: Pollution Issues. Arctic Monitoring and Assessment Programme (AMAP), 859 s.

Andersen T. J., 2017: Some Practical Considerations Regarding the Application of ^{210}Pb and ^{137}Cs Dating to Estuarine Sediments. Applications of Paleoenvironmental Techniques in Estuarine Studies. Developments in Paleoenvironmental Research (DPER), Vol. 20, p 121-140.

Braastad, G. 2000: Kort innføring i toksikologi – økotoksikologisk risikovurdering – veiledning – Del IIA. SFT-rapport TA 1756, 46 s.

Bøe R., Dolan M., Thorsnes T., Lepland A., Olsen H., Totland O. & Elvenes S. 2010: Standard for geological seabed mapping offshore. NGU-rapport 2010.033, 15 s.

Dehairs, F., Chesselet, R., and Jedwab, J., 1980. Discrete suspended particles of barite and the barium cycle in the ocean. Earth Planetary Science Letters, vol. 49, s. 528 – 550.

Farmer J. G. and Lovell M. A., 1986. Natural enrichment of arsenic in Loch Lomond sediments. Geochimica et Cosmochimica Acta, Vol. 50, issue 9, pp. 2059 – 2067.

Jensen, H.K.B., Knies, J., Finne, T.E. og Thorsnes, T. 2007: MAREANO 2006 - miljøgeokjemiske resultater fra Tromsøflaket, Ingøydjupet og Sørøysundet, NGU-rapport 2007.059, 249 sider inkl. vedlegg.

Jensen, H.K.B., Knies, J., Finne, T.E. og Thorsnes, T. 2008: MAREANO 2007 - miljøgeokjemiske resultater fra Troms II og Troms III, NGU-rapport 2008.077, 253 sider inkl. vedlegg.

Jensen, H.K.B., Knies, J., Finne, T.E. og Thorsnes, T. 2009: MAREANO 2008 – miljøgeokjemiske resultater fra fra havområdene utenfor Lofoten – Troms, NGU-rapport 2009.057, 31sider inkl. CD med vedlegg.

Jensen, H.K.B., Knies, J., Finne, T.E. og Thorsnes, T. 2010a: MAREANO 2009 – miljøgeokjemiske resultater fra Eggakanten, NGU-rapport 2010.016, 31 sider inkl. CD med vedlegg.

Jensen H. K. B, Knies J., Finne, T.E. og Thorsnes, T. 2010b: MAREANO 2009 – miljøgeokjemiske resultater fra Eggakanten, Tromsøflaket og Nordland VII, NGU-rapport 2010.063, 36 sider inkl. CD med vedlegg.

Jensen H. K. B., Finne T. E. og Thorsnes T., 2011. MAREANO 2010 – miljøgeokjemiske resultater av overflatesedimenter fra områder utenfor Finnmark, Troms III og Nordland VI. NGU-rapport 2011.052, 22 sider og vedlegg.

Jensen H. K. B., Knies J., Finne T. E. og Thorsnes T., 2013. Miljøkjemiske data og dateringsresultater fra fire sedimentkjerner i Nordkapptransektet, Troms III og Nordland VI. 28 sider og vedlegg.

Jensen H. K. B., Finne T. E. og Thorsnes T., 2013. Miljøkjemiske data og dateringsresultater fra Finnmark, Nordland VI og Mørebankene. NGU-rapport 2013.041, 76 sider.

Jensen H. K. B., Plassen, L., Finne T. E. og Thorsnes T., 2014. Miljøkjemiske data og dateringsresultater fra Norskehavet og Tidligere Omstridt Område (TOO) – MAREANO. NGU-rapport 2014.025, 82 sider.

Jensen H. K. B., Seither A. og Knies J., 2016. Miljøkjemiske data og dateringsresultater fra Barentshavet Øst og Norskehavet. NGU-rapport 2016.025, 66 sider.

Jensen H. K. B., Knies J. og Bellec V., 2018. Miljøkjemiske data og dateringsresultater fra Kong Karls Land – Bjørnøyrenna-transektet og Nordkapp-Sørkapp-transektet – MAREANO. NGU rapport 2018.001, 61 sider.

Jensen H. K. B. og Cramer J., 2017. MAREANOs pilotprosjekt på mikroplast – resultater for forslag til oppfølgning. NGU-rapport 2017.043, 51sider.

Knies, J., Jensen, H.K.B., Finne, T.E., Lepland, A. & Sæther, O. M. 2006: Sediment composition and heavy metal distribution in Barents Sea surface samples: Results from Institute of Marine Research 2003 and 2004 cruises. NGU-report 2006.067, 1-35.

Knutsen, H., Singdal-Larsen C. and Cyvin J. B., 2019. Microplastic contents in Svalbard fjord and Bjørnøy transect sediments. NGI rapport (på engelsk), 107 sider inkl. appendikser.

Lepland, A., Sæther O. M. & Thorsnes T. 2000: Accumulation of barium in recent Skagerrak sediments: sources and distribution control. Marine Geology, vol. 163, s. 13 – 26.

MAREANO kjemidata, 2003 – 2017. http://www.mareano.no/datanedlasting/kjemidata.

Miljødirektoratet veileder M-608, 2016. Grenseverdier for klassfisering av vann, sedimenter og biota. 24 sider.

Molvær, J., Knutzen, J., Magnusson, J., Rygg, B., Skei, J. & Sørensen, J. 1997: Klassifisering av miljøkvalitet i fjorder og kystvann. Veiledning. SFT-rapport 97:03, TA-1467, 36 sider.

Norsk oljehistorie i korte trekk, 2002. http://www.ptil.no/ord-og-uttrykk/norsk-oljehistorie-i-korte-trekk-article882-38.html.

Nuernberg C. C., Bohrmann G., Schlueter M. og Frank M., 1997. Barium accumulation in the Atlantic sector of the Southern Ocean. Results from 190,000-year records. Paleoceanography. Vol. 12 (4), s. 594 – 603.

Olsgård F. and Gray J., 1995. A comprehensive analysis of the effects of offshore oil and gas exploration and production on the benthic communities of the Norwegian continental shelf. Marine Ecology Progress Series, vol. 122, pp. 277 – 306.

Ottesen R. T., Bogen J., Finne T. E., Andersson M., Dallmann W. K., Eggen O. E., Jartun M., Lundquist Q., Pedersen H. R. and Volden, T., 2010. Geochemical atlas of Norway. Part 2: Geochemical Atlas of Spitsbergen. NGU, 160 pages.

Pathirana I., Knies J., Felix M. and Mann U., 2014. Towards an improved organic carbon budget for the western Barents Sea shelf. Climate of the Past, vol. 10, pp. 569-587.

Rise, L. og Brendryen, J. 2013. Leirinnhold i jordarter – en sammenlignende studie med vekt på Coulter Laser 200 og Sedigraph, og forslag til beregning av ekvivalent leirinnhold i prosent. NGU Rapport 2013.012, 35 s.

Rye H., 1996. Miljøeffekter av utslipp fra borekjemikalier. Rapport fra OLF. IKU Petroleumsforskning. Rapport nr. 42.4053.00/01/96. 98 sider.

SFT 2007: Veileder for klassifisering av miljøkvalitet i fjorder og kystfarvann. Revidering av klassifisering av metaller og organiske miljøgifter i vann og sedimenter. SFT-veileder 2229, 11 s.

Steinsund P.I. and Hald M., 1993. Recent calcium carbonate dissolution in the Barents Sea: Paleoceanographic applications. Marine Geology, vol. 117, pp. 303-316.

Sværen I., 2013. Cs-137 aktivitet i sediment og datering av kjernar i MAREANO-prosjektet. HI-rapport 2013.

Sæther O. M., Faye G., Thorsnes T., Rise L., Longva O. and Bøe R., 1996. Regional distribution of manganese, phosphorus, heavy metals, barium, and carbon in sea-bed sediments (0-2 cm) from the northern part of the Norwegian Skagerrak. Geological Survey of Norway Bull., no. 430, p. 103-112.

Thorsnes T. and Klungsøyr J., 1997. Contamination of Skagerrak sediments due to man-made inputs during the last 200 years. In: O. Longva and T. Thorsnes (Editors), Skagerrak in the past and at the present - an integrated study of geology, chemistry, hydrography and microfossil ecology. Geological Survey of Norway. Special Publication, vol. 8, p. 52-79.

Winkelmann D. and Knies J., 2005. Recent distribution and accumulation of organic carbon on the continental margin west off Spitsbergen. Geochemistry, Geophysics and Geosystems, Vol. 6, no. 9, pp. 1-22.

Vedlegg 2

Cd, Cr, Cu, Zn og ^{137}Cs kart i prøvene 0-1 cm dyp og sedimentasjonsrater basert på ^{210}Pb-data.

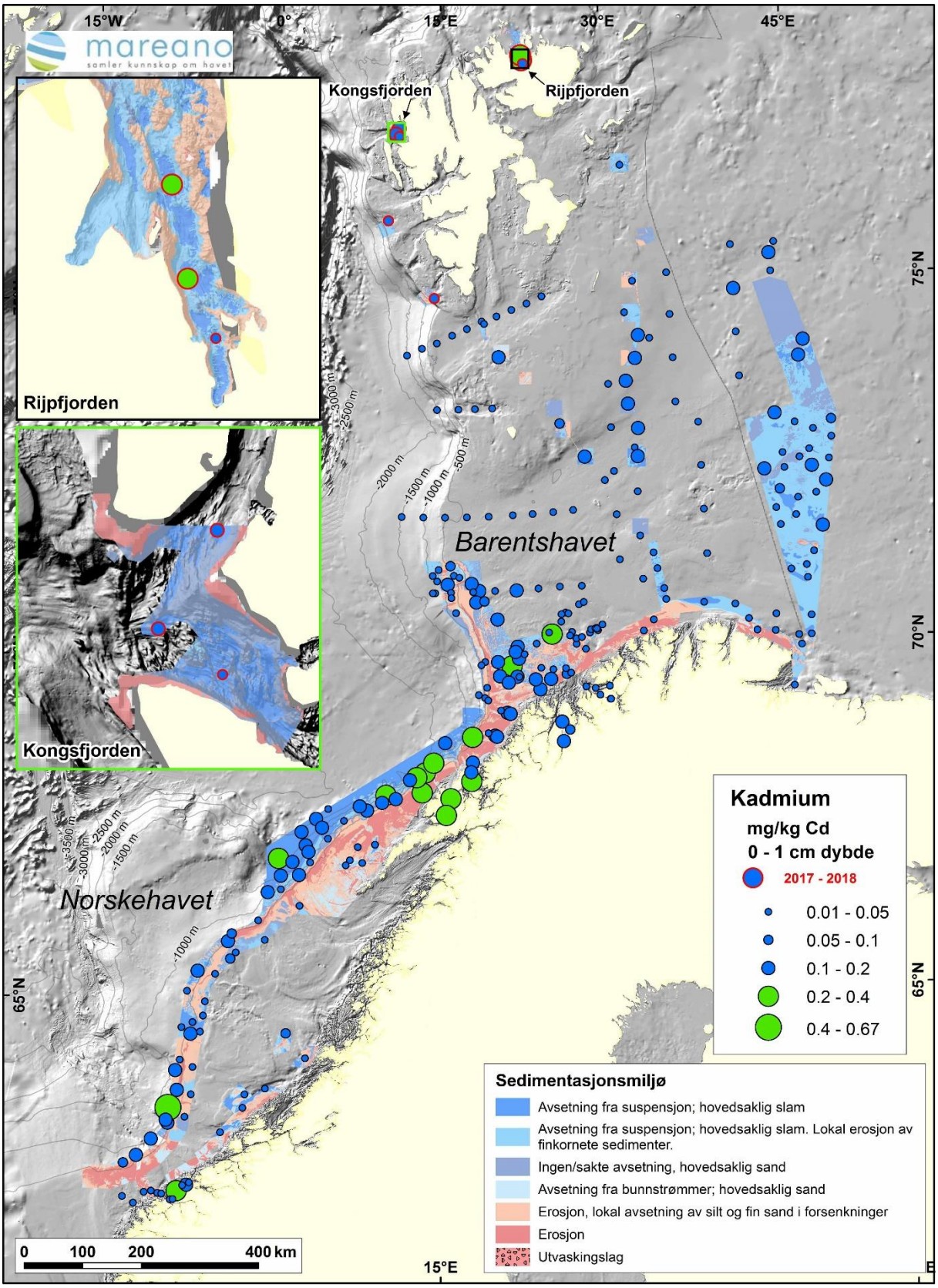
mareano
samler kunnskap om havet
15°W
0°
15°E
30°E
45°E
75°N
70°N
65°N
Kongsfjorden
Rijpfjorden
Barentshavet
Norskehavet
-3000 m
-2500 m
-2000 m
-1500 m
-1000 m
-500 m
-3500 m
Kadmium
mg/kg Cd
0 - 1 cm dybde
2017 - 2018
0.01 - 0.05
0.05 - 0.1
0.1 - 0.2
0.2 - 0.4
0.4 - 0.67
Sedimentasjonsmiljø
Avsetning fra suspensjon; hovedsaklig slam
Avsetning fra suspensjon; hovedsaklig slam. Lokal erosjon av finkornete sedimenter.
Ingen/sakte avsetning, hovedsaklig sand
Avsetning fra bunnstrømmer; hovedsaklig sand
Erosjon, lokal avsetning av silt og fin sand i forsenkninger
Erosjon
Utvaskingslag
0
100
200
400 km

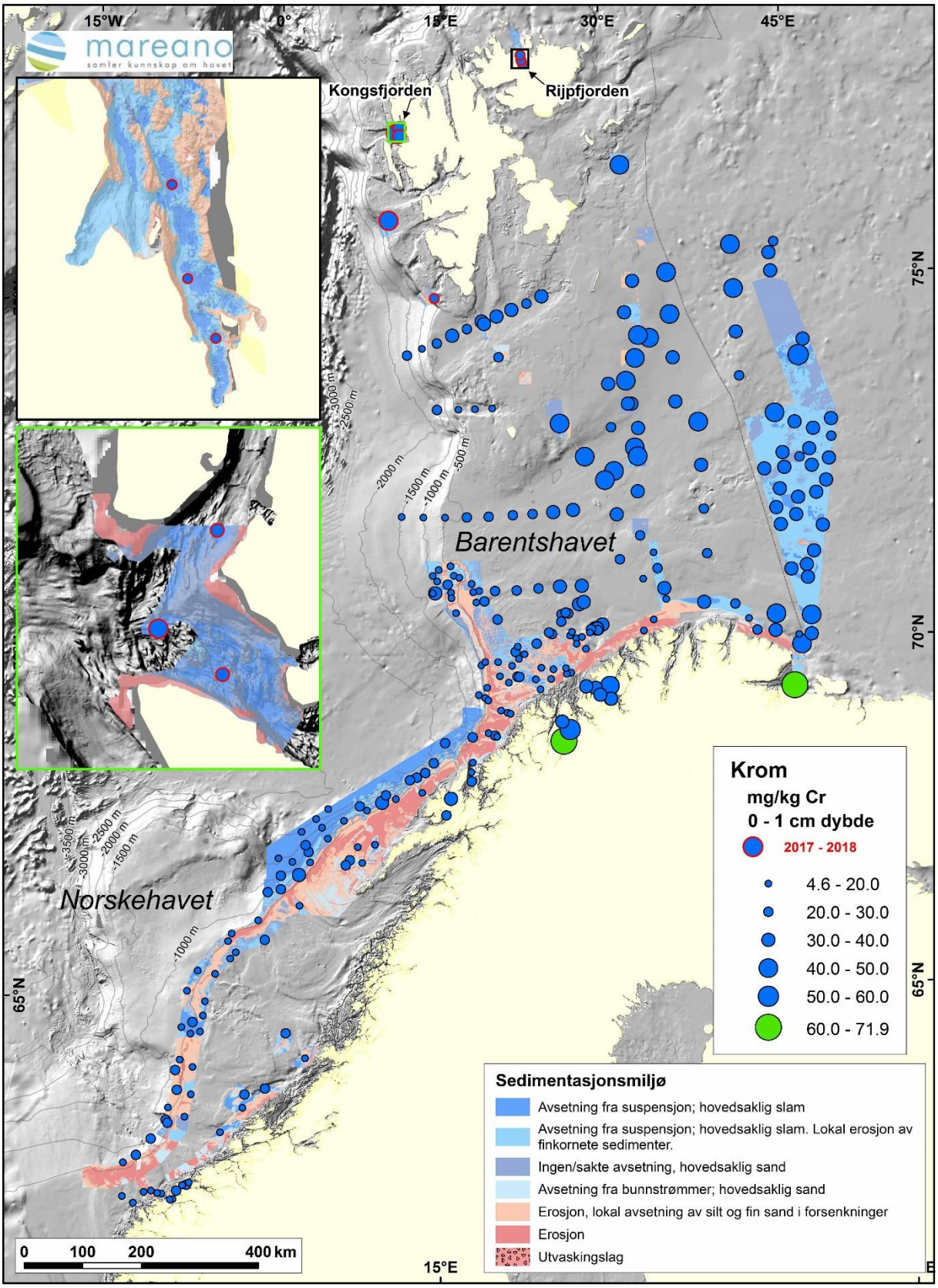
mareano
samler kunnskap om havet
15°W
0°
15°E
30°E
45°E
75°N
70°N
65°N
Kongsfjorden
Rijpfjorden
Barentshavet
Norskehavet
-3000 m
-2500 m
-2000 m
-1500 m
-1000 m
-500 m
-3500 m
Krom
mg/kg Cr
0 - 1 cm dybde
2017 - 2018
4.6 - 20.0
20.0 - 30.0
30.0 - 40.0
40.0 - 50.0
50.0 - 60.0
60.0 - 71.9
Sedimentasjonsmiljø
Avsetning fra suspensjon; hovedsaklig slam
Avsetning fra suspensjon; hovedsaklig slam. Lokal erosjon av finkornete sedimenter.
Ingen/sakte avsetning, hovedsaklig sand
Avsetning fra bunnstrømmer; hovedsaklig sand
Erosjon, lokal avsetning av silt og fin sand i forsenkninger
Erosjon
Utvaskingslag
0
100
200
400 km

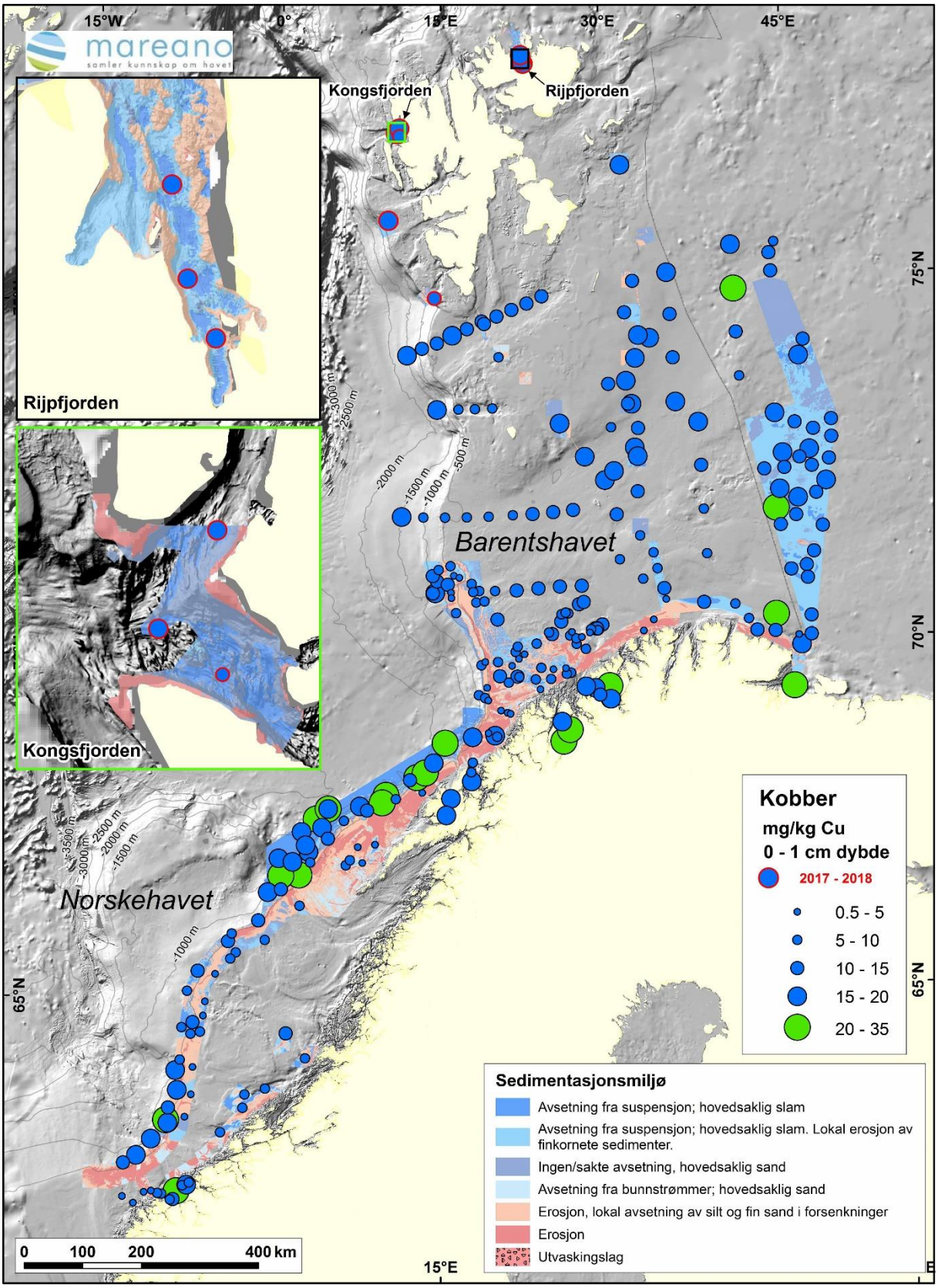
mareano
samler kunnskap om havet
15°W
0°
15°E
30°E
45°E
75°N
70°N
65°N
Kongsfjorden
Rijpfjorden
Rijpfjorden
Kongsfjorden
-3000 m
-2500 m
-2000 m
-1500 m
-1000 m
-500 m
Barentshavet
Norskehavet
-3500 m
-3000 m
-2500 m
-2000 m
-1500 m
-1000 m
Kobber
mg/kg Cu
0 - 1 cm dybde
2017 - 2018
0.5 - 5
5 - 10
10 - 15
15 - 20
20 - 35
Sedimentasjonsmiljø
Avsetning fra suspensjon; hovedsaklig slam
Avsetning fra suspensjon; hovedsaklig slam. Lokal erosjon av finkornete sedimenter.
Ingen/sakte avsetning, hovedsaklig sand
Avsetning fra bunnstrømmer; hovedsaklig sand
Erosjon, lokal avsetning av silt og fin sand i forsenkninger
Erosjon
Utvaskingslag
0
100
200
400 km
15°E

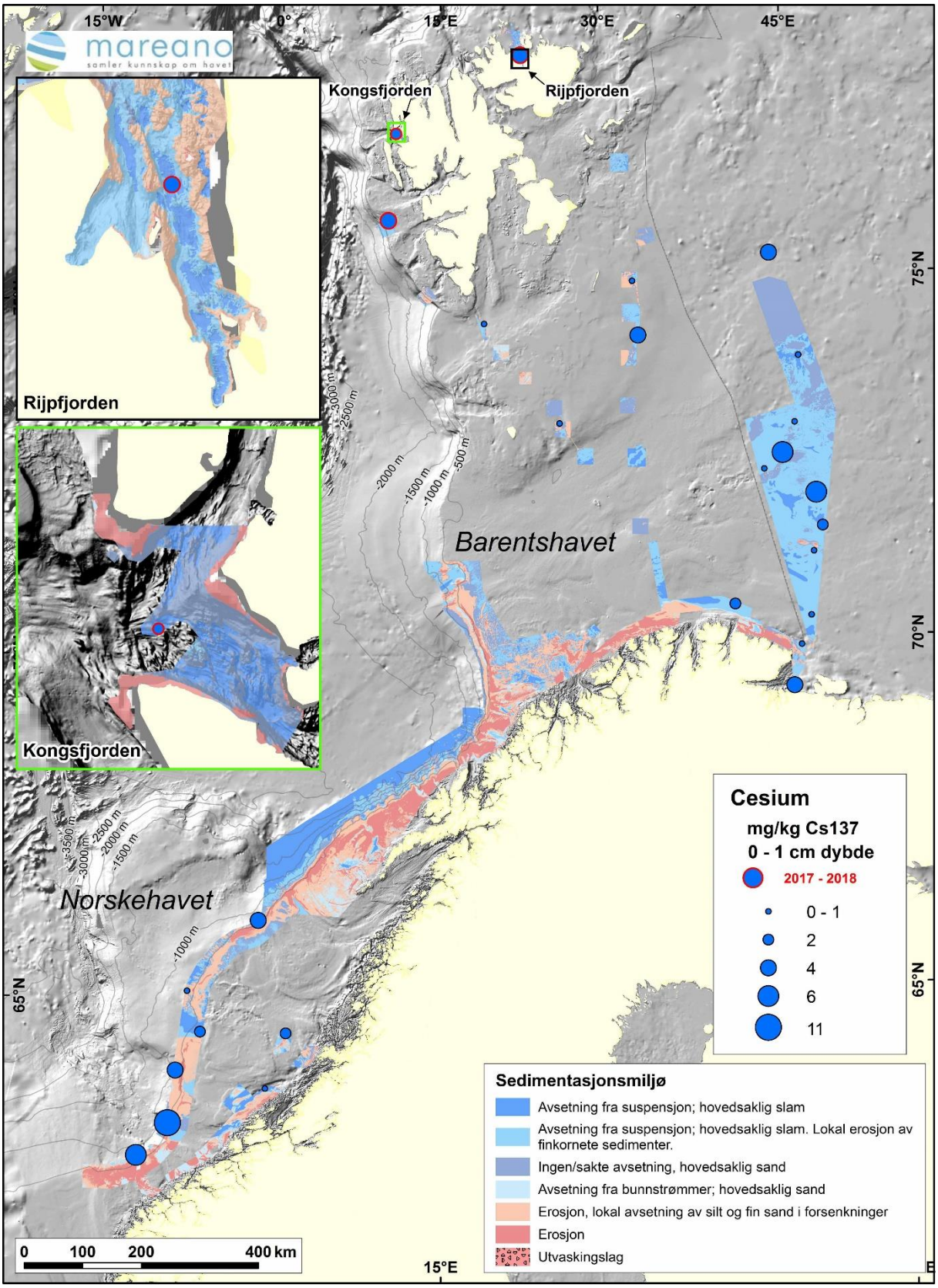
mareano
samler kunnskap om havet
15°W
0°
15°E
30°E
45°E
75°N
70°N
65°N
Kongsfjorden
Rijpfjorden
Rijpfjorden
Kongsfjorden
-3000 m
-2500 m
-2000 m
-1500 m
-1000 m
-500 m
Barentshavet
Norskehavet
Cesium
mg/kg Cs137
0 - 1 cm dybde
2017 - 2018
0 - 1
2
4
6
11
Sedimentasjonsmiljø
Avsetning fra suspensjon; hovedsaklig slam
Avsetning fra suspensjon; hovedsaklig slam. Lokal erosjon av finkornete sedimenter.
Ingen/sakte avsetning, hovedsaklig sand
Avsetning fra bunnstrømmer; hovedsaklig sand
Erosjon, lokal avsetning av silt og fin sand i forsenkninger
Erosjon
Utvaskingslag
0
100
200
400 km

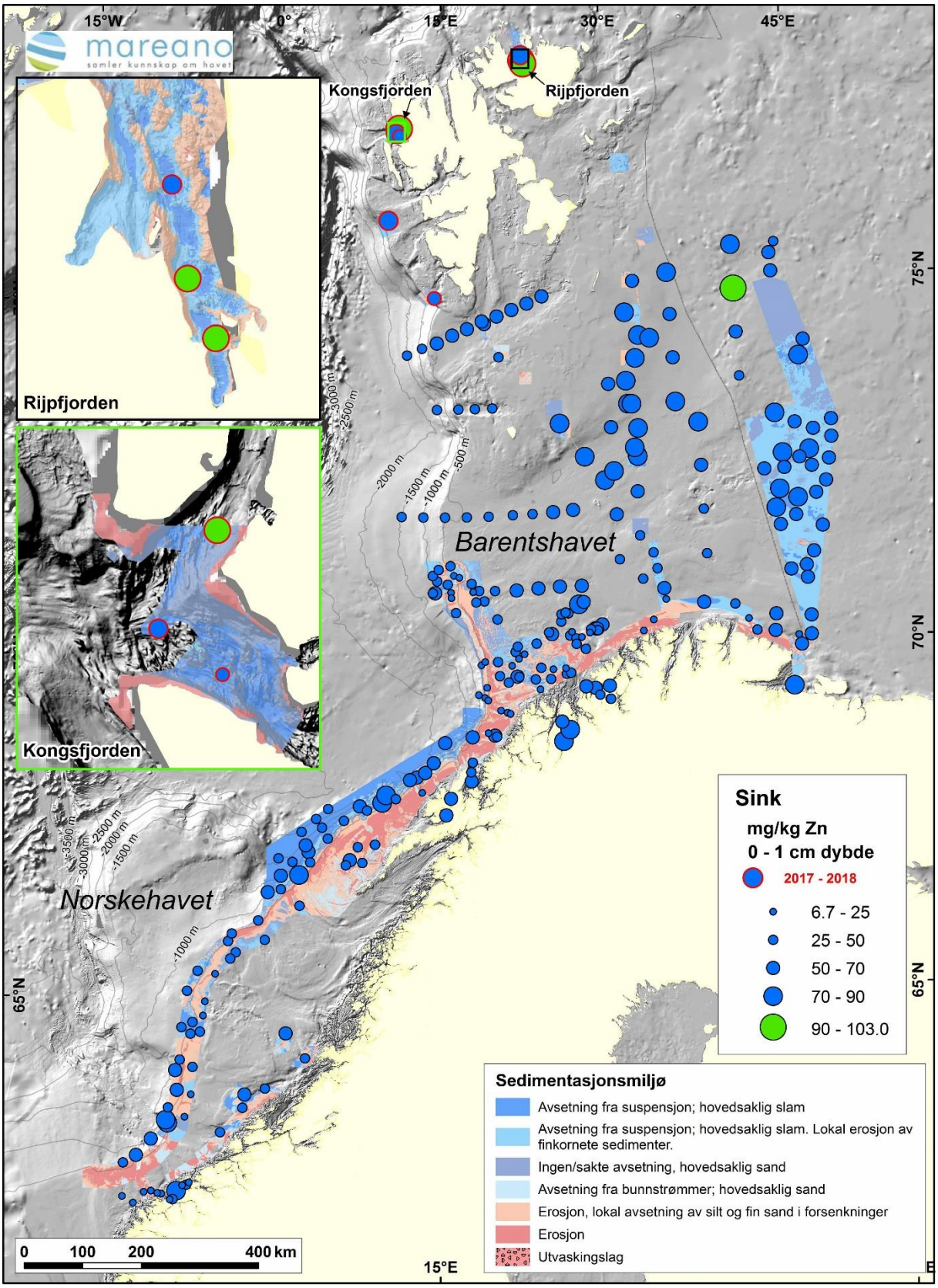
mareano
samler kunnskap om havet
Kongsfjorden
Rijpfjorden
Rijpfjorden
Kongsfjorden
Barentshavet
Norskehavet
15°W
0°
15°E
30°E
45°E
75°N
70°N
65°N
-3000 m
-2500 m
-2000 m
-1500 m
-1000 m
-500 m
-3500 m
Sink
mg/kg Zn
0 - 1 cm dybde
2017 - 2018
6.7 - 25
25 - 50
50 - 70
70 - 90
90 - 103.0
Sedimentasjonsmiljø
Avsetning fra suspensjon; hovedsaklig slam
Avsetning fra suspensjon; hovedsaklig slam. Lokal erosjon av finkornete sedimenter.
Ingen/sakte avsetning, hovedsaklig sand
Avsetning fra bunnstrømmer; hovedsaklig sand
Erosjon, lokal avsetning av silt og fin sand i forsenkninger
Erosjon
Utvaskingslag
0
100
200
400 km

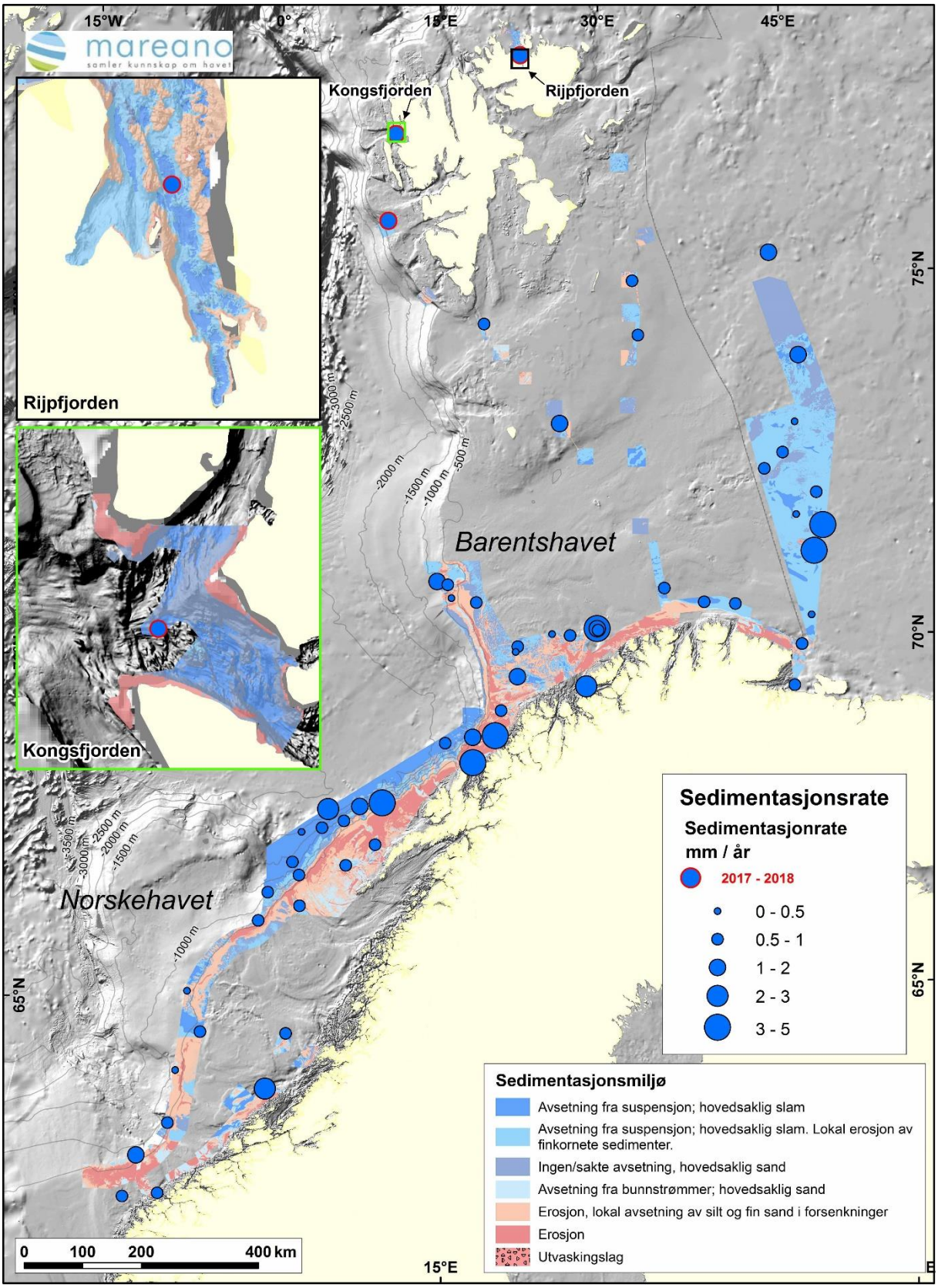
mareano
samler kunnskap om havet
15°W
0°
15°E
30°E
45°E
75°N
70°N
65°N
Kongsfjorden
Rijpfjorden
Rijpfjorden
Kongsfjorden
-3000 m
-2500 m
-2000 m
-1500 m
-1000 m
-500 m
Barentshavet
Norskehavet
-3500 m
-3000 m
-2500 m
-2000 m
-1500 m
-1000 m
Sedimentasjonsrate
Sedimentasjonrate
mm / år
2017 - 2018
0 - 0.5
0.5 - 1
1 - 2
2 - 3
3 - 5
Sedimentasjonsmiljø
Avsetning fra suspensjon; hovedsaklig slam
Avsetning fra suspensjon; hovedsaklig slam. Lokal erosjon av finkornete sedimenter.
Ingen/sakte avsetning, hovedsaklig sand
Avsetning fra bunnstrømmer; hovedsaklig sand
Erosjon, lokal avsetning av silt og fin sand i forsenkninger
Erosjon
Utvaskingslag
0
100
200
400 km
15°E

Vedlegg 3

XRI-bilder av sedimentkjerner

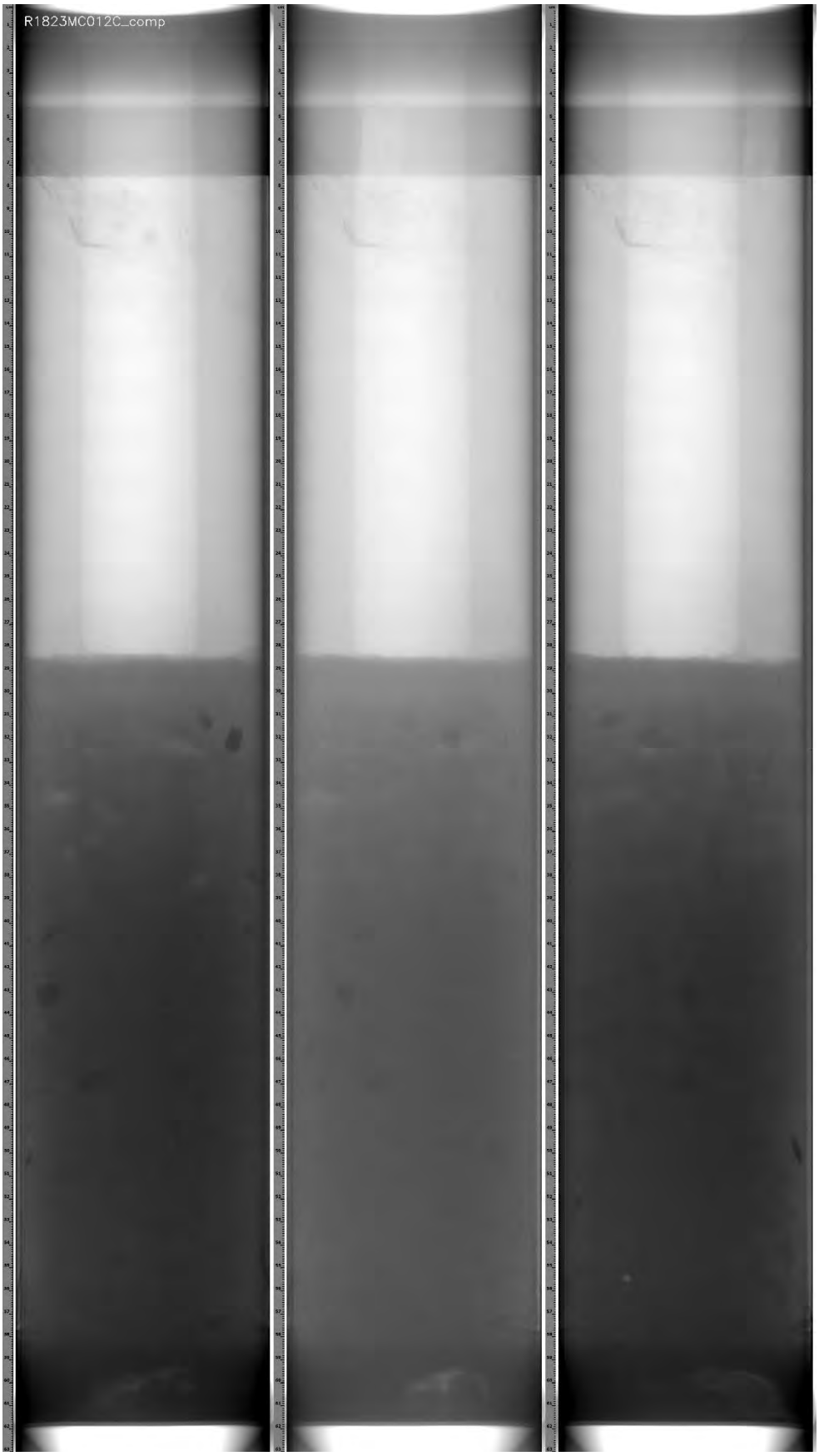

R1823MC012C

0 grader 45 grader 90 grader

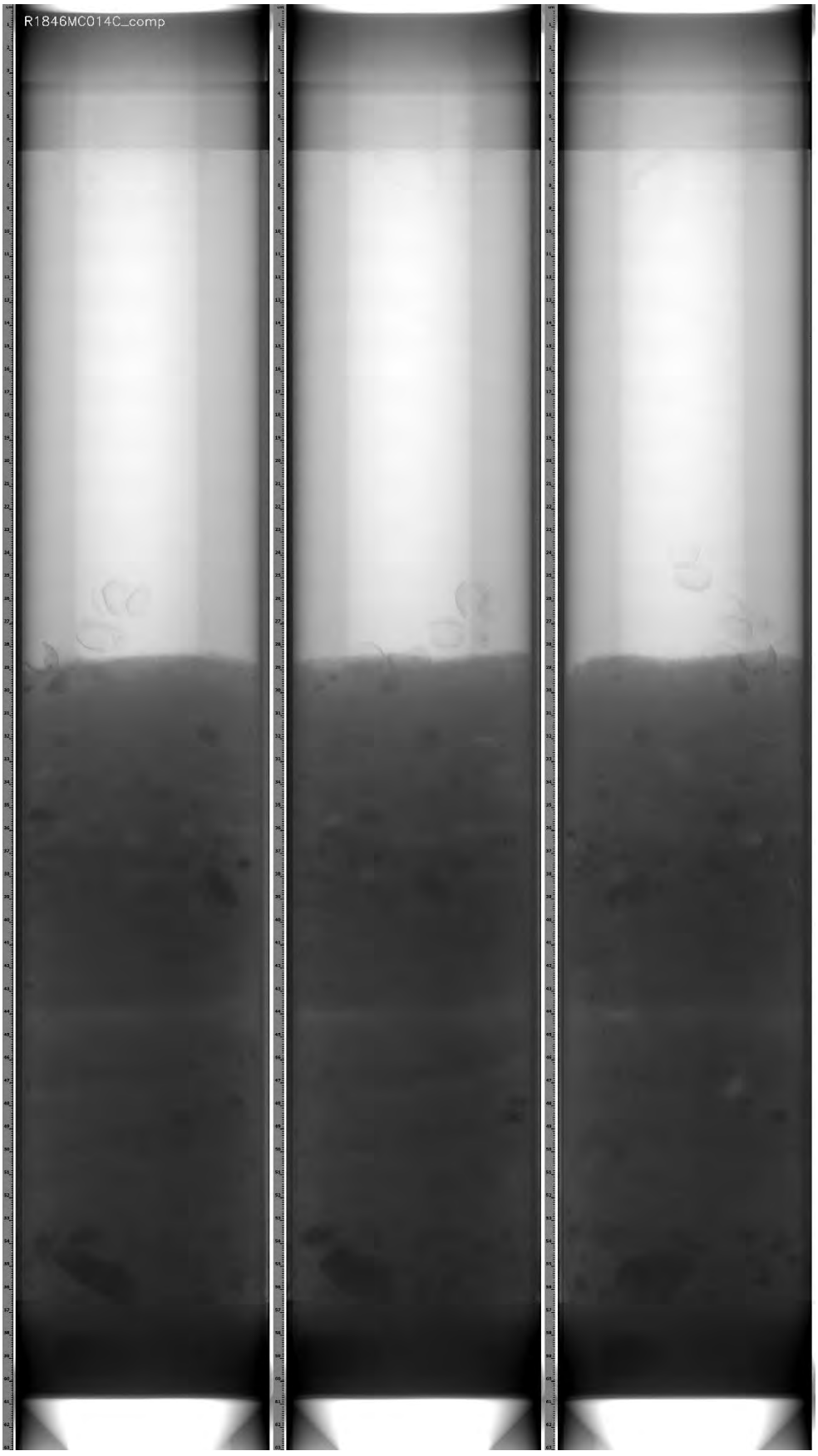

R1846MC014C

0 grader 45 grader 90 grader

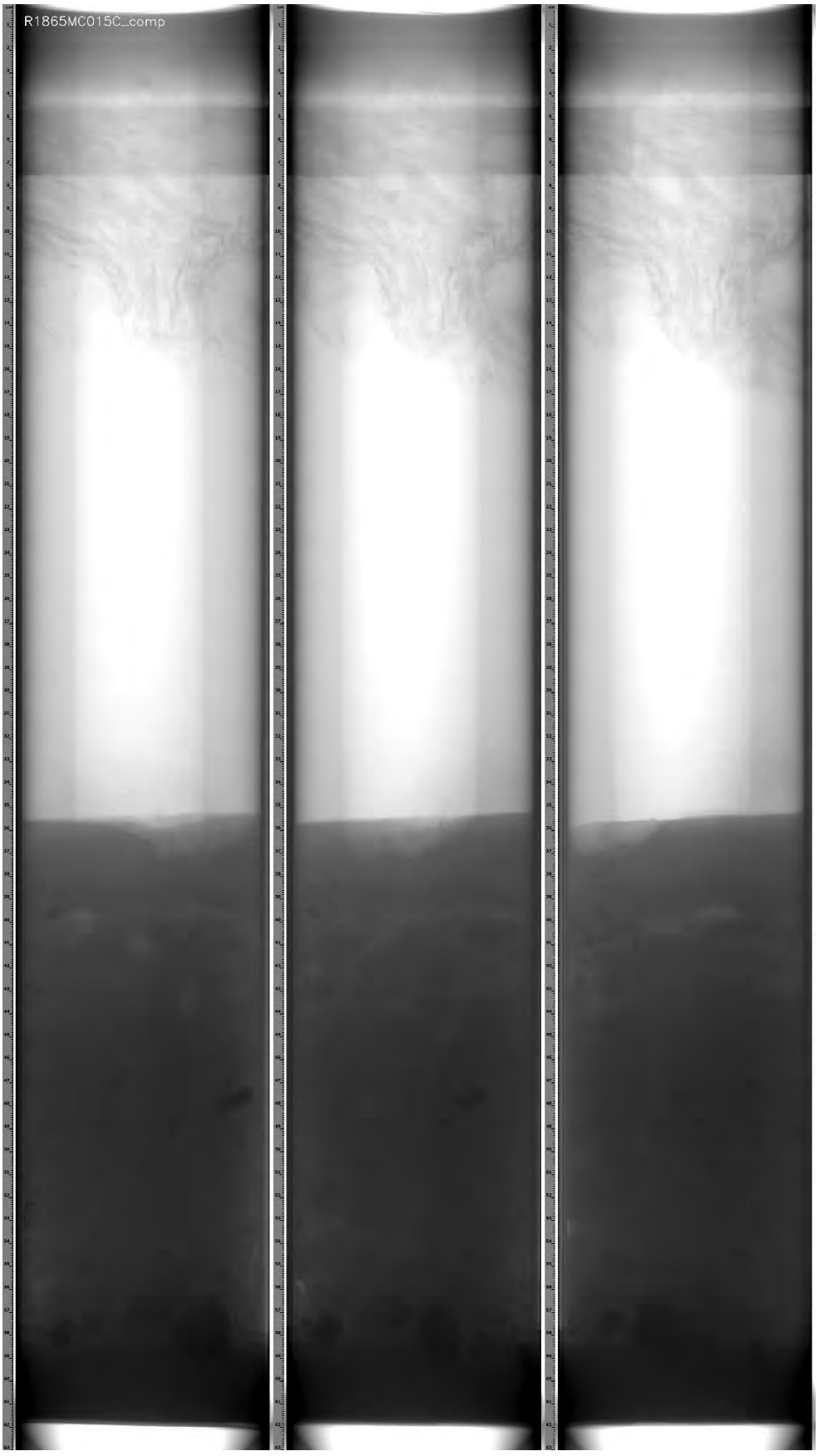

R1865MC015C

0 grader 45 grader 90 grader

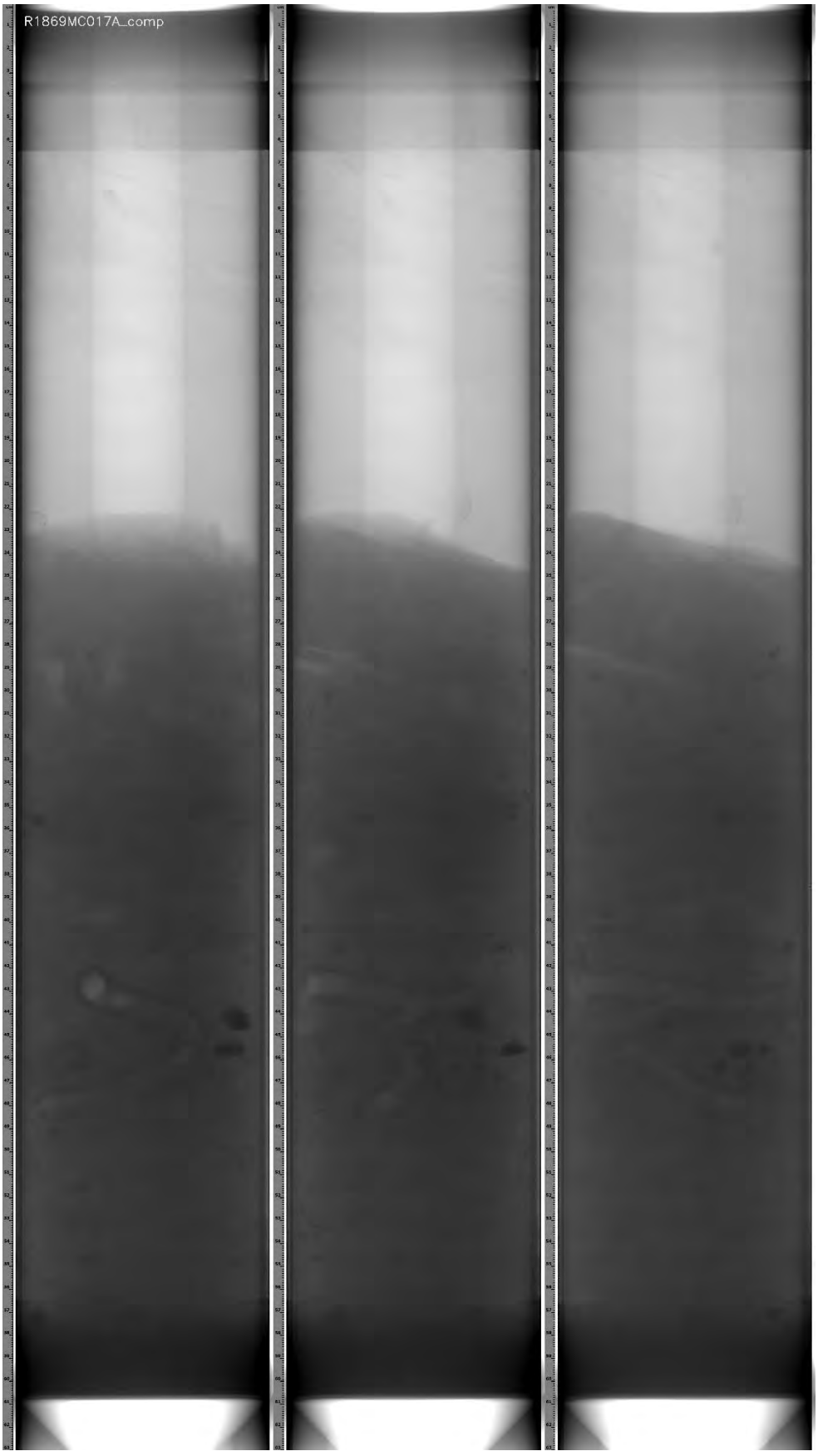

R1869MC016C

0 grader 45 grader 90 grader

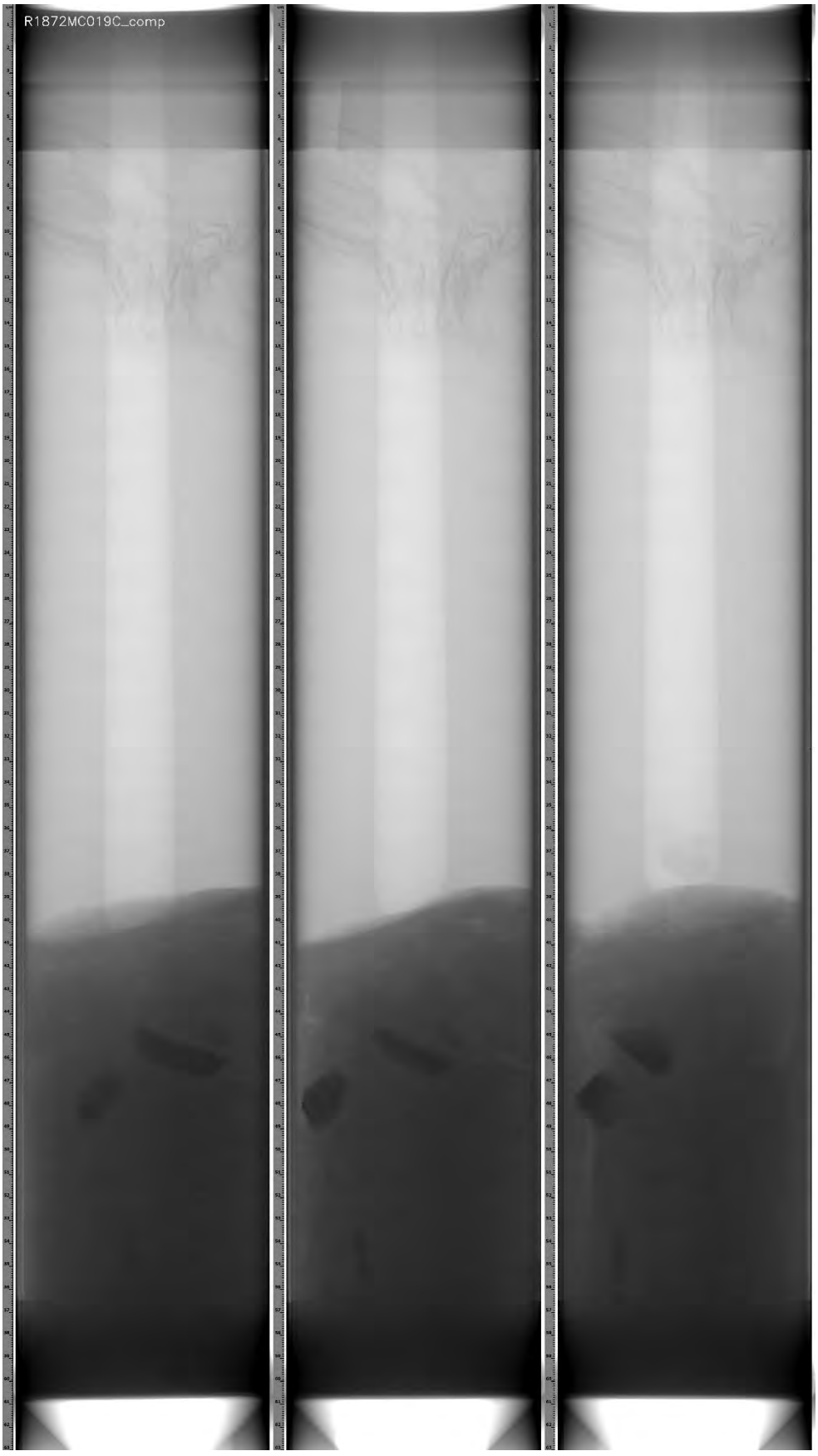

R1872MC019C

0 grader 45 grader 90 grader

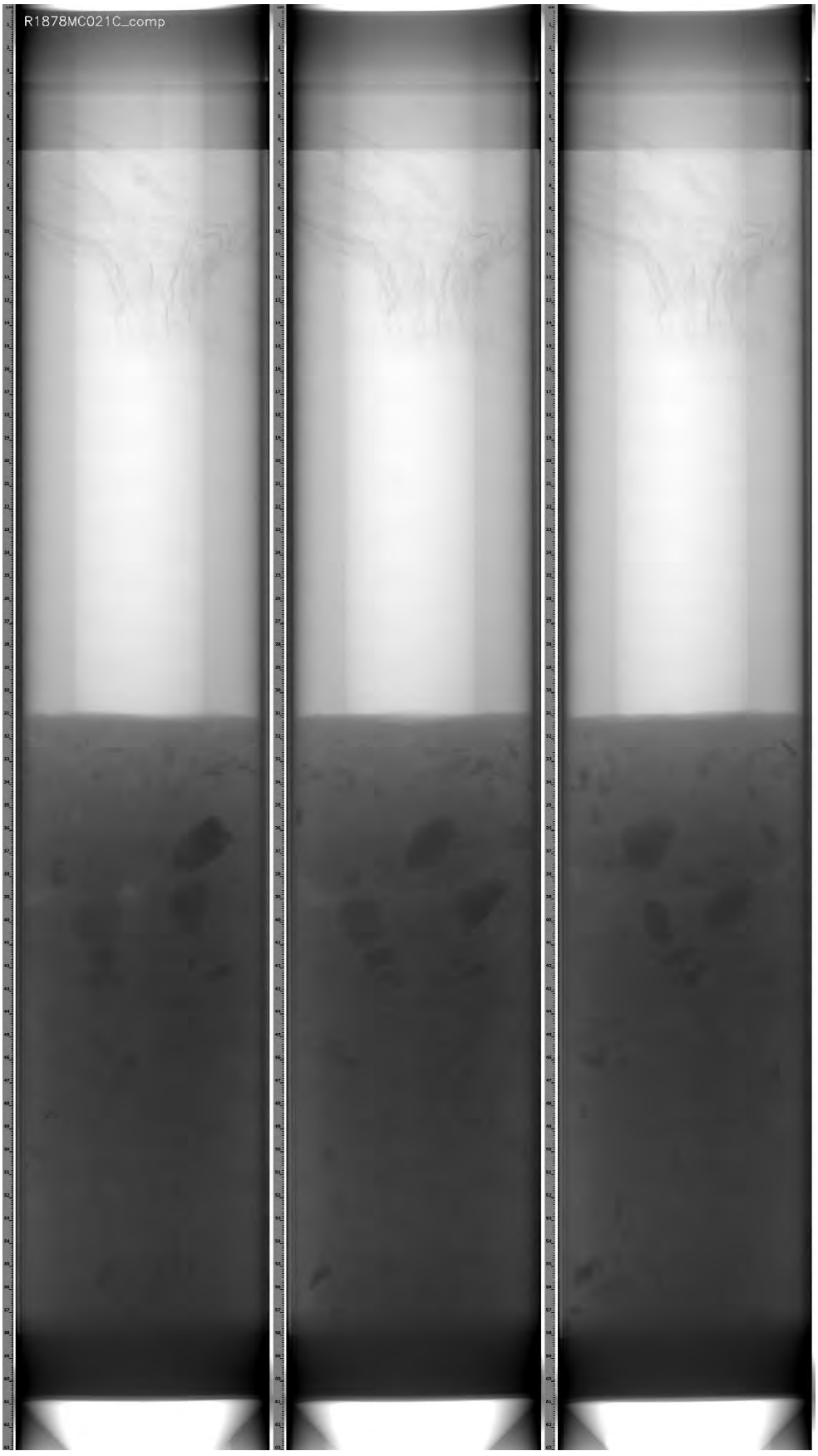

R1878MC021C

0 grader 45 grader 90 grader

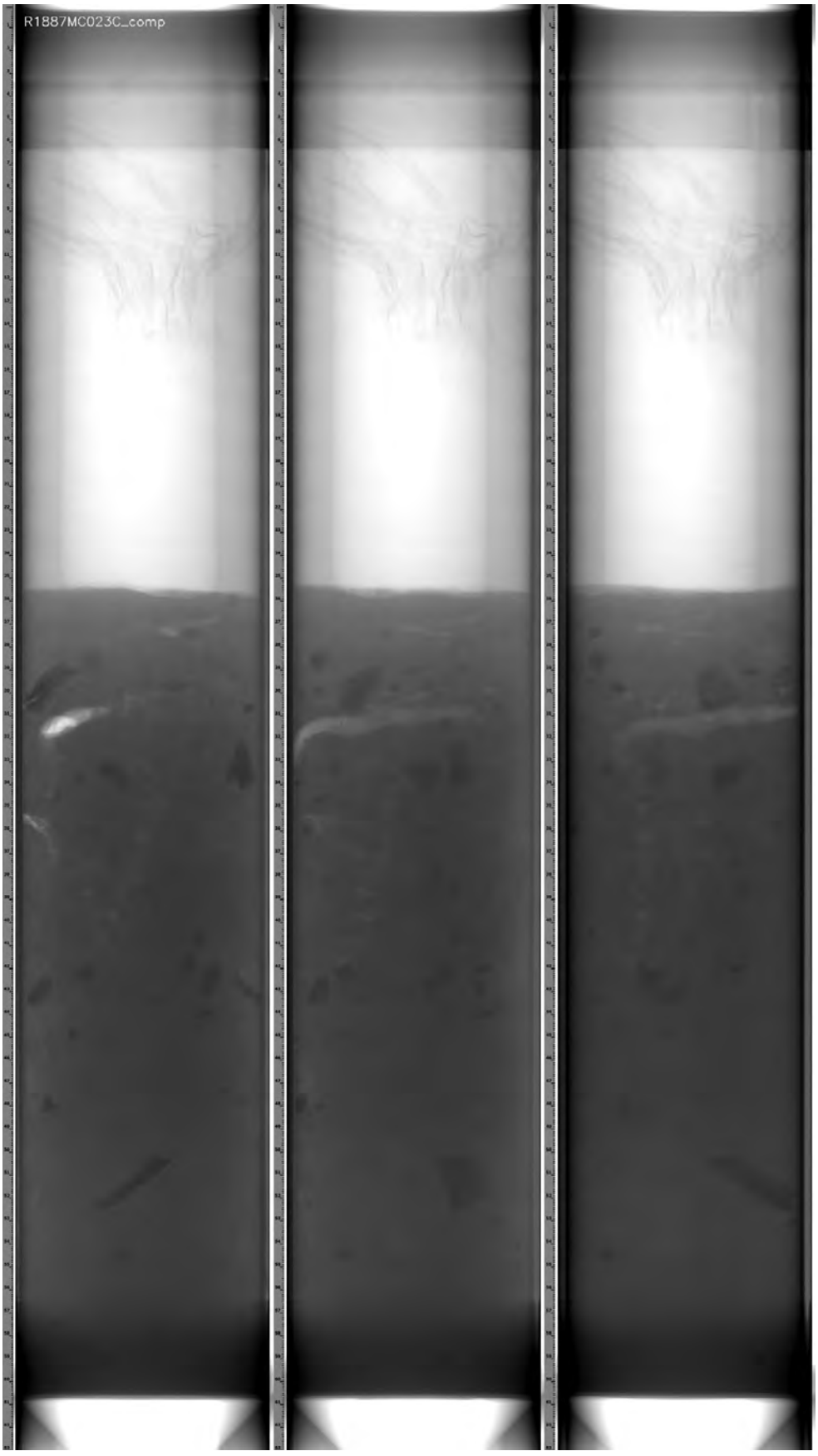

R1887MC023C

0 grader 45 grader 90 grader

Vedlegg 4

^{137}Cs aktivitet og ^{210}Pb datering av 3 sedimentkjerner (R1823MC008A, R1869MC016A, R1887MC023A). Leverandør av data: Gamma Dating Center (GDC), Københavns Universitet, Danmark

Gamma Dating Center Copenhagen

Copenhagen, August 19th, 2019

Thorbjørn J. Andersen
Department of Geosciences and Natural Resource Management (IGN)
University of Copenhagen
Oester Voldgade 10
1350 Copenhagen K
e-mail tja@ign.ku.dk
phone +45 35 32 25 03
fax +45 35 32 25 01

Dating of core R1823MC12A

Dating of core R1823MC12A

Methods

The samples have been analysed for the activity of ^{210}Pb, ^{226}Ra and ^{137}Cs via gammaspectrometry at the Gamma Dating Center, Institute of Geography, University of Copenhagen. The measurements were carried out on a Canberra ultralow-background Ge-detector. ^{210}Pb was measured via its gamma-peak at 46,5 keV, ^{226}Ra via the granddaughter ^{214}Pb (peaks at 295 and 352 keV) and ^{137}Cs via its peak at 661 keV.

Results

The core showed surface contents of unsupported ^{210}Pb of around 660 Bq kg^{-1} with a clear tendency for exponential decline with depth (fig 1). The calculated flux of unsupported ^{210}Pb is 827 Bq m^{-2} y^{-1} which is 5-10 times higher than the expected flux (based on data shown in Appleby, 2001). This indicates that the site is subject to intense sediment focusing.

The content of the isotope ^{137}Cs was low and only consistently above detection limits in the upper 10 cm of the core.

CRS-modelling has been applied on the profile using a modified method (Appleby, 2001; Andersen 2017) where the activity below 22 cm is calculated on the basis of the regression shown in fig 2. The result is given in table 2 and fig 3 and 4.

The chronology given in table 2 is only valid if bioturbation and other sediment mixing is negligible. If this is not the case, ages given in table 2 are underestimated and accumulation rates are overestimated. However, the profile of unsupported ^{210}Pb showed a fairly consistent exponential decline with depth which indicates that mixing is not significant. Additionally, measurable content of ^{137}Cs was only detected in the upper part of the core which also indicates that mixing cannot be severe and the chronology is therefore believed to be reliable.

Copenhagen, August 19th 2019

Thorbjørn J Andersen
Professor,
IGN, University of Copenhagen
Oester Voldgade 10, 1350 Copenhagen K, Denmark

Reference:

Andersen, T.J., 2017. Some Practical Considerations Regarding the Application of ^{210}Pb and ^{137}Cs Dating to Estuarine Sediments. Applications of Paleoenvironmental Techniques in Estuarine Studies . Developments in Paleoenvironmental Research (DPER), Vol. 20, p 121-140.

Appleby, P.G., 2001. Chronostratigraphic techniques in recent sediments. In: Last, W.M & Smol, J.P. (eds) Tracking environmental change using lake sediments. Volume 1: Basin analysis, coring and chronological techniques. Kluwer Academic Publishers, the Netherlands.

Table 1. Raw data, R1823MC12A

Depth	Pb-210tot	error Pb-210 tot	Pb-210 supp	error pb-210 supp	Pb-210 unsup	error pb-210 unsup	Cs-137	error Cs-137
cm	Bq kg-1	Bq kg-1	Bq kg-1	Bq kg-1	Bq kg-1	Bq kg-1	Bq kg-1	Bq kg-1
0.5	692	34	32	0	660	34	3	2
1.5	657	36	33	2	624	38	5	2
2.5	576	30	27	6	549	37	2	2
4.5	540	29	32	3	508	31	5	2
5.5	500	38	45	7	455	45	0	0
6.5	136	10	29	6	106	16	7	2
7.5	236	16	23	0	213	16	4	1
8.5	303	19	36	4	267	23	7	2
9.5	215	15	37	2	178	17	3	2
10.5	143	9	36	2	107	11	0	0
11.5	153	12	28	0	125	13	0	2
12.5	126	8	35	2	91	10	1	1
13.5	101	9	29	3	72	12	1	2
14.5	108	10	32	3	76	13	3	2
15.5	74	4	30	1	44	6	1	1
20.5	38	4	29	1	9	5	0	1
21.5	43	4	31	2	12	6	0	0

Table 2, chronology core R1823MC12A

Depth	Age	error age	Date	acc rate	error rate	Date acc rate
cm	y	y	y	(kg m-2 y-1)	(kg m-2 y-1)	y
			2018			
0.5	2	1	2016	1.22	0.07	2017
1.5	5	1	2013	1.16	0.08	2015
2.5	9	1	2009	1.13	0.08	2011
4.5	19	1	1999	1.01	0.08	2004
5.5	26	2	1992	0.85	0.09	1995
6.5	31	2	1987	1.21	0.18	1989
7.5	34	2	1984	1.87	0.16	1985
8.5	40	2	1978	1.08	0.10	1981
9.5	47	2	1971	0.95	0.10	1974
10.5	53	2	1965	1.22	0.14	1968
11.5	59	3	1959	1.25	0.15	1962
12.5	66	3	1952	1.10	0.14	1956
13.5	72	3	1946	1.18	0.21	1949
14.5	80	4	1938	1.04	0.20	1942
15.5	88	5	1930	1.01	0.17	1934
20.5	125	15	1893	1.20	0.84	1911
21.5	131	7	1887	1.43	0.33	1890

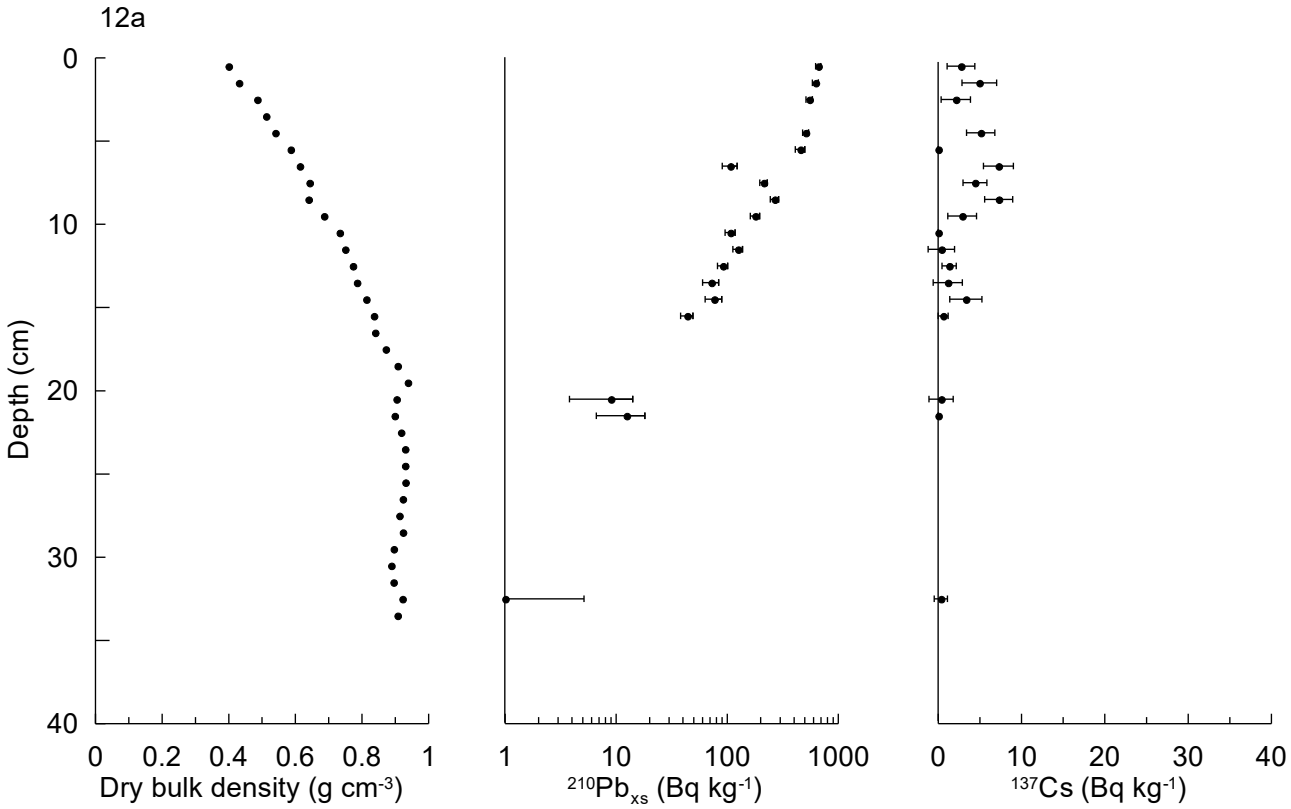

Fig 1

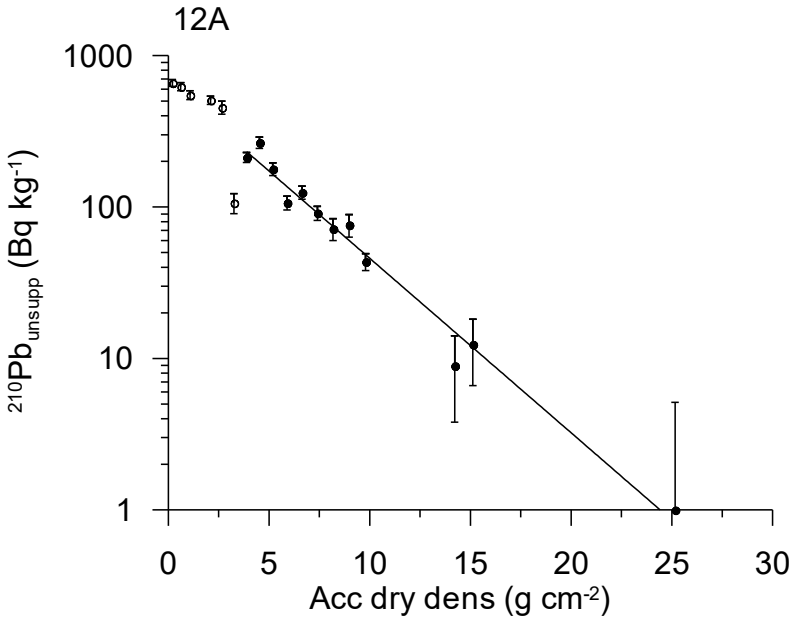

Fig 2. Regression of unsupported ^{210}Pb vs accumulated dry density.

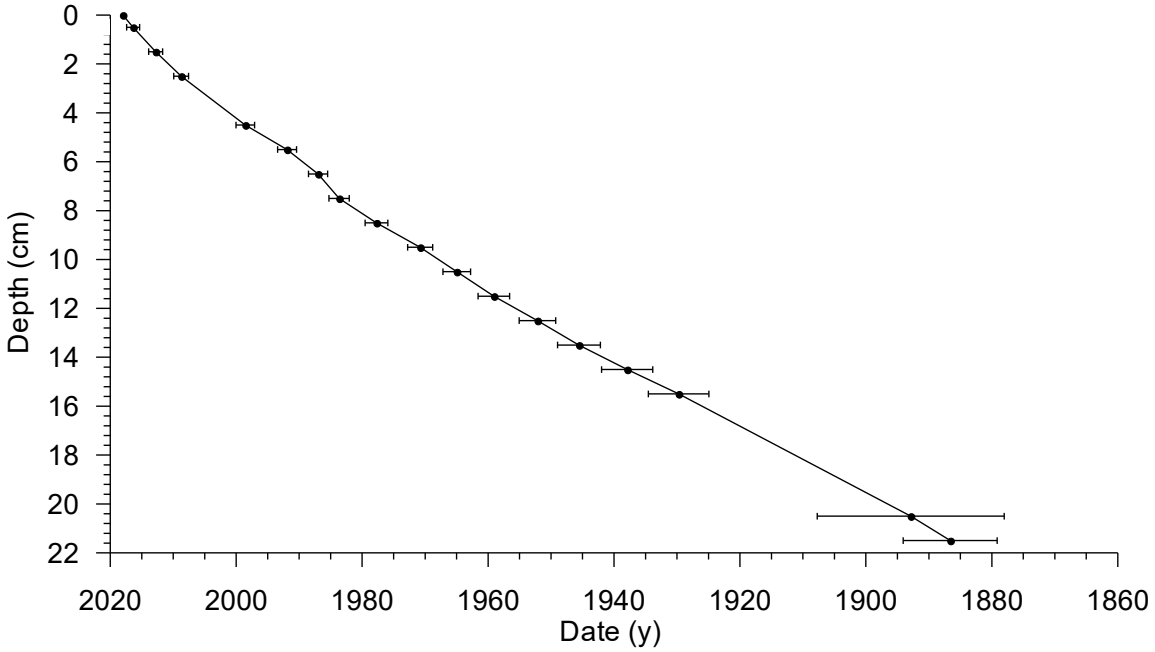
Depth (cm)
0
2
4
6
8
10
12
14
16
18
20
22
2020
2000
1980
1960
1940
1920
1900
1880
1860
Date (y)

Fig 3

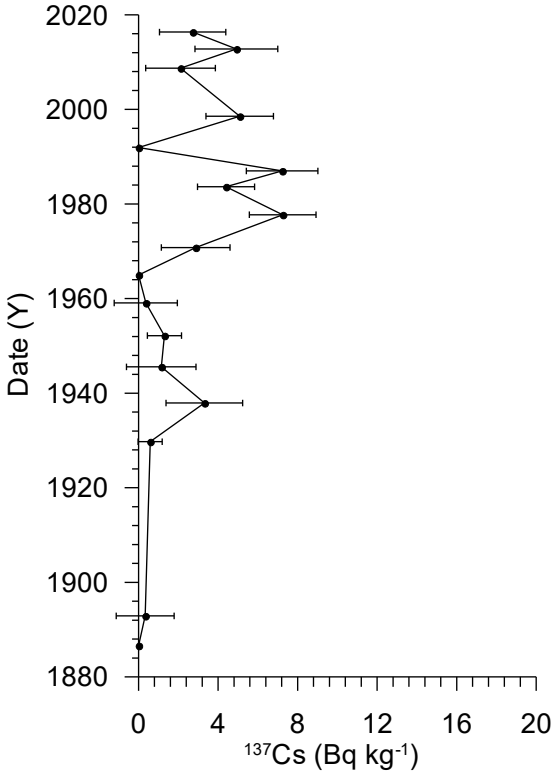
Date (Y)
2020
2000
1980
1960
1940
1920
1900
1880
0
4
8
12
16
20
137Cs (Bq kg-1)

Fig 4

Gamma Dating Center Copenhagen

Copenhagen, August 19th, 2019

Thorbjørn J. Andersen
Department of Geosciences and Natural Resource Management (IGN)
University of Copenhagen
Oester Voldgade 10
1350 Copenhagen K
e-mail tja@ign.ku.dk
phone +45 35 32 25 03
fax +45 35 32 25 01

Dating of core R1869MC016A

Dating of core R1869MC016A

Methods

The samples have been analysed for the activity of ^{210}Pb, ^{226}Ra and ^{137}Cs via gammaspectrometry at the Gamma Dating Center, Institute of Geography, University of Copenhagen. The measurements were carried out on a Canberra ultralow-background Ge-detector. ^{210}Pb was measured via its gamma-peak at 46,5 keV, ^{226}Ra via the granddaughter ^{214}Pb (peaks at 295 and 352 keV) and ^{137}Cs via its peak at 661 keV.

Results

The core showed surface contents of unsupported ^{210}Pb of around 340 Bq kg^{-1} with a clear tendency for exponential decline with depth (fig 1). The calculated flux of unsupported ^{210}Pb is 420 Bq m^{-2} y^{-1} which is about 3 times higher than the expected flux (based on data shown in Appleby, 2001). This indicates that the site is subject to sediment focusing.

The content of the isotope ^{137}Cs was low and only consistently above detection limits in the upper 8 cm of the core.

CRS-modelling has been applied on the profile using a modified method (Appleby, 2001; Andersen 2017) where the activity below 22 cm is calculated on the basis of the regression shown in fig 2. The result is given in table 2 and fig 3 and 4.

The chronology given in table 2 is only valid if bioturbation and other sediment mixing is negligible. If this is not the case, ages given in table 2 are underestimated and accumulation rates are overestimated. However, the profile of unsupported ^{210}Pb showed a fairly uniform exponential decline with depth which indicates that mixing is not significant. Additionally, measurable content of ^{137}Cs was only detected in the upper part of the core which also indicates that mixing cannot be severe and the chronology is therefore believed to be reliable.

Copenhagen, August 19th 2019

Thorbjørn J Andersen
Professor,
IGN, University of Copenhagen
Oester Voldgade 10, 1350 Copenhagen K, Denmark

Reference:

Andersen, T.J., 2017. Some Practical Considerations Regarding the Application of ^{210}Pb and ^{137}Cs Dating to Estuarine Sediments. Applications of Paleoenvironmental Techniques in Estuarine Studies . Developments in Paleoenvironmental Research (DPER), Vol. 20, p 121-140.

Appleby, P.G., 2001. Chronostratigraphic techniques in recent sediments. In: Last, W.M & Smol, J.P. (eds) Tracking environmental change using lake sediments. Volume 1: Basin analysis, coring and chronological techniques. Kluwer Academic Publishers, the Netherlands.

Table 1. Raw data, R1869MC016A

Depth	Pb-210tot	error Pb-210 tot	Pb-210 supp	error Pb-210 sup	Pb-210 unsup	error Pb-210 unsup	Cs-137	error Cs-137
cm	Bq kg-1	Bq kg-1	Bq kg-1	Bq kg-1	Bq kg-1	Bq kg-1	Bq kg-1	Bq kg-1
0.50	369	25	25	6	344	31	2	1
1.50	348	48	34	0	314	48	4	8
2.50	309	27	26	4	283	31	7	1
3.50	231	31	20	6	210	37	5	3
4.50	231	20	24	2	207	22	3	1
5.50	216	15	25	0	192	16	5	1
6.50	146	16	15	8	132	24	3	1
7.50	113	13	22	2	91	16	5	1
8.50	85	11	22	4	63	15	2	1
9.50	91	8	24	3	67	12	1	1
10.50	81	10	24	0	57	10	2	1
14.50	59	8	24	1	35	9	0	0
15.50	51	8	23	2	29	10	0	0
18.50	33	3	21	2	11	5	0	0
20.50	26	4	22	4	4	8	0	0

Table 2, chronology core R1869MC016A

Depth	Age	error age	Date	acc rate	error rate	Date acc rate
cm	y	y	y	(kg m-2 y-1)	(kg m-2 y-1)	y
			2018			
0.5	2	2	2016	1.19	0.12	2017
1.5	6	2	2012	1.13	0.17	2014
2.5	11	2	2007	1.08	0.13	2010
3.5	16	2	2002	1.13	0.20	2005
4.5	21	2	1997	1.14	0.14	2000
5.5	27	2	1991	1.00	0.11	1994
6.5	34	3	1984	1.01	0.19	1987
7.5	40	3	1978	1.21	0.23	1981
8.5	44	4	1974	1.48	0.36	1976
9.5	49	4	1969	1.51	0.31	1971
10.5	55	5	1963	1.34	0.26	1966
14.5	85	12	1933	1.07	0.47	1948
15.5	95	9	1923	0.80	0.27	1928
18.5	131	24	1887	0.66	0.53	1905

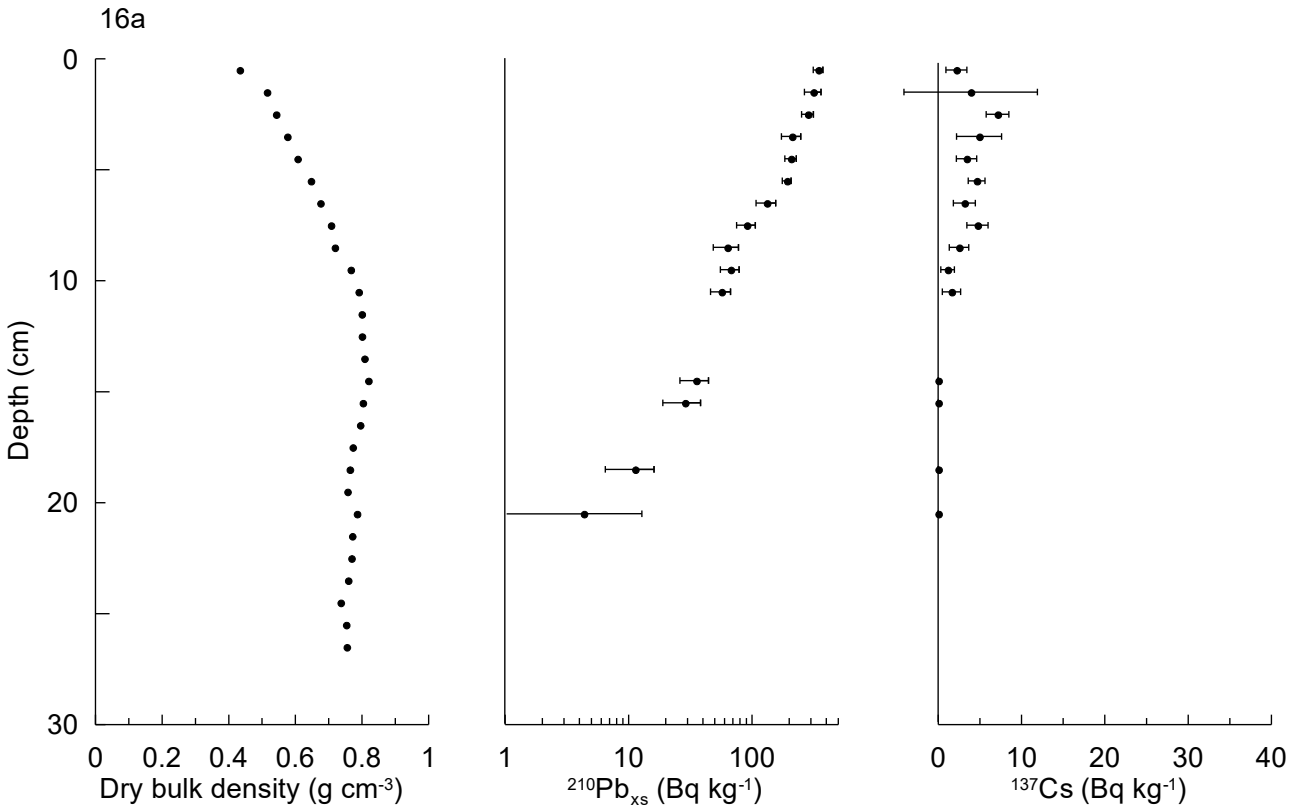

Fig 1

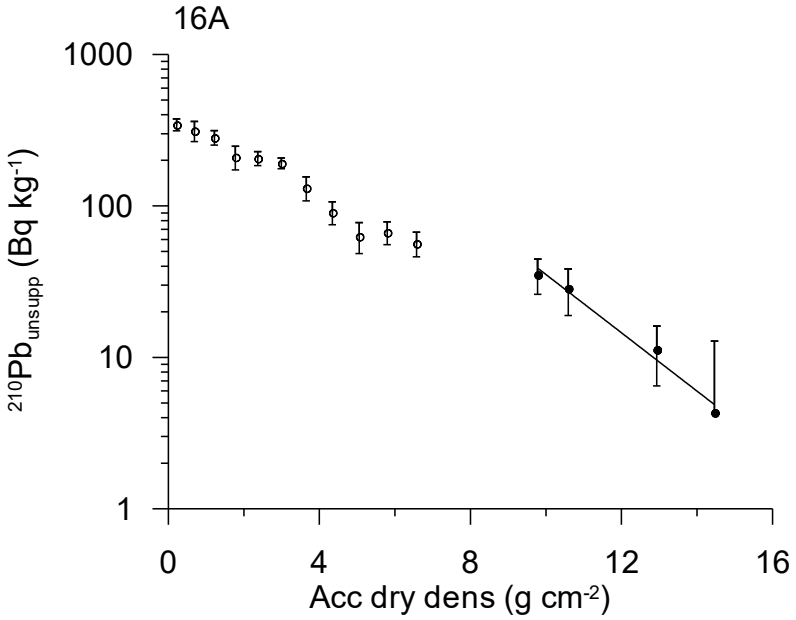

Fig 2. Regression of unsupported ^{210}Pb vs accumulated dry density.

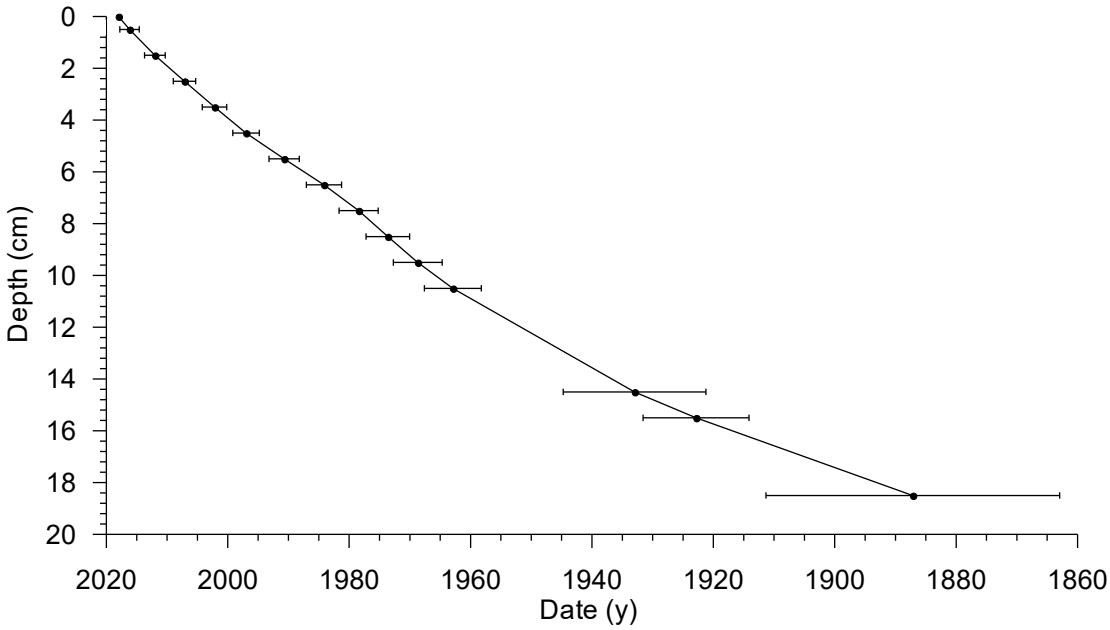
Depth (cm)
0
2
4
6
8
10
12
14
16
18
20
2020
2000
1980
1960
1940
1920
1900
1880
1860
Date (y)

Fig 3

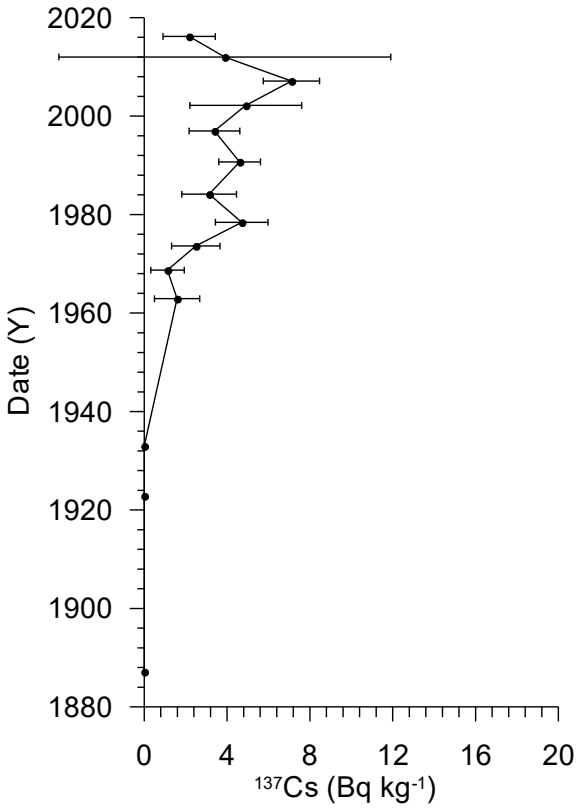
Date (Y)
2020
2000
1980
1960
1940
1920
1900
1880
0
4
8
12
16
20
137Cs (Bq kg-1)

Fig 4

Gamma Dating Center Copenhagen

Copenhagen, August 19th, 2019

Thorbjørn J. Andersen
Department of Geosciences and Natural Resource Management (IGN)
University of Copenhagen
Oester Voldgade 10
1350 Copenhagen K
e-mail tja@ign.ku.dk
phone +45 35 32 25 03
fax +45 35 32 25 01

Dating of core R1887MC022A

Dating of core R1887MC022A

Methods

The samples have been analysed for the activity of ^{210}Pb, ^{226}Ra and ^{137}Cs via gammaspectrometry at the Gamma Dating Center, Institute of Geography, University of Copenhagen. The measurements were carried out on a Canberra ultralow-background Ge-detector. ^{210}Pb was measured via its gamma-peak at 46,5 keV, ^{226}Ra via the granddaughter ^{214}Pb (peaks at 295 and 352 keV) and ^{137}Cs via its peak at 661 keV.

Results

The core showed surface contents of unsupported ^{210}Pb of around 260 Bq kg^{-1} with a clear tendency for exponential decline with depth (fig 1). The calculated flux of unsupported ^{210}Pb is 355 Bq m^{-2} y^{-1} which is about 3 times higher than the expected flux (based on data shown in Appleby, 2001). This indicates that the site is subject to sediment focusing.

The content of the isotope ^{137}Cs was fairly low and only consistently above detection limits in the upper 17 cm of the core. However, a distinct peak was observed at a depth of 12.5 cm.

CRS-modelling has been applied on the profile using a modified method (Appleby, 2001; Andersen 2017) where the activity below 22 cm is calculated on the basis of the regression shown in fig 2. The chronology calculated on the basis of this places the peak in 137Cs to 1954 which is clearly before the likely date of 1963. A final chronology has therefore been calculated in which the peak is set to 1963. The result is given in table 2 and fig 3 and 4.

The chronology given in table 2 is only valid if bioturbation and other sediment mixing is negligible. However, the distinct peak in ^{137}Cs indicates that mixing must be very limited and the chronology is therefore believed to be reliable.

Copenhagen, August 19th 2019

Thorbjørn J Andersen
Professor,
IGN, University of Copenhagen
Oester Voldgade 10, 1350 Copenhagen K, Denmark

Reference:

Andersen, T.J., 2017. Some Practical Considerations Regarding the Application of ^{210}Pb and ^{137}Cs Dating to Estuarine Sediments. Applications of Paleoenvironmental Techniques in Estuarine Studies . Developments in Paleoenvironmental Research (DPER), Vol. 20, p 121-140.

Appleby, P.G., 2001. Chronostratigraphic techniques in recent sediments. In: Last, W.M & Smol, J.P. (eds) Tracking environmental change using lake sediments. Volume 1: Basin analysis, coring and chronological techniques. Kluwer Academic Publishers, the Netherlands.

Table 1. Raw data, R1887MC022A

Depth	Pb-210tot	error Pb-210 tot	Pb-210 supp	error Pb-210 sup	Pb-210 unsup	error Pb-210 unsup	Cs-137	error Cs-137
cm	Bq kg-1	Bq kg-1	Bq kg-1	Bq kg-1	Bq kg-1	Bq kg-1	Bq kg-1	Bq kg-1
0.5	300	23	44	1	256	24	4	2
1.5	308	28	54	4	254	32	3	3
2.5	282	26	53	2	229	28	3	0
3.5	240	13	65	2	176	16	7	1
4.5	231	25	50	1	181	26	10	3
5.5	220	22	39	4	181	26	7	2
6.5	177	20	51	7	126	27	11	2
8.5	148	16	39	5	109	21	10	2
10.5	83	11	41	3	42	14	5	2
11.5	97	13	43	6	54	19	5	2
12.5	83	12	30	10	53	22	32	3
14.5	74	10	49	3	25	13	2	2
16.5	64	6	43	3	21	9	3	1
20.5	46	7	48	0	1	8	1	2
22.5	58	7	43	1	15	8	2	1
26.5	44	6	42	1	2	7	0	0

Table 2, chronology core R1887MC022A

Depth	Age	error age	Date	acc rate	error rate	Date acc rate
cm	y	y	y	(kg m-2 y-1)	(kg m-2 y-1)	y
			2018			
0.5	1	2	2017	1.36	0.15	2017
1.5	5	2	2013	1.27	0.17	2015
2.5	8	2	2010	1.20	0.17	2012
3.5	12	2	2006	1.28	0.15	2008
4.5	16	3	2002	1.28	0.21	2004
5.5	22	3	1996	1.09	0.18	1999
6.5	27	4	1991	1.08	0.23	1994
8.5	40	5	1978	1.06	0.25	1984
10.5	52	6	1966	1.12	0.42	1972
11.5	57	7	1961	1.34	0.52	1963
12.5	64	8	1954	1.01	0.43	1958
14.5	77	12	1941	1.03	0.61	1948
16.5	89	15	1929	1.19	0.70	1935
20.5	107	25	1911	1.57	10.32	1920
22.5	118	26	1900	1.36	1.15	1905

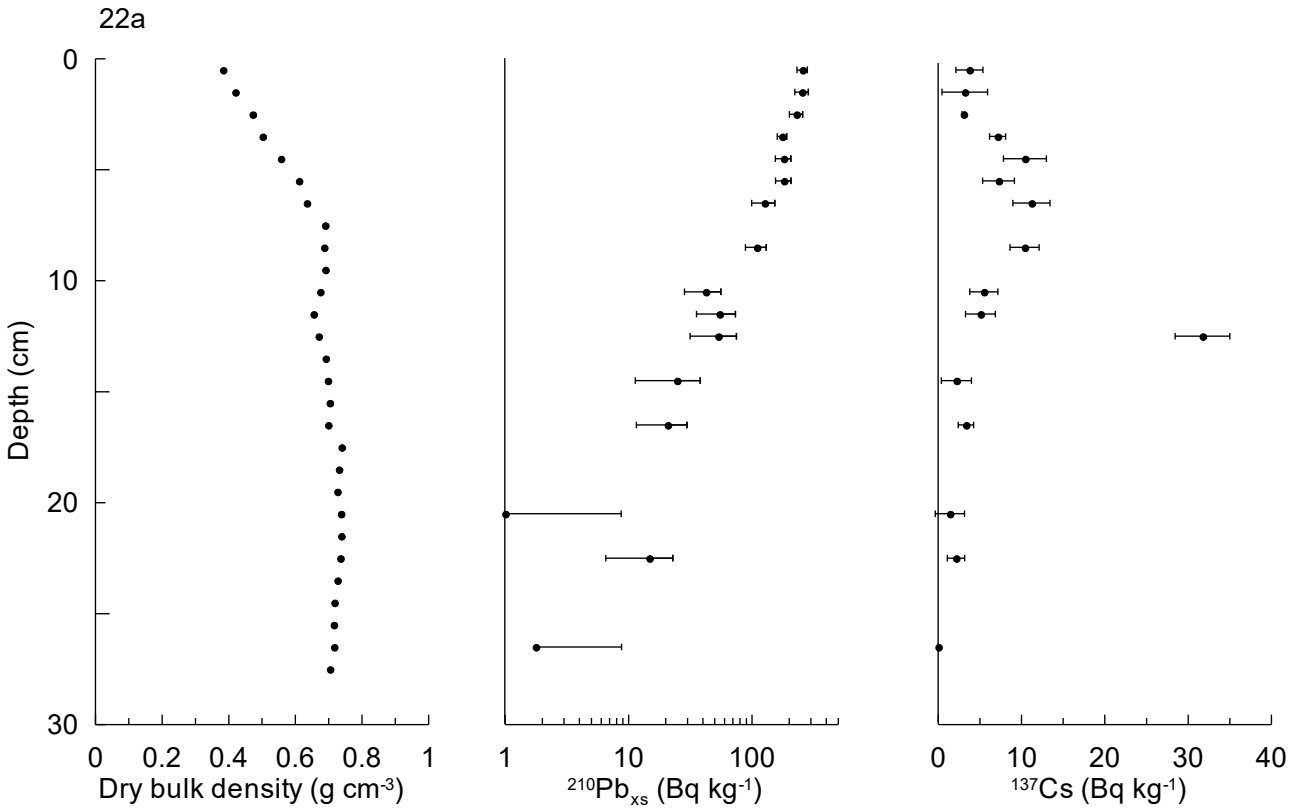

Fig 1

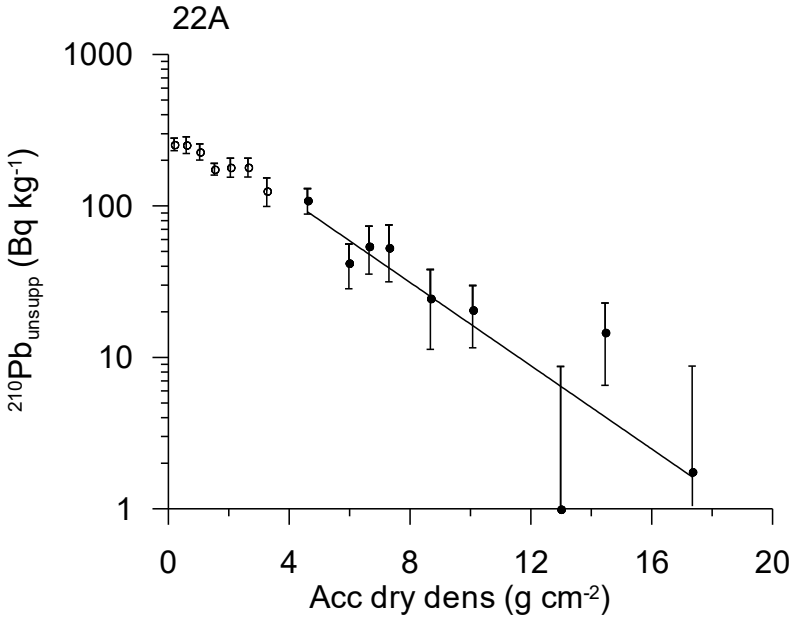

Fig 2. Regression of unsupported ^{210}Pb vs accumulated dry density.

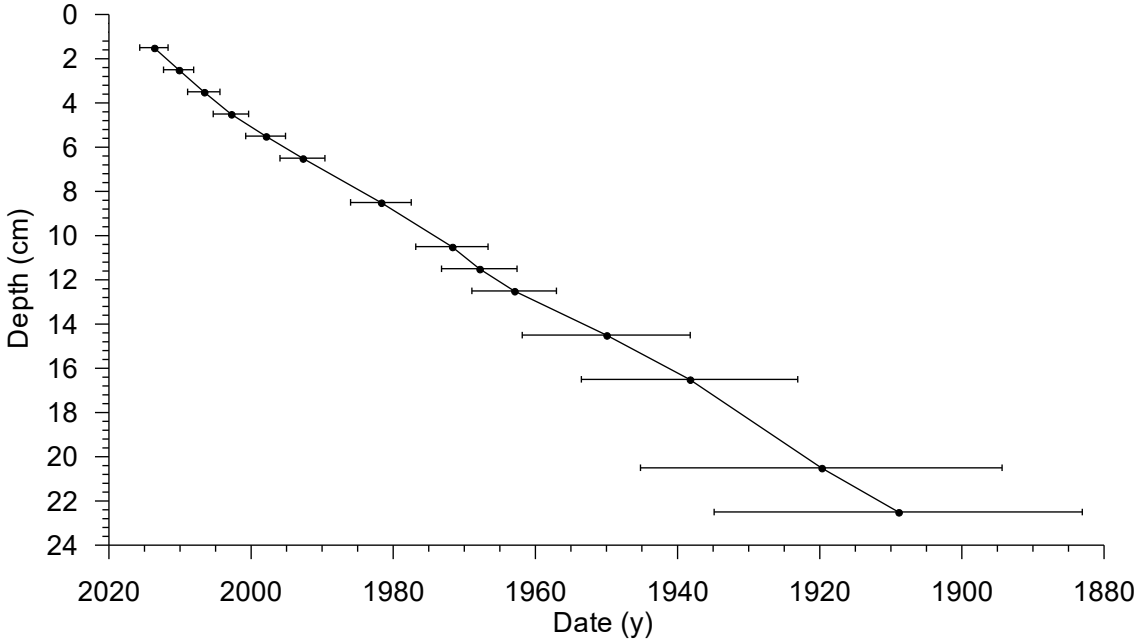
Depth (cm)
0
2
4
6
8
10
12
14
16
18
20
22
24
2020
2000
1980
1960
1940
1920
1900
1880
Date (y)

Fig 3

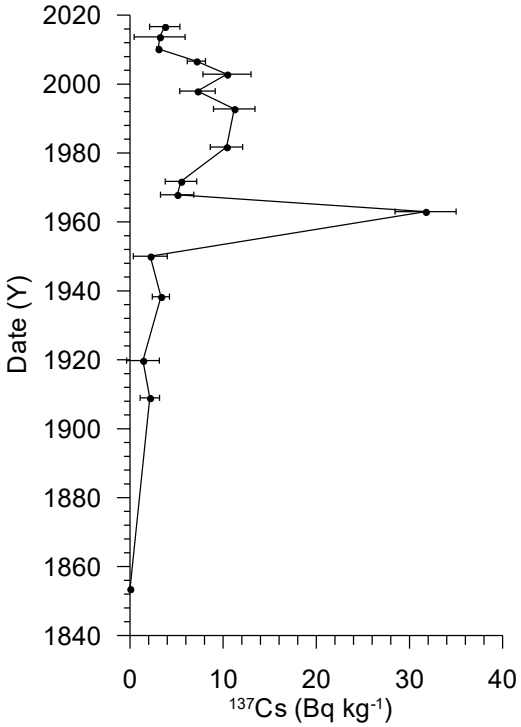
Date (Y)
2020
2000
1980
1960
1940
1920
1900
1880
1860
1840
0
10
20
30
40
137Cs (Bq kg-1)

Fig 4

Vedlegg 5

AMS^{14}C dateringsanalyser

Leverandør: ^{14}Chrono Centre

Queens University, Belfast,

Nord-Irland.

UBANo	Sample ID	Material Type	^{14}C Age	±	F14C	±	mg Graphite
UBA-41563	R1869MC016A 24-25 cm	foraminifers	692	18	0.9174	0.0020	0.981

Henning K. B.
Jensen Jensen
Geological Survey of
Norway
Leiv Eirikssonsvei 39
Trondheim 7491
Norway
Customer No.
2310390

^{14}CHRONO
Centre
Queens University
Belfast
42 Fitzwilliam
Street
Belfast BT9 6AX
Northern Ireland

Radiocarbon Date Certificate

Laboratory Identification:	UBA-41563
Date of Measurement:	2019-09-25
Site:	R1869MC016A
Sample ID:	R1869MC016A 24-25 cm
Material Dated:	shell or other carbonates
Pretreatment:	Acid Etch
mg Graphite:	0.981
Submitted by:	Henning K. B. Jensen Jensen

Conventional ^{14}C Age:	692±18 BP
Fraction corrected	using AMS δ^{13}C

Information about radiocarbon calibration

RADIOCARBON CALIBRATION PROGRAM*
CALIB REV7.0.1

*To be used in conjunction with:
Stuiver, M., and Reimer, P.J., 1993, Radiocarbon, 35, 215-230.
Annotated results (text) - -

41563
UBA-41563
Radiocarbon Age BP 692 +/- 18
Calibration data set: intcal13.14c # Reimer et al. 2013

% area enclosed	cal AD age ranges	relative area under probability distribution
68.3 (1 sigma)	cal AD 1279- 1292	1.000
95.4 (2 sigma)	cal AD 1273- 1300	0.905
	1369- 1381	0.095

References for calibration datasets:
Reimer PJ, Bard E, Bayliss A, Beck JW, Blackwell PG, Bronk Ramsey C, Buck CE Cheng H, Edwards RL, Friedrich M, Grootes PM, Guilderson TP, Haflidason H, Hajdas I, HattÃ© C, Heaton TJ, Hogg AG, Hughen KA, Kaiser KF, Kromer B, Manning SW, Niu M, Reimer RW, Richards DA, Scott EM, Southon JR, Turney CSM, van der Plicht J.
IntCal13 and MARINE13 radiocarbon age calibration curves 0-50000 years calBP
Radiocarbon 55(4). DOI: 10.2458/azu_js_rc.55.16947

Comments:
* This standard deviation (error) includes a lab error multiplier.
** 1 sigma = square root of (sample std. dev.^2 + curve std. dev.^2)
** 2 sigma = 2 x square root of (sample std. dev.^2 + curve std. dev.^2)
where ^2 = quantity squared.
[ ] = calibrated range impinges on end of calibration data set
0* represents a "negative" age BP
1955* or 1960* denote influence of nuclear testing C-14

NOTE: Cal ages and ranges are rounded to the nearest year which may be too precise in many instances. Users are advised to round results to the nearest 10 yr for samples with standard deviation in the radiocarbon age greater than 50 yr.

<>

Vedlegg 6

NGI rapport: Mikroplastdata fra indre Kongsfjorden, indre Rijpfjorden, Bjørnøytransektet,
samt testanalyser for kontaminering.

REPORT

Microplastics in Svalbard fjords and Bjørnøy transect sediments

MAREANO SURVEY OF SVALBARD

DOC.NO. 20190263-01-R
REV.NO. 0 / 2019-11-20

NORWEGIAN GEOTECHNICAL INSTITUTE
NGI.NO

Project

Project title:	Microplastics in Svalbard fjords and Bjørnøy transect Sediments
Document title:	MAREANO survey of Svalbard
Document no.:	20190263-01-R
Date:	2019-11-20
Revision no. /rev. date:	0

Client

Client:	NGU
Client contact person:	Henning Jensen
Contract reference:	Contract signed 2019-05-20

for NGI

Project manager:	Heidi Knutsen
Prepared by:	Heidi Knutsen, Cecilie Singdahl-Larsen og Jakob Bonnevie Cyvin
Reviewed by:	Hans Peter Arp

NORWEGIAN GEOTECHNICAL INSTITUTE
NGI.NO

Main office
PO Box 3930 Ullevaal St.
NO-0806 Oslo
Norway

Trondheim office
PO Box 5687 Torgarden
NO-7485 Trondheim
Norway

T 22 02 30 00
F 22 23 04 48
NGI@ngi.no

BIC NO. DNBANOKK
IBAN NO26 5096 05 01281
ORGANISATION NO.
958 254 318MVA

ISO 9001/14001
CERTIFIED BY BSI
FS 32989/EMS 612006

Summary

MAREANO surveys at Svalbard and a transect from the continental shelf to the slope west of Bjørnøya (Bjørnøy transect) were conducted in 2018 and 2019, where sediment samples from Kongsfjorden, Rijpfjorden and the Bjørnøy transect were sampled for the analysis of microplastics and other contaminants. The Norwegian Geotechnical Institute (NGI) has, on behalf of NGU, performed the microplastics analyses of the sediment samples, as described in this report.

Since the study focussed on a remote area that is expected to have low concentrations of microplastics, particular focus was placed on analysis of blanks. The following blanks were tested: method blanks, quantifying microplastics in the lab analysis method; sampling blanks, quantifying microplastics from the expedition and equipment used; deep-sediment field blanks, quantifying microplastics appearing in sediment from the bottom of the sediment cores (i.e. samples dated previous to the existence of plastic); tube contact blanks, quantifying microplastics in samples over the entire sediment core diameter vs those sampled in the middle of the sediment core; and recovery blanks, quantifying the recovery rates of spiked plastic.

Method blanks (n=3) were found to be a major source of microplastics contamination in general. Sampling blanks (n=4) only had slightly larger microplastic concentrations than method blanks. Thus, it was concluded that the contribution of airborne microplastic contamination from the field work on board RV G.O Sars was insignificant compared to the analytical method. The amount of microplastics in the field blanks (n=3) ranged from not detected (n.d.) to 260 particles/kg dry sediment (mean ± standard deviation: 120 ± 130 particles/kg). PVC and PE-chlorinated were among the most abundant microplastics. The origin of these microplastics is most likely the PVC tubes used for the sediment core sampling. This is the best type of blank to use for sediment analysis; however, the PVC/PE-chlorinated data were considered compromised based on the choice of sampling tube.

Surface sediments (top 2 cm) from Svalbard (inner Kongsfjord, n=3; and inner Rijpfjord, n=3) and the Barents Sea (Bjørnøy transect, n=4) have been analysed for microplastics. Overall, the amount of microplastic particles (45-1000 µm) ranged widely, from n.d. to 560 particles/kg dry sediment (230 ± 180 particles/kg). There were no statistically significant geographical differences. These concentrations are lower than found in a previous study that looked at microplastics in Arctic deep-sea sediments from the HAUSGARTEN observatory, west of Svalbard (n = 9; 42-6595 particles/kg). This difference can to some extent be explained by differences in the methods between the studies. Whereas the previous study looked at plastic particles from 10 µm – 1mm, this one focussed on microplastics between 45 µm – 1mm. The relatively high microplastic quantities in the HAUSGARTEN sediments is due in part to this difference in size fractions and also that HAUSGARTEN may be in or close to a plastic accumulation area.[1]

The results for the Barents Sea compare well with an earlier study using a similar method[2, 3], where microplastic concentrations ranged from 53 to 810 particles/kg (320 ± 330 particles/kg) in four Barents Sea samples, whereas this study reported microplastic abundances from 46 to 430 particles/kg (220 ± 190 particles/kg; n = 4). In both studies phenoxy resin, PE-oxidized and rubber resins were commonly found along with other microplastics.

The following recommendations are suggested for the future:

Future field sampling:

- Use tubes with a less common plastic than PVC (e.g. polycarbonate/plexiglass) for sampling of sediment cores, or alternatively steel sediment corers. Be sure to keep the tubes sealed until use, to minimize airborne microplastics contamination.
- Use deep sediment (i.e. deep in the sampling tubes, ideally older than the 20th century) as field blanks to correct for contamination during sampling, transport and laboratory analysis.
- Limit the use of plastic equipment as much as possible. For instance, use glass jars sealed with aluminium foil instead of Rilsan® bags (nylon) for sampling.
- Select location well suited for taking out samples from sediment cores for microplastic analysis (e.g. a "clean room").
- Continue with field blanks, method blanks and other control samples as part of sampling strategy.

Laboratory considerations:

- If field blanks are not available, include as a minimum method blanks to control for laboratory contamination. In this study, the method blanks showed that the laboratory method was the most substantial source of plastic contamination in the samples.
- Use analytical equipment to identify potential microplastics and other particles (e.g. FT-IR or Raman spectroscopy).
- Limit the use of plastic equipment as much as possible.
- Report method specific details, as these are important for comparison of results (e.g. size of microplastics investigated, chemicals for oxidation, density of separation fluid if used, etc.)
- Record particle size distribution for better comparison with literature.

Contents

Appendix

Review and reference page

1 Introduction

1.1 MAREANO survey at Svalbard

The Geological Survey of Norway (NGU) participates in the MAREANO programme as part of the Executive Groups responsible for carrying out field sampling and other scientific activities. The MAREANO programme maps depth and topography, sediment composition, biodiversity, habitats and biotopes as well as pollution in the seabed in Norwegian offshore areas, to address critical questions related to the Norwegian seabed.

In 2018, a MAREANO survey at Svalbard was conducted, where sediment samples from inner Kongsfjord (n = 3) and inner Rijpfjord (n = 3) were sampled for the analysis of microplastics and other contaminants. In 2019 a MAREANO survey adjacent to Bjørnøya in the Bjørnøy transect was conducted, and samples from four locations were collected. The Norwegian Geotechnical Institute (NGI) has, on behalf of NGU, performed the microplastic analyses of the 10 sediment samples, as described in this report.

Figure 1 MAREANO survey in Svalbard and Bjørnøya 2018 – 2019.

1.2 Plastic pollution

In 2015 the production rate of plastic was 380 million metric tons (MT) plastic, and since then production rates are forecasted to be increasing.[4] Unfortunately, many countries still have inefficient waste management and water treatment systems that allow for leakage to the environment. Mismanaged plastic waste could triple from 60-99 million MT in 2015 to 155-265 MT by 2060, assuming a business-as-usual scenario.[5] Plastics are designed to be extremely durable and resistant to decay. While these characteristics are highly valued during usage, it has the implication that plastic emitted into the environment will remain for long periods of time. Plastic is currently found to be accumulating on remote islands, the sea surface, within the water column of the sea and on deep seafloor.

Recently, concern has been raised regarding smaller plastic pieces, referred to as microplastics; which may pose a threat to sensitive marine ecosystems. Microplastics are generally defined as plastic items smaller than 5 mm. These can originate from weathering of larger plastic items due to the influence of e.g. UV-light, mechanic abrasion, waves and temperature fluctuations (so-called secondary microplastics), or from direct emissions of plastics that were manufactured smaller than 5 mm (so-called primary microplastics). A variety of studies suggest that the seafloor is the ultimate sink for microplastics.[1, 6, 7]. However, there have been relatively few surveys of microplastics on the sea floor, and few studies on the impacts of microplastics on benthic ecosystems as well.

Previously, microplastics (between 10 and 275 µm) have been found in marine sediments west of Svalbard, at the HAUSGARTEN observatory.[1] Nine sediment samples were taken from depths of 2342-5570 meters. The results indicate the wide spread of high numbers of microplastics (42-6595 particles/kg sediment; mean ± standard error: 4356 ± 675). Chlorinated polyethylene accounted for the largest proportion (38 %), followed by polyamide (22 %) and polypropylene (16 %). The results were among the first to demonstrate that microplastics are settling in arctic deep ocean-floor sediments. In a recent study, microplastics (between 11 and 475 µm) were also found in Arctic snow from Svalbard.[8] The concentration of microplastic particles in arctic snow was significantly lower (0-14x10^3 particles/L) than in European snow (0.19-154x10^3 particles/L), thus verifying that microplastics, like persistent organic pollutants, are capable of long range atmospheric transport. Material composition in the Arctic snow samples varied, but varnish materials, rubber, polyethylene and polyamide dominated overall. It can therefore be considered factual that both the atmospheric and oceanic currents can lead to arctic accumulation of microplastics. The MAREANO sediment samples reported here are of great interest regarding the distribution and presence of microplastics in the Arctic.

2 Materials and methods

2.1 Field work and sampling strategy

Sediment cores were sampled during sampling cruises with IMR research vessel, G.O. Sars, at different stations at Svalbard in August 2018 (inner Kongsfjord, 3 stations, and inner Rijpfjord, 3 stations) and April 2019 in the Barents Sea (Bjørnøy transect, 4 stations), as shown in Figure 2. Core samples were sampled by NGU and HI using a multicorer (produced by KC-Denmark, model 73.000), which gives six sediment cores with a maximum depth of ca. 50 cm. The multicorer tubes consist of transparent PVC-tubes with an inner diameter of 106 mm. The sampling was performed as described in MAREANO's chemistry program (www.mareano.no/resources/Metodedokument-Kjemiprogram-MAREANO-sluttversjon20190128-003-.pdf).

Samples were briefly (for 2-3 s) opened during tube recovery from the multicorer, and then kept sealed until opening at NGU in Trondheim, Norway. Care was taken to avoid potential contamination, which is difficult in the case of microplastics, as they are abundant in ambient air. Due to logistical reasons, the samples were opened outdoors at a small parking lot at NGU (Photo 1) with no traffic during sampling. Different sample types were sampled / prepared for microplastics analysis, as described in the following.

Figure 2 Sampling stations for surface samples S-01 – S-10. S-01 – S-03: inner Kongsfjord; S-04 - S-06: inner Rijpfjord; S-07 to S-10: Bjørnøy transect.

Photo 1 Overview of sealed sediment core in PVC tube (left) and detail photo of surface sediment (right).

The samples were placed in Rilsan® bags (FT-IR analysis at NGI showed these were made of nylon) and sent from NGU to NGI with DHL shipping. At NGI, the samples were stored at 2-4 °C until processing.

2.1.1 Surface samples

Sediment surface samples (n = 10, Table 1 and Figure 2) were prepared from the sediment cores, by slicing off the top 2 cm with a metal spatula. The outermost part, which had been in contact with the PVC sampling tube, was discarded to minimize contamination (illustrated in Figure 3 and Photo 2).

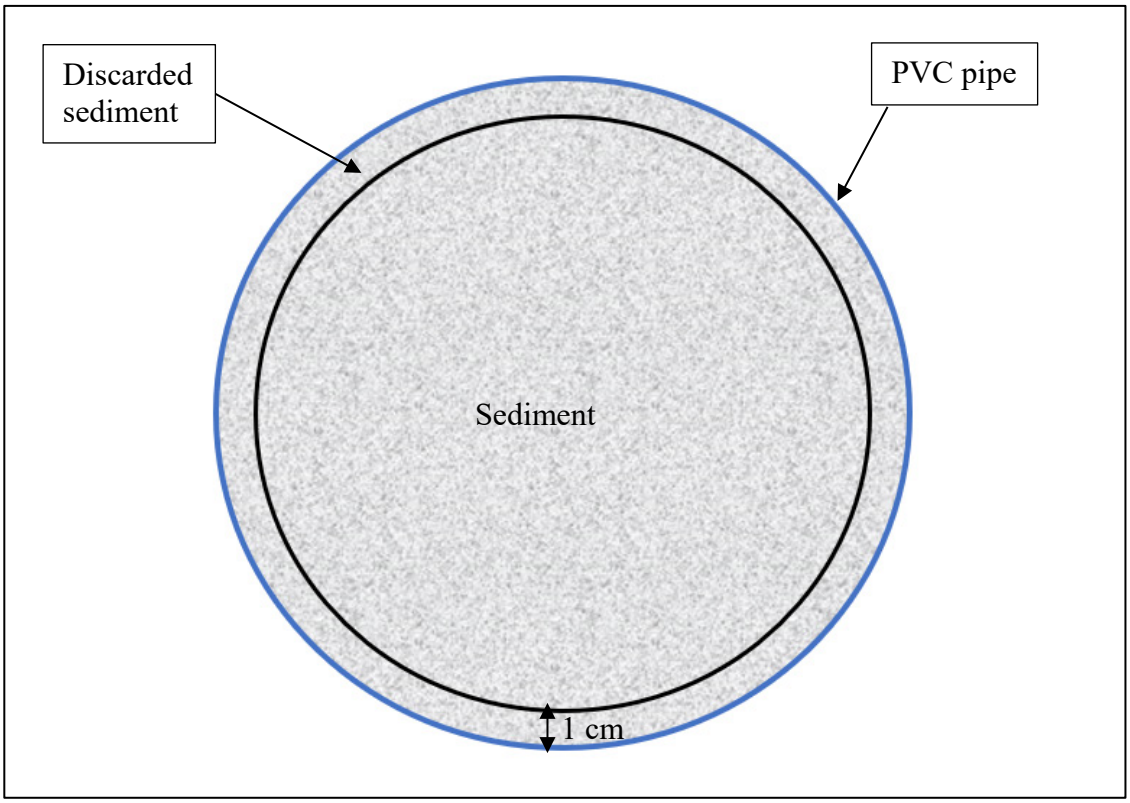

Figure 3 Schematic presentation of sediment core seen from above. The outer part (about 0-1 cm) was discarded, as this part had been in contact with the PCV tube used for core sampling.

Photo 2 Collection of surface sediment, showing how the outer part of sediment was sliced off with a metal spatula and discarded due to contact with the PVC tube.

Table 1 List of surface samples with station specific information

Sample ID	Sample depth (cm)	Station	Latitude	Longitude	Bottom depth (m)
S-01	0-2	R1846MC014	78.98480	11.70747	311.42
S-02	0-2	R1865MC015	79.10484	11.64824	274.63
S-03	0-2	R1869MC016	79.01981	11.41530	345.53
S-04	0-2	R1872MC019	80.03960	22.25330	144.65
S-05	0-2	R1878MC021	80.09196	22.15351	212.87
S-06	0-2	R1887MC022	80.17150	22.13449	208.04
S-07	0-2	R1951MC001	74.78769	18.56757	246.26
S-08	0-2	R1965MC002	74.80772	17.63731	301.84
S-09	0-2	R1994MC003	74.92973	14.60875	1477.45
S-10	0-2	R1998MC004	74.80246	13.52051	2089.10

2.1.2 Sampling blank

Sampling blanks (n = 4) were prepared by taking pre-washed, empty glass jars on the field trip and exposing them to the surroundings during sampling. Thus, the samples were not in direct contact with the sampling equipment, but were included to control for other field effects, such as airborne contamination from the transport route, contamination from the containers themselves etc.

2.1.3 Field blank

A field blank is often defined as a sample which is initially free of analyte (here microplastics), prepared in the field and treated as a real sample (includes contact with sampling equipment and exposure to the sampling site, stored in the same way as regular samples and which undergoes the analytical procedure). This type of blank controls for both field and analytical contamination.

In this project, field blanks (n = 3, Table 2) were prepared by sampling deep-sediment (> 30 cm depth) from sediment cores in the same area as the surface samples, assuming that the deeper sediment was from a time prior to plastic production (meaning they should in theory be free from microplastics). In agreement with the surface samples, the outermost part of the field blanks was discarded, as this had been in contact with the PVC tube used for sampling (illustrated in Figure 3). The purpose of the field blanks was to correct for microplastics abundance in the surface samples.

Table 2 List of field blanks used for correction of surface results.

Sample ID	Sample depth (cm)	Station	Area	Comment
B-1	32-34	R1869MC016	Inner Kongsfjord	From the same core as S-03
B-2	30-32	R1887MC022	Inner Rijpfjord	From the same core as S-06
S-12	33-35	R1965MC002	Bjørnøy transect	From the same core as S-08

Sediment cores from the same stations as B-1 and B-2 have been dated via gamma spectrometry at the Gamma Dating Centre, Institute of Geography, University of Copenhagen. According to the dating reports, sample B-1 and B-2 should both represent a time prior to year 1900 (Appendix C). B-1 has a sedimentation rate of approximately 1.5 mm per year, which suggests that B-1 at 32 – 34 cm depth is equivalent to approx. 200 years ago, i.e. early 19th century. A higher Pb^{210} sedimentation rate is measured in B-2, implying that the B-2 sample is 150 – 160 years back in time (i.e. 1858 – 1868). Thus, the selected sediment layers are well prior to introduction of microplastics to the marine environment, and beyond the depth of bioturbating animals. As the first plastic types were not commercially produced until in the late 1920s, it is assumed the field blanks should be plastic-free. Also, the selected samples B-1 at 32 – 34 cm depth and B-

2 at 30 – 32 cm depth are well below the depth of bioturbating animals, which potentially could mix microplastics into deeper sediment layers. With respect to sample S-12, there are no ^{210}Pb dating results from this core. However, based on ^{210}Pb data from locations to the north and east of the Bjørnøy transect (Jensen et al., 2018)[9], sedimentation rates are in the range 0.9-1.7 mm/year in this part of the Barents Sea. S-12 is therefore likely to have deposited in the 19th century, i.e. well before the introduction of microplastic.

2.1.4 PVC-tube contact test samples

To examine whether the PVC tubes used in core sampling were a source of PVC contamination, 10 deep-sediment samples (> 20 cm depth) were collected from five different stations / cores, assuming the depth was large enough to represent sediment from a time prior to plastic production. For each station, one sample was collected directly from the core (meaning it had been in direct contact with the PVC tube), whereas the other was sampled in the same way as the surface and field samples (i.e. the outer part of sediment was discarded, Figure 3).

Table 3 List of deep-sediment samples to test for contamination from the PVC sampling tubes. The station data are extracted from www.mareano.no chemistry database.

Sample ID	Sample depth (cm)	Station	Latitude	Longitude	Bottom depth (m)	Contact with PVC tube?
S-11	31-33	R1965MC002	70.4743	31.72450	399.56	Yes
S-12[1]	33-35	R1965MC002	70.4743	31.72450	399.56	No
S-13	26-28	R1225MC038	70.4743	31.7245	485.00	Yes
S-14	28-30	R1225MC038	70.4743	31.7245	485.00	No
S-15	20-22	R1512MC095	64.9880	5.9210	767.18	Yes
S-16	22-24	R1512MC095	64.9880	5.9210	767.18	No
S-17	30-32	R1349MC416	63.5907	5.5732	251.28	Yes
S-18	32-34	R1349MC416	63.5907	5.5732	251.28	No
S-19	25-27	R1359MC418	63.7195	6.1248	399.56	Yes
S-20	27-29	R1359MC418	63.7195	6.1248	399.56	No

[1]*This is the same sample as S-12 in Table 2*

2.2 Microplastics analysis

2.2.1 Sediment preparation

The first step of sample preparation was to homogenize the sediment by stirring the sample with a metal spoon in an aluminium tray. Then a portion of it (ca. 25 g wet weight) was transferred to a pre-weighed aluminium tray for dry matter analysis. The weight of the wet sediment sample was noted, and the sample was put in the oven at 60 °C for at least two days. Then, the dry weight was obtained and used to calculate the percent dry matter (DM%, Formula 1). A temperature of 60 °C was used instead of 110 °C, which is normally used to calculate DM%, in order to prevent the potential melting of microplastics in the sample.

$$\text{DM\%} = \frac{dry\ weight\ (g)}{wet\ weight\ (g)} * 100\% \qquad \textit{Formula 1}$$

Then, another portion from the same sample (ca 100 g wet weight) was transferred to a new pre-weighed aluminium tray. This sediment was used for the microplastics-sediment separation. A slurry was made by adding $ZnCl_2$-$CaCl_2$ (ρ ~1.52 g/cm^3) (from now on referred to as zinc-chloride) to the sediment.

2.2.2 Sediment density separation

NGI's Bauta Microplastic-Sediment Separator (BMSS) was used to separate microplastics from sediment (Figure 4). The BMSS was inspired by Munich Plastic-Sediment Separator (MPSS) by Imhof et al.[10] The setup of the BMSS consists of a 650 mm high glass column with a separate sample separation chamber on top. The separation chamber has a ½" ball valve on the top and a shut-off valve on the bottom. This unit makes it possible to separate the top-layer of the solution, which after density separation includes non-colloidal particles with a density less than the separation fluid used (i.e. microplastics, organic material and debris with ρ < 1.52 g/cm^3), whereas all denser particles are collected in the sediment chamber.

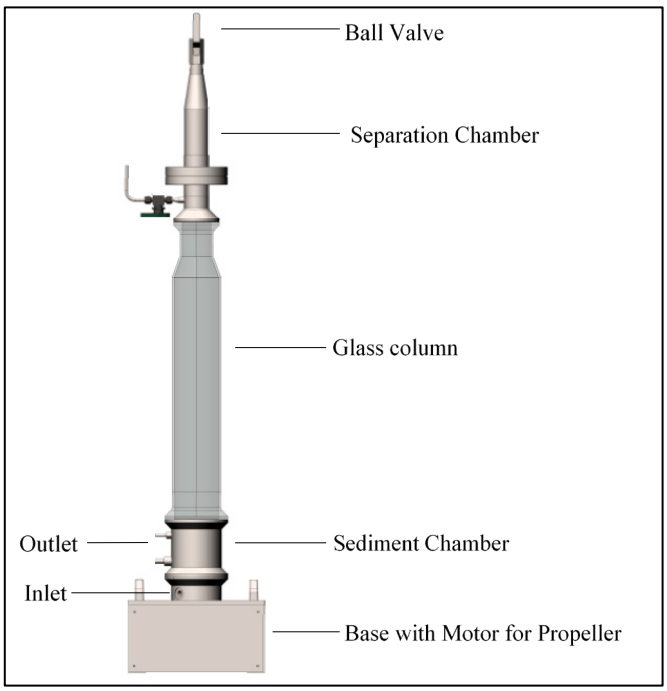

Figure 4 NGI's Bauta Microplastic-Sediment Separator

The BMSS was thoroughly cleaned, flushed with distilled water and inspected before each use, to ensure minimal particle contamination. The filtered (Whatman glass microfiber filter, grade GF/D, pore size 2.7 µm and diameter 150 mm) high-density zinc-chloride solution ($\rho \geq 1.52$ g/cm^3)[11] was filled from the bottom of the sediment chamber and into the glass column (until the constriction of the column). Then, the slurry of sediment and zinc-chloride was added to the BMSS from the top, using a spoon. After stirring, the sample was left for sedimentation overnight, or longer if needed.

After sedimentation, the separation chamber was attached to the top of the column, and the zinc-chloride solution was elevated by addition of zinc-chloride solution through the inlet valve. After 5 minutes, the separation chamber was closed to collect the separated microplastics. Then the zinc-chloride solution level was lowered, and the separator unit was taken off for the separation and filtration onto a 45 µm stainless steel mesh filter (#300 Mesh - 0.045mm Aperture - 0.04mm Wire Diameter - SS316 Grade - Woven Wire, purchased from the Mesh Company, Warrington UK), using a vacuum pump and flushing with MilliQ-water and methanol. The filtration step was done twice, and a pre-washed and dried steel spoon was used to loosen particles that stuck to the walls on the constriction of the glass column.

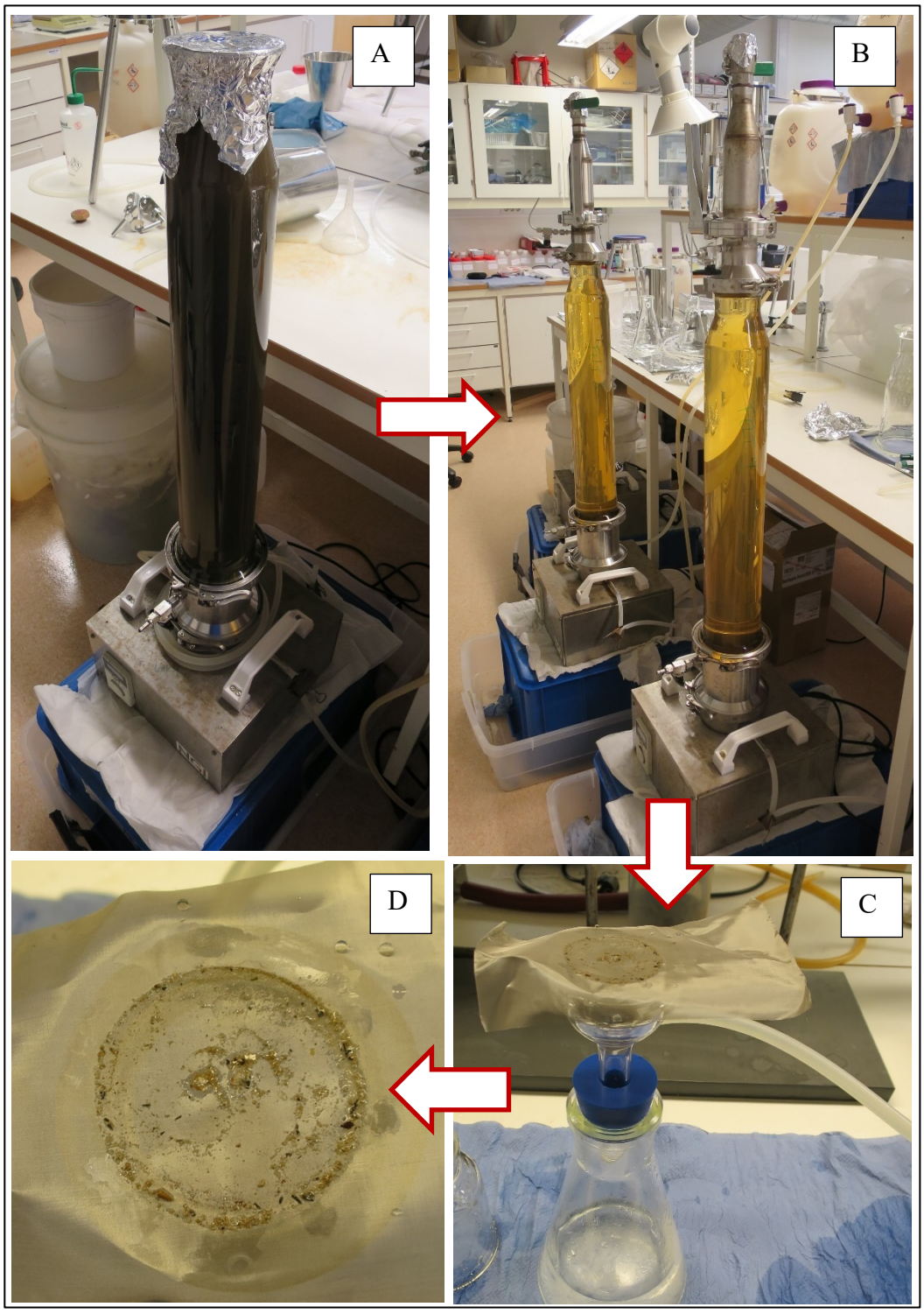

Figure 5 A: sediment sample and zinc chloride solution ($\rho \geq 1.52$ g/cm^3) for separation; B: after 24 hours of density separation; C: filtered microplastics sample; D: close-up of filtered sample.

The steel mesh filter containing the combined filtrate sample after rinsing several times (see part D in Figure 5) was carefully folded into a "tea-bag" like form and tied up with a pre-weighed steel wire. Finally, the samples were dried over night at 60 °C and weighed before treatment by oxidation of organic matter.

2.2.3 Oxidation of organic matter

Organic material was removed by performing a chemical digestion process that consisted of two parts. Biogenic polymers, such as chitin and cellulose, were dissolved in the first step by using a mixture of urea, thiourea and NaOH.[12, 13] In the second step, the remaining sample is digested with 30 % H_2O_2 (prepared from 50 % stock solution) and 10 M NaOH. This process was done at least once for the separated samples.

2.2.4 Visual microscopy

Visual microscopy was performed to collect descriptive and qualitative data for the density separated and oxidized samples. First, the processed samples were transferred from the "tea bag" steel mesh filters and onto pre-cut, spherical steel mesh filters (pore size of 45 µm) with a diameter of 13 mm, which were used for both visual microscopy and subsequently for Fourier Transform Infrared Spectroscopy (FT-IR) microscope analysis of material composition. The sample material was transferred to the 13 mm filters by opening the “tea bag” filters into MilliQ water followed by vacuum filtration.

The processed samples were investigated by visual analysis using a microscope. The microscope was set at x10 and x40 magnification. As a basis for discerning plastic from non-plastic/biological material during the counting approach, MERIs “Guide to microplastic identification” was used.[14] In short, the particles that resembled microplastics were visually distinguished according to the following criteria: no cellular or organic structure visible, fibers should be equally thick throughout the entire length, and particles should present a clear and homogenous color. However, visual microscopy may lead to misidentification of microplastics, and several authors have therefore concluded that the visual identification error rate is unacceptably high, ranging from 33 to 70 %.[15] Therefore, FT-IR-analysis was performed to determine material composition (chapter 2.2.5).

Table 4 was used to categorize particles by shape, size and colour. The shape was divided into three categories: fibre, layer and granule. The size was divided into four categories: A, B, C and D, where group A are particles ≥ 45 µm to 100 µm, group B are particles between 100-300 µm, group C are particles between 300 - 1000 µm and group D are particles from 1 to 5 mm. The colour was divided into clear/white, light brown, dark brown, black, blue, red, green, orange and yellow. Particles with a pink colour were categorized as red, and the ones with a grey colour were categorized as black.

Table 4 Spreadsheet used to log data from visual microscopy. Size group A-D: A: ≥ 45 – 100 µm; B: 100 – 300 µm; C: 300 – 1000 µm; D: 1 – 5 mm.

Colour	Fiber 1D				Layer 2D				Granule 3D			
Clear/white												
Light brown												
Dark brown												
Black												
Blue												
Red												
Green												
Orange												
Yellow												

There were too many particles to be truly quantitative, so extrapolations were done based on parts of the filter, and unusual particles, the most abundant size fraction and the amount of clear/white, brown and black particles were consistently noted. Particles identified with visual microscopy were further analysed with FT-IR for determination of material composition.

2.2.5 FT-IR analysis

The micro FT-IR system used here was a Perkin Elmer Spotlight 200i FT-IR microscope, equipped with a Frontier FTIR spectrometer. The system consists of a microscope, spectrometer, PC, stage controller and joystick (Figure 6).

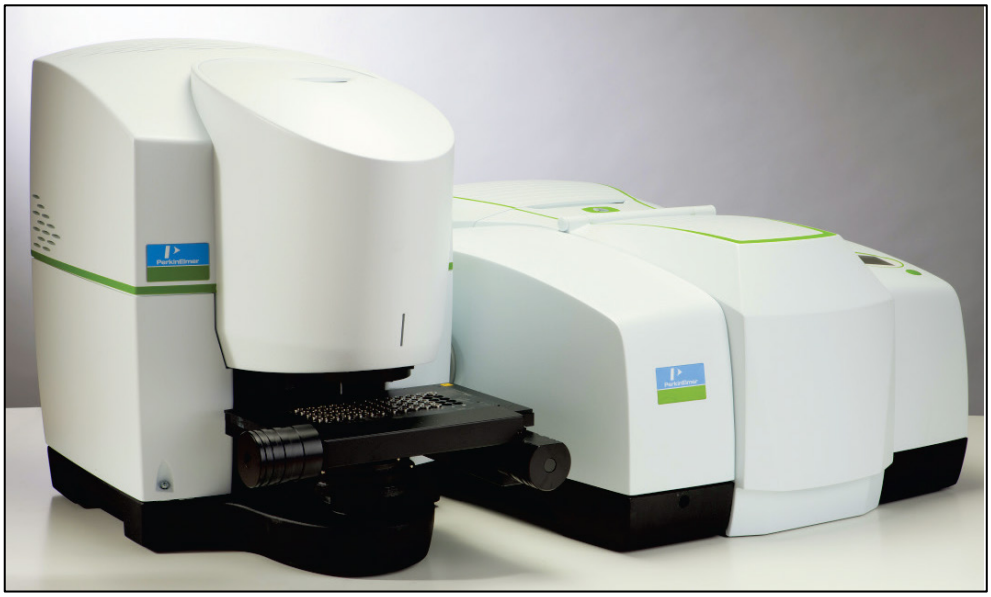

Figure 6 Spotlight 200i – microscope and Frontier IT System

Prior to analysis, the Spotlight 200i was set up, and the microscope was focussed as described in the Spotlight 200 User's Guide. The scan parameters were set to the following settings: resolution: 8-16 cm^{-1}, wave number range: 4000-600 cm^{-1}, 4 number of accumulations.

For samples with larger particles, large enough to be picked up by tweezers, their length was measured using Vernier callipers, and thereafter individual particle analyses using the Frontier ATR assembly was conducted. The ATR crystal was cleaned with methanol between each analysis to reduce the chance of cross-contamination between samples. For particles too small to be picked up, the analysis was performed in transmittance mode.

In transmittance mode, the infrared radiation penetrates the particle before arriving at the detector, giving an infrared spectrum of the entire volume of the particle. This mode works best with thin or translucent particles. Using the ATR technique allows for the analysis of materials that are too opaque for transmission measurements and too strongly absorbing for good reflectance measurements. The FT-IR microscope only scans the inner 10 mm of the total 13 mm filter, and thereby excludes some of particles on the edge of the filter (though these were a minority).

The obtained IR spectrums were compared with libraries of polymer spectra available through Perkin-Elmer, namely "Polymer", "ATR-Spectra", "Transmission-Spectra" and "Fluka". Particle identification is done through the software, which compares the obtained spectrum with those in the spectrum libraries, which includes a wide variety of plastic polymers, organic substances, salts and minerals, many of which are highly unlikely to be a major component of marine samples. The "Polymer" library also included typical polymer blends (e.g. polyethylene and polypropylene blends). Particles with a quality index ≥ 0.7 (i.e. 70 % match with FT-IR library) were accepted, whereas particles with a quality index <0.7 were rejected and are denoted "unknown" in this report. The identified items were categorized into the groups in Table 5.

Table 5 Particle categories used in this report.

Particle Category	Description
Unknown	Particles identified by FT-IR with a quality index < 0.7
Mineral	Particles with no organic chemical bond visible in the IR spectrum (such as inorganic salts, glass, etc.)
Oxy-resins*	Particles containing oxy-resins, such as ethoxy resin, epoxy resin, phenoxy resin, or bisphenol-a containing particles.
Petro-Pyro	Typical petroleum substances, such as hydrocarbon resins, petroleum products, etc.
Plastic*	Commercial synthetic polymers, or a weathered derivative thereof, such as oxygenated polymers; semi-synthetics derived from biopolymers like cellulose, such as rayon, viscose etc are not included
Rubber*	Particles identified as rubbers, polymers used as rubbers (e.g. SBR, silicon rubber), or resins containing rubber compounding products
Organic	Particles identified as organic macromolecules like cellulose, rayon, chitin, proteins, or in general particles containing organic carbon molecular bonds, that do not fit into any of the above categories

**Microplastics are in this report defined as oxy-resins, plastic polymers and rubbers.*

Plastic polymers were further subdivided into the plastic types in the table below. In case of blends, the main polymers in the composition was chosen.

Table 6 Plastic particle categories used in this report.

Plastic category	**Description**
PE	Polyethylene (E.g. LDPE, HDPE, LLDPE, etc.)
PE-chlorinated	Chlorinated polyethylene
PE-chlorosulfonated	Chlorosulfonated polyethylene
PE-oxidized	Oxidized polyethylene
PE:PP	Blends of polyethylene:polypropylene
PP	Polypropylene
PET	Polyester, polyethylene terephthalates
PS	Polystyrene
PTFE	Polytetrafluoroethylenes
PP-chlorinated	Chlorinated polypropylenes
PAM	Polyacrylamide
PMMA	Polymethylmethacrylate and other polyacrylates
PU	Polyurethane foam
PVF	Polyvinyl fluoride
PVC	Polyvinyl chloride
Melamine	Melamine (all resin blends)
Nylon	Nylon and polyamide
Unresolved	Synthetic polymers not belonging to the above list

2.3 Chemicals and solvents

Chemicals used during solution preparation are listed below.

Table 7 Chemicals

Chemical	Molecular formula	Manufacturer/ Distributor	Purity (%)
Zink chloride	$ZnCl_2$	VWR International	97
Calcium chloride	$CaCl_2$		90-98
Hydrogen peroxide	50 % H_2O_2		Analytical grade
Urea	$CO(NH_2)_2$	Sigma Aldrich	≥ 98
Sodium dodecyl sulphate	$CH_3(CH_2)_{11}OSO_3Na$		≥ 99
Thiourea	CH_4N_2S	Merck K GaA	≥ 98
Sodium hydroxide	NaOH		99-100

Table 8 Microplastics used in spiked blanks

Form	Polymer type	Manufacturer/ Distributor	Properties	
			Density (g/cm^3)	Diameter (µm)
Powder	Polyester (PET)	Goodfellow Cambridge Ltd. (UK)	1.40	75-300
Fibre	Polyester (PET)		1.39	17
Granulate	Polyester (PET)		1.40	3000-5000

2.4 Quality assurance

Contamination control was carried out throughout the sampling, processing and analysis. Several steps were taken to reduce contamination, which included:

- Lab coats, cotton clothing and hairnet were used in the laboratory.
- All glassware was flushed with MilliQ water and visually inspected before each use.
- All steel mesh filters were inspected with visual microscopy before use. If particles were observed, ultrasonic cleaning in MilliQ was performed.
- The samples were sealed as much as possible to prevent airborne contamination.

Presence of contamination in blank samples was accounted for in the results.

2.4.1 Method blank

Method blanks (n = 3) were used to check for contamination from the laboratory method. Method blanks were prepared in the laboratory, by adding zinc chloride to a sediment-free aluminium tray and followed by the exact same analysis as for sediment samples.

2.4.2 Sampling blank

The sampling blanks (n = 4) were introduced to the BMSS by flushing the empty glass containers from the field work with a wash bottle with zinc chloride, followed by analysis. The sampling blanks were used to control for contamination from shipping and the laboratory method.

2.4.3 Field blank

The field blanks (n = 3) were analysed in the same way as sediment samples and used to correct the microplastic concentrations in surface samples from the same geographical area. The field blanks were thus used to correct for contamination from the sampling, transport and laboratory method.

2.4.4 Spiked blanks

Spiked blanks were prepared after processing an actual sample by transferring some of the remaining "high-density material-free sediment" after separation in the BMSS from the sediment chamber, to a pre-weighed aluminium tray and spiked with either plastic fibres and granules or plastic powder and granules (Table 8). Five granules were used, and the weight of the granules, fibres and powder was noted before spiking the sediment. The spiked sediment was then re-introduced to the bauta. The purpose of the spiked blanks was to test the recoveries of the method. The spiked sample recovery ($f_{recovery}$) was calculated by using the following equation:

$$f_{recovery}(\%) = \frac{m_{recovery\ blank} - (m_{filter} + m_{wire})}{m_{spiking\ material}} \qquad \textit{Formula 2}$$

2.5 Microplastic concentrations

The number of particles of a specific type of microplastic based on the type of polymer in the analysed sediment surface samples ($n_{p,sample}$), was corrected according to the average number of corresponding particles in the field blanks ($n_{p,field\ blank}$) and the method blank ($n_{p,method\ blank}$). The results were further corrected according to the recovery correction factor ($f_{recovery}$) obtained from the spiked blanks as shown in Formula 3.

$$n_{plastic} = (n_{p,sample} - n_{p,field\ blank} - n_{p,method\ blank})/f_{recovery} \qquad \textit{Formula 3}$$

The field blank should account for microplastics introduced from the field sampling as well as from the laboratory method, but as the method blank samples could contain additional microplastics that were not all present in the field blanks, it was considered important to include this.

Based on the weight of the processed samples after density separation and chemical digestion (mg potential MP) and the percentage of identified microplastics in the samples, microplastic concentrations were estimated on weight basis.

$$c_{MP}\left(\frac{mg\ MP}{kg\ d.w.}\right) = \frac{mg\ potential\ MP}{kg\ d.w.} * \frac{n_{plastic}}{n_{tot}} \qquad \textit{Formula 4}$$

Microplastic concentrations were also calculated as number of microplastic particles (blank-corrected) per kg sediment:

$$c_{MP}\left(\frac{items\ MP}{kg\ d.w.}\right) = \frac{n_{plastic}}{kg\ d.w.} \qquad \textit{Formula 5}$$

The presence of non-plastic particles (organic, mineral, petro-pyro and unknown particles) in the sediment surface samples were corrected according to the respective amounts in the sampling blanks.

3 Results and discussion

3.1 Visual microscopy

Pictures from visual microscopy are shown in Appendix A. The particles encountered in the samples were mostly from 90 to 135 µm (size category A and B). Particles with the colour blue, red, green, orange and yellow were observed in most samples (Appendix A). The largest granule and layer particles were classified as size group C (between 300 and 1000 µm). The most abundant particle shape was fibre (observed in every sample). Some of the samples contained several particles, which made it difficult to see the fibres. The type of particle with the greatest length that was found were fibres. Blue fibres with a length of 2.5 mm were found in sample S-03 and S-06, clear fibres with a length of 3.2 mm were found in S-01 and S-11, and a black fibre with a length of 3.4 mm was found in S-13.

Some of the samples contained white/clear particles that looked like shell fragments (microfossils), which did not dissolve during chemical digestion. The abundance of these particles was especially high in samples S-01, S-02 and S-03 from inner Kongsfjord, as well as in sample S-04 from inner Rijpfjord (Appendix A). The relatively higher occurrence of microfossils in the samples from Kongsfjord agrees with their higher carbonate content compared to Rijpfjord (Table 9). Carbonate in surface sediments is suspected to originate from organisms with carbonate shells.

Table 9 Levels of total carbon (TC), total organic carbon (TOC) and carbonate ($CaCO_3$) in surface sample S-01 to S-06 (TC and TOC-levels provided by NGU – results from LECO analyses).

Sample ID	Area	TC (%)	TOC (%)	Carbonate content (%)[1]
S-01 (0-1 cm)	Inner Kongsfjord	3.2	1.4	15
S-02 (0-1 cm)		2.8	1.1	14
S-03 (0-1 cm)		3.3	1.8	12
S-04 (0-1 cm)	Inner Rijpfjord	1.5	1.1	3.7
S-05 (0-1 cm)		1.8	1.3	4.2
S-06 (0-1 cm)		1.8	1.2	4.3

[1]*Calculated as (TC – TOC) x 8.33. Assumes that inorganic carbon is bound as $CaCO_3$.*

Sample S-06 (inner Rijpfjord), S-08, S-11 and S-12 (Barents Sea) contained several black and shiny granules (Appendix A), which according to FT-IR analysis were likely to be petro-pyro particles, such as coal or oil residues. These samples, as well as the ones with relatively high abundance of microfossils (S-01 to S-04 from Svalbard), were among the ones with the highest weight of remaining sample material after density separation and chemical oxidation (i.e. non-digestible particles with a density less than the separation fluid used (zinc-chloride, ρ ~1.52 g/cm^3)).

3.2 Quality assurance

3.2.1 Method blanks

As described previously, method blanks (n = 3) were prepared and analysed for microplastics to control for contamination resulting from the laboratory method. The number of particles in the method blanks are shown in the table below.

Table 10 Number of microplastic particles and other particles in method blanks within each defined FT-IR category. Colouring in the table corresponds to the colouring in Table 5. SD = standard deviation.

Particle		Blank 1	Blank 2	Blank 3	Mean ± SD
Plastic polymer	PE	2	0	0	1 ± 1
	PP	2	4	3	3 ± 1
	PET	2	3	3	3 ± 1
	PS	0	1	0	0 ± 1
	PMMA	0	1	0	0 ± 1
	PE-oxidized	4	0	0	1 ± 2
	Melamine	2	1	0	1 ± 1
	Nylon	0	2	2	1 ± 1
	Other	0	0	2	1 ± 1
	Total	12	12	10	11 ± 9
Oxy-resin		0	0	0	0 ± 0
Rubber		0	0	0	0 ± 0
Petro-Pyro		0	0	0	0 ± 0
Organic		12	35	28	25 ± 12
Mineral		0	0	0	0 ± 0
Unknown		24	33	40	32 ± 8

As evident from Table 10, there was relatively low contamination in the blank samples, with PP and PET particles being the most abundant (mean: 3 ± 1 particles). An average of 11 ± 9 microplastic particles were detected in the method blanks. Further, each method blank contained an average of 25 organic particles, and 32 unknown particles (i.e. particles with a match score < 0.7 with the FT-IR library). The impurities collected on the steel mesh filters contributed to 2 ± 1 mg (mean ± standard deviation) average additional weight after chemical digestion.

As shown in Appendix B, relatively high levels of PTFE particles (granules and fibres) were found in the method blanks (mean: 34 ± 33 particles per blank sample). PTFE is a thermoplastic polymer of tetrafluoroethylene. PTFE, or Teflon, and it has several applications, such as a non-stick coating for pans and other cookware, due to its

hydrophobic characteristics. The source of PTFE particles was, after analysis of our laboratory equipment, found to be the inner parts of the ball valve used in the density separator. Due to the high abundance of PTFE resulting from the analytical method, it was decided that the method did not yield quantitative results for this plastic type. Therefore, results for PTFE in the sediment samples are not reported.

3.2.2 Sampling blanks

The number of particles in the sampling blanks (n = 4) are shown in the table below. As described previously, these were prepared and analysed for microplastics to control for airborne contamination resulting from the transport and analytical method.

Table 11 Number of microplastic particles and other particles in sampling blanks within each defined FT-IR category. Colouring corresponds to the colouring in Table 5. SD = standard deviation.

Particle		FBlank 1	FBlank 2	FBlank 3	FBlank4	Mean ± SD
Plastic polymer	PE	2	2	3	0	2 ± 1
	PP	8	12	3	3	7 ± 4
	PET	0	2	3	2	2 ± 1
	PE:PP	2	0	1	1	1 ± 1
	PVC	0	0	1	0	0 ± 1
	Melamine	0	0	1	0	0 ± 1
	Nylon	0	4	0	2	2 ± 2
	Unverified	0	0	3	1	1 ± 1
	Total	12	20	15	9	14 ± 5
Oxy-resin		0	0	0	0	0 ± 0
Rubber		0	0	0	0	0 ± 0
Petro-Pyro		0	0	0	0	0 ± 0
Organic		10	46	8	18	21 ± 18
Mineral		0	0	1	0	0 ± 1
Unknown		40	92	30	49	53 ± 27

In agreement with the method blanks, relatively high levels of PTFE particles were found in the sampling blanks (mean: 39 ± 17 particles, see Appendix B). Further, the abundance of other microplastics were in the same range, although somewhat higher in the sampling blanks, with PP, PET, PE and nylon being the most abundant (Figure 7). The sampling blanks were used to correct the results for the deeper sediment samples (i.e. field blanks and PVC-tube contamination samples). Approximately 42 % of the analysed particles were microplastics.

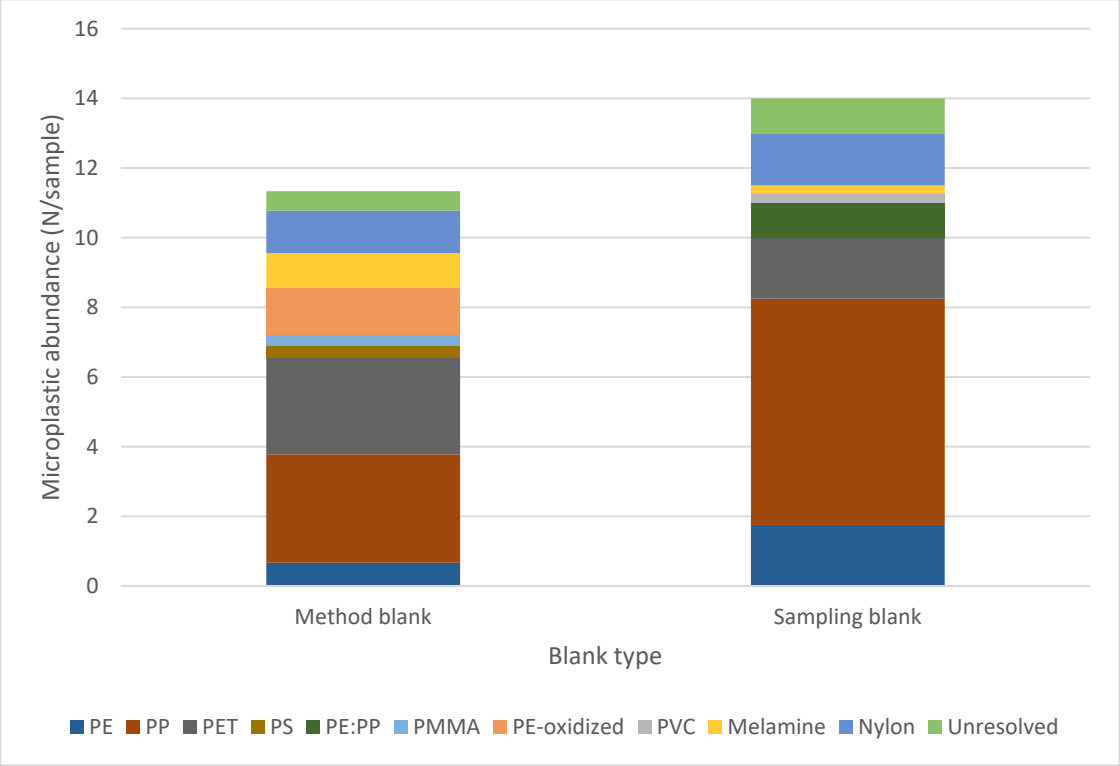

Figure 7 Comparison of average number of microplastics encountered in method blanks (n = 3) and field blanks (n = 4) (with the exclusion of PTFE particles, see Appendix B).

As the number of microplastics in the method blanks was comparable to the sampling blanks (Figure 7), it seems that the contribution of airborne microplastics contamination from the field work was insignificant compared to the analytical method.

The impurities collected on the method blank steel mesh filters contributed to 2 ± 1 mg average additional weight after chemical digestion. The limit of detection (LOD) was therefore set to 2 mg. The dry weights of the remaining potential microplastics in the sediment samples collected on the steel mesh filters after density separation and chemical oxidation were thus blank corrected by subtracting 2 ± 1 mg, with values less than zero being considered < LOD on weight basis. On concentration basis, this corresponds to approximately 16 mg microplastic/kg dry sediment, based on a "blank" weight of 2 mg divided by an average sample weight of 0.052 kg and considering that 42 % of particles in the method blank was identified as plastic (i.e. LOD of 16 mg microplastic/kg sediment = 0.42 * 2 mg / 0.052 kg).

3.2.3 Spiked blanks

Five spiked blanks were prepared and weighed to predict the recovery rates of microplastics from the environmental samples, as shown in the table below.

Table 12 Recovery rates for three types of microplastics used for spiking. SD = standard deviation.

Spiked blank	Date	Density of ZnCl2:CaCl2 (g/cm^3)	Weight recovery fraction (%)*		
			PET powder	PET fibre	PET pellet
S-08	30.05.2019	1.53	79	-	100
S-09	30.05.2019	1.53	68	-	100
S10	30.05.2019	1.53	-	31	100
S-06[1]	24.08.2019	1.53	-	-1	100
S-19	24.08.2019	1.53	-	19	100
Mean ± SD		1.53 ± 0	73 ± 7.8	16 ± 16	100 ± 0

**Based on blank corrected weight results*
[1]Sediment sample seemed to have a relatively high clay content => poor separation

The total average recovery fraction obtained for PET powder was 73 %. Thus, a fraction ($f_{recovery}$) of 0.73 was used for recovery correction for the dry weights of sample microplastics.

Average recovery rate for PET fibres was relatively low, and with a high standard deviation (16 ± 16 %). Previous spiking with PE fibres (density of 0.92 g/cm^3 and a larger diameter than PET fibres) has resulted in relatively higher recoveries (91 ± 6 % in DNV and NGI (2018a)).[2] Thus, it seems that a substantial amount of the PET fibres used for spiking in this study either got dissolved during the digestion procedure or failed to separate from the sediment because of aggregation with clay particles. In addition, fibre loss could result from a leakage from the steel mesh filters during filtration. The PET fibres used had a diameter of 17 µm and are made up of a weave of even smaller fibers, which are less than the pore size of the steel mesh filters of 45 µm. However, fibres were observed in all spiked samples, as well as in the environmental samples, but as the recovery rates were relatively low, the method was not able to correctly quantify the amount of fibres in the samples.

3.2.4 PVC-tube contact samples

The microplastics concentrations in the samples that were used to test PVC contamination from the sampling tubes (n = 10) are shown in Table 13. As seen in the table, microplastics particles were found in all samples, except for S-12 and S-16. Sample S-12 contained several petro-pyro particles (Figure 11). Sample S-11, which was sampled from the same core as S-12, also had petro-pyro particulates. Overall, the microplastic concentrations ranged from not detected (n.d.) to 750 particles/kg (mean: 340 ± 250). The abundance of PVC and PE-chlorinated particles, possibly originating from the PVC tubes, ranged from n.d. to 750 particles/kg (mean: 160 ± 240). Thus, the results indicate that microplastics were present in the sediment samples from deep down in the cores (> 25 cm, Table 3 and Table 13), though because these sediments pre-date plastic, this is mostly attributable to sample contamination. However, on weight basis, all microplastic concentrations were below the LOD of 16 mg/kg because of the low weight of remaining sample material on the steel mesh filters after density separation and oxidation, except for sample S-18 (38 mg MP/kg dry sediment),

Table 13 Microplastic (MP) abundance (dry weight basis) in PVC-tube contact samples (sample blank corrected). LOD = 16 mg/kg. n.d. = not detected. Bold marking indicates outliers / extreme observations in the respective groups. SD = standard deviation.

Sample ID	Station	Contact with PVC	mg MP/kg d.w.	MP particles/kg	PVC and PE-chlorinated particles/kg	Most frequent plastic
S-11	R1965MC002	Yes	< LOD	320	n.d.	Phenoxy resin, rubber
S-12		No	< LOD	n.d.	n.d.	n.d.
S-13	R1225MC038	Yes	< LOD	470	250	PE-chlorinated, PET
S-14		No	< LOD	750	**750**	PE-chlorinated
S-15	R1512MC095	Yes	< LOD	**40**	n.d.	PET
S-16		No	< LOD	n.d.	n.d.	n.d.
S-17	R1349MC416	Yes	< LOD	420	280	PE-chlorinated, PVC, rubber
S-18		No	**38**	520	170	PE:PP, PVC
S-19	R1359MC418	Yes	< LOD	430	50	PE-oxidized, PE:PP
S-20		No	< LOD	440	55	PE:PP, rubber
All (mean ± SD)			-	340 ± 250	160 ± 240	-
Contact with PVC-tube (mean ± SD)				340 ± 170	120 ± 140	-
No contact with PVC-tube (mean ± SD)				340 ± 330	200 ± 320	-

[1]*FT-IR match: 'PLASTHALL P-1070'*

Box plots (Figure 8 - Figure 9) were made to show the distribution of data. The extreme/outlier observations are highlighted with bold in Table 13. Statistical analyses (ANOVA with Tukey test) were performed to check for significant differences between samples that had been in contact with the PVC tubes vs. the samples that had not been in contact with the tube. No significant differences were found, regardless if the outliers/extremes were included in the analyses or not. Therefore, it is not possible to state if efforts to sample within the tube were effective. The rubber particulates (associated with the trade names Plasthall® and Resinall®) in several samples may be due to sediment core slicing near the parking lot. The presence of PE, PE:PP and PET is most likely due to ambient contamination, as these were spotted in the method and sampling blanks.

For future sampling of sediment cores for microplastics analysis, it is recommended to use non-plastic core tube materials (e.g. metal), or to use tubes with a less common plastic than PVC (e.g. polycarbonate) so that PVC in sediment can be more accurately quantified. Samples in this study and others should be interpreted with contamination risks in mind. For the surface samples, this was to some extent corrected for by the use of field blanks.

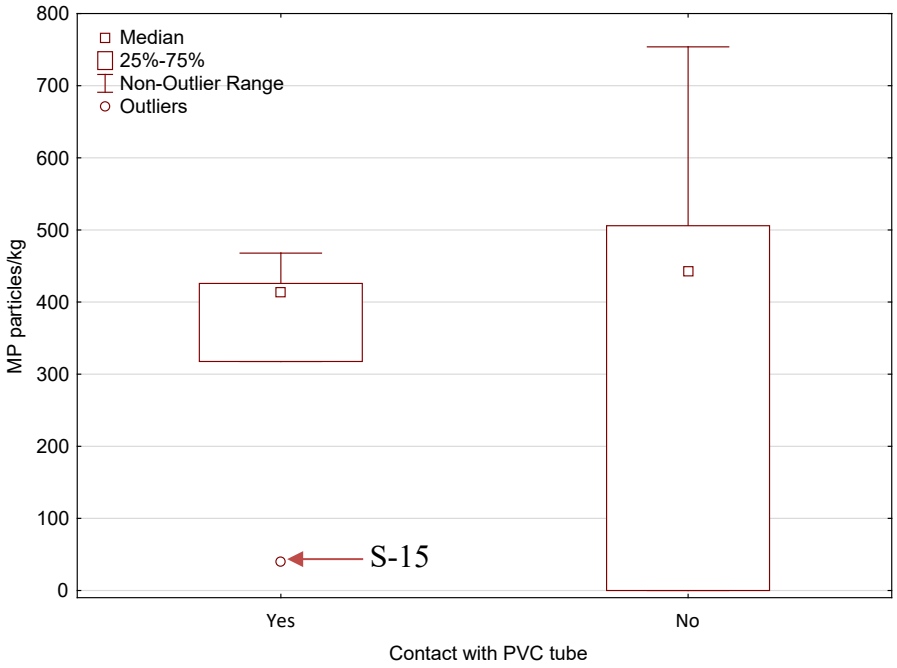

Figure 8 Box plot of microplastic concentrations (particles/kg dry sediment) in sediment samples which have been in contact with the PVC tube (denoted 'yes' in the figure), as well as samples obtained from the interior of the core (denoted 'no' in the figure).

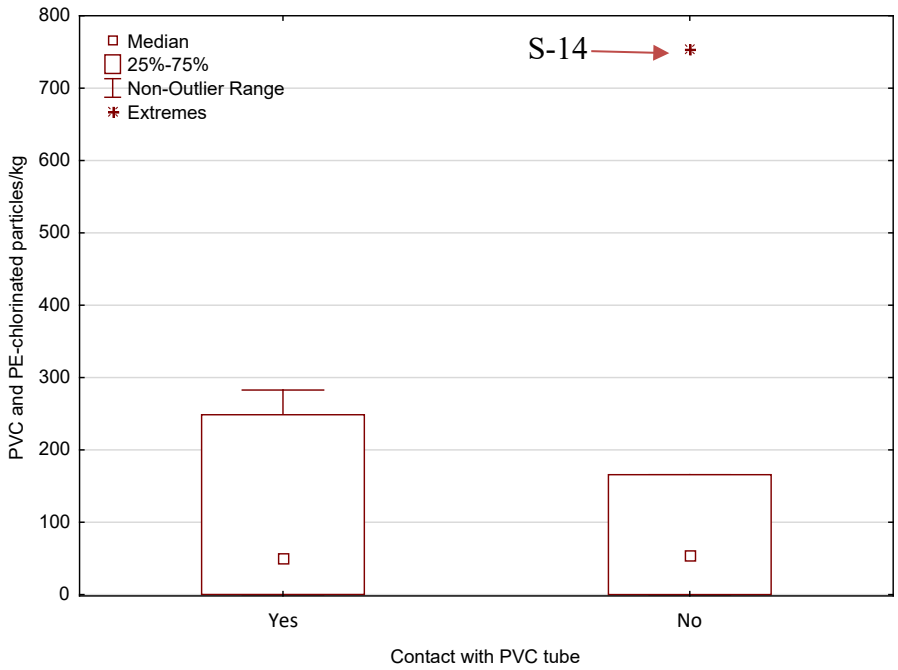

Figure 9 Box plot of microplastic concentrations (PVC and PE-chlorinated particles/kg dry sediment) in sediment samples which have been in contact with the PVC tube (denoted 'yes' in the figure), as well as samples obtained from the interior of the core (denoted 'no' in the figure).

3.2.5 Field blanks

The amount of microplastics in the field blanks (n = 3) are shown in Table 14, and ranged from n.d. to 260 particles/kg (mean: 120 ± 130), of which PVC and PE-chlorinated particles ranged from n.d. to 110 particles/kg (mean: 66 ± 58). On weight basis, the microplastic concentrations were < LOD.

Table 14 Microplastics (MP) abundance (dry weight basis) in field blank samples (sample blank corrected). LOD = 16 mg/kg. Grey colour: < LOQ. n.d. = not detected. SD = standard deviation.

Sample ID	Depth (cm)	Area	mg MP/kg d.w.	MP particles/kg	PVC and PE-chlorinated particles/kg	Most frequent plastic
B-1	32-34	Kongsfjorden	< LOD	104	86	PVC (50 %) and PE-chlorinated (33 %)
B-2	30-32	Rjipfjorden	< LOD	260	110	PE-chlorinated (44 %) and PE (38 %)
S-12	33-35	Bjørnøy transect	< LOD	n.d.	n.d.	n.d.
All (mean ± SD)			-	120 ± 130	66 ± 58	-

It is noteworthy that field blank S-12 from the Bjørnøy transect was free of microplastics according to the method used. As previously mentioned, this was a sample that contained several black and shiny granules (photos in Appendix A). These were identified as petro-pyro particles (Figure 11). The relatively high abundance of petro-pyro particles in field blank S-12 (13 % of total particle composition, compared to 5 % and 1 % for B-1 and B-2, respectively, see Appendix D) may have resulted in difficulties obtaining high-quality spectra for potential microplastics, as these could have been 'hidden' in the black-particle matrix.

For B-1 and B-2, microplastics (plastic polymers and rubber) accounted for approximately 40 % and 90 %, respectively (Figure 10). The most frequent plastic polymers were PE-chlorinated, PVC, and PE. As these fjord sediment samples originate from a time prior to plastic production, it is assumed that these plastics are related to contamination from sampling. The most likely source for contamination is the PVC sampling tube itself, despite efforts to sample from the interior of the core (i.e. not in contact with the PVC tube) (see section 2.1). The FT-IR spectra of PE-chlorinated is somewhat comparable to that of PVC, as both polymers have a similar chemical structure, which could result in PVC-particles being mistakenly identified as PE-chlorinated. The presence of PE in B-2 is more of a mystery but is likely due to sampling bias.

It is uncertain to which extent the presence of microplastics in the field blanks was influenced by contamination during sampling, transport, processing and analysis, though this was to some degree accounted for by the sampling blanks. For instance, the subsampling from the PVC tubes was performed nearby a parking lot, which could explain the presence of a rubber particle in sample B-2, as this could have been originating from car tires.

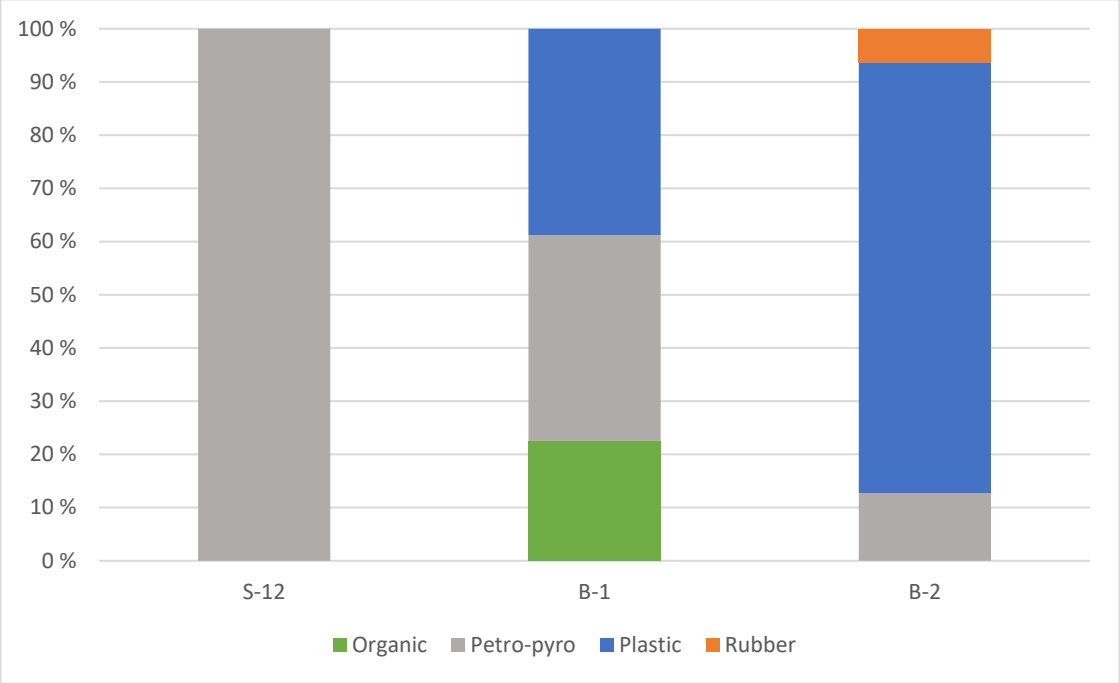

Figure 10 Material composition of identified particles in the field blanks, shown as percentage of each category group, with the exclusion of unknown particles (FT-IR score < 0.7), which accounted for > 80 % of the particles in all samples

3.2.6 Limitations of the method

Density limitation

Typical densities for sand or other sediments are approximately 2.65 g/cm^3, whereas density values for virgin plastic resins range from 0.8 to 1.4 g/cm^3.[16] Density separation with zinc-chloride solution ($\rho \sim 1.52$ g/cm^3) will thus separate the lighter plastic particles from the heavier sediment grains. However, there are some types of plastic with densities higher than this, such as pure teflon and mixtures of polymers and glass, polymers and minerals or polymers and metals. This means that plastics with a density higher than the zink-chloride solution are not extracted from the sediment, which might have led to an underestimation of the total microplastics concentration present in the sample.

Particle size limitation

Due to the filter size of 45 µm, the results in this report may have been underestimated. Bergmann et al. (2017) reported that a significant amount of the counted microplastic particles were smaller than 25 µm in their study.[1] Thus, some of the smaller particles (including nanoplastics) would have gone unnoticed in this study. Though these particles would have minimum influence on the weight.

Digestion limitation

The digestion method used here was optimised to be as destructive as possible to organic matter (including cellulose, chitin, proteins, lipids, etc.), while leaving synthetic polymers intact. During the method development, this was tested systematically, and recalcitrant organic matter like cellulose was found to be digested 98 ± 4 %, while there was no weight change to microplastic granules.[13]

Most of the material separated in the BMSS was < 1 mm. Thus, it is likely that the digestion removed most of the organic matter, as it is more difficult and time consuming to completely digest larger organic matter particles than smaller ones. Some organic matter did survive, as evident from the FT-IR results. Further, other low-density carbonaceous materials like coal, charcoal, bitumen, etc., or possibly non-carbonaceous low-density materials such as porous glass and ceramics, would have been unaffected by digestion.

Characterisation by FT-IR microscopy

There are also limitations regarding to the FT-IR analysis used. In literature, it is common to use a quality index of 0.7 as the limit.[17] This limit was also used in this study. However, weathering of the polymers affects their surface and thereby their spectra, which makes comparison with reference spectra more difficult. Therefore, a score limit of 0.7 could lead to an underestimation of plastics, as particles with a lower score in fact could be plastics. At the same time, the cut-off of 0.7 could have resulted in an overestimation of plastics if the limit is not conservative enough, as the uncertainty increases with decreasing score.

Furthermore, there are uncertainties associated with the actual FT-IR apparatus. For instance, to obtain high quality spectra in transmission mode, it is best with samples that are translucent, and they should sit as flat on the window as possible. However, particles from environmental samples, like in this project, are often irregularly shaped and with an uneven surface, or they can be highly opaque and thick, which may reduce the quality of the recorded spectra using ATR. It is uncertain to what extent this may have led to an underestimation of the results.

3.3 Microplastics in surface samples

3.3.1 Microplastic abundance

Microplastic concentrations in the sediment surface (0-2 cm) samples (n = 10) are provided in the following table (dry weight basis). The amount of microplastics on weight basis (mg microplastic/kg sediment) was below the LOD of 16 mg/kg for all samples. However, the number of microplastic particles per kg sediment ranged from n.d. to 560 (230 ± 180 particles/kg, Table 15). Unlike the deeper sediment samples (chapter 3.2.4 and 3.2.5), PVC particles were quantified in only one of the samples (S-09), whereas the rest were PVC-free (although S-05 contained one PE-chlorinated particle prior to blank correction).

The relatively lower number of PVC particles in the surface samples may be due to less contact with the PVC-tube compared to the deeper sediment samples, where the PVC-tube is pressed into the sediment so that PVC particles may have loosened in contact with the sediment grains. Thus, the results indicate that PVC-tube sampling is not as critical for surface sediment samples as for deeper samples. However, the use of PVC-free sampling tubes is recommended for future sampling campaigns also for surface samples. The microplastic composition of the surface samples are further discussed in chapter 3.3.3.

Table 15 Microplastics (MP) abundance (dry weight basis) in surface samples (field blank corrected). LOD = 16 mg/kg. n.d. = not detected. SD = standard deviation.

Sample ID	Area	Mg MP/kg dry sediment	MP particles/kg dry sediment	PVC and PE-chlorinated particles/kg
S-01	Inner Kongsfjord	< LOD	300	n.d.
S-02		< LOD	89	n.d.
S-03		< LOD	n.d.	n.d.
S-04	Inner Rijpfjord	< LOD	300	n.d.
S-05		< LOD	200	n.d.
S-06		< LOD	560	n.d.
S-07	Bjørnøy transect	< LOD	46	n.d.
S-08		< LOD	320	n.d.
S-09		< LOD	77	29
S-10		< LOD	430	n.d.
Mean ± SD (min-max)	All areas	-	230 ± 180 (0-560)	2.9 ± 9.1
	Inner Kongsfjord		130 ± 160 (0-300)	n.d.
	Inner Rijpfjord		350 ± 190 (200-560)	n.d.
	Bjørnøy transect		220 ± 190 (46-430)	7.2 ± 14

As seen by the following figure, there were no clear geographical differences between the surface samples (not statistically significant).

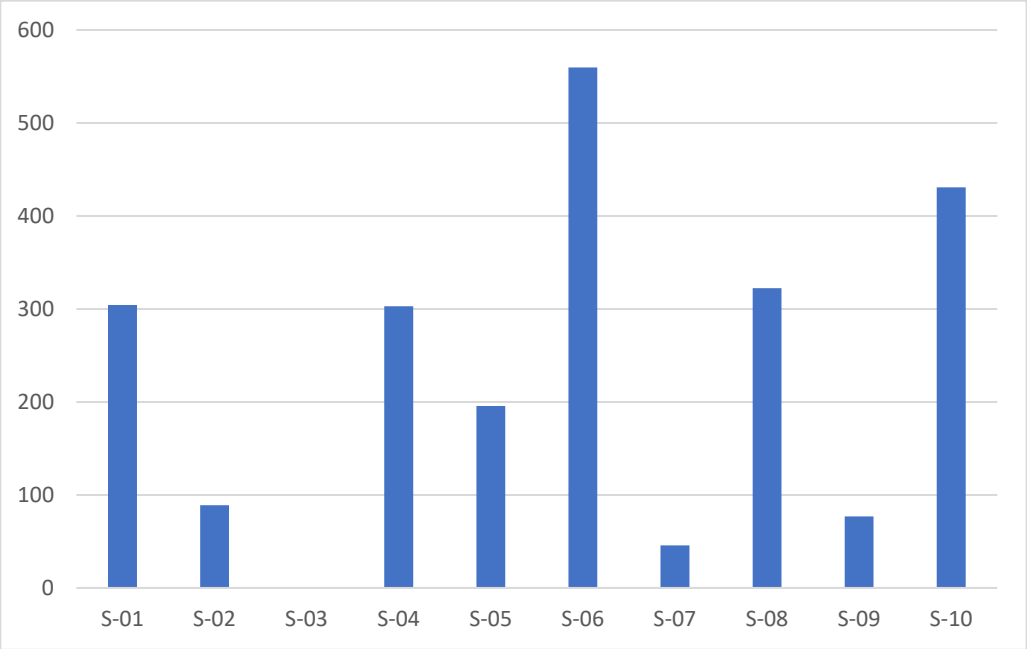

Figure 11 Microplastic (MP) abundance (mg MP/kg dry sediment) in samples from inner Kongsfjord (S-01 to S-03), inner Rijpfjord (S-04 to S-06) and the Bjørnøy transect (S-07 to S-10).

3.3.2 Comparison of microplastic abundance with literature

Microplastics have been found in sediments worldwide, although the majority of reported sediment monitoring studies have had greater focus on beach and nearshore sediments.[15] It is difficult to make direct comparisons across different regions because of variability and differences in the sampling techniques, sample preparation and detection methods used. In the table below, there is a list of studies of microplastics in sediment from nearby geographical areas and with some methodological similarities to this study. For meaningful comparisons, it is important to define specific methodological conditions, such as the density of the density-solution used and in particular the size range of microplastics quantified, as particle number is expected to increase with decreasing particle size.[1] Differences in methodology which could affect comparison are discussed in the text.

Table 16 Summary of reported microplastic concentrations in sediments. The concentrations are expressed as particles/kg (dry weight basis). SD = standard deviation; SE = standard error; n = number of samples.

Location	Location specification	Particle size (n)	Measured concentration (min-max range and/or mean)	Reference
Svalbard/ Arctic	Arctic and Barents Sea	45 µm – 1 mm[a] (10)	0 – 560 particles/kg (220 ± 180 SD)	This study
	Barents Sea	45 µm – 1 mm[a] (4)	46 – 430 particles/kg (220 ± 190 SD)	
Svalbard/ Arctic	HAUSGARTEN observatory	10 – 275 µm (9)	42 – 6595 particles/kg (4356 ± 675 SE)	Bergmann et al., 2017
Norway	Norwegian Continental Shelf	5 µm – 1 mm (10)	23 – 290 particles/kg (120 ± 97 SD)	NGU, 2018[18]
Norway[b]	Norwegian Continental Shelf	45 µm – 5 mm[c] (35)	0 – 3400 particles/kg (370 ± 690 SD)	DNV and NGI, 2018[2, 3]
	Barents Sea	45 µm – 5 mm[c] (5)	53 – 810 particles/kg (320 ± 330 SD)	
Belgium	Belgium Continental Shelf	38 µm – 1 mm (6)	72 – 270 particles/kg (97 ± 19 SD)	Claessens et al., 2011

[a]*With the exception of some longer fibres, no granules/layers were over 1 mm in this study.*
[b]*The concentrations in this table differ from the reported ones in DNV and NGI (2018)[3], as the previously reported concentrations were recalculated due to the hard FT-IR cut-off of 0.7 in this study, compared to previously where data between 0.6 and 0.7 was included. Data from the NCS study using the 0.7 FT-IR cut-off is presented in Appendix E.*
[c]*Most particles were in the size range 45-1000 µm, although some were in size group 1-5 mm.*

A study of microplastics in Arctic deep-sea sediments from the HAUSGARTEN Observatory (2340-5570 m depth) in the Fram Strait at N79°, west of Svalbard, recorded concentrations of microplastics from 42 to 6595 particles/kg sediment dry weight, with an overall mean number of 4356 (± 675 standard error) items/kg.[1] The sampling and analytical technique used was similar to this study, though with some differences. In short, sediment cores were sampled using a multiple corer, and the top 5 cm were sliced with a metal spatula for microplastics analysis. A Microplastic Sediment Separator (MPSS) filled with $ZnCl_2$ solution (1.7-1.8 g/cm^3) was used for density separation. The filtered sample (steel mesh filter with 20 µm cut-off) was, after chemical oxidation with Fenton's reagent, analysed both visually and with FT-IR analysis. To account for possible laboratory contamination, a procedural blank was run (comparable to method blanks in this study).

The results in Bergmann et al.[1] consist of substantially higher microplastics concentrations compared to this study (Table 16). However, it should be kept in mind that the HAUSGARTEN study quantified microplastics ≥ 10 µm, while this study investigated particles ≥ 45 µm. Also, Bergmann et al. reported that the majority of all particles were ≤ 25 µm.[1] Thus, this could be one explanation of why they found more microplastics than the present study. Further, the results in this study were field blank

corrected, whereas the samples in the HAUSGARTEN study were only method blank corrected, which may additionally explain why they reported higher concentrations. Interestingly, they found PTFE particles in all samples (although the density of PTFE (2.10-2.30 g/cm^3) is higher than the $ZnCl_2$ solution used). Further, the microplastic quantities in sediments from the HAUSGARTEN observatory are among the highest recorded from benthic sediments across the globe[19]. The relatively high microplastic quantities may indicate that this is in or close to a plastic accumulation area.[1]

Recently, snow samples from ice floes in Fram Strait were analysed to assess whether atmospheric transport plays a role regarding microplastics pathways to the North. The microplastic concentrations (11 – 100 µm) of Arctic snow (from 0 to 14.4x10^3 particles/liter) were significantly lower than European snow (from 0.19x10^3 to 154x10^3 particles/liter), but still substantial.[8] It is worth noting that in this snow study, 80 % of all detected MPs were ≤ 25 µm, and 98% of all particles were <100 µm.

In 2016-2017, NGU performed a pilot within the MAREANO program to investigate microplastics in 10 sediment samples, which were sampled on several MAREANO surveys covering relatively large areas along the Norwegian Continental Shelf (NCS).[18] The microplastic abundances ranged from 23 to 290 particles/kg (mean: 120 ± 97, Table 16), which is somewhat lower, but in the same range as this study. However, despite the similar results, they are not directly comparable due to important differences in the laboratory method (see next paragraph). The sampling strategy for eight of the sediment cores was similar to this study (multicorer), while two of the samples were collected using boxcorer sediment cores. The top 3 cm were sliced (in-door at NGU) with a metal spatula and sent in glass containers to Ghent University in Belgium for microplastics analysis.

The method, in short, used in the previous NGU study was: sediment samples were oxidized with H_2O_2, diluted with deionized water and centrifuged for 5 minutes at 3500 rpm. The supernatant was filtered through a cellulose nitrate membrane filter with a pore size of 5 µm, and the residue was re-suspended in NaI solution (1.6 g/cm^3). After centrifugation, the supernatant was again filtered through a 5 µm filter. The residue was again re-suspended in NaI, and the centrifugation and filtration steps were repeated. The filters were visually inspected under a microscope, and microplastics were further confirmed by the "hot needle technique". Raman spectroscopy was performed on selected particles for eight of the ten samples. Plastic polymers were only identified in two of the eight samples.[18] The differences between the two NGU studies can thus to a large extent be explained by differences in methodology. In general, with microplastics analysis, confirmation of plastic identity with FT-IR, Raman, or similar methods are considered as more reliable than visual analysis.

During the regional environmental sediment monitoring on the NCS on behalf of the oil and gas industry in 2017, 35 sediment samples from the North Sea and the Barents Sea were sampled, including many stations in the vicinity of offshore oil platforms.[2, 3] The samples were collected by Van Veen Grabs, and the top 1 cm was sent to NGI for analysis of microplastics, using the same analytical method as in this study. Microplastic

concentrations in the whole study area ranged from n.d. to 3400 particles/kg (370 ± 690 particles/kg) (Table 16 and Appendix E), which is a much broader range than observed in this study. One of the reasons for the larger range in microplastics in the 2017 samples is the greater diversity in geographical areas, including the proximity of some samples to oil and gas activities, which tended to have higher microplastic concentrations.[2, 3] A better comparison is to look only at samples collected from the Barents Sea. Microplastic concentrations in the previous study (n = 5) ranged from 53 to 810 particles/kg (320 ± 330 particles/kg), which is somewhat higher though largely overlaps with the results of this study (range: 43-430 particles/kg; mean: 220 ± 190 particles/kg, Table 16). Many of the same plastic types were found frequently in the Barents Sea in both studies, such as phenoxy resin, PE-oxidized, rubber resins and PP, as discussed more closely in chapter 3.3.4.

The relatively higher microplastic abundances in the Barents Sea samples from 2017 may have been affected by differences in sampling and quantification. I.e. the 2017 sediments (0-1 cm) were sampled using van Veen grabs, while a multicorer was used for sediments (0-2 cm) in this study. Differences in sampling depth may be of importance for the results, especially in areas where there are very slow sedimentation rates (e.g. < 1 mm per year), as in such areas microplastic can be a dominating particle type of sediment in the surface (1 cm) layer. Further, washout of fine fine-grained sediment is an issue with van Veen grab sampling, and blockage of the jaws by coarser particles often leads to sample loss. Furthermore, the sample recovered is to some extent mixed and the original seabed structure is not preserved. The penetration depth is also inaccurate and depends on soil composition. Corers, on the other hand, will give more undisturbed sediment samples. It should be also mentioned that field blanks were not included in the previous NCS/Barents Sea study, only method blanks. Thus, the contribution of microplastics from sampling was not corrected for in the results, which may have also contributed to relatively higher concentrations than this study.

In 2011, Claessens et al. published results on microplastics abundance in Belgian marine sediments collected in harbours, on beaches and off shore (on the Belgian Continental Shelf, BCS, n = 25).[20] The concentrations in sediment samples from the BCS (n = 6) ranged from 72 to 270 particles/kg (mean: 97 ± 19), corresponding to from 0.89 to 1.30 mg/kg.[20] The results were in the same range, although somewhat lower than in the present study.

Claessens et al. separated microplastics from sediment by using the method of Thompson et al. (2014)[21], with some modification. In short, concentrated saline solution (density not provided) was added to wet sediment and the mixture stirred. After 1 h settlement, the supernatant was poured through a 38 µm mesh sieve, and microplastics < 1 mm was quantified. The collected particles were examined under a microscope, followed by FT-IR spectroscopy. Spiked blanks were analysed to obtain correction factors for calculating the microplastic concentrations reported.[20]

To summarize, some of the observed differences in quantified microplastic concentrations in literature may be due to the use of different methodologies, as there is a wide variety of approaches used to identify and quantify microplastics. However, the microplastic concentrations in this study (in the Arctic) were comparable to other studies on the Norwegian and the Belgian continental shelf. The overlap was most obvious for Barents Sea sediments, but was less obvious for Svalbard sediments, considering the HAUSGARTEN observatory west of Svalbard. This latter discrepancy could be due to the importance of accounting for particles smaller than 45 µm or because HAUSGARTEN is closer to a deep sea plastic accumulation area than the other areas studied.[1]

3.3.3 Composition of microplastics

As seen in Table 17, PS, PET, PE, rubber resins, phenoxy resin, PE-oxidized, nylon and PAM were among the most frequent plastic types encountered in the sediment samples.

Table 17 List of most frequently identified (i.e. FT-IR match > 0.7) microplastics (defined as plastic polymers, oxy-resin and rubber) in the surface samples.

Sample ID	Area	Most frequent (percentage of total microplastics)	Second most frequent (percentage of total microplastics)
S-01	Inner Kongsfjord	Unresolved (64 %)[1]	PET (36 %)
S-02		PS (73 %)	Unresolved (27 %)[1]
S-03		n.d.	n.d.
S-04	Inner Rijpfjord	PS (71 %)	PET (29 %)
S-05		PET (82 %)	PS (11 %)
S-06		PAM (35 %)	Rubber[2] (35 %)
S-07	Bjørnøy transect	PE (64 %)	PET (36 %)
S-08		Phenoxy Resin (54 %)	Nylon (46 %)
S-09		Rubber (38 %)	PVC (38 %)
S-10		Rubber (30 %)	PE-oxidized (21 %)

[1]*FT-IR match: "CYANOX 53";* [2]*Poly(butadiene:acrylonitrile)*

As shown in Figure 12, the samples from the inner Kongsfjord and -Rijpfjord mainly comprised of PET and PS polymers, except for sample S-06 which had a more heterogenous microplastics composition. This sample consisted of different rubber particles and PAM. In addition to sample S-06, relatively high abundance of rubber particles was found in samples S-08 to S-10 from the Bjørnøy transect. Due to their similarities in material composition, these samples were clustered (i.e. grouped together) in the PCA biplot in Figure 13. Generally, the samples from the Bjørnøy transect contained a variety of microplastics.

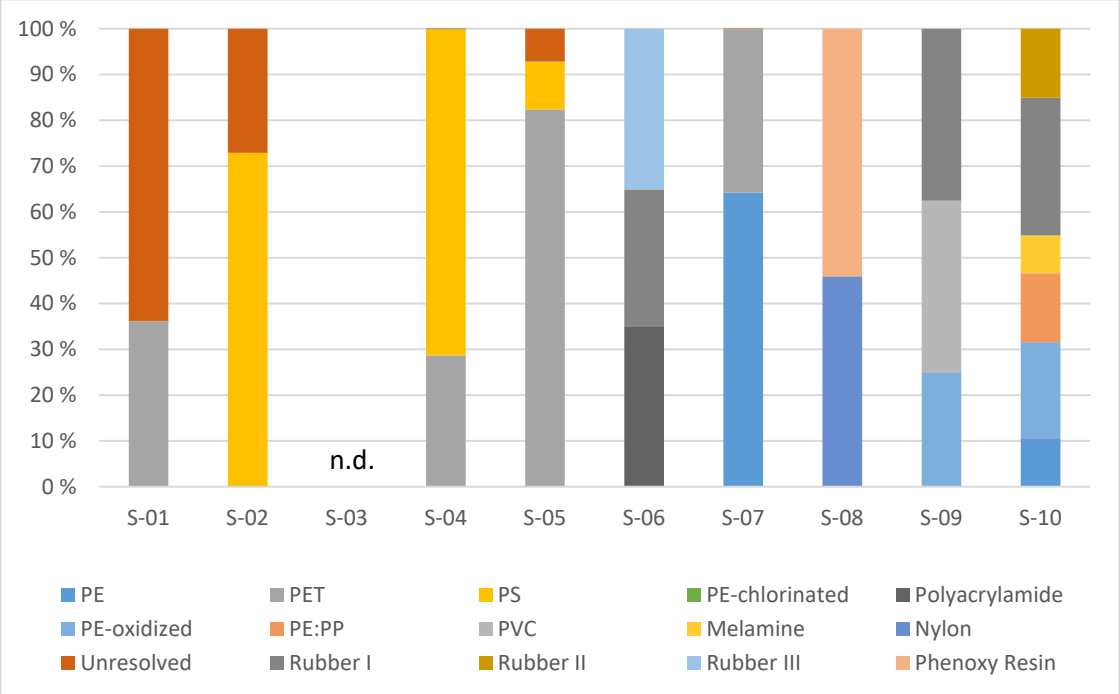

Figure 12 Microplastics composition (%) of surface sample S-01 to S-10. n.d. = not detected.

The density of surface seawater ranges from about 1.020 to 1.029 g/cm^3, while deep seawater can reach a density of 1.050 g/cm^3 or higher. In Table 18, typical densities of (pristine) plastic polymers identified in the surface samples are listed. As evident by the table, most polymers in the samples had a density higher than seawater, thus expected to sink in the water column after being transported by currents. However, low-density polymers like PE were also found. There are several mechanisms which affect the sinking behaviour of microplastics. For instance, biofouling may increase the specific density, and thereby enhance its sinking behaviour.[22] Other mechanisms could be flocculation with higher density particles and sinking as part of phytoplankton excrement pellets.[23] Different hydrodynamic processes will also influence the distribution of microplastics in the marine environment.[24]

Table 18 Density of pristine plastic polymers identified in the surface samples in this study.

Polymer type	Density (g/cm^3)	Reference
PET	1.37-1.45	Hidalgo-Ruz et al., 2012[16]
PE	0.92-0.97	
PS	1.04-1.1	
Nylon	1.02-1.05	
PAM	1.20-1.30	www.polymerdatabase.com

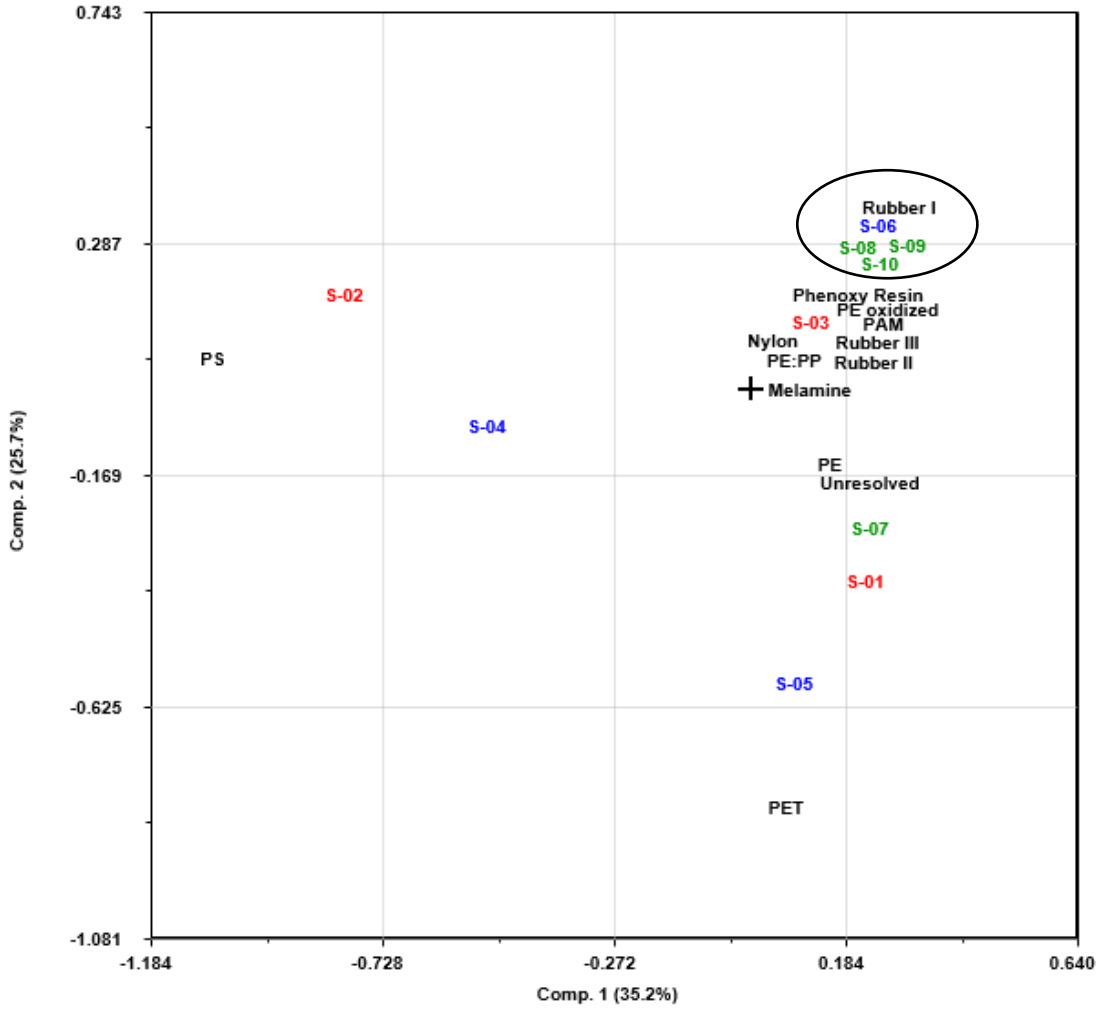

Figure 13 PCA biplot of objects (sample S-01 to S-10) and variables (types of microplastics). Approximately 60 % of the variance is explained by principal component 1 and 2. Red = inner Kongsfjord; blue = inner Rijpfjord; green = Bjørnøy transect.

A short description of some of the most frequently detected microplastics is as follows:

- PET is the most common thermoplastic of the polyester family. Often used in fibres for clothing, containers for liquids and foods, and in combination with glass fibre for engineering resins.
- PS in its solid form is clear, hard and brittle. It is widely employed in the food-service industry as rigid trays and containers, disposable eating utensils, lids and in protective packaging.
- PAM is a water-soluble polymer that can be used as a flocculating agent. PAM is commonly used as a flocculant in water and wastewater treatment, as well as enhanced oil recovery. It's presence in sediments could therefore be due to flocs containing PAM, from such uses.

- Synthetic rubbers are artificial elastomers. Rubber material is the core component in tyres, which has been suggested to be one of the most important sources of microplastics in the environment.
- Phenoxy resin is one of the most typical oxy-resin-particulates, commonly used as a marine varnish.
- PE is the most common plastic type. Its primary use is in packaging (plastic bags, containers such as shampoo bottles and more).
- Nylon is a generic designation for a family of synthetic polymers based on polyamides. It is a thermoplastic silky material that can be melt-processed into fibres, films or shapes. Nylon filaments are primarily used in toothbrushes and string trimmers, as well as in fishing lines. As mentioned in section 2.1, the Rilsan® bags used for the sediment samples were made of nylon. Thus, these plastics could be related to contamination from the Rilsan® bags.

3.3.4 Comparison of microplastic composition with literature

Differences in microplastic detection method used, particle categorization, reporting units and surveyed particle sizes makes comparisons of microplastics composition in environmental samples somewhat biased. However, a short comparison is given in the following.

In the HAUSGARTEN study (west of Svalbard) by Bergmann et al.,[1] PE-chlorinated was the most abundant plastic type. This plastic was not identified in the surface samples in this study (prior to blank correction, one PE-chlorinated particle was found in sample S-05). However, this plastic polymer was one of the most abundant microplastics in the deeper samples (field blanks and test for PVC tube contamination samples). As the FT-IR spectra of PVC potentially could be mistaken for PE-chlorinated due to similarities in their chemical structure, the presence of PE-chlorinated in the deep core samples could originate from the PVC-tubes used. The second most abundant plastic type in the HAUSGARTEN study was polyamide, which could refer to nylon or possibly also PAM – both of which were found in this study. In agreement with this study, several different rubber types were also reported in their samples.[1]

According to a review by Burns et al. (2018), polymer type trends in the literature are similar in the water column and sediment, with the greatest proportion of particles being PE, followed by PET and PAM in water and PP in sediment.[15] With the exception of PP, all these polymer types were found in the ten sediment samples in this study.

A variety of microplastics, including rubber, phenoxy resins and PE-oxidized particles have previously been identified as some of the most frequent microplastics in sediment samples from the Barents Sea.[3] In contrast to this study, where chlorinated-PE particles were infrequently found in surface samples, PE-chlorinated particles were also among the most frequent plastics in the previous study (similar to the HAUSGARTEN study).[3] Constant et al 2019, also found PET, PAM, PE and PS as some of the most abundant microplastics (0.063-5 mm) in beach sediments from the micro-tidal Northwestern

Mediterranean Sea.[25] PAM has also been found in sandy beach samples of the Baja California peninsula.[26] According to de Jesus Piñon-Colin et al.[26] PAM was identified in many of the fibres, which could be due to its use as a finishing agent in the textile industry (provides anti-wrinkle and anti-mold properties to textile).

3.3.5 Composition of microplastics and other particles

The percentage composition of particles categorized as unknown (match score < 0.7 with the FT-IR library), organic, oxy-resin, petro-pyro, plastic and rubber are listed in the following table (mineral particles were not identified). Pie charts with average, relative compositions for each geographical area are shown in Figure 14.

Table 19 Percent composition of particles in the surface samples, as classified by FT-IR.

Sample ID	Area	Unknown	Organic	Oxy-resin[1]	Petro-pyro	Plastic polymer[1]	Rubber[1]
S-01	Inner Kongsfjord	98	0	0	0	1	0
S-02		98	0	0	0	2	0
S-03		99	1	0	0	0	0
All		99 ± 1	0 ± 1	0 ± 0	0 ± 0	1 ± 1	0 ± 0
S-04	Inner Rijpfjord	97	0	0	0	3	0
S-05		56	7	0	5	32	0
S-06		83	1	0	15	1	1
All		79 ± 21	3 ± 4	0 ± 0	7 ± 8	12 ± 17	0 ± 1
S-07	Bjørnøy transect	99	0	0	0	1	0
S-08		68	0	1	29	1	0
S-09		0	0	0	43	36	21
S-10		86	4	0	0	5	4
All		63 ± 44	1 ± 2	0 ± 1	18 ± 22	11 ± 17	6 ± 10
All areas		79 ± 31	1 ± 2	0 ± 0	9 ± 15	8 ± 14	3 ± 7

[1]*Total microplastic concentrations were in this report calculated based on the amount of oxy-resins, plastic polymers and rubber particles.*

As shown in Table 19, most of the particles were classified as unknown (79 %), followed by petro-pyro (9 %), plastic polymers (8 %), rubber (3 %) and organic (1 %). The samples from the Inner Kongsfjord locations contained especially high percentages of unknown particles (≥ 98 %). Visually, the majority of these resembled microfossils (Appendix A). Substantial amounts of microfossils were also observed in sample S-04 from the inner Rijpfjord, which contained 97 % unknown particles. In addition to the fact that the particles classified as unknown may have been particles missing in the library database, their relatively low scores could be caused by other factors, such as differences between the surface of the reference sample and measurement target. E.g. if the surface of the sample is weathered and oxidized, or if it is coated, the spectrum will not match well with the reference. A relatively poorer match is also expected if an analysed microplastics particle consists of a mixture of different polymers and additives,

such as many oxy-resins and epoxides. The samples with the highest amounts of petro-pyro particles (S-06, S-08 and S-09) contained several black and shiny granules; thus, in these samples many of the unknown particles are likely of petrogenic or pyrogenic origin. It is not certain whether the petro-pyro particles are to be considered anthropogenic or natural, as they can be both.

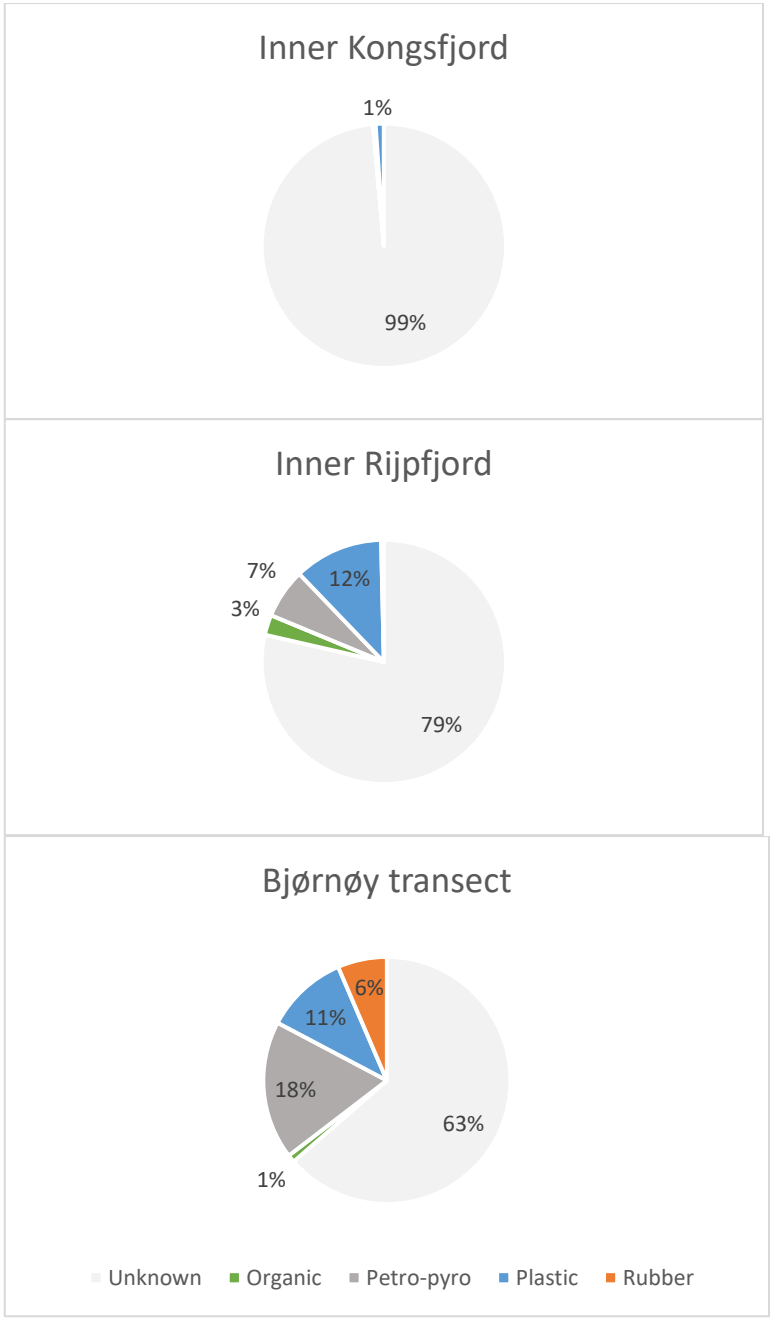

Figure 14 Average percentage composition of identified particles in the samples from the inner Kongsfjord (n = 3), inner Rijpfjord (n = 3) and Bjørnøy transect (n = 4).

In agreement with the results in this study, Bergmann et al. found that other particles than microplastics accounted for 22-100 % of the total particles in Arctic snow. These particles comprised chitin, charcoal, coal, animal fur, plant fibres, and sand.[8]

4 Conclusions

The following conclusions can be drawn based on this study:

- Several different blank sample types were included in the study, to address and correct for contamination sources during sampling, transport and analysis.
- Sampling blanks (n = 4) were prepared by taking empty glass jars on the field trip and exposing them to the surroundings during sampling. Thus, the samples were included to control for field effects, such as airborne contamination from the transport route, contamination from the containers themselves etc. Since the number of microplastic particles in the laboratory method blanks (n = 3) was comparable to the sampling blanks, it was concluded that the contribution of airborne microplastics contamination from the field work was insignificant compared to the analytical method blank.
- Field blanks (n = 3) were prepared by sampling deep-sediment (> 30 cm depth) from cores in the same areas as the surface samples, assuming the deeper sediment was from a time prior to plastic production (meaning they should in theory be free from microplastics). This type of blank controls for both field and analytical contamination. The purpose of the field blanks was to correct for microplastics abundance in the surface samples. Overall microplastic concentrations ranged from < LOD to 38 mg/kg, corresponding to from n.d. to 260 particles/kg. PVC and PE-chlorinated were among the most abundant microplastics (ranging from n.d. to 110 particles/kg), probably originating from the PVC sampling tubes, since the sediments were pre-date plastic. This is the best type of blank to use for sediment analysis.
- 10 deep-sediment (> 25 cm) samples were sampled to verify if the PVC tube was a contamination source. This was done by comparing sediment samples obtained from the interior of the core (away from the tube wall, n = 5) with sediment that had been in contact with the PVC tube (n = 5). As microplastics were found in both sample types, it was not possible to state if efforts to sample within the tube were effective. However, these deep sediments are assumed to originate from a time prior to plastic production, so the abundance of microplastics is mostly attributable to sample contamination.
- Sediment samples from Svalbard (inner Kongsfjord, n = 3; and inner Rijpfjord, n = 3) and the Barents Sea (Bjørnøy transect, n = 4) have been analysed for microplastics. Overall, the amount of microplastics (45-1000 µm) ranged widely, from n.d. to 560 particles/kg dry sediment (mean ± standard deviation: 230 ± 180 particles/kg). There were no statistically significant geographical differences.
- The results for the Barents Sea compare well with an earlier study[2, 3] using the same method, both in terms of microplastics abundance and types of

microplastics. The previous study reported concentrations of 53-810 particles/kg (320 ± 330 particles/kg) in four Barents Sea samples, whereas this study reported 46-430 particles/kg (220 ± 190 particles/kg), which is in the same range. In both studies phenoxy resin, PE-oxidized and rubber resins were commonly found, along with other microplastics.

5 Recommendations

Based on the results in this study, the following recommendations are suggested for the future:

Future field sampling:

- Use tubes with a less common plastic than PVC (e.g. polycarbonate/plexiglass) for sampling of sediment cores, or alternatively steel sediment corers. Be sure to keep the tubes sealed until use, to minimize airborne microplastics contamination.
- Use deep sediment (i.e. deep in the sampling tubes, ideally older than 1900) as field blanks to correct for contamination during sampling, transport and laboratory analysis.
- Limit the use of plastic equipment as much as possible. For instance, use glass jars sealed with aluminium foil instead of Rilsan® bags (nylon) for sampling.
- Select location well suited for taking out samples from sediment cores for microplastic analysis (e.g. a "clean room").
- Continue with field blanks, method blanks and other control samples as part of sampling strategy and as a control of whether recommendations have worked well or not.

Laboratory considerations:

- If field blanks are not available, include as a minimum method blanks to control for laboratory contamination. In this study, the method blanks showed that the laboratory method was the most substantial source of plastic contamination in the samples.
- Use analytical equipment to identify potential microplastics and other particles (e.g. FT-IR or Raman spectroscopy).
- Limit the use of plastic equipment as much as possible.
- Report method specific details, as these are important for comparison of results (e.g. size of microplastics investigated, chemicals for oxidation, density of separation fluid if used, etc.)
- Record particle size distribution for better comparison with literature.

6 References

1. M. Bergmann, V. Wirzberger, T. Krumpen, C. Lorenz, S. Primpke, M. B. Tekman and G. Gerdts, High quantities of microplastic in Arctic deep-sea sediments from the HAUSGARTEN observatory, *Environmental science & technology*, 2017, **51**, 11000-11010.
2. DNV and NGI, *Microplastics in sediments on the Norwegian Continental Shelf*, 2018.
3. DNV and NGI, *Microplastic in sediments on the Norwegian Continental Shelf II: Identification through FT-IR analysis*, Report 2018-1226, Rev. 00, 2018.
4. R. Geyer, J. R. Jambeck and K. L. Law, Production, use, and fate of all plastics ever made, *Science advances*, 2017, **3**, e1700782.
5. L. Lebreton and A. Andrady, Future scenarios of global plastic waste generation and disposal, *Palgrave Communications*, 2019, **5**, 6.
6. E. Goldberg, Plasticizing the seafloor: an overview, *Environ. Technol.*, 1997, **18**, 195-201.
7. L. C. Woodall, A. Sanchez-Vidal, M. Canals, G. L. Paterson, R. Coppock, V. Sleight, A. Calafat, A. D. Rogers, B. E. Narayanaswamy and R. C. Thompson, The deep sea is a major sink for microplastic debris, *Royal Society open science*, 2014, **1**, 140317.
8. M. Bergmann, S. Mützel, S. Primpke, M. B. Tekman, J. Trachsel and G. Gerdts, White and wonderful? Microplastics prevail in snow from the Alps to the Arctic, *Science Advances*, 2019, **5**, eaax1157.
9. H. K. B. Jensen, J. Knies and V. Bellec, *Miljøkjemiske data og dateringsresultater fra Kong Kalrs Land - Bjørnøyrenna-transektet og Nordkapp-Sørkapp-transektet - MAREANO*, 2018.
10. H. K. Imhof, J. Schmid, R. Niessner, N. P. Ivleva and C. Laforsch, A novel, highly efficient method for the separation and quantification of plastic particles in sediments of aquatic environments, *Limnology and oceanography: methods*, 2012, **10**, 524-537.
11. C. Hudgins, Solubility and Density Studies of the CaCl2-ZnCl2-H2O System at 0 and 25 C, *Journal of Chemical & Engineering Data*, 1964, **9**, 434-436.
12. S. Zhang, W.-C. Wang, F.-X. Li and J.-Y. Yu, Swelling and dissolution of cellulose in NaOH aqueous solvent systems, *Cellul. Chem. Technol.*, 2013, **47**, 671-679.
13. L. M. B. Olsen, H. Knutsen, S. Mahat, E. J. Wade and H. P. H. Arp, unpublished work.
14. MERI, *Guide to microplastic identification*, 2012.
15. E. E. Burns and A. B. Boxall, Microplastics in the aquatic environment: Evidence for or against adverse impacts and major knowledge gaps, *Environ. Toxicol. Chem.*, 2018, **37**, 2776-2796.
16. V. Hidalgo-Ruz, L. Gutow, R. C. Thompson and M. Thiel, Microplastics in the marine environment: a review of the methods used for identification and quantification, *Environmental science & technology*, 2012, **46**, 3060-3075.

17. R. W. Obbard, S. Sadri, Y. Q. Wong, A. A. Khitun, I. Baker and R. C. Thompson, Global warming releases microplastic legacy frozen in Arctic Sea ice, *Earth's Future*, 2014, **2**, 315-320.
18. NGU, *MAREANOs pilotprosjekt på mikroplast - resultater og forslag til videre arbeid*, https://www.ngu.no/upload/Publikasjoner/Rapporter/2017/2017_043.pdf, 2018.
19. SINTEF, Microplastic in global and Norwegian marine environments: Distributions, degradation mechanisms and transport, 2017.
20. M. Claessens, S. De Meester, L. Van Landuyt, K. De Clerck and C. R. Janssen, Occurrence and distribution of microplastics in marine sediments along the Belgian coast, *Marine pollution bulletin*, 2011, **62**, 2199-2204.
21. R. C. Thompson, Y. Olsen, R. P. Mitchell, A. Davis, S. J. Rowland, A. W. John, D. McGonigle and A. E. Russell, Lost at sea: where is all the plastic?, *Science*, 2004, **304**, 838-838.
22. C. D. Rummel, A. Jahnke, E. Gorokhova, D. Kühnel and M. Schmitt-Jansen, Impacts of biofilm formation on the fate and potential effects of microplastic in the aquatic environment, *Environmental Science & Technology Letters*, 2017, **4**, 258-267.
23. M. Cole, P. K. Lindeque, E. Fileman, J. Clark, C. Lewis, C. Halsband and T. S. Galloway, Microplastics alter the properties and sinking rates of zooplankton faecal pellets, *Environmental science & technology*, 2016, **50**, 3239-3246.
24. H. Zhang, Transport of microplastics in coastal seas, *Estuarine, Coastal and Shelf Science*, 2017, **199**, 74-86.
25. M. Constant, P. Kerhervé, M. Mino-Vercellio-Verollet, M. Dumontier, A. S. Vidal, M. Canals and S. Heussner, Beached microplastics in the Northwestern Mediterranean Sea, *Marine pollution bulletin*, 2019, **142**, 263-273.
26. T. de Jesus Piñon-Colin, R. Rodriguez-Jimenez, M. A. Pastrana-Corral, E. Rogel-Hernandez and F. T. Wakida, Microplastics on sandy beaches of the Baja California Peninsula, Mexico, *Marine pollution bulletin*, 2018, **131**, 63-71.

Appendix A

PHOTOS FROM MICROSCOPY

Contents

A1 Method blanks

A1.1 MBlank 1

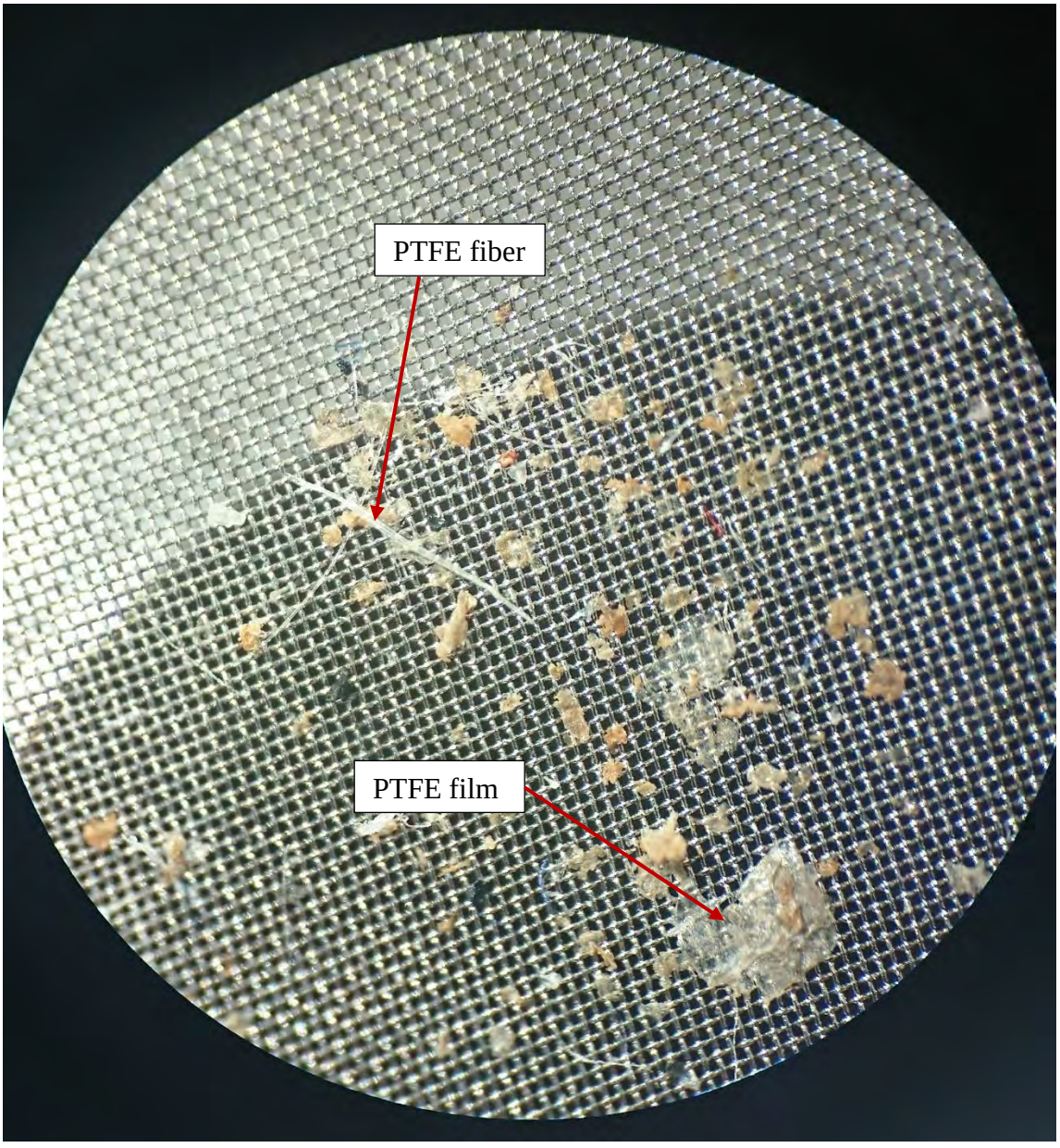

Figure A1 1 Method blank 1. Most particles were PTFE, also some PE, PP, PET and melamine particles.

A1.2 Mblank 2

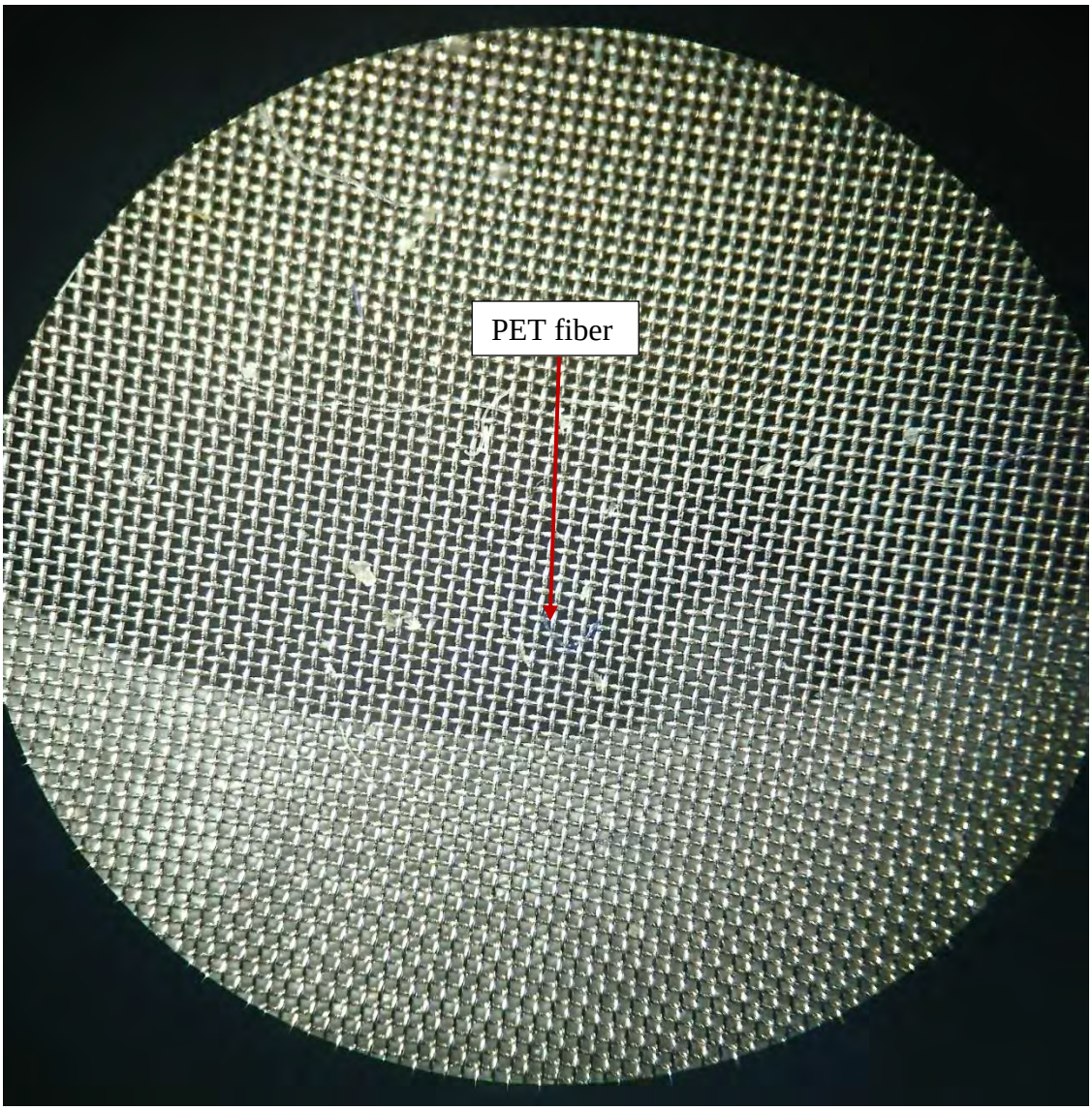

Figure A1 2 Method blank 2. Granules mostly PTFE, PP and PET particles.

A1.3 Mblank 3

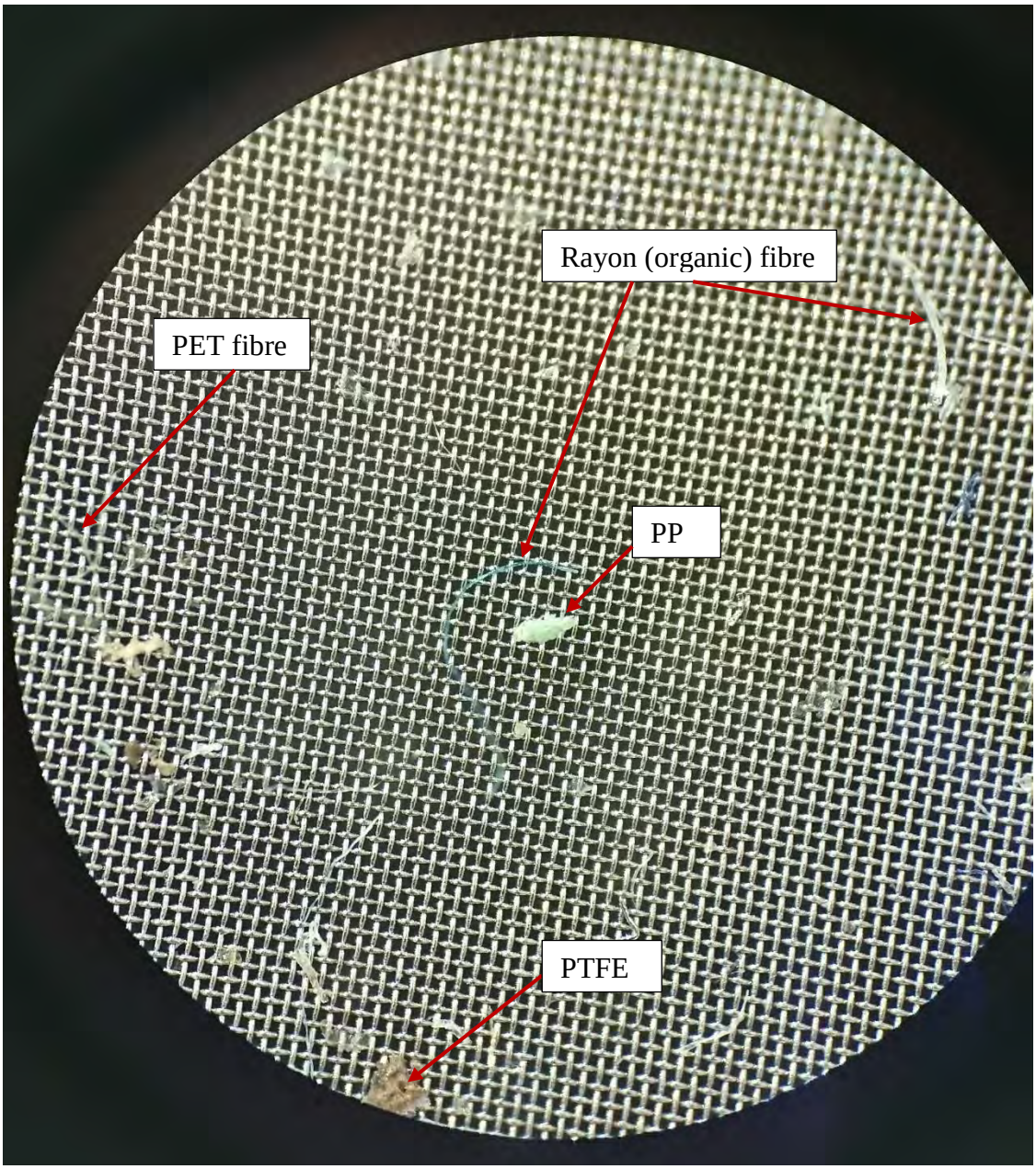

Figure A1 3 Method blank 3. Granules mostly PTFE, PP and PET.

A2 Sampling blanks

A2.1 SBlank 1

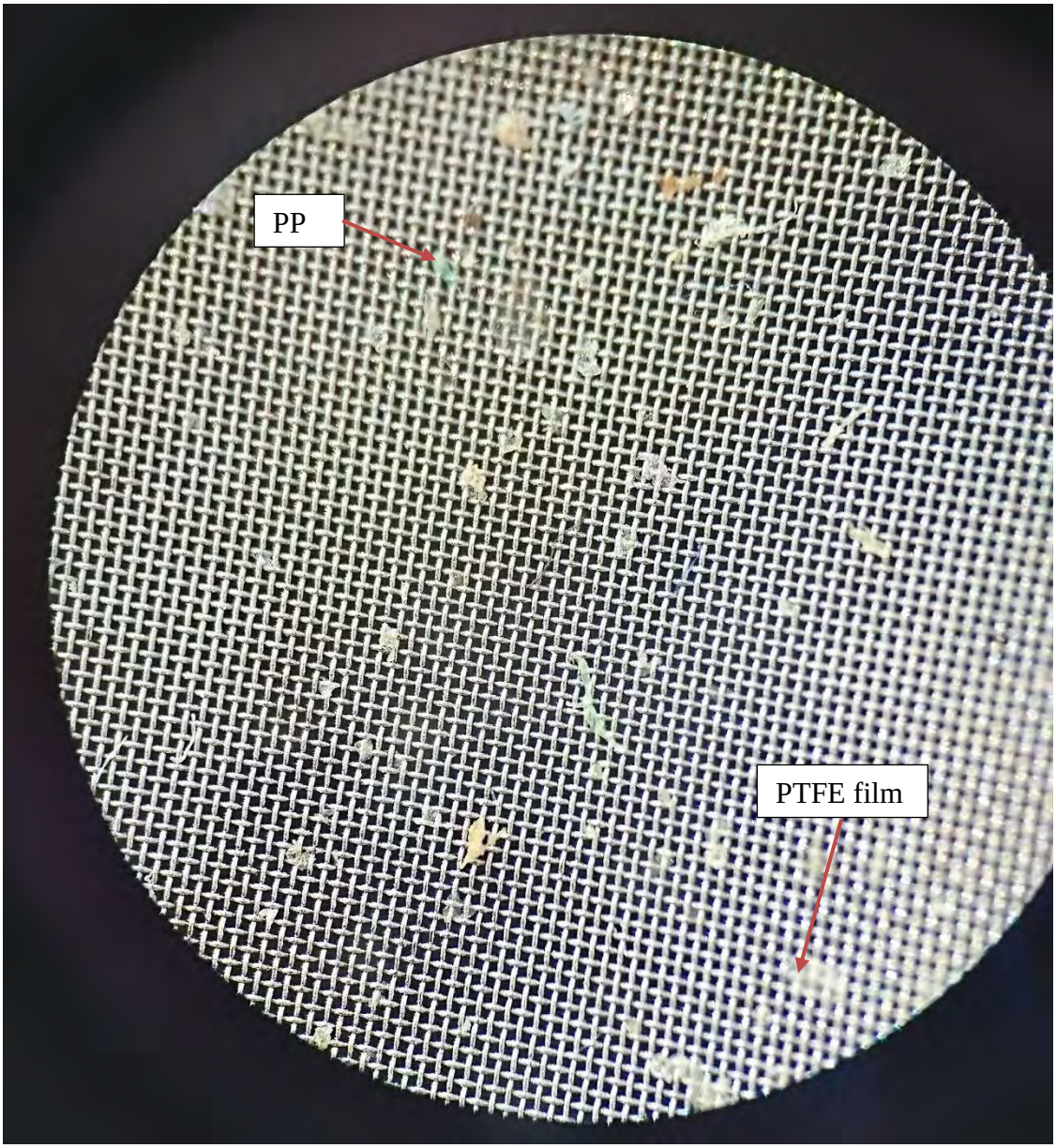

Figure A2 1 Sampling blank 1. Mostly PTFE particles and some PP and PE.

A2.2 Sblank 2

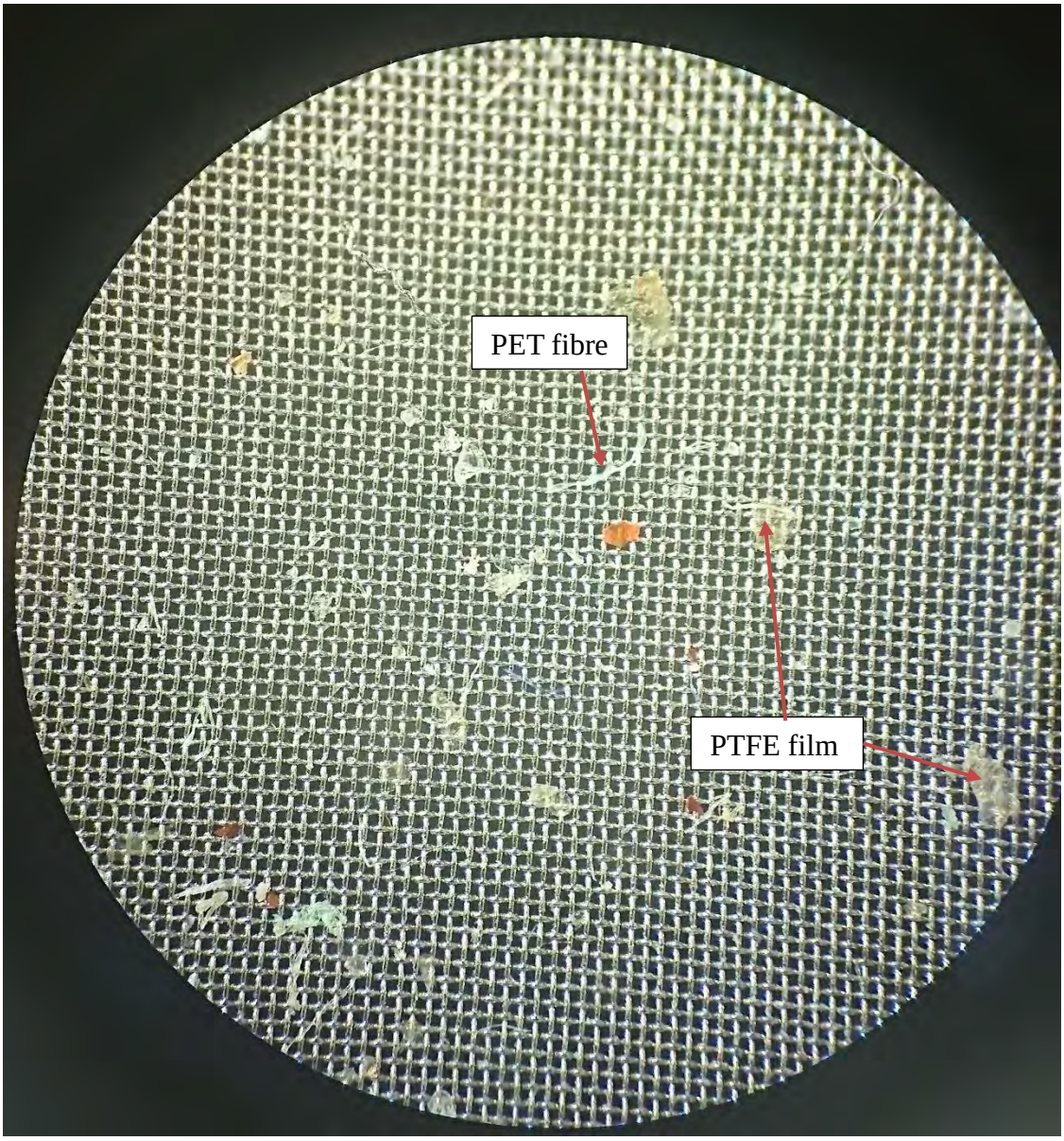

Figure A2 2 Sampling blank 2. Mostly PTFE particles, and some PP, nylon, PE and PET.

A2.3 Sblank 3

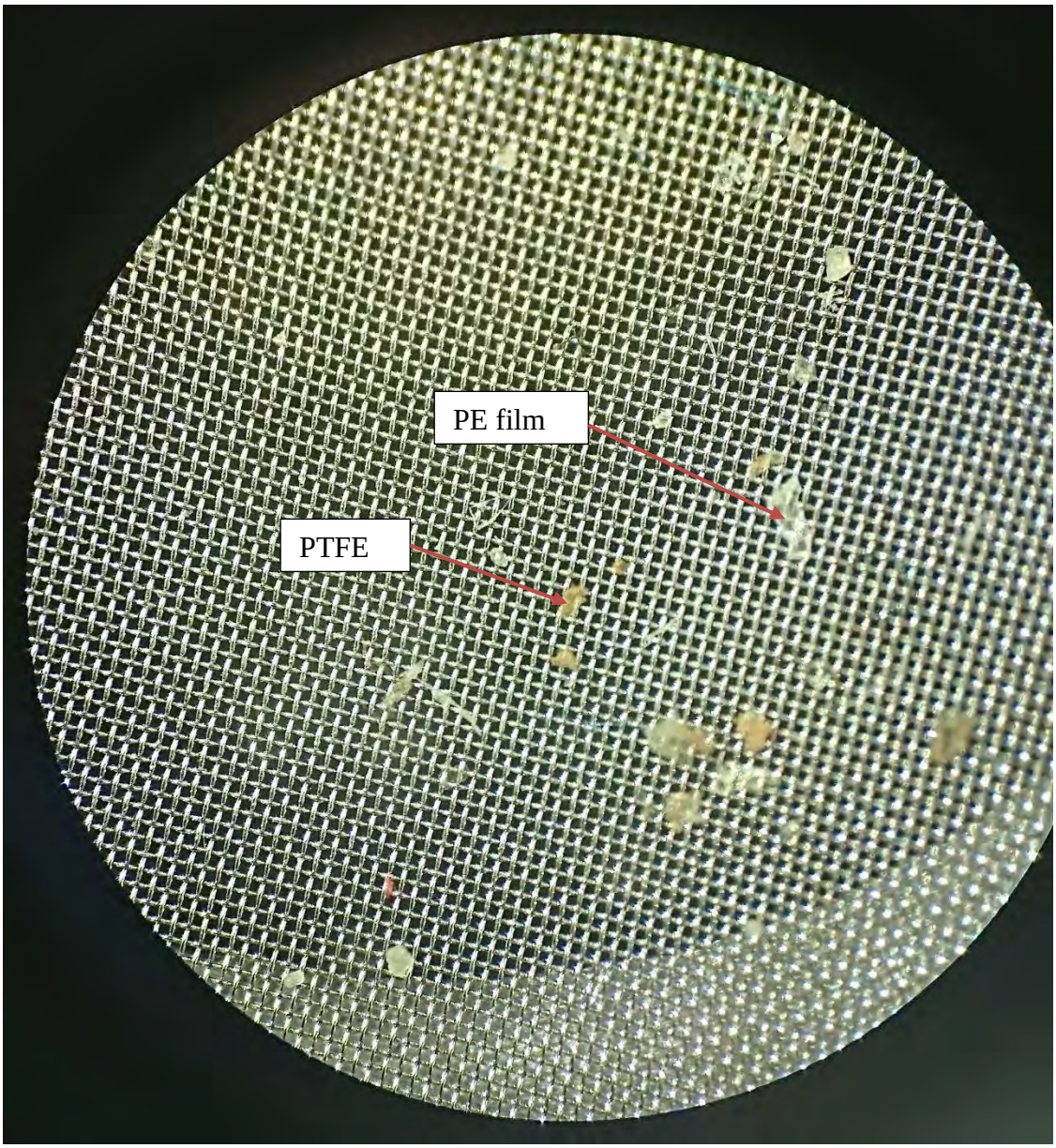

Figure A2 3 Sampling blank 3. Mostly PTFE particles, and some PE, PET, melamine, PP and PVC.

A2.4 Sblank 4

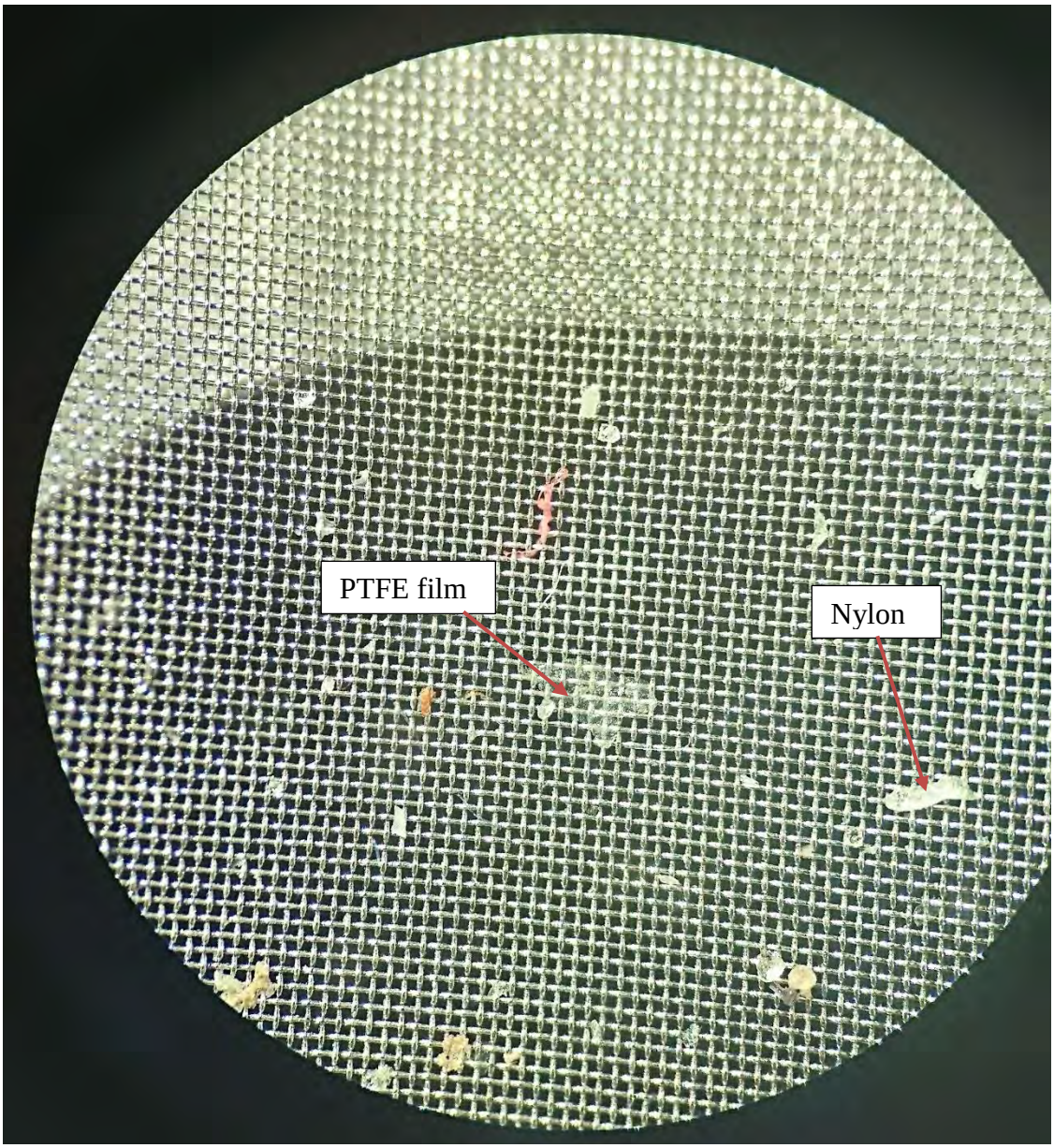

Figure A2 4 Sampling blank 4. Mostly PTFE particles, and some PP, PET and nylon.

A3 Sediment samples

A3.1 S-01

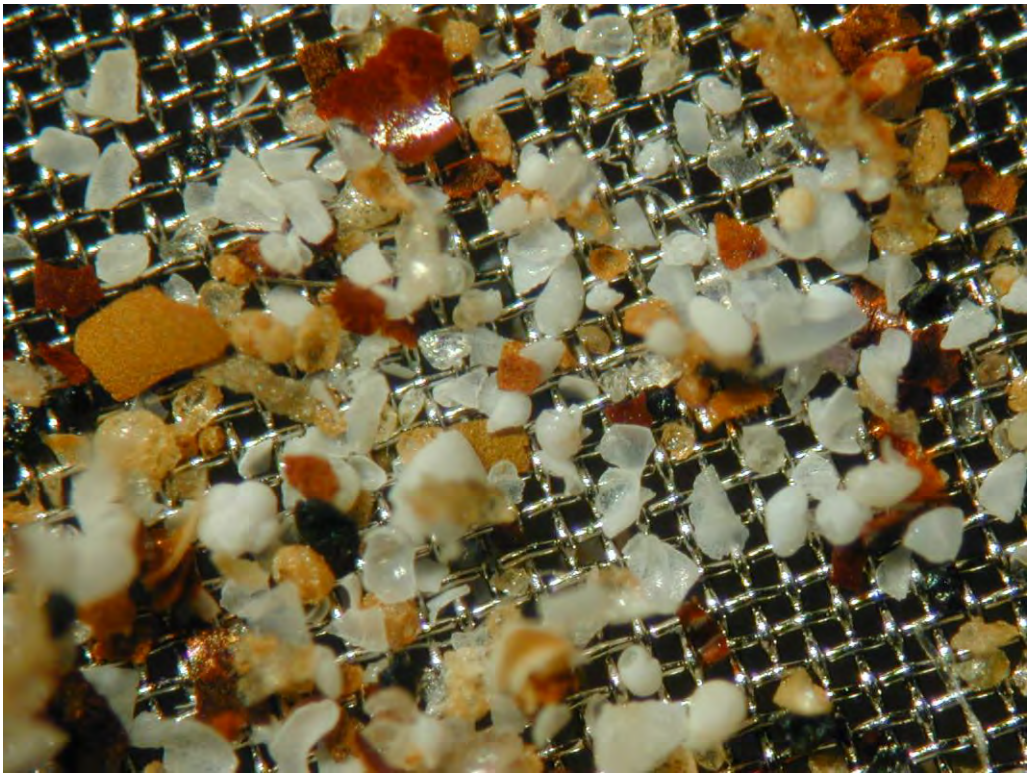

Figure A3 1 Sample S-01. Heterogenous composition. Microfossils observed.

Material composition:

- 80 % white to clear particles
- 15 % brown particles
- 5 % black particles

A3.2 S-02

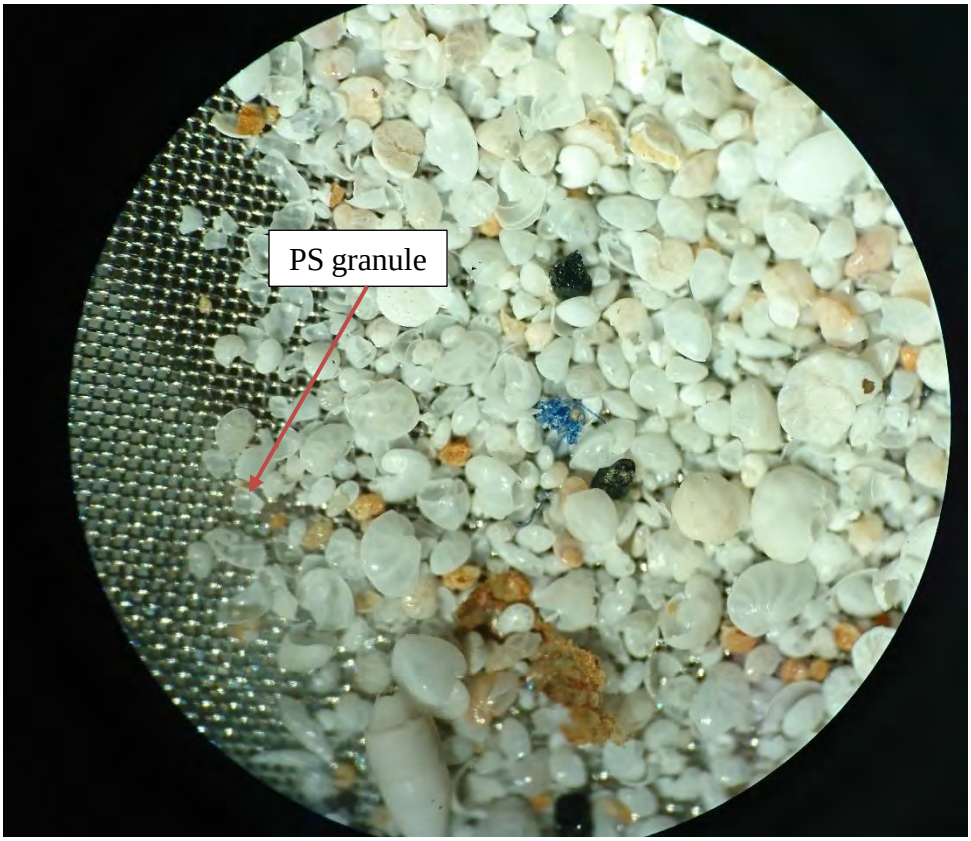

Figure A3 2 Sample S-02. High quantities of microfossils.

Material composition:

- 96 % white to clear particles
- 3 % brown particles
- 1 % black particles

A3.3 S-03

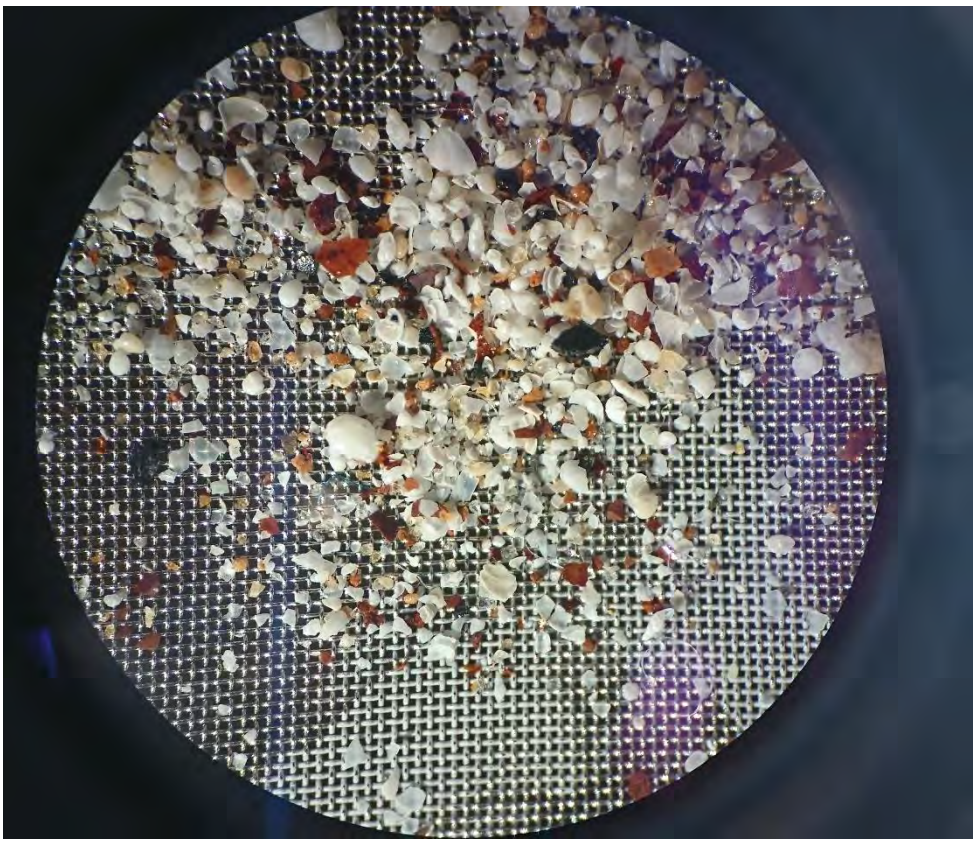

Figure A3 3 Sample S-03. Heterogenous composition. Microfossils observed.

Material composition:

- 60 % white to clear particles
- 35 % brown particles
- 5 % black particles

A3.4 S-04

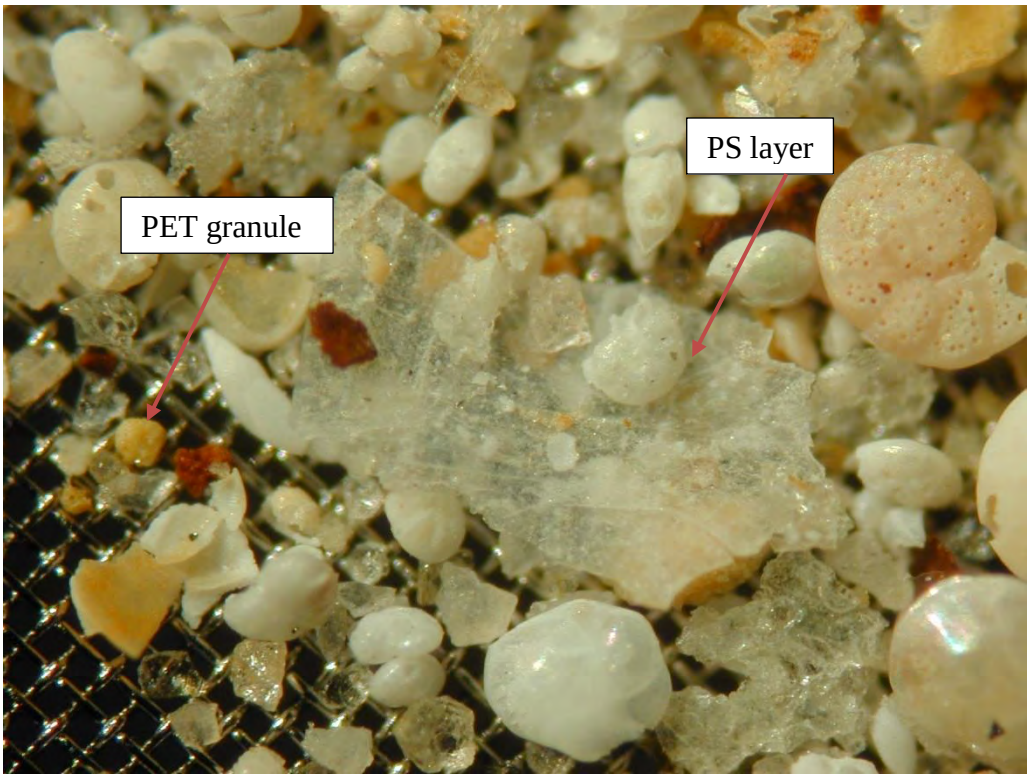

Figure A3 4 S-04. Heterogenous composition. Microfossils and polystyrene (PS) layer.

Material composition:

- 90 % white to clear particles
- 10 % brown particles

A3.5 S-05

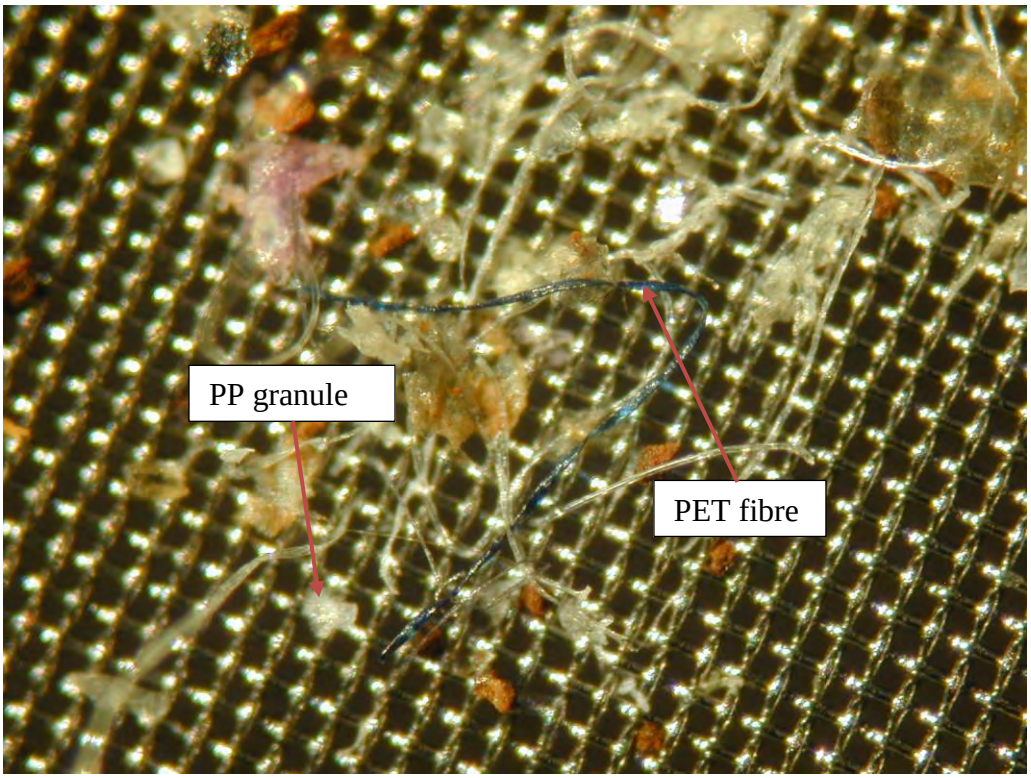

Figure A3 5 S-05. Blue PET fibre and various cotton and cellulose fibres.

Material composition:

- 70 % white to clear particles
- 30 % brown particles

A3.6 S-06

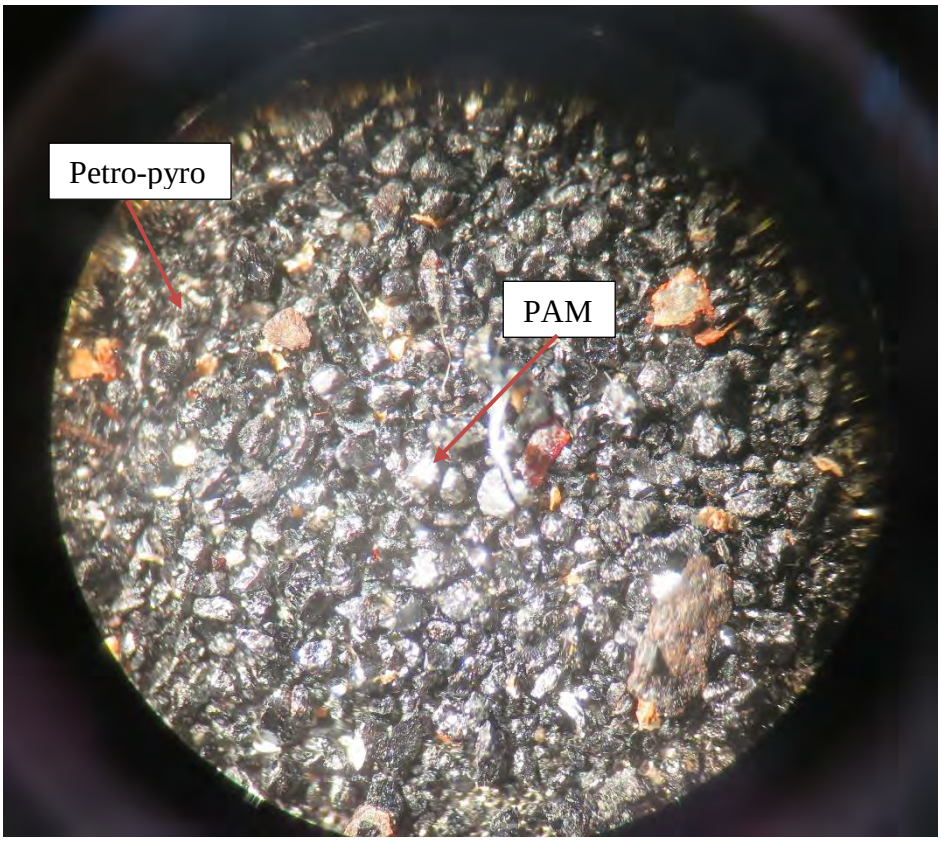

Figure A3 6 S-06. Lots of black granules.

Material composition:

- 94 % black particles
- 4 % brown particles
- 2 % white to clear particles

A3.7 S-07

Figure A3 7 S-07. Heterogenous composition.

Material composition:

- 97 % brown particles
- 2 % white to clear particles
- 1 % black particles

A3.8 S-08

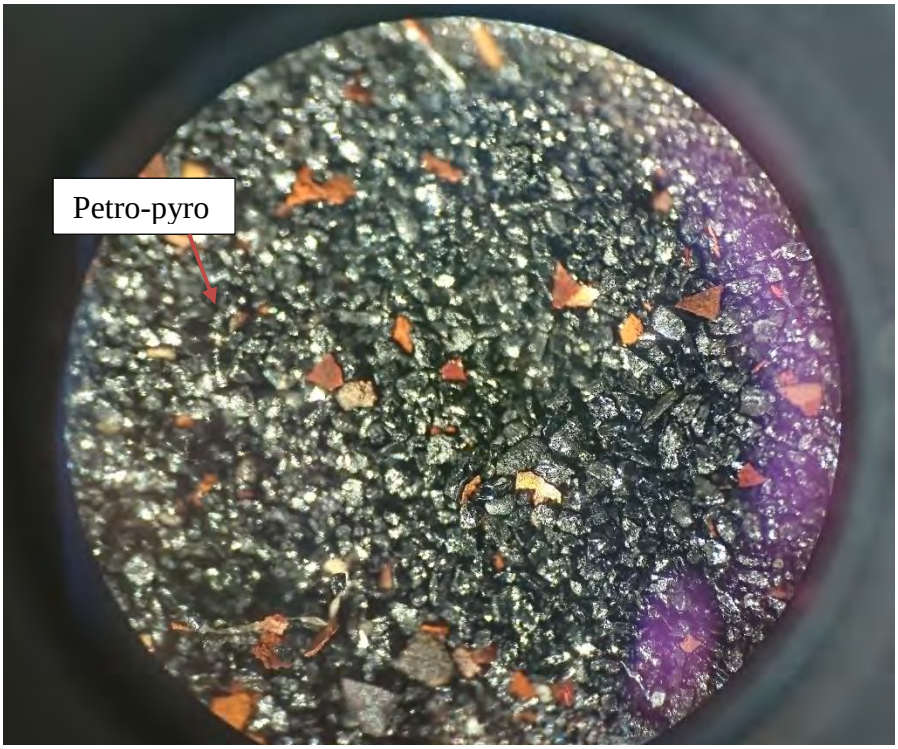

Figure A3 8 S-08. Lots of black granules.

Material composition:

- 89 % black particles
- 10 % brown particles
- 1 % white to clear particles

A3.9 S-09

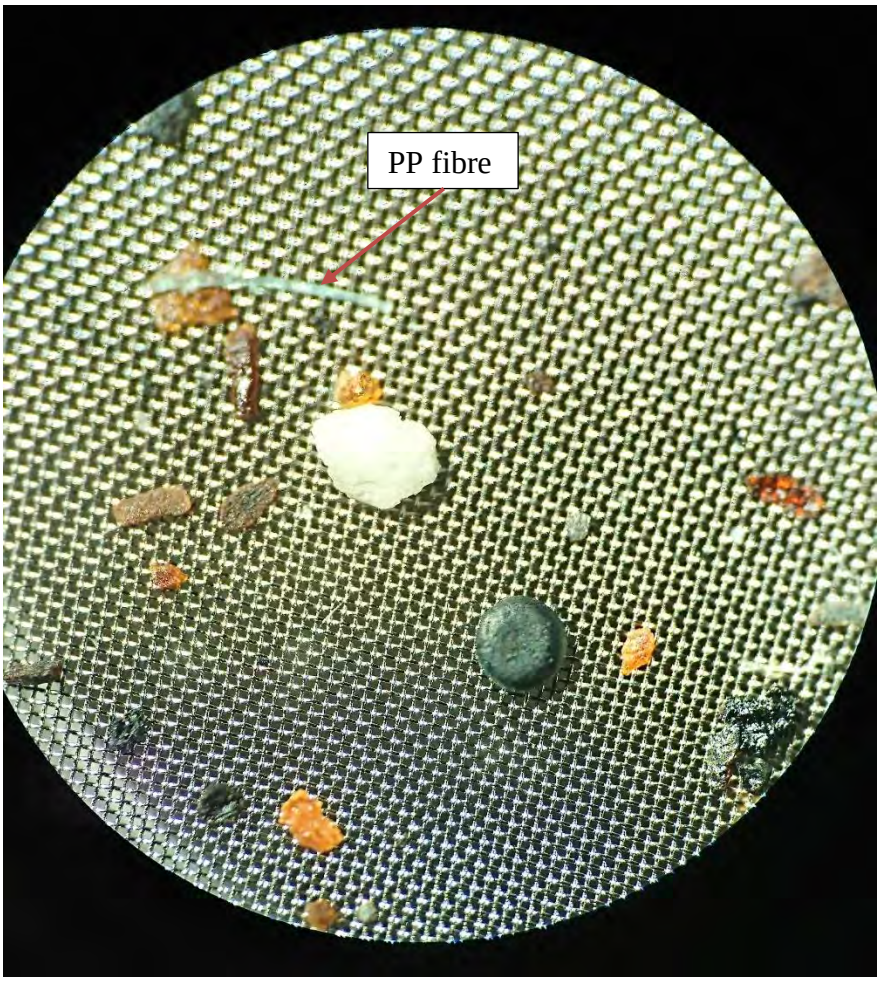

Figure A3 9 S-09. Heterogenous composition.

Material composition:

- 55 % black particles
- 35 % brown particles
- 10 % white to clear particles

A3.10 S-10

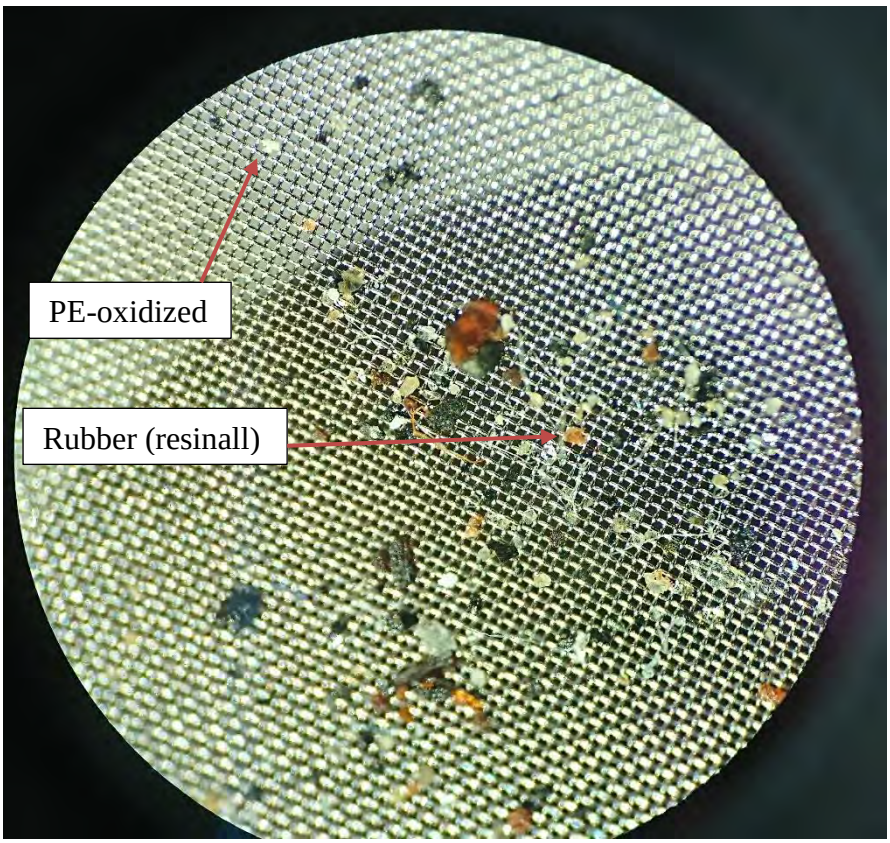

Figure A3 10 S-10. Heterogenous composition.

Material composition:

- 45 % white to clear particles
- 35 % brown particles
- 20 % black particles

A3.11 S-11

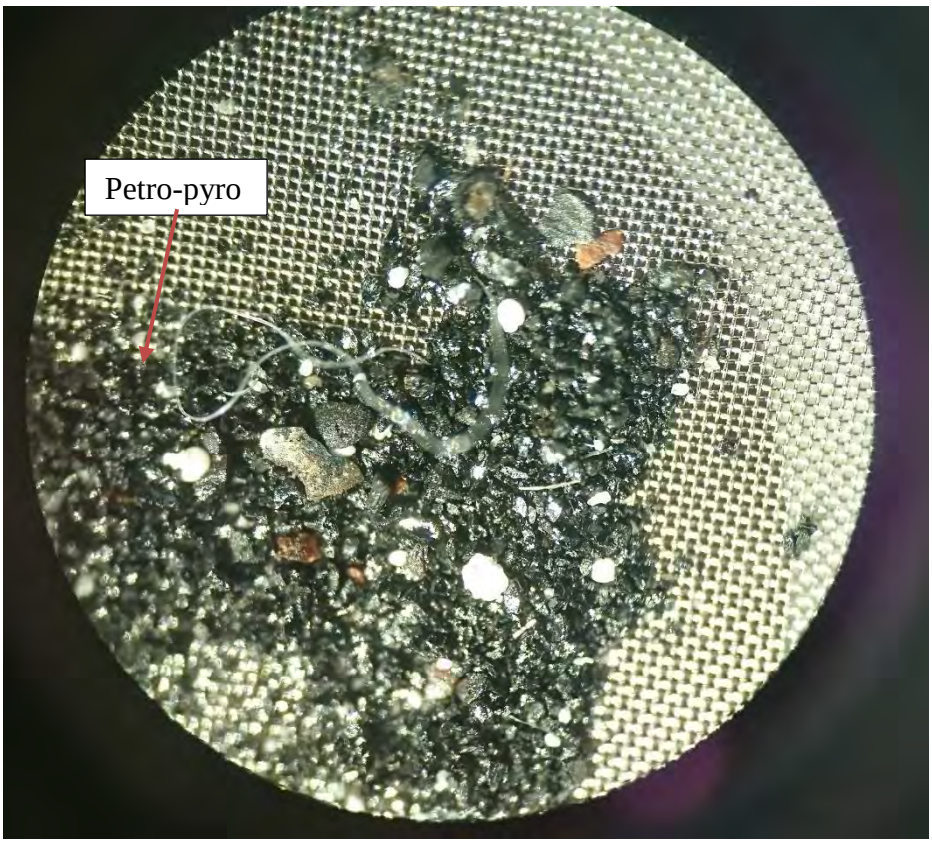

Figure A3 11 S-11. Lots of black granules.

Material composition:

- 6 % white to clear particles
- 1 % brown particles
- 93 % black particles

A3.12 S-12

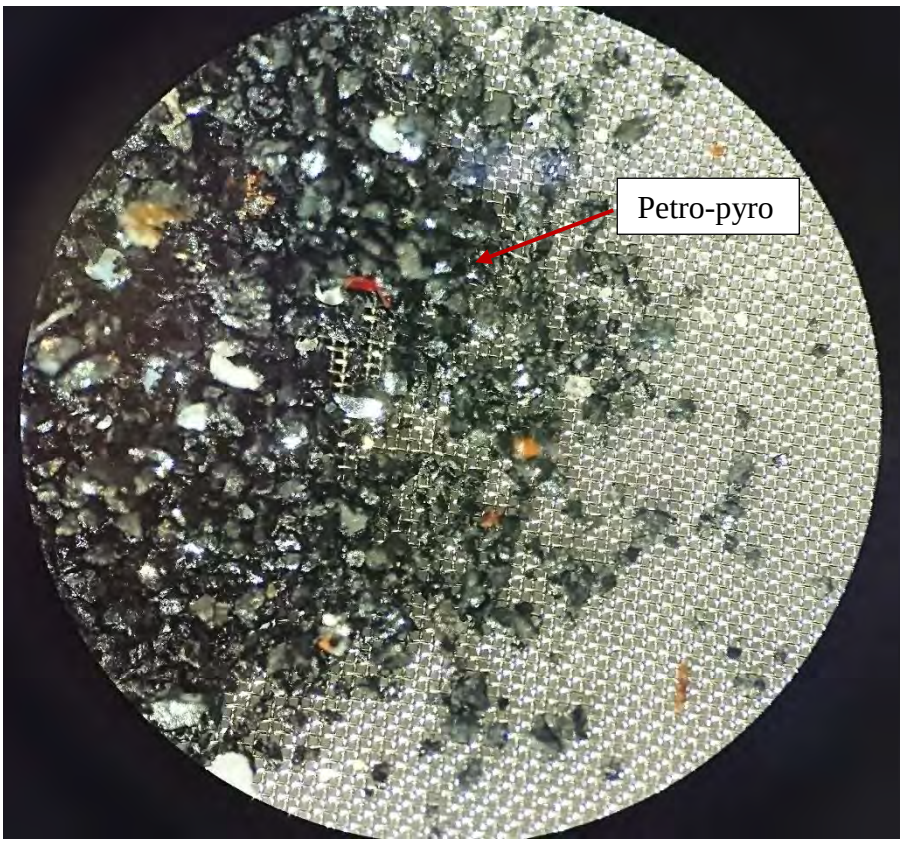

Figure A3 12 S-12. Lots of black granules.

Material composition:

- 8 % white to clear particles
- 2 % brown particles
- 90 % black particles

A3.13 S-13

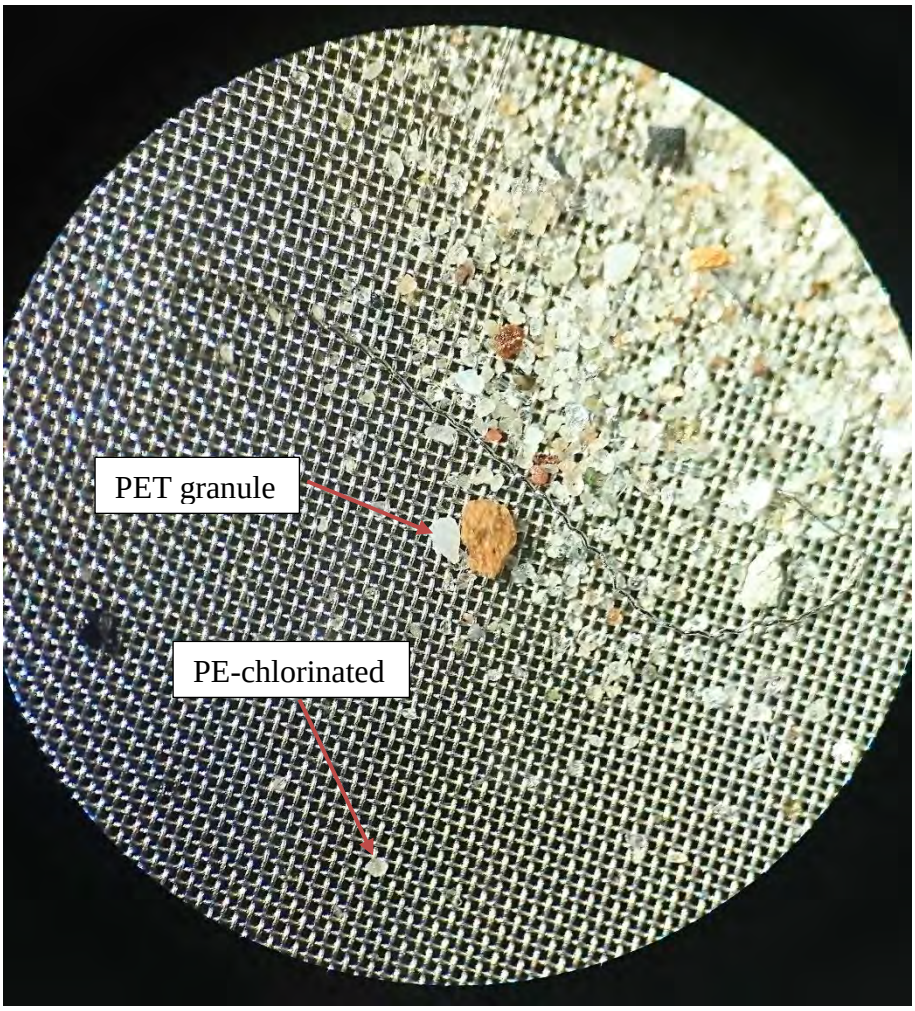

Figure A3 13 S-13. Mostly white to clear granules.

Material composition:

- 95 % white to clear particles
- 4 % brown particles
- 1 % black particles

A3.14 S-14

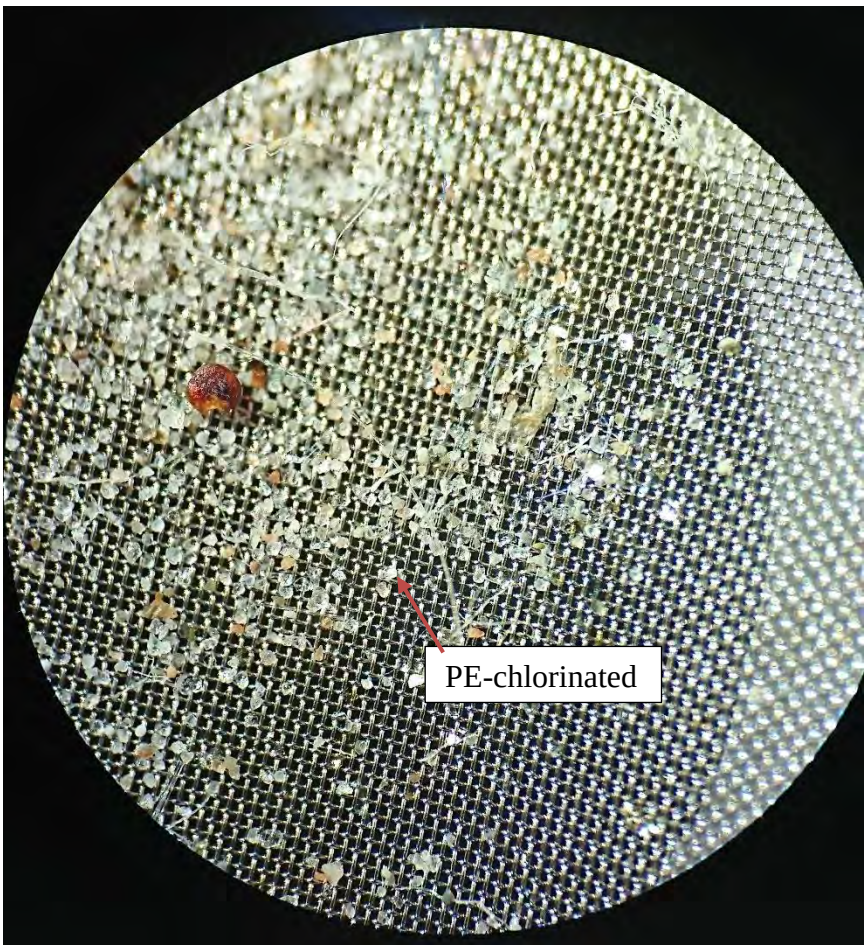

Figure A3 14 S-14. Mostly white to clear granules.

Material composition:

- 95 % white to clear particles
- 4 % brown particles
- 1 % black particles

A3.15 S-15

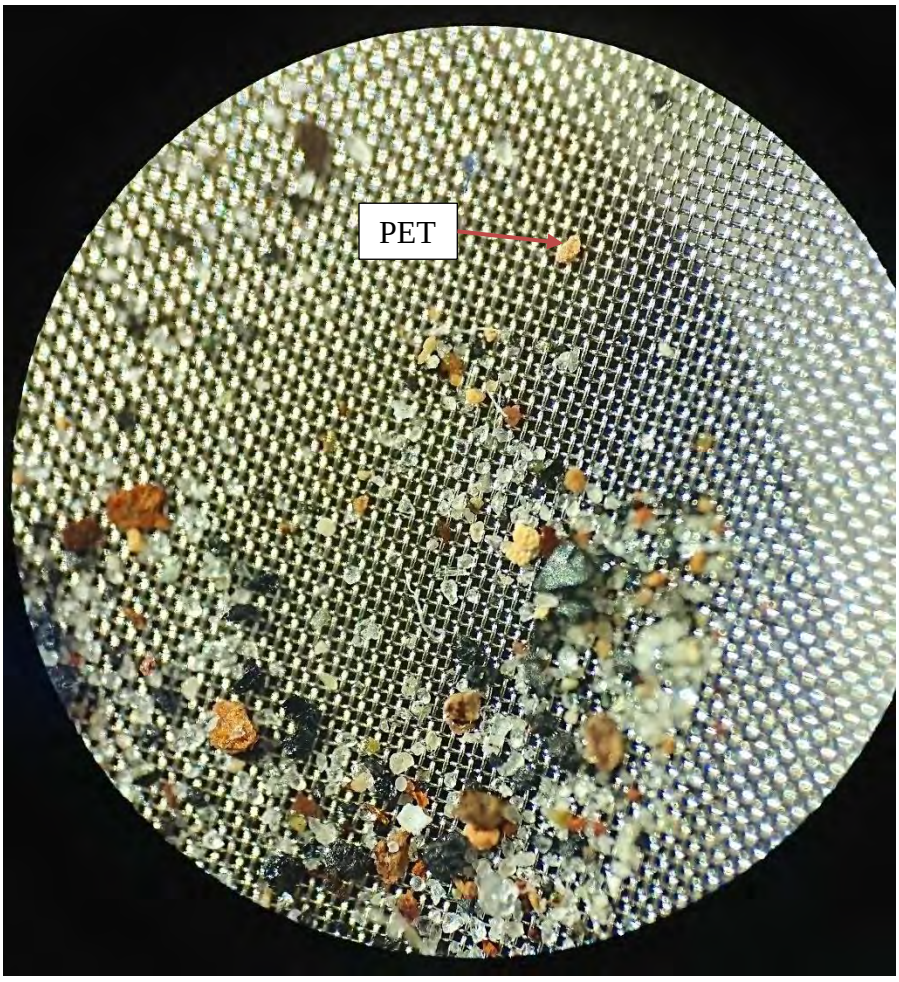

Figure A3 15 S-15. Heterogenous composition.

Material composition:

- 55 % white to clear particles
- 10 % brown particles
- 35 % black particles

A3.16 S-16

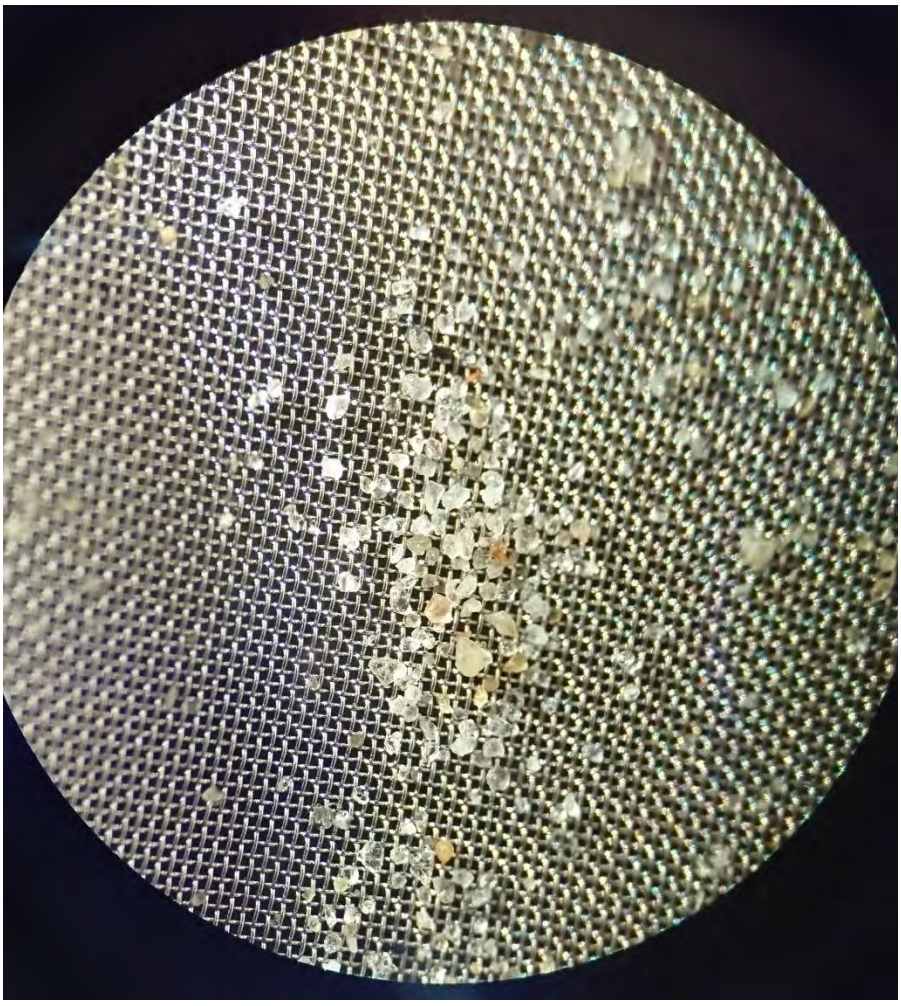

Figure A3 16 S-16. Mostly white to clear granules.

Material composition:

- 6 % white to clear particles
- 1 % brown particles
- 93 % black particles

A3.17 S-17

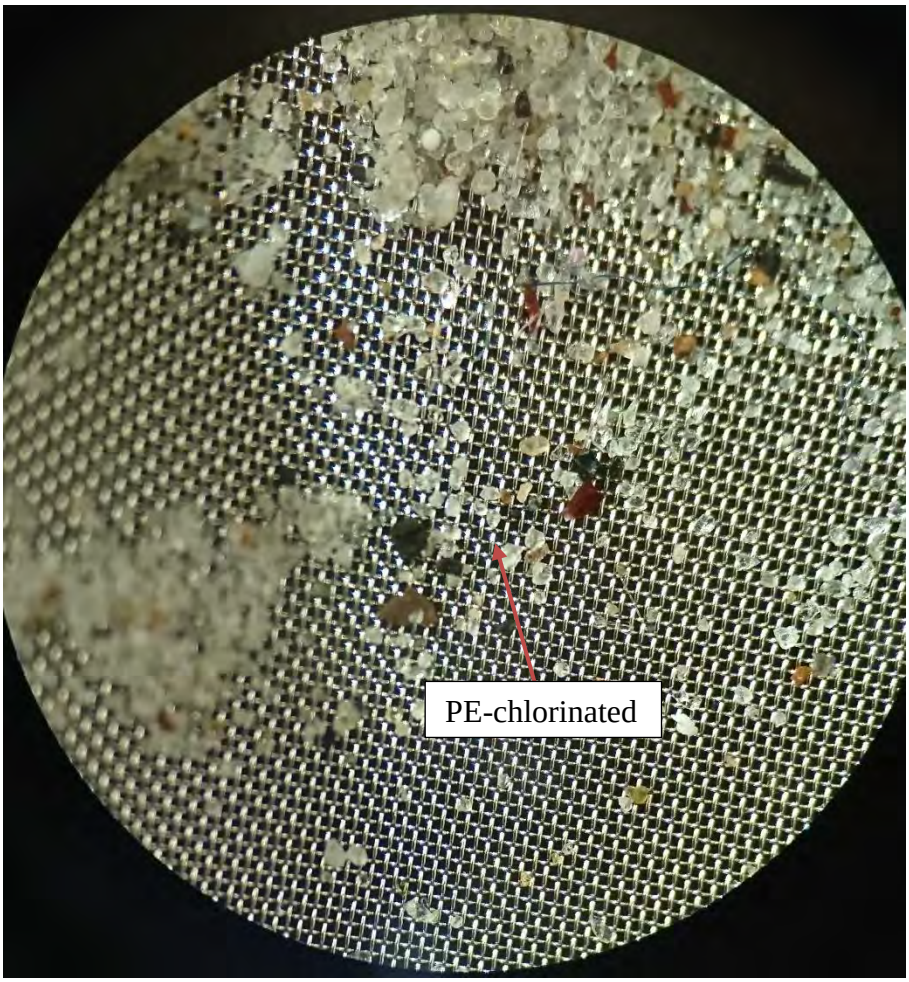

Figure A3 17 S-17. Mostly white to clear granules.

Material composition:

- 90 % white to clear particles
- 8 % brown particles
- 3 % black particles

A3.18 S-18

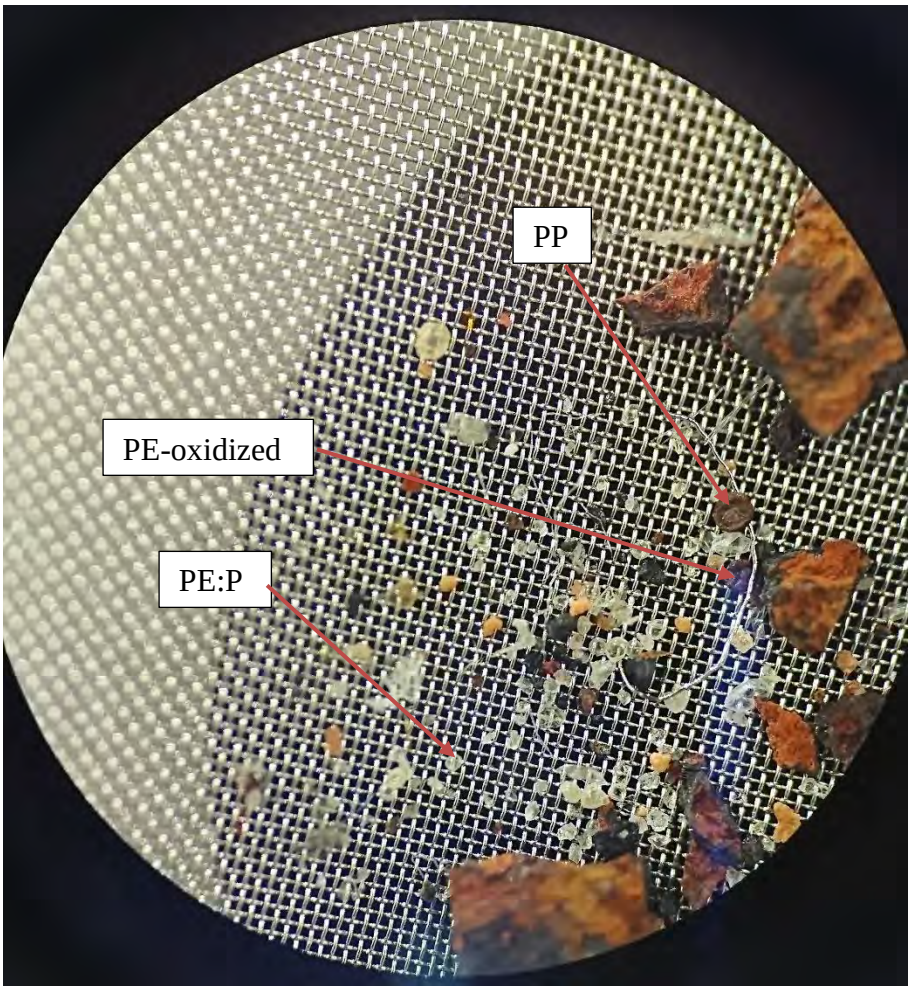

Figure A3 18 S-18. Heterogenous composition.

Material composition:

- 15 % white to clear particles
- 84 % brown particles
- 1 % black particles

A3.19 S-19

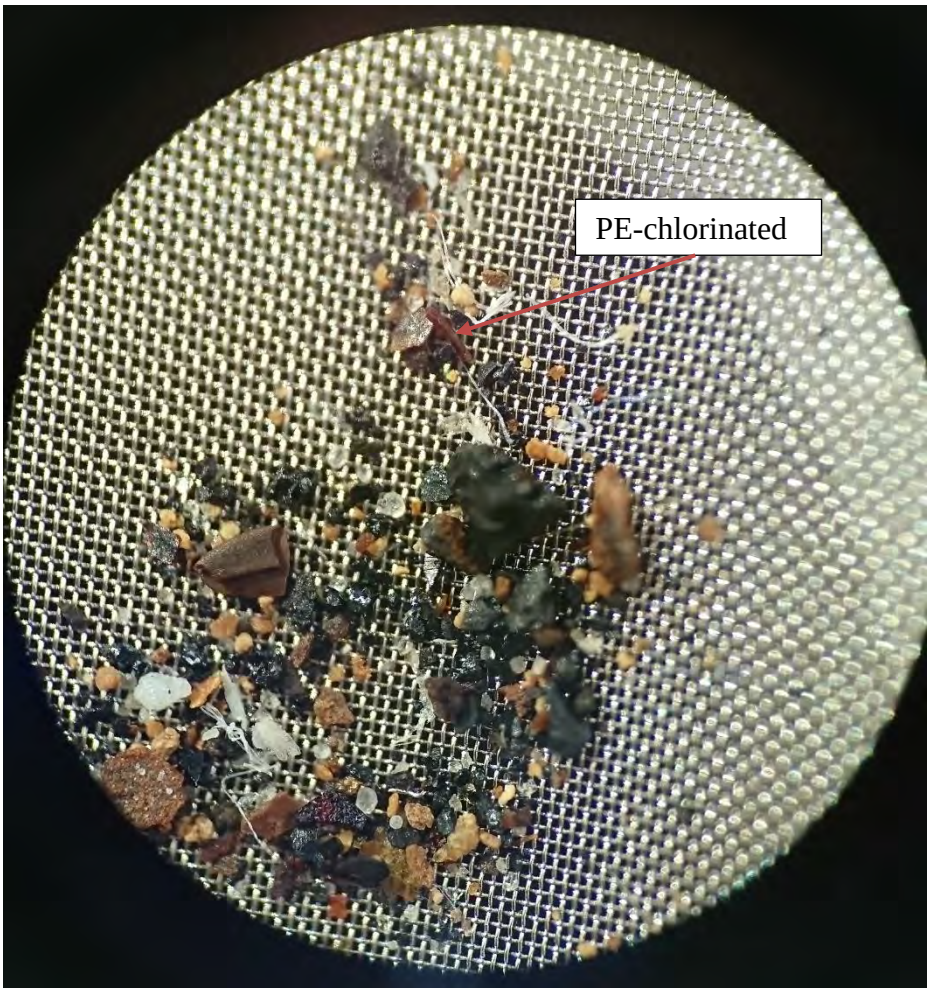

Figure A3 19 S-19. Several black granules. Heterogenous composition.

Material composition:

- 15 % white to clear particles
- 30 % brown particles
- 55 % black particles

A3.20 S-20

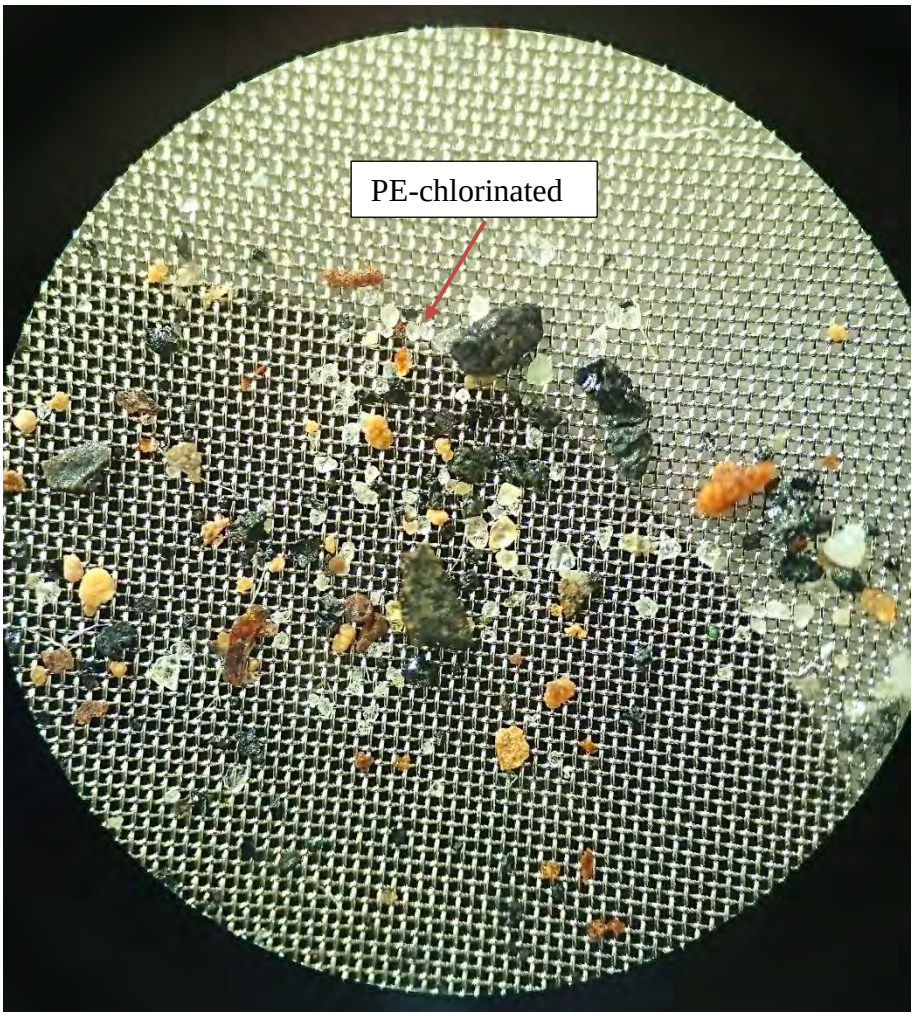

Figure A3 20 S-20. Heterogenous composition.

Material composition:

- 10 % white to clear particles
- 40 % brown particles
- 50 % black particles

A3.21 B-1

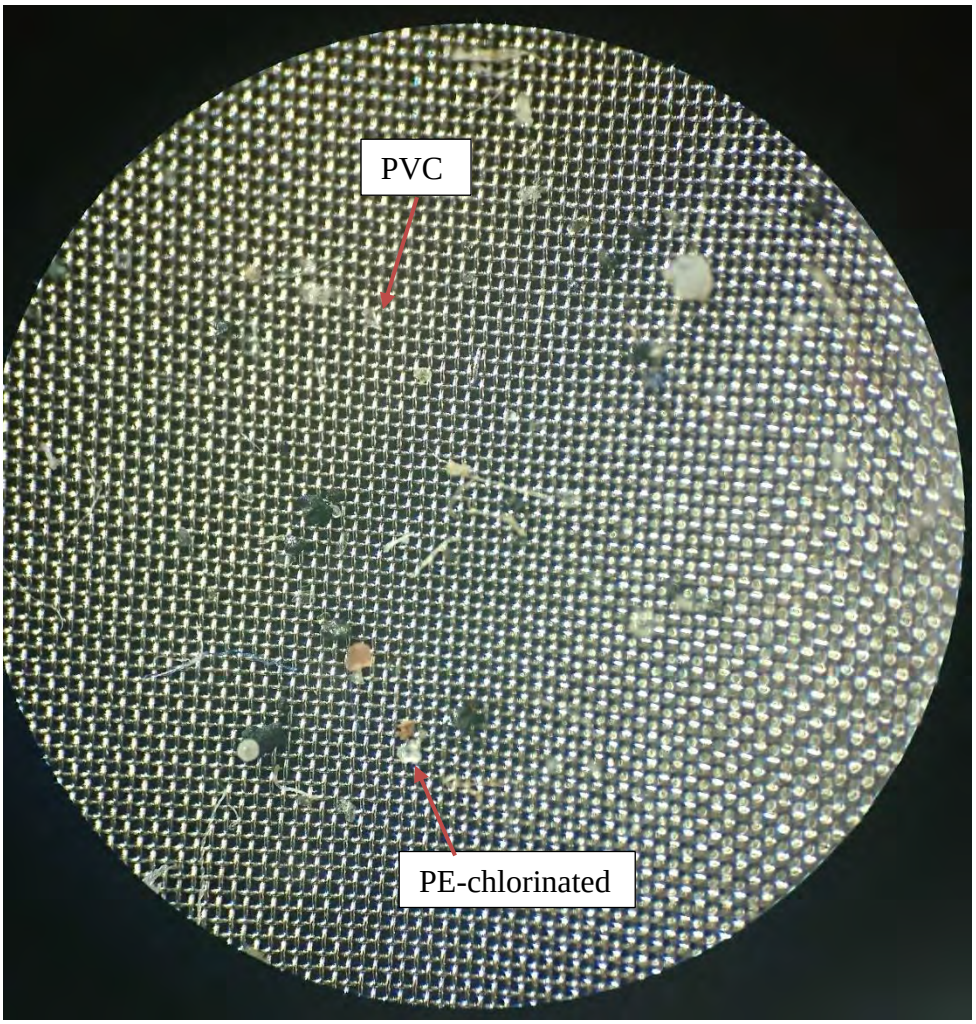

Figure A3 21 B-1. Heterogenous composition.

Material composition:

- 60 % white to clear particles
- 1 % brown particles
- 39 % black particles

A3.22 B-2

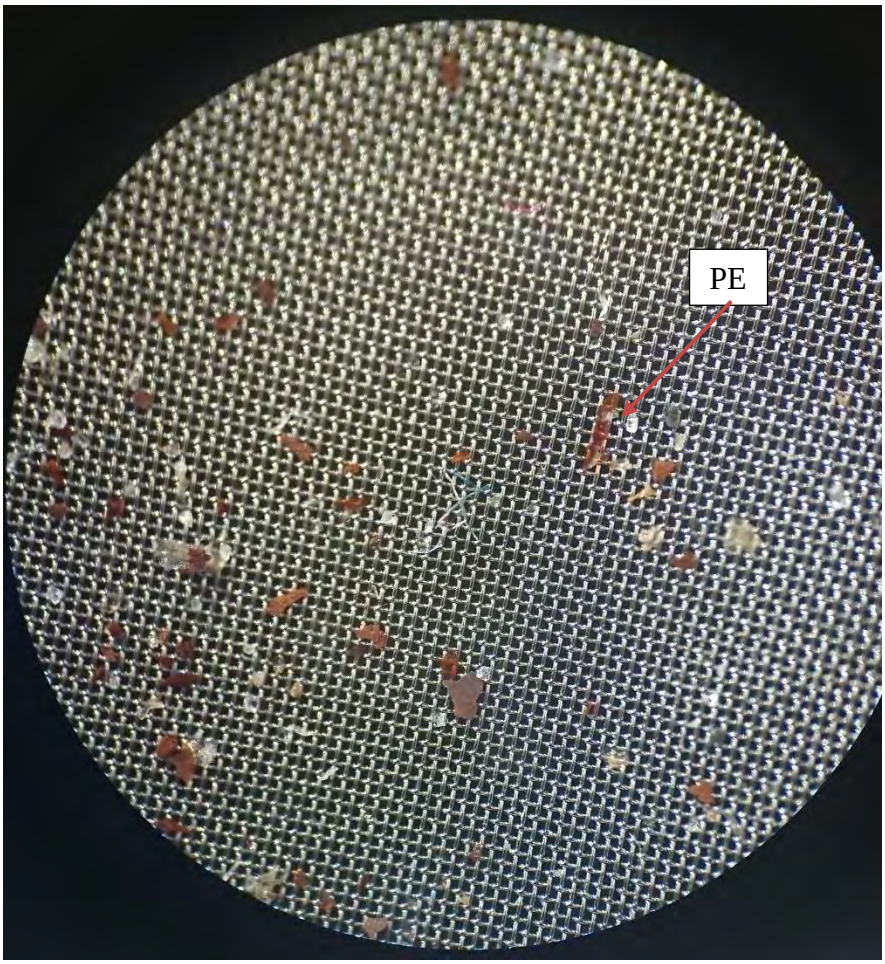

Figure A3 22 Heterogenous composition. Several brown particles.

Material composition:

- 65 % white to clear particles
- 34 % brown particles
- 1 % black particles

Appendix B

RESULTS FOR METHOD- AND SAMPLING BLANKS

Contents

B1 Method blanks

Method blanks (n = 3) were prepared and analysed for microplastics to control for contamination resulting from the laboratory method. The number of particles in the method blanks are shown in the table below.

Table B1 1 Number of microplastic particles and other particles in method blanks within each defined FT-IR category. SD = standard deviation.

Particle		Blank 1	Blank 2	Blank 3	Mean ± SD
Plastic polymer	PE	2	0	0	1 ± 1
	PP	2	4	3	3 ± 1
	PET	2	3	3	3 ± 1
	PS	0	1	0	0 ± 1
	PTFE*	72	10	20	34 ± 33
	PMMA	0	1	0	0 ± 1
	PE-oxidized	4	0	0	1 ± 2
	Melamine	2	1	0	1 ± 1
	Nylon	0	2	2	1 ± 1
	Other	0	0	2	1 ± 1
	Total-PTFE (Total*)	12 (84)	12 (22)	10 (30)	11 ± 9 (45 ± 43)
Oxy-resin		0	0	0	0 ± 0
Rubber		0	0	0	0 ± 0
Petro-Pyro		0	0	0	0 ± 0
Organic		12	35	28	25 ± 12
Mineral		0	0	0	0 ± 0
Unknown		24	33	40	32 ± 8

**PTFE was excluded due to a local contamination*

As seen by the table, relatively high levels of PTFE particles were found in the method blanks (mean: 34 ± 33 particles/sample, corresponding to approximately 80 % of the detected microplastics). As mentioned in the main report, the source of PTFE particles was, after analysis of our laboratory equipment, found to be the inner parts of the ball valve used in the density separator. Due to the high abundance of PTFE resulting from the analytical method, it was decided that the method did not yield quantitative results for this plastic type. Therefore, results for PTFE in the sediment samples are not reported.

B2 Sampling blanks

The number of particles in the sampling blanks (n = 4) are shown in the table below. As described in the main report, these were prepared and analysed for microplastics to control for airborne contamination resulting from the transport and analytical method.

Table B2 2 Number of microplastic particles and other particles in sampling within each defined FT-IR category. SD = standard deviation.

Particle		FBlank 1	FBlank 2	FBlank 3	FBlank4	Mean ± SD
Plastic polymer	PE	2	2	3	0	2 ± 1
	PP	8	12	3	3	7 ± 4
	PET	0	2	3	2	2 ± 1
	PTFE*	62	24	27	41	39 ± 17
	PE:PP	2	0	1	1	1 ± 1
	PVC	0	0	1	0	0 ± 1
	Melamine	0	0	1	0	0 ± 1
	Nylon	0	4	0	2	2 ± 2
	Unverified	0	0	3	1	1 ± 1
	Total-PTFE (Total*)	12 (74)	20 (44)	15 (42)	9 (50)	14 ± 5 (53 ± 15)
Oxy-resin		0	0	0	0	0 ± 0
Rubber		0	0	0	0	0 ± 0
Petro-Pyro		0	0	0	0	0 ± 0
Organic		10	46	8	18	21 ± 18
Mineral		0	0	1	0	0 ± 1
Unknown		40	92	30	49	53 ± 27

**PTFE was excluded due to a local contamination*

In agreement with the method blanks, relatively high levels of PTFE particles were found in the sampling blanks (mean: 39 ± 17 particles, corresponding to more than 70 % of the detected microplastics). As previously mentioned, this was due to local contamination source. Hence, the method did not yield quantitative results for this plastic type. Therefore, the results for PTFE in the sediment samples were not reported.

Further, the abundance of other microplastics were in the same range, although somewhat higher in the sampling blanks, with PP, PET, PE and nylon being the most abundant.

Appendix C

DATING RESULTS OF CORE R1869MC016 AND R1887MC022

Contents

C1 Dating of core R1869MC016

Gamma Dating Center Copenhagen

Copenhagen, August 19th, 2019

Thorbjørn J. Andersen
Department of Geosciences and Natural Resource Management (IGN)
University of Copenhagen
Oester Voldgade 10
1350 Copenhagen K
e-mail tja@ign.ku.dk
phone +45 35 32 25 03
fax +45 35 32 25 01

Dating of core R1869MC016A

Dating of core R1869MC016A

Methods

The samples have been analysed for the activity of ^{210}Pb, ^{226}Ra and ^{137}Cs via gammaspectrometry at the Gamma Dating Center, Institute of Geography, University of Copenhagen. The measurements were carried out on a Canberra ultralow-background Ge-detector. ^{210}Pb was measured via its gamma-peak at 46,5 keV, ^{226}Ra via the granddaughter ^{214}Pb (peaks at 295 and 352 keV) and ^{137}Cs via its peak at 661 keV.

Results

The core showed surface contents of unsupported ^{210}Pb of around 340 Bq kg^{-1} with a clear tendency for exponential decline with depth (fig 1). The calculated flux of unsupported ^{210}Pb is 420 Bq m^{-2} y^{-1} which is about 3 times higher than the expected flux (based on data shown in Appleby, 2001). This indicates that the site is subject to sediment focusing.

The content of the isotope ^{137}Cs was low and only consistently above detection limits in the upper 8 cm of the core.

CRS-modelling has been applied on the profile using a modified method (Appleby, 2001; Andersen 2017) where the activity below 22 cm is calculated on the basis of the regression shown in fig 2. The result is given in table 2 and fig 3 and 4.

The chronology given in table 2 is only valid if bioturbation and other sediment mixing is negligible. If this is not the case, ages given in table 2 are underestimated and accumulation rates are overestimated. However, the profile of unsupported ^{210}Pb showed a fairly uniform exponential decline with depth which indicates that mixing is not significant. Additionally, measurable content of ^{137}Cs was only detected in the upper part of the core which also indicates that mixing cannot be severe and the chronology is therefore believed to be reliable.

Copenhagen, August 19th 2019

Thorbjørn J Andersen
Professor,
IGN, University of Copenhagen
Oester Voldgade 10, 1350 Copenhagen K, Denmark

Reference:

Andersen, T.J., 2017. Some Practical Considerations Regarding the Application of ^{210}Pb and ^{137}Cs Dating to Estuarine Sediments. Applications of Paleoenvironmental Techniques in Estuarine Studies . Developments in Paleoenvironmental Research (DPER), Vol. 20, p 121-140.

Appleby, P.G., 2001. Chronostratigraphic techniques in recent sediments. In: Last, W.M & Smol, J.P. (eds) Tracking environmental change using lake sediments. Volume 1: Basin analysis, coring and chronological techniques. Kluwer Academic Publishers, the Netherlands.

Table 1. Raw data, R1869MC016A

Depth	Pb-210tot	error Pb-210 tot	Pb-210 supp	error Pb-210 sup	Pb-210 unsup	error Pb-210 unsup	Cs-137	error Cs-137
cm	Bq kg-1	Bq kg-1	Bq kg-1	Bq kg-1	Bq kg-1	Bq kg-1	Bq kg-1	Bq kg-1
0.50	369	25	25	6	344	31	2	1
1.50	348	48	34	0	314	48	4	8
2.50	309	27	26	4	283	31	7	1
3.50	231	31	20	6	210	37	5	3
4.50	231	20	24	2	207	22	3	1
5.50	216	15	25	0	192	16	5	1
6.50	146	16	15	8	132	24	3	1
7.50	113	13	22	2	91	16	5	1
8.50	85	11	22	4	63	15	2	1
9.50	91	8	24	3	67	12	1	1
10.50	81	10	24	0	57	10	2	1
14.50	59	8	24	1	35	9	0	0
15.50	51	8	23	2	29	10	0	0
18.50	33	3	21	2	11	5	0	0
20.50	26	4	22	4	4	8	0	0

Table 2, chronology core R1869MC016A

Depth	Age	error age	Date	acc rate	error rate	Date acc rate
cm	y	y	y	(kg m-2 y-1)	(kg m-2 y-1)	y
			2018			
0.5	2	2	2016	1.19	0.12	2017
1.5	6	2	2012	1.13	0.17	2014
2.5	11	2	2007	1.08	0.13	2010
3.5	16	2	2002	1.13	0.20	2005
4.5	21	2	1997	1.14	0.14	2000
5.5	27	2	1991	1.00	0.11	1994
6.5	34	3	1984	1.01	0.19	1987
7.5	40	3	1978	1.21	0.23	1981
8.5	44	4	1974	1.48	0.36	1976
9.5	49	4	1969	1.51	0.31	1971
10.5	55	5	1963	1.34	0.26	1966
14.5	85	12	1933	1.07	0.47	1948
15.5	95	9	1923	0.80	0.27	1928
18.5	131	24	1887	0.66	0.53	1905

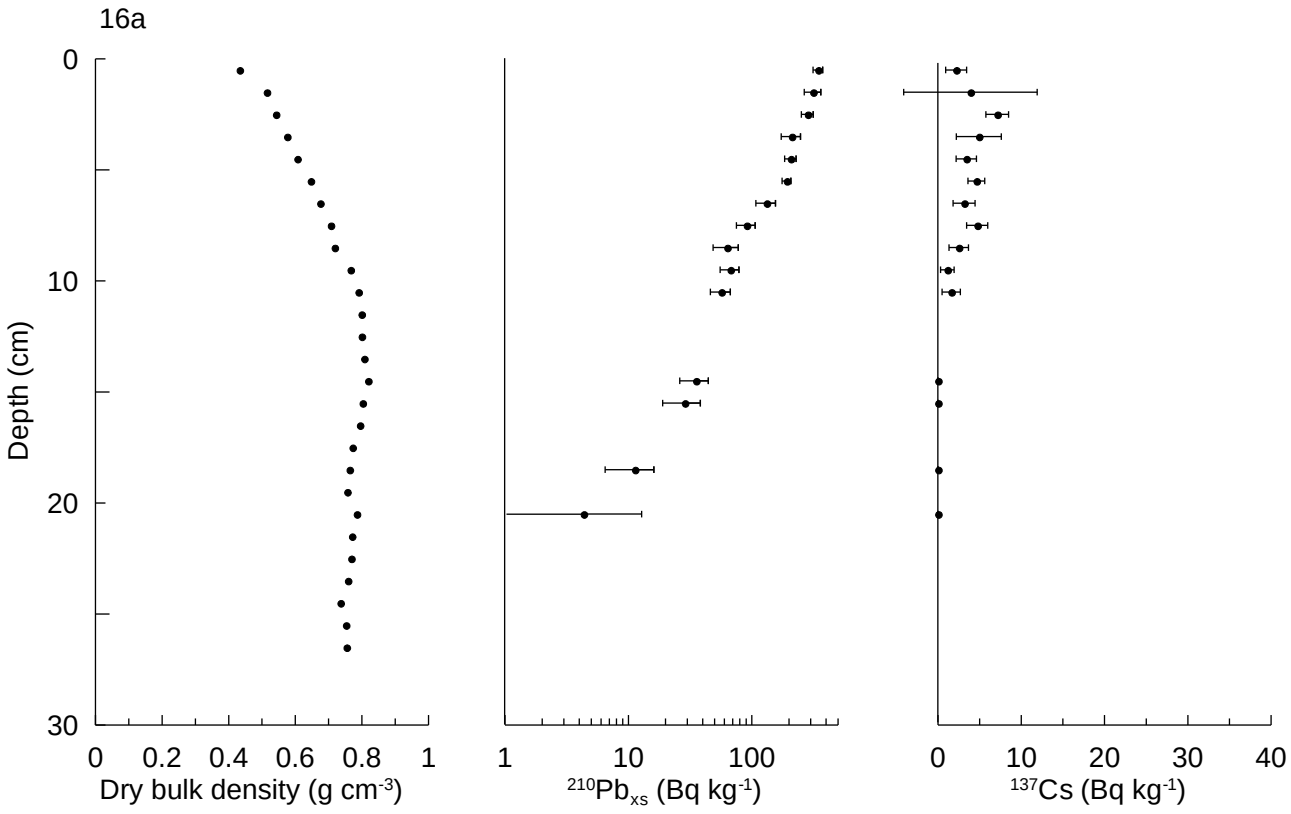

Fig 1

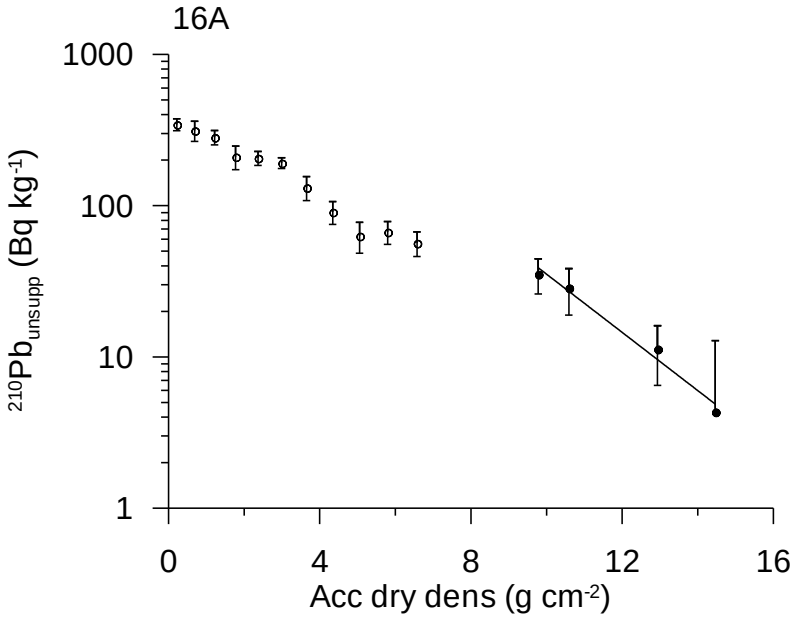

Fig 2. Regression of unsupported ^{210}Pb vs accumulated dry density.

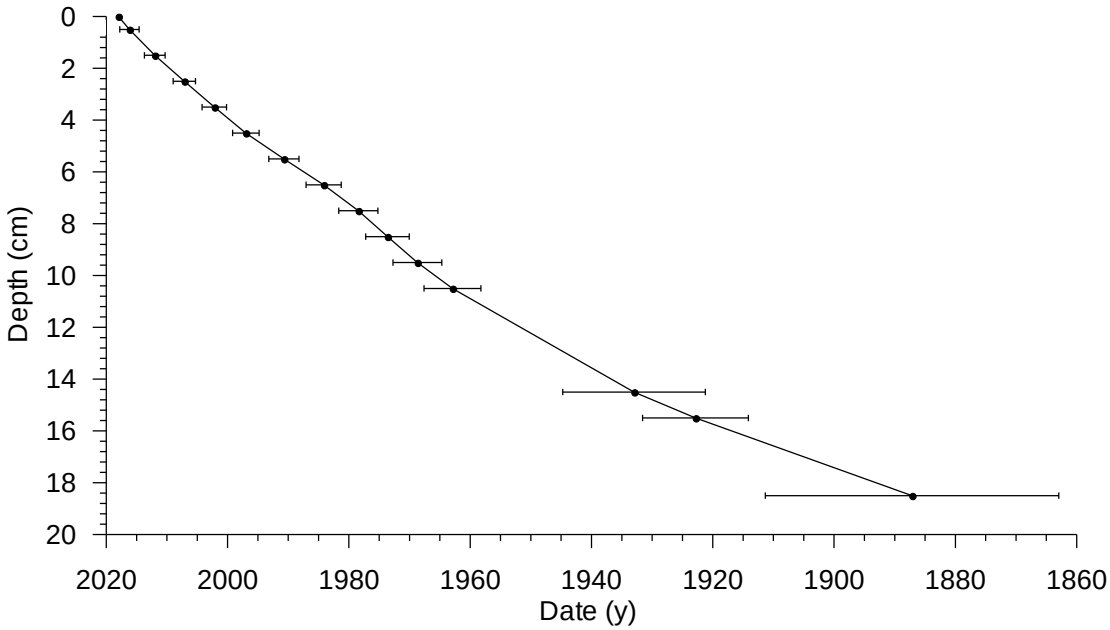
Depth (cm)
0
2
4
6
8
10
12
14
16
18
20
2020
2000
1980
1960
1940
1920
1900
1880
1860
Date (y)

Fig 3

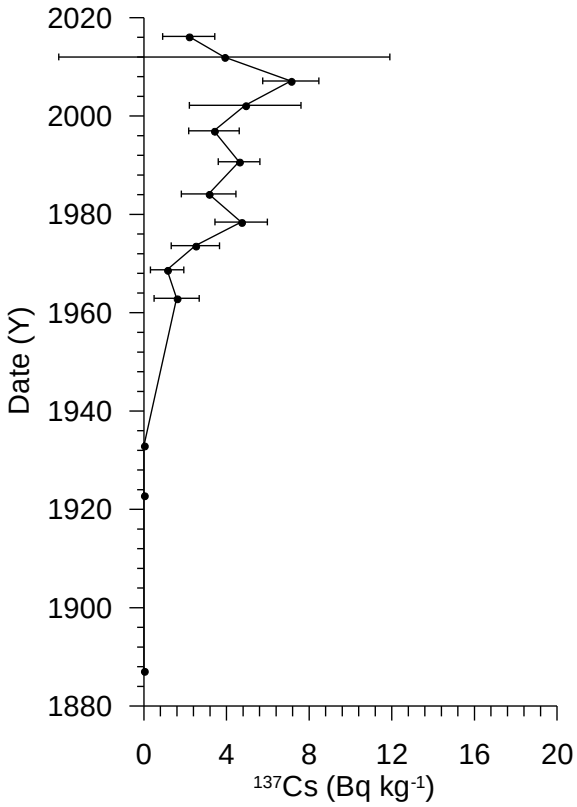
Date (Y)
2020
2000
1980
1960
1940
1920
1900
1880
0
4
8
12
16
20
137Cs (Bq kg-1)

Fig 4

C2 Dating of core R1887MC022

Gamma Dating Center Copenhagen

Copenhagen, August 19th, 2019

Thorbjørn J. Andersen
Department of Geosciences and Natural Resource Management (IGN)
University of Copenhagen
Oester Voldgade 10
1350 Copenhagen K
e-mail tja@ign.ku.dk
phone +45 35 32 25 03
fax +45 35 32 25 01

Dating of core R1887MC022A

Dating of core R1887MC022A

Methods

The samples have been analysed for the activity of ^{210}Pb, ^{226}Ra and ^{137}Cs via gammaspectrometry at the Gamma Dating Center, Institute of Geography, University of Copenhagen. The measurements were carried out on a Canberra ultralow-background Ge-detector. ^{210}Pb was measured via its gamma-peak at 46,5 keV, ^{226}Ra via the granddaughter ^{214}Pb (peaks at 295 and 352 keV) and ^{137}Cs via its peak at 661 keV.

Results

The core showed surface contents of unsupported ^{210}Pb of around 260 Bq kg^{-1} with a clear tendency for exponential decline with depth (fig 1). The calculated flux of unsupported ^{210}Pb is 355 Bq m^{-2} y^{-1} which is about 3 times higher than the expected flux (based on data shown in Appleby, 2001). This indicates that the site is subject to sediment focusing.

The content of the isotope ^{137}Cs was fairly low and only consistently above detection limits in the upper 17 cm of the core. However, a distinct peak was observed at a depth of 12.5 cm.

CRS-modelling has been applied on the profile using a modified method (Appleby, 2001; Andersen 2017) where the activity below 22 cm is calculated on the basis of the regression shown in fig 2. The chronology calculated on the basis of this places the peak in 137Cs to 1954 which is clearly before the likely date of 1963. A final chronology has therefore been calculated in which the peak is set to 1963. The result is given in table 2 and fig 3 and 4.

The chronology given in table 2 is only valid if bioturbation and other sediment mixing is negligible. However, the distinct peak in ^{137}Cs indicates that mixing must be very limited and the chronology is therefore believed to be reliable.

Copenhagen, August 19th 2019

Thorbjørn J Andersen
Professor,
IGN, University of Copenhagen
Oester Voldgade 10, 1350 Copenhagen K, Denmark

Reference:

Andersen, T.J., 2017. Some Practical Considerations Regarding the Application of ^{210}Pb and ^{137}Cs Dating to Estuarine Sediments. Applications of Paleoenvironmental Techniques in Estuarine Studies . Developments in Paleoenvironmental Research (DPER), Vol. 20, p 121-140.

Appleby, P.G., 2001. Chronostratigraphic techniques in recent sediments. In: Last, W.M & Smol, J.P. (eds) Tracking environmental change using lake sediments. Volume 1: Basin analysis, coring and chronological techniques. Kluwer Academic Publishers, the Netherlands.

Table 1. Raw data, R1887MC022A

Depth	Pb-210tot	error Pb-210 tot	Pb-210 supp	error Pb-210 sup	Pb-210 unsup	error Pb-210 unsup	Cs-137	error Cs-137
cm	Bq kg-1	Bq kg-1	Bq kg-1	Bq kg-1	Bq kg-1	Bq kg-1	Bq kg-1	Bq kg-1
0.5	300	23	44	1	256	24	4	2
1.5	308	28	54	4	254	32	3	3
2.5	282	26	53	2	229	28	3	0
3.5	240	13	65	2	176	16	7	1
4.5	231	25	50	1	181	26	10	3
5.5	220	22	39	4	181	26	7	2
6.5	177	20	51	7	126	27	11	2
8.5	148	16	39	5	109	21	10	2
10.5	83	11	41	3	42	14	5	2
11.5	97	13	43	6	54	19	5	2
12.5	83	12	30	10	53	22	32	3
14.5	74	10	49	3	25	13	2	2
16.5	64	6	43	3	21	9	3	1
20.5	46	7	48	0	1	8	1	2
22.5	58	7	43	1	15	8	2	1
26.5	44	6	42	1	2	7	0	0

Table 2, chronology core R1887MC022A

Depth	Age	error age	Date	acc rate	error rate	Date acc rate
cm	y	y	y	(kg m-2 y-1)	(kg m-2 y-1)	y
			2018			
0.5	1	2	2017	1.36	0.15	2017
1.5	5	2	2013	1.27	0.17	2015
2.5	8	2	2010	1.20	0.17	2012
3.5	12	2	2006	1.28	0.15	2008
4.5	16	3	2002	1.28	0.21	2004
5.5	22	3	1996	1.09	0.18	1999
6.5	27	4	1991	1.08	0.23	1994
8.5	40	5	1978	1.06	0.25	1984
10.5	52	6	1966	1.12	0.42	1972
11.5	57	7	1961	1.34	0.52	1963
12.5	64	8	1954	1.01	0.43	1958
14.5	77	12	1941	1.03	0.61	1948
16.5	89	15	1929	1.19	0.70	1935
20.5	107	25	1911	1.57	10.32	1920
22.5	118	26	1900	1.36	1.15	1905

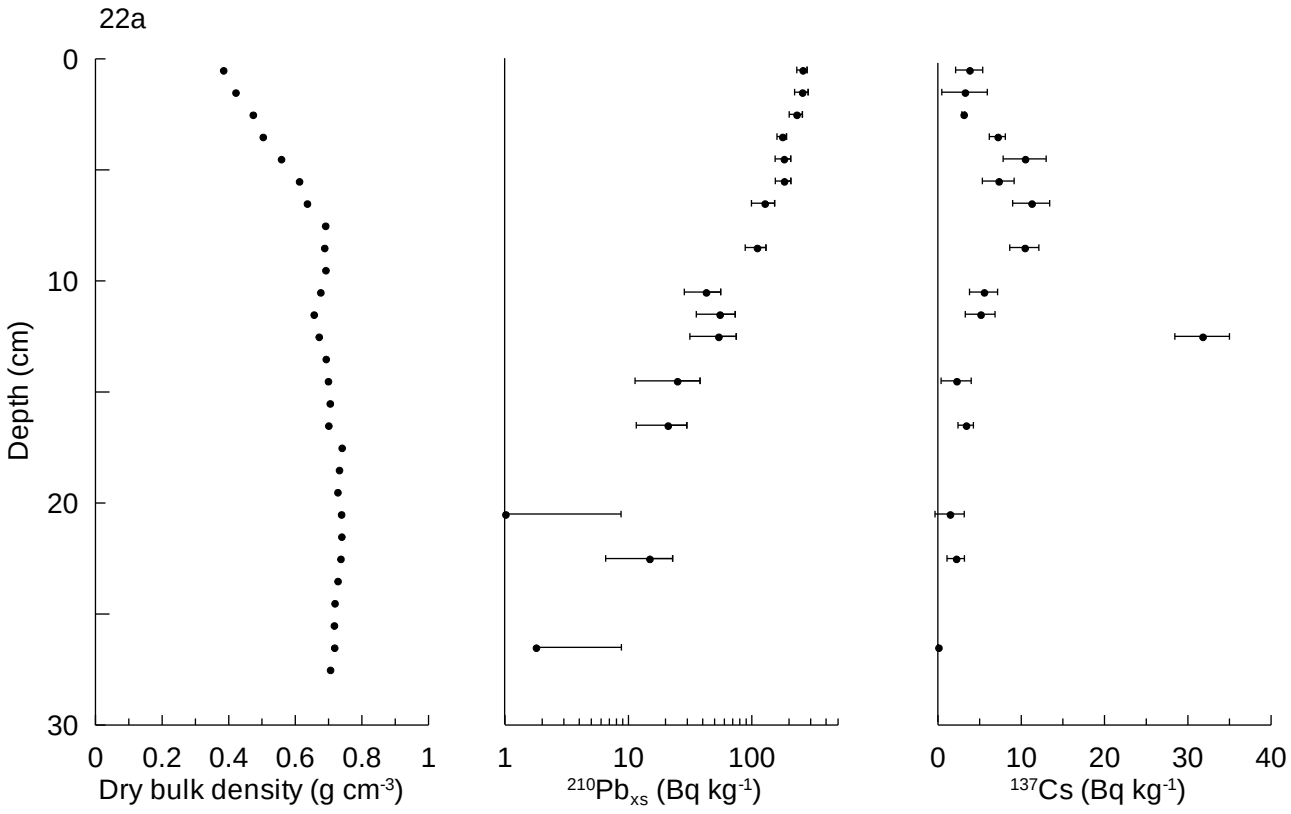

Fig 1

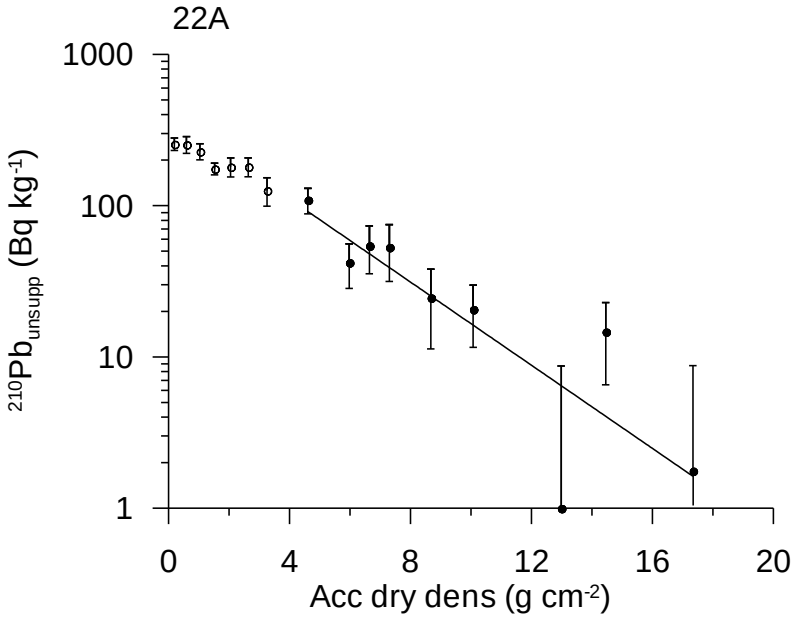

Fig 2. Regression of unsupported ^{210}Pb vs accumulated dry density.

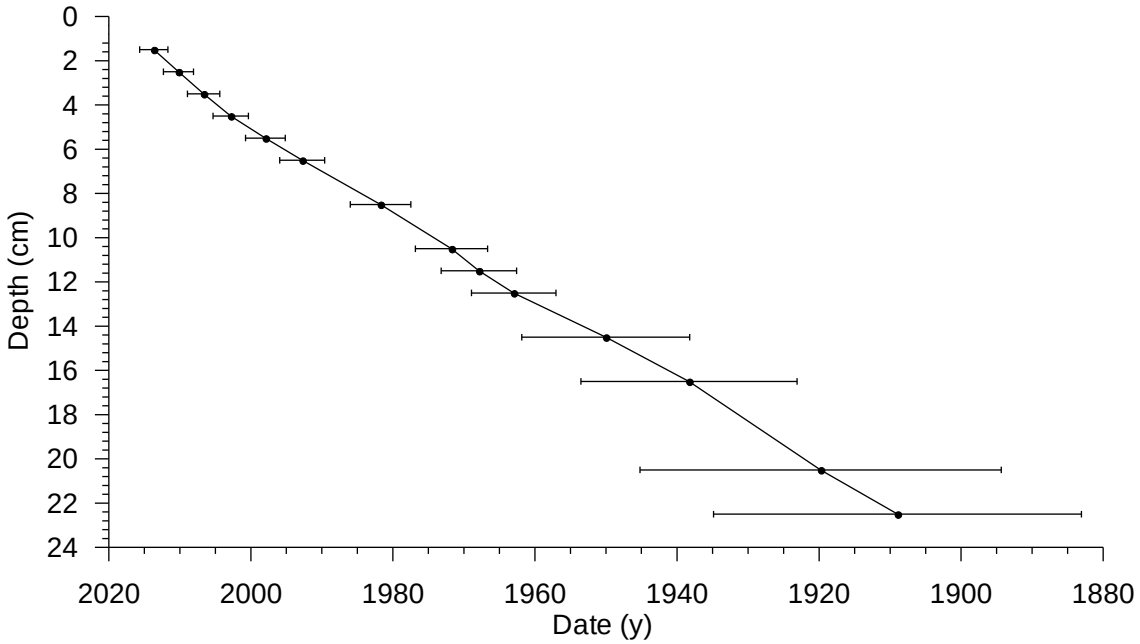
Depth (cm)
0
2
4
6
8
10
12
14
16
18
20
22
24
2020
2000
1980
1960
1940
1920
1900
1880
Date (y)

Fig 3

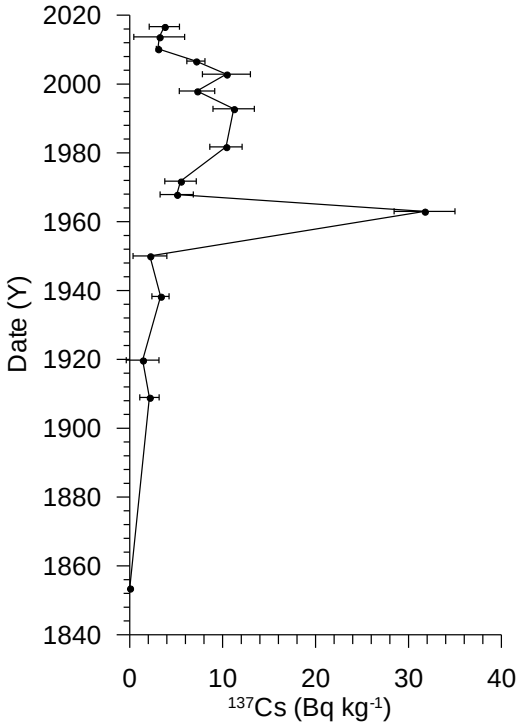
Date (Y)
2020
2000
1980
1960
1940
1920
1900
1880
1860
1840
0
10
20
30
40
137Cs (Bq kg-1)

Fig 4

Appendix D

MATERIAL COMPOSITION

Table D 1 Percent composition of particles in the sediment samples, as classified by FT-IR.

Sample ID	Depth (cm)	Unknown	Mineral	Organic	Oxy-resin	Petro-pyro	Plastic	Rubber	Most frequent plastic (plastic, rubber, oxy-resin) identified	Second most frequent plastic (plastic, rubber, oxy-resin) identified
S-01	0-2	98 %	0 %	0 %	0 %	0 %	1 %	0 %	Unresolved	PET
S-02	0-2	98 %	0 %	0 %	0 %	0 %	2 %	0 %	PS	Unresolved
S-03	0-2	99 %	0 %	1 %	0 %	0 %	0 %	0 %	n.d.	n.d.
S-04	0-2	97 %	0 %	0 %	0 %	0 %	3 %	0 %	PS	PET
S-05	0-2	56 %	0 %	7 %	0 %	5 %	32 %	0 %	PET	PS
S-06	0-2	83 %	0 %	1 %	0 %	15 %	1 %	1 %	PAM	Rubber
S-07	0-2	99 %	0 %	0 %	0 %	0 %	1 %	0 %	PE	PET
S-08	0-2	68 %	0 %	0 %	1 %	29 %	1 %	0 %	Phenoxy Resin	Nylon
S-09	0-2	0 %	0 %	0 %	0 %	43 %	36 %	21 %	Rubber	PVC
S-10	0-2	86 %	0 %	4 %	0 %	0 %	5 %	4 %	Rubber	PE-oxidized
S-11	31-33	61 %	0 %	0 %	1 %	37 %	1 %	1 %	Phenoxy Resin	Rubber I
S-12	33-35	87 %	0 %	0 %	0 %	13 %	0 %	0 %	PE	nd
S-13	26-28	94 %	1 %	0 %	0 %	0 %	5 %	0 %	PE-chlorinated	PET
S-14	28-30	87 %	0 %	6 %	0 %	0 %	7 %	0 %	PE-chlorinated	nd

Sample ID	Depth (cm)	Unknown	Mineral	Organic	Oxy-resin	Petro-pyro	Plastic	Rubber	Most frequent plastic (plastic, rubber, oxy-resin) identified	Second most frequent plastic (plastic, rubber, oxy-resin) identified
S-15	20-22	92 %	0 %	8 %	0 %	0 %	1 %	0 %	PET	nd
S-16	22-24	100 %	0 %	0 %	0 %	0 %	0 %	0 %	nd	nd
S-17	30-32	96 %	1 %	2 %	0 %	0 %	1 %	1 %	Rubber I	PVC
S-18	32-34	67 %	0 %	12 %	3 %	1 %	15 %	2 %	PE:PP	PVC
S-19	25-27	79 %	0 %	7 %	2 %	4 %	6 %	3 %	PE-oxidized	Tin-Paint
S-20	27-29	81 %	0 %	9 %	1 %	3 %	4 %	2 %	PE:PP	Rubber II
B-1	32-34	86 %	0 %	3 %	0 %	5 %	5 %	0 %	PVC	PE-chlorinated
B-2	30-32	94 %	0 %	0 %	0 %	1 %	5 %	0 %	PE-chlorinated	PE

Appendix E

MICROPLASTICS IN SEDIMENTS FROM THE NORWEGIAN CONTINENTAL SHELF

Contents

E1 Microplastics in sediments from the Norwegian Continental Shelf

During the regional environmental sediment monitoring on the Norwegian Continental Shelf (NCS) on behalf of the oil and gas industry in 2017, 35 sediment samples from the North Sea and the Barents Sea were sampled, including many stations near offshore oil platforms.[1, 2] The samples were analysed for microplastics at NGI, using the same analytical method as in this study. However, in the 2017 study, the microplastic concentrations were calculated based on the FT-IR cut-off of 0.6 with the reference library, while in the present study, a cut-off of 0.7 was used. Thus, the microplastic concentrations in sediments from the NCS were recalculated for comparison with the MAREANO sediments in this study. Data from the NCS study using the 0.7 cut-off is presented in the following table.

Table E 1 Microplastic abundance (defined as plastic polymers, oxy-resins and rubbers) in sediments (dry weight) from the Norwegian Continental Shelf (NCS). Results are based on FT-IR match score ≥ 0.7 with the reference library.

Station	Location area	mg MP/kg	mg/m^2	Items/kg	Items/m^2
Reg-01[1]	Central North Sea	<LOD	<LOD	n.d.	n.d.
Reg-02[1]		<LOD	<LOD	n.d.	n.d.
Reg-03[1]		2.6	21	190	1600
Reg-04[1]		<LOD	<LOD	n.d.	n.d.
Reg-06[1]		13	110	980	8300
Reg-07[1]		0.68	6.0	52	450
Reg-08[1]		2.2	20	170	1500
Reg-09[1]		0.48	2.2	76	350
Reg-11[1]		<LOD	<LOD	n.d.	n.d.
Reg-14[1]		<LOD	<LOD	110	900
EKO-12[2]		1.6	13	120	960
EKO-14[2]		0.89	10	68	810
EKO-21[2]		22	190	1700	15000
GYDA-18[2]		1.1	7.8	69	460
GYDA-21[2]		<LOD	<LOD	n.d.	n.d.
VAL-02[2]		5.3	39	390	3000
VAL-04[2]		<LOD	<LOD	n.d.	n.d.
VAL-05[2]		3.3	26	250	2000
VAL-15[2]		1.2	9.3	89	700
ULA-06[2]		25	196	1900	15000
Reg-12[1]	Northern North Sea	<LOD	<LOD	n.d.	n.d.
SNB-16R[1]		<LOD	<LOD	500	1900
VI-RB[1]		<LOD	<LOD	100	210
STC-06R[1]		<LOD	<LOD	n.d.	n.d.
KV-14[2]		0.51	6.4	39	490
KV-02[2]		5.3	54	400	4100
VI-01[2]		7.1	36	540	2800
VI-03[2]		5.9	35	170	1000
VI-30[2]		46	146	3400	11000
Vega-R[2]		<LOD	<LOD	98	270
STT-2[1]	Barents Sea	1.9	4.9	150	380
KF2-6[1]		0.91	4.2	71	320
SC3-4[1]		6.9	22	540	1600
KRT-14[1]		0.90	3.4	54	190
GRS-2[1]		11	27	800	2000

[1]Stations at sufficient distance from oil and gas fields ("regional" samples).
[2]Stations in close vicinity to oil and gas fields.

E2 References to the Appendix

1. DNV and NGI, *Microplastics in sediments on the Norwegian Continental Shelf*, 2018.
2. DNV and NGI, *Microplastic in sediments on the Norwegian Continental Shelf II: Identification through FT-IR analysis*, Report 2018-1226, Rev. 00, 2018.

Kontroll- og referanseside/ Review and reference page

Dokumentinformasjon/*Document information*		
Dokumenttittel/*Document title* MAREANO survey of Svalbard		**Dokumentnr./*Document no.*** 20190263-01-R
Dokumenttype/*Type of document* Rapport / Report	**Oppdragsgiver/*Client*** NGU	**Dato/*Date*** 2019-11-20
Rettigheter til dokumentet iht kontrakt/ *Proprietary rights to the document according to contract* NGI		**Rev.nr.&dato/*Rev.no.&date*** 0
Distribusjon/*Distribution* BEGRENSET: Distribueres til oppdragsgiver og er tilgjengelig for NGIs ansatte / LIMITED: Distributed to client and available for NGI employees		
Emneord/*Keywords* Microplastics, sediment, Svalbard, Mareano, Bauta		

Stedfesting/*Geographical information*	
Land, fylke/*Country* Norway	**Havområde/*Offshore area***
Kommune/*Municipality*	**Feltnavn/*Field name***
Sted/*Location*	**Sted/*Location***
Kartblad/*Map*	**Felt, blokknr./*Field, Block No.***
UTM-koordinater/*UTM-coordinates* **Zone: East: North:**	**Koordinater/*Coordinates*** **Projection, datum: East: North:**

Dokumentkontroll/*Document control*

Kvalitetssikring i henhold til/*Quality assurance according to NS-EN ISO9001*

Rev/ *Rev.*	**Revisjonsgrunnlag/*Reason for revision***	**Egenkontroll av/ *Self review by:***	**Sidemanns-kontroll av/ *Colleague review by:***	**Uavhengig kontroll av/ *Independent review by*:**	**Tverrfaglig kontroll av/ *Interdisciplinary review by:***
0	Original document	2019-11-19 Heidi Knutsen	2019-11-19 Hans Peter Arp		

Dokument godkjent for utsendelse/ *Document approved for release*	**Dato/*Date***	**Prosjektleder/*Project Manager***
	20 November 2019	Heidi Knutsen

NGI (Norwegian Geotechnical Institute) is a leading international centre for research and consulting within the geosciences. NGI develops optimum solutions for society and offers expertise on the behaviour of soil, rock and snow and their interaction with the natural and built environment.

NGI works within the following sectors: Offshore energy – Building, Construction and Transportation – Natural Hazards – Environmental Engineering.

NGI is a private foundation with office and laboratories in Oslo, a branch office in Trondheim and daughter companies in Houston, Texas, USA and in Perth, Western Australia

www.ngi.no

NGI (Norges Geotekniske Institutt) er et internasjonalt ledende senter for forskning og rådgivning innen ingeniørrelaterte geofag. Vi tilbyr ekspertise om jord, berg og snø og deres påvirkning på miljøet, konstruksjoner og anlegg, og hvordan jord og berg kan benyttes som byggegrunn og byggemateriale.

Vi arbeider i følgende markeder: Offshore energi – Bygg, anlegg og samferdsel – Naturfare – Miljøteknologi.

NGI er en privat næringsdrivende stiftelse med kontor og laboratorier i Oslo, avdelingskontor i Trondheim og datterselskaper i Houston, Texas, USA og i Perth, Western Australia.

www.ngi.no

NGI
OSLO
TRONDHEIM
HOUSTON
PERTH

NORWEGIAN GEOTECHNICAL INSTITUTE
NGI.NO

Main office
PO Box 3930 Ullevaal St.
NO-0806 Oslo
Norway

Trondheim office
PO Box 5687 Torgarden
NO-7485 Trondheim
Norway

T (+47)22 02 30 00
F (+47)22 23 04 48
NGI@ngi.no

BIC NO. DNBANOKK
IBAN NO26 5096 0501 281
ORGANISATION NO.
958 254 318MVA

ISO 9001/14001
CERTIFIED BY BSI
FS 32989/EMS 612006

NORGES
GEOLOGISKE
UNDERSØKELSE

· NGU ·

Norges geologiske undersøkelse
Postboks 6315, Sluppen
7491 Trondheim, Norge

Besøksadresse
Leiv Eirikssons vei 39
7040 Trondheim

Telefon 73 90 40 00
E-post ngu@ngu.no
Nettside www.ngu.no